INVESTIGATING THE ROLE OF THE CALCIUM-SENSING RECEPTOR (CaSR) IN LUNG REMODELLING

Richard Bruce, BSc.

A thesis presented for the degree of Doctor of Philosophy

July 2023

Supervisor: Professor Daniela Riccardi
Co-supervisor(s): Dr Zoe Prytherch & Professor Paul Kemp

School of Biosciences
Cardiff University
Museum Avenue
Cardiff
CF10 3AX

GRAPHICAL SUMMARY

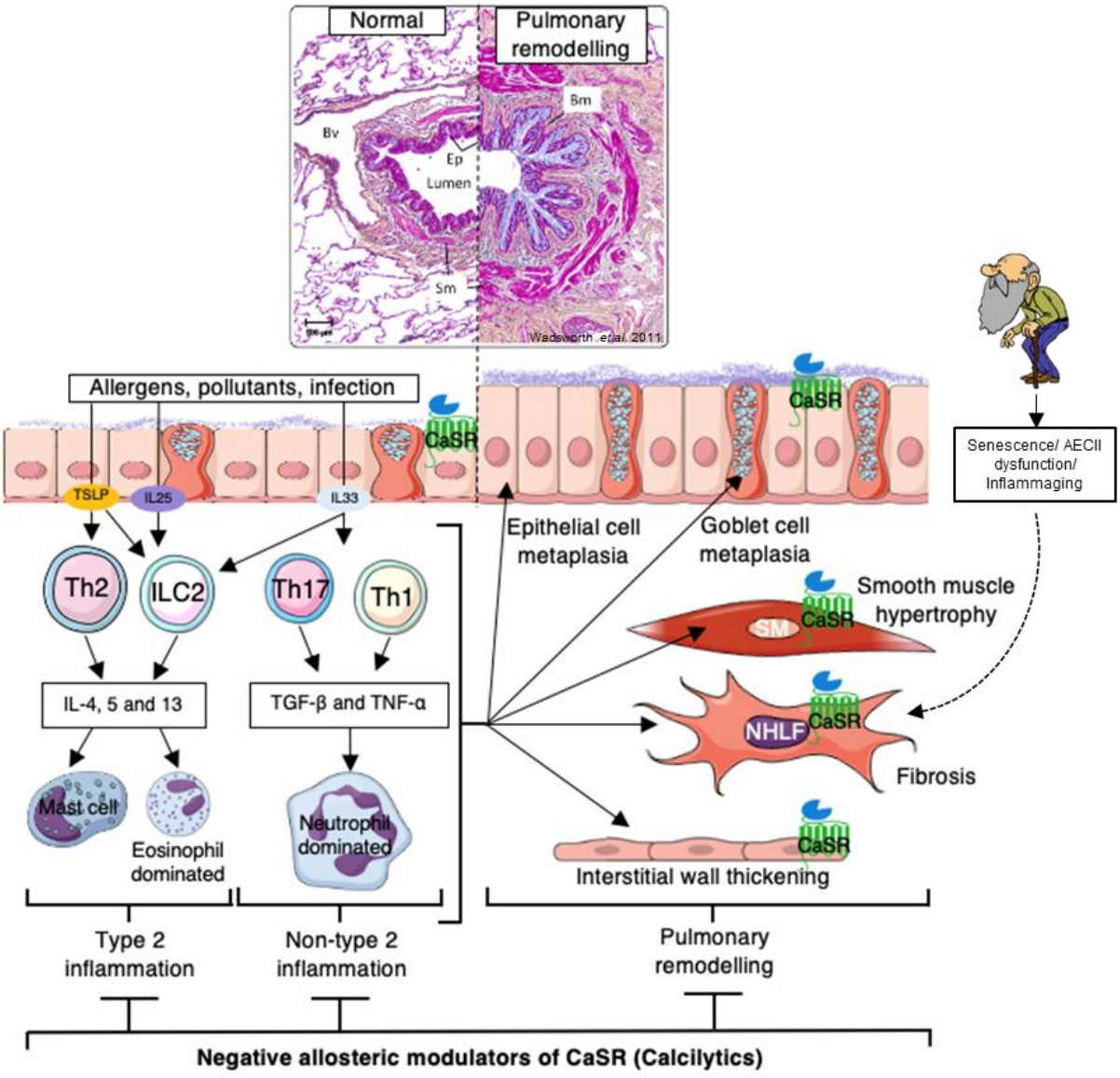

Age- and disease-related lung remodelling limits airflow and devastates the lung architecture without option for effective treatment. Allergens, pollutants and infections have been identified as activators of chronic inflammation and injury in the lung where immune cells (e.g. eosinophils and neutrophils), resident cells (e.g. epithelial cells and fibroblasts) and remodelling mediators (e.g. interleukin-13 (IL-13) and transforming growth factor-ß (TGF-ß)) drive lung remodelling by mechanisms that are not yet fully understood.

Previous studies have demonstrated an extracellular cation-sensor, the calcium-sensing receptor (CaSR), plays a central role in lung development, tissue morphogenesis and inflammation in the lung as well as tissue remodelling in other organs. However, the role of the CaSR in lung remodelling is currently unknown.

During my PhD I have 1) developed novel methods for determining airway and interstitial lung remodelling *in vivo*; 2) investigated the role of the CaSR in age-related lung remodelling *in vivo* using aging mice with targeted CaSR-deletion from SM22α-positive cells; 3) investigated the role of the CaSR in pre-clinical models of IgE/Th2 asthma, alarmin-driven asthma and COPD-like neutrophilic exacerbation in the presence or absence of inhaled negative allosteric modulators (NAM) of the CaSR; and 4) investigated the role of the CaSR in cell signalling and remodelling processes *in vitro* using human lung fibroblasts exposed to a remodelling mediator, TGF-β, in the presence of absence of NAM treatment. The key findings of this thesis are:

1. The CaSR in SM22α-positive cells is central to age-related airway and interstitial ECM remodelling.
2. Inhaled NAM treatment ameliorates airway remodelling, particularly goblet cell metaplasia, in models of IgE/Th2 asthma and interstitial remodelling and/or inflammation in alarmin-driven asthma.
3. The CaSR is expressed in human lung fibroblasts and NAM treatment ameliorates TGF-β1-induced upregulation of CaSR and associated G-protein expression; non-canonical TGF-β signalling; and cellular processes implicated in lung remodelling, including cell-adhesion, apoptosis, secretion, growth, proliferation and extracellular matrix (ECM) remodelling.

Together these findings strongly indicate that the CaSR plays a central role in physiological and pathophysiological lung remodelling.

PUBLICATIONS

Peer-reviewed articles

Yarova, P.L., Huang, P., Schepelmann, M.W., Bruce, R., Ecker, R., Nica, R., Telezhkin, V., Traini, D., Dos Reis, L.G., Kidd, E.J. and Ford, W.R., (2021). Characterization of negative allosteric modulators of the calcium-sensing receptor for repurposing as a treatment of asthma. *Journal of Pharmacology and Experimental Therapeutics*, *376*(1), pp.51-63.

Pre-print (Peer review pending)

Wolffs, K., Mansfield, B., Bruce, R., Huang, P., Schepelmann, M.W., Brennan, S.C., Verckist, L., Adriaensen, D., De Araújo, R.P., Mur, L.A. and Attanoos, R., (2020). Calcium-sensing receptor antagonism as a novel therapeutic for pulmonary fibrosis. *medRxiv*.

Published abstracts

Bruce, R., Huang, P., Yarova, P., Schepelmann, M., Wolffs, K., Mansfield, B., Ford, W., Kidd, E., Chang, W., Ecker, R. and Nica, R., Ying, S., Kemp, P.J., and Riccardi, D., (2019). Calcium-sensing receptor (CaSR) drives lung ECM remodelling and fibrosis in murine asthma models and in ageing mice. [European Respiratory Society Abstract]

In Preparation

Bruce, R., Huang, P., Yarova, P., Schepelmann, M., Wolffs, K., Mansfield, B., Ford, W., Kidd, E., Chang, W., Ecker, R. and Nica, R., Ying, S., Kemp, P.J., and Riccardi, D., Calcium-sensing receptor (CaSR) drives airway and interstitial remodelling in murine asthma models.

CONTRIBUTIONS

This project was highly collaborative in nature and all *in vivo* models of age-related fibrosis and inflammatory lung disease were organised and performed by Dr Martin Schepelmann, Dr Polina Yarova and Ping Huang of our laboratory as well as other external collaborators. Furthermore, Dr Kasope Wolffs of our laboratory designed and performed the *in vitro* experiments using normal human lung fibroblasts, with my occasional aid. All contributors or data obtained through external means are referenced in the text. All data analysis and interpretation of results provided in the results chapters are my own.

ACKNOWLEDGEMENTS

I would like to say a special thank you to Professor Daniela Riccardi for being a fantastic, encouraging and supportive supervisor, I could not have asked for more! I would also like to thank Dr Polina Yarova, Dr Martin Schepelmann, Ping Huang, and Dr Kasope Wolffs who's hard work with models of aging and disease made the studies in this thesis possible. I would also like to say a huge thank you to Dr Rupert Ecker and Robert Nica at TissueGnostics who provided access and support with the fantastic image analysis software, StrataQuest. I would also like to thank Dr Anthony Hayes, Derek Scarborough, Mark, and Claire Gealy at the Cardiff University Bioimaging Hub who provided a huge amount of histology and microscopy support as well as Dr Daniel Pass, Angela Marchbank and Andrew Ells at the Genome Hub that supported me with RNA-sequencing and bioinformatics.

Finally, I would like to say a special thank you to my parents, you have provided the emotional and financial support that made all of this possible!

TABLE OF CONTENTS

LIST OF ABBREVIATIONS

3-PG	3-Phosphoglyceric acid
3-PHP	3-Phosphohydroxypyruvate
3-PS	3-Phosphoserine
4E-BP1	4E-binding protein 1
7TM	Seven transmembrane
AB	Alcian blue
ACTA2	Alpha smooth muscle actin gene
ADCY	Adenyl Cyclase
AHR	Airway hyperresponsiveness
Akt	Protein kinase B
AKT	Akt isoform 3
AKTIP	Akt interacting protein
ALDH	Aldehyde dehydrogenase
ALDH18A1	Aldehyde dehydrogenase 18A1
ANOVA	Analysis of variance
AP-1	Activator protein-1
APC	Adenomatous polyposis coli
AS	Modified Ashcroft score
ASM	Airway smooth muscle
ASNS	Asparagine synthetase
AT	Austria
ATF	Activating transcription factor
ATF4	Activating transcription factor 4
ATG	Autophagy related
ATP	Adenosine triphosphate
AU	Arbitrary units
Balb	Bagg and Albino
BALF	Bronchoalveolar lavage fluid
BP	Base pair
BRAF	B-Raf isoform

Ca^{2+}_i	Intracellular free ionised calcium
Ca^{2+}_i	Intracellular free ionised calcium
c-Abl	c-Abelson
CALR	Calreticulin
CAMK2A	Calcium/calmodulin dependent protein kinase II alpha
CAMK2D	Calcium/calmodulin dependent protein kinase II delta
CAMK2G	Calcium/calmodulin dependent protein kinase II gamma
CAMK2N1	Calcium/calmodulin dependent protein kinase II inhibitor 1
CaMKKβ	Calmodulin
cAMP	Cyclic adenosine monophosphate
CaN	Calcineurin
CaSR	Extracellular calcium (cation)-sensing receptor
CaSR-KO	Targeted CaSR deletion from SM22α-positive cells
CDC42	Cell division cycle 42
CDK	Cyclin-dependent kinase
CDKN	Cyclin-dependent kinase inhibitors
CF	Cofactors
CFTR	Cystic fibrosis transmembrane conductance regulator
CK-1	Casein kinase-1
COL	Collagen gene
COPD	Chronic obstructive pulmonary disease
CR	Cysteine-rich
CREB	cAMP response element-binding protein
CTGF	Connective tissue growth factor
CTHRC1	Collagen triple helix repeat containing 1
CXCL	Chemokine C-X-C motif ligand
DAG	Diacylglycerol
DAPI	4,6-Diamidino-2-phenylindole
DEP	Disheveled/Egl-10/pleckstrin
DEPTOR	DEP domain containing mTOR interacting protein
DMSO	Dimethyl sulfoxide
DNA	Deoxyribonucleic acid
DVL	Dishevelled

ECM	Extracellular matrix
ECP	Eosinophilic cationic protein
EGFR	Epidermal growth factor receptor
ELN	Elastin
EMT	Epithelial to mesenchymal transition
ER	Endoplasmic reticulum
ERK	Extracellular signal-regulated kinase
ES	Embryonic stem cells
ET	Epithelial tissue
F6P	Fructose 6-phosphate
FBM	Fibroblast basal medium
FBS	Fetal bovine serum
FEV1	Forced expiratory volume in one second
FFPE	Formalin-fixed paraffin-embedded
FGF	Fibroblast growth factor
FGFR	Fibroblast growth factor receptor
FGM	Fibroblast growth medium
FIJI	Fiji is Just ImageJ
FN1	Fibronectin 1
FOSL2	Fos-like 2 AP-1 transcription factor subunit
FP	Fluticasone propionate
FSCN1	Fascin actin-bundling protein 1
FZD	Frizzled
G protein	Guanine nucleotide-binding protein
G_{11}	Guanine nucleotide-binding protein subunit alpha (11)
G_{12}	Guanine nucleotide-binding protein subunit alpha (12)
G_{13}	Guanine nucleotide-binding protein subunit alpha (13)
GAG	Glycosaminoglycan
GAP	GTPase-activating protein
GC	Goblet cells
GDI	Guanine nucleotide dissociation inhibitor
GEF	Guanine nucleotide exchange factor
G_i	Guanine nucleotide-binding protein subunit alpha (i)

GM-CSF	Granulocyte-macrophage colony-stimulating factor
GNA	Guanine nucleotide-binding protein subunit alpha gene isoform
GNB	Guanine nucleotide-binding protein subunit beta gene isoform
GNY	Guanine nucleotide-binding protein subunit gamma gene isoform
GO	Gene ontology
G_o	Guanine nucleotide-binding protein subunit alpha (o)
GPCR	G-protein coupled receptor
G_q	Guanine nucleotide-binding protein subunit alpha (q)
Grb2	Growth factor receptor binding protein 2
Grp75	Glucose regulated protein 75
G_s	Guanine nucleotide-binding protein subunit alpha (s)
GSK-3	Glycogen synthase kinase-3
GSK3β	Glycogen synthase kinase 3 beta
GTP	Guanosine triphosphate
G_β	Guanine nucleotide-binding protein subunit beta
G_γ	Guanine nucleotide-binding protein subunit gamma
HBEC	Human bronchial epithelial cell
HEK293	Human embryonic kidney 293
Het	Heterozygous
Hom	Homozygous
HRAS	H-Ras isoform
HRCT	High-resolution computed tomography
HSPB1	Heat shock protein family B1
IgE	Immunoglobulin E
IgG	Immunoglobulin G
IgG2a	Immunoglobulin G isotype 2a
IKK	IκB kinase
IL	Interleukin
IL1βR	IL1β receptor
ILC2	Type 2 innate lymphoid cells
IN	Intranasal
IP	Intraperitoneal
IP_3	Inositol 1,4,5-trisphosphate

IP_3R	IP_3 receptor
IPF	Idiopathic pulmonary fibrosis
ITPR	Inositol 1,4,5-trisphosphate receptor
JIP	Jun N-terminal kinase-interacting protein
JNK	Jun N-terminal kinase
LABA	Long-acting ß2-adrenoceptor agonists
LAMA	Long-acting muscarinic antagonists
LB	Lobe
LDH	Lactate dehydrogenase
LDHA	Lactate dehydrogenase A
LEF	Lymphoid enhancer binding factor
LPS	Lipopolysaccharide
LRP	Low-density lipoprotein receptor-related protein
LRP5/6	Low-density lipoprotein receptor-related protein 5 and 6
MAPK	Mitogen-activated protein kinase
MAPKAPK-2	Mitogen-activated protein kinase activated protein kinase-2
MARCKS	Myristoylated alanine rich protein kinase c substrate
MBP	Major basic protein
MEK	MAPK/ERK Kinase
MEKK	MAPK/ERK kinase kinase
mGluR5	Metabotropic glutamate receptor 5
MICU	Mitochondrial calcium uptake
MKK	Mitogen activation protein kinase kinase
MLK3	Mixed lineage kinase 3
MLPH	Melanophilin
mLST8	GTPase ß-subunit like protein gßL
MMP	Matrix metalloproteinase
mPTP	Mitochondrial permeability transition pore
mRNA	Messenger ribonucleic acid
mSIN1	Mammalian stress-activated protein kinase-interacting protein
MSK1	Ribosomal protein S6 kinase
mTOR	Mechanistic target of rapamycin
mTORC	Mechanistic target of rapamycin complex

NAM	Negative allosteric modulator of the Calcium-sensing receptor
NFκB	Nuclear factor kappa-light-chain-enhancer of activated B cells
NFκB	Nuclear factor kappa-light-chain-enhancer of activated B cells
NHLF	Normal human lung fibroblast
NLRP3	Nucleotide-binding oligomerization domain like receptor P3
NRAS	N-Ras isoform
NRTK	Non-receptor tyrosine kinases
ORMDL-3	Orosomucoid-like 3
ORMDL3	Orosomucoid-like 3 gene
OVA	Ovalbumin
P5C	Pyrroline-5-carboxylate
P5CS	Pyrroline-5-carboxylate synthetase
P5CS	Δ1-pyrroline-5-carboxylate synthetase
PAM	Positive allosteric modulator of the Calcium-sensing receptor
PAS	Periodic acid Schiff
PBS	Phosphate buffered saline
PC	Peribronchial collagen
PCR	Polymerase chain reaction
PDGF	Platelet-derived growth factor
PFKFB3	6-Phosphofructo-2-kinase/fructose-2,6-biphosphatase 3
PHGDH	Phosphoglycerate dehydrogenase
PI3K	Phosphatidylinositol 3-kinase
PIK3AP1	Phosphatidylinositol 3-kinase adaptor protein 1
PIK3CA	Class I phosphatidylinositol 3-kinase catalytic subunit alpha
PIK3CB	Class I phosphatidylinositol 3-kinase catalytic subunit beta
PIK3CD	Class I phosphatidylinositol 3-kinase catalytic subunit delta
PIK3R1	Phosphatidylinositol 3-kinase regulatory subunit 1
PIP2	Phosphatidylinositol 4,5-bisphosphate
PIP4K2C	Phosphatidylinositol-5-phosphate 4-kinase type 2 gamma
PKC	Protein kinase C
PLAU	Plasminogen activator urokinase
PLAUR	Plasminogen activator urokinase receptor
PLC	Phospholipase C

PLCD	Phospholipase C delta
Plg	Plasminogen
PO_2	Partial pressure of oxygen
POLR1	RNA polymerase I
POLR2	RNA polymerase II
POLR3	RNA polymerase III
PPID	Cyclophilin-D
PPP3CC	Protein phosphatase 3 catalytic subunit gamma
PPP3R1	Protein phosphatase 3 regulatory subunit B alpha
PRAS40	Proline-rich AKT substrate of 40 kDa
PRKCA	Protein kinase C alpha
PRKCD	Protein kinase C delta
PRKCE	Protein kinase C epsilon
PRKCI	Protein kinase C iota
PRKCSH	Protein kinase C substrate 80Kda H
Protor	Proline-rich protein 5
PSAT1	Phosphoserine aminotransferase 1
PSPH	Phosphoserine phosphatase
PTH	Parathyroid hormone
PTH1R	Parathyroid hormone 1 receptor
Px	Pixels
PYCR	Pyrroline-5-carboxylate reductases
PYCR	P5C reductase
qHACC	Quantitative histomorphometry of airway cross-section components
qHIT	Quantitative histomorphometry of interstitial tissue
RAB	Ras-related protein
Raptor	Regulatory-associated protein of TOR
Ras	Rat sarcoma
Rb	Retinoblastoma protein
RCF	Relative centrifugal field
Rheb	Ras homolog enriched in brain
Rho	Ras-homologous
RhoK	Ras-homologous kinases

Rictor	Rapamycin-insensitive companion of TOR
RNA-seq	RNA-sequencing
ROCK	Rho Associated Coiled-Coil Containing Protein Kinase
ROCK1	Rho-associated coiled-coil containing protein kinase 1
ROCK2	Rho-associated coiled-coil containing protein kinase 2
ROI	Regions of interest
RRAS	R-Ras isoform
rRNA	ribosomal RNA
RTK	Receptor tyrosine kinases
S6K1	p70-S6 kinase 1
SAPK	Stress-activated protein kinase
SARA	Smad anchor for receptor activation
SERPINE1	Plasminogen activator inhibitor-1
Shc	Src homology 2 domain-containing transforming protein C
SHMT2	Serine hydroxymethyltransferase 2
SIRT1	Sirtuin-1
SLC	Solute carrier
SLC2A1	Solute carrier 2A1
SM	Smooth muscle
SM22α	Smooth muscle protein 22 alpha (aka Transgelin)
Smad	Small mother against decapentaplegic
Sos	Son Of Sevenless
SPARC	Secreted protein acidic and rich in cysteine
STAR	Spliced Transcripts Alignment to a Reference
STAT	Signal transducer and activator of transcription proteins
STX	Syntaxin
TAGLN	Transgelin gene (aka Smooth muscle protein 22 alpha gene)
TCF	Transcription factor
TEER	Transepithelial electrical resistance
TF	Transcription factor
TGFBRAP1	Transforming growth factor beta receptor associated protein 1
TGF-β	Transforming growth factor beta 1
TGF-βR	Transforming growth factor beta receptor

TGIF	Transforming growth-interacting factor
Th1	T helper 1
Th17	T helper 17
Th2	T helper 2
TIF1A	Transcription intermediary factor 1-alpha
TIMP	Tissue inhibitor of metalloproteinase
TNFα	Tumour necrosis factor alpha
TSC	Tuberous Sclerosis
TSLP	Thymic stromal lymphopoietin
TSPO	Translocator protein
Ubf	Upstream binding transcription factor
UIP	Usual interstitial pneumonia
ULK1	Unc-51 like autophagy activating kinase 1
VAMP	Vesicle associated membrane protein
VDAC	Voltage dependent anion channel
VEGFB	Vascular endothelial growth factor B
VFT	Venus flytrap
Wnt	Wingless-related integration site
WNT5A	Wingless-related integration site 5A isoform
WNT5B	Wingless-related integration site 5B isoform
WT	Wild type
ZO-1	Tight junction protein 1
αSMA	Alpha smooth muscle actin
αvß6	Integrin alpha-v beta-6
ß-catenin	Beta-catenin

CHAPTER 1: INTRODUCTION

Lung remodelling is a characteristic of aging and chronic lung disease in humans. In fact, irreversible respiratory dysfunction is the direct result of lung remodelling. This is defined as the structural change in molecular, cellular or tissue quantity, composition and organisation (Hogg et al., 2009). This introduction will present an overview of lung physiology, the changes that occur in pathophysiology and what is currently understood about remodelling mechanisms. It will also introduce the extracellular calcium-sensing receptor (CaSR) and the current evidence suggesting the CaSR plays a central role in lung remodelling as well as a hypothesis, aims and objectives.

1.1 Lung physiology and remodelling

1.1.1 Morphology and cellular composition

The lung is the primary site for gaseous exchange, providing the body with oxygen for the process of producing energy from complex organic substances as well as expulsion of the internal respiration and metabolic product, carbon dioxide (Lammert et al., 2014). At least 40 cell types have been identified in the lung so far; however, the recent discovery of novel cell types, such as the airway epithelium ionocyte and lipofibroblasts, suggests current knowledge of the cellular composition of the lung is incomplete (Franks et al., 2008; Montoro et al., 2018; Plasschaert et al., 2018; Schiller et al., 2019).

In humans, the bifurcating larger airways (bronchi) have an epithelium consisting primarily of pseudostratified, columnar, ciliated epithelial cells; mucus-secreting goblet cells; columnar cells; and basal cells attached to a basement membrane. These cells play a central role in defence by secreting mucosubstances, trapping foreign particles and removing them from the lung by mucociliary clearance.

The subepithelial region, also termed the submucosa, consists of mucus-secreting submucosal glands, neutrophils, dendritic cells and fibroblasts supported by a layer of collagen- and elastin-rich connective extracellular matrix (ECM) (lamina propria).

A layer of smooth muscle is found between the subepithelial region and the peribronchial adventitia that can constrict the airway to prevent passage of harmful substances into the lung, such as methacholine (Bossé et al., 2008). Finally, the peribronchial region (adventitia) consists of cartilage, fibroblasts and a supporting non-cellular ECM.

The ECM is composed of over 300 structural proteins, adhesion proteins and glycoproteins, including collagen, elastin, fibronectin, tenascin, glycosaminoglycans (GAGs) and proteoglycans, of which collagen fibres are the most abundant (Olczyk et al., 2014; Kular et al., 2014). Fibroblasts and the ECM provide structural rigidity and elasticity but also regulate tissue morphology by processes such as cell adhesion, migration, and proliferation through stiffness, integrin binding site availability and signalling molecules, called matrikines (Hoyles et al., 2011; Burgstaller et al., 2018; Burgess et al., 2018; Hough et al., 2020). The airways are also highly vascularised to perform their function with each airway being associated with a vein and an artery (Lammert et al., 2014; **Figure 1.1A**).

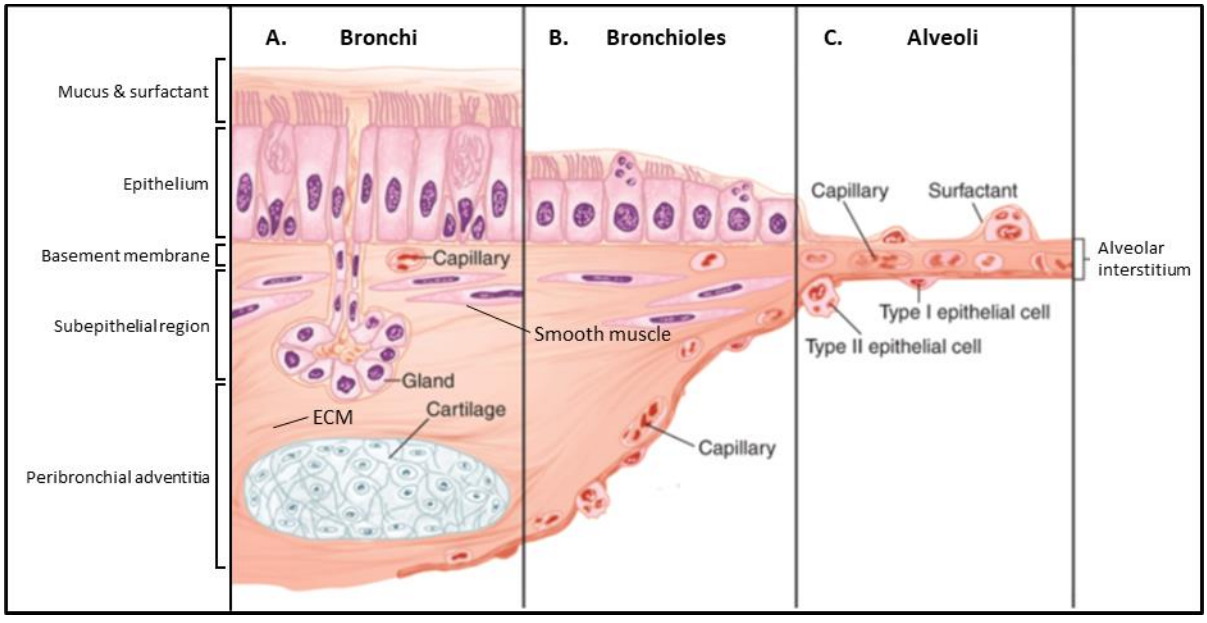

Figure 1.1. The structure and cellular composition of the lower airways. This is a graphical representation of the cellular and structural composition of the (**A**) larger airways (bronchi), (**B**) smaller airways (bronchioles) and (**C**) alveoli. Reproduced from Barrett et al. (2016). ECM: extracellular matrix.

The smaller airways (bronchioles, terminal bronchioles and respiratory bronchioles) consist primarily of ciliated, simple columnar or cuboidal epithelium with fewer goblet cells and submucosal glands, increased surfactant-secreting Clara cells and a reduced peribronchial ECM (**Figure 1.1B**). Finally, alveolar ducts feed the alveolar sacs that are especially thin to maximise surface area and aid gaseous exchange to and from the dense alveolar capillary network (West, 2011; Lammert et al., 2014). The alveoli consist of squamous-like type I alveolar epithelium cells, larger cuboidal surfactant-producing type II alveolar epithelial progenitor cells and capillary endothelial cells attached to a supporting alveolar interstitial extracellular matrix (**Figure 1.1C**).

1.1.2 Protective mechanisms and repair

Bacterial or viral infections, inflammation, allergic reactions, exposure to xenobiotics (e.g. cigarette smoke, pollution), physical trauma (e.g. mechanical ventilation), cancer, or pathology of unknown origin can cause injury to the lung epithelium (Crosby & Waters, 2010). Despite region-dependent variation in the response to persistent lung injury, the acute inflammatory response following initial injury is consistent throughout the lung.

Injury to the airway epithelium activates tissue remodelling processes to re-establish integrity and organisation by releasing signalling molecules, such as cytokines, interleukins, matrikines and growth factors, such as TGF-ß. These signalling molecules then mediate cellular repair mechanisms by activating signalling cascades, such as the small mother against decapentaplegic (Smad) pathway; Jun N-terminal kinase (JNK), extracellular signal-regulated kinase (ERK) and p38 mitogen-activated protein (MAP) kinase pathways; the phosphatidylinositol 3-kinase (PI3K)/Akt pathway, the Ras homolog (Rho) pathway; and Wingless-related integration site (Wnt) signalling pathways (Crosby & Waters, 2010). These pathways display a high degree of overlap and collectively orchestrate remodelling processes, such as cell adhesion, growth, proliferation, differentiation, migration, cytoskeletal organisation, apoptosis, and ECM component synthesis and turnover, as shown in **Figure 1.2** (Crosby & Waters, 2010).

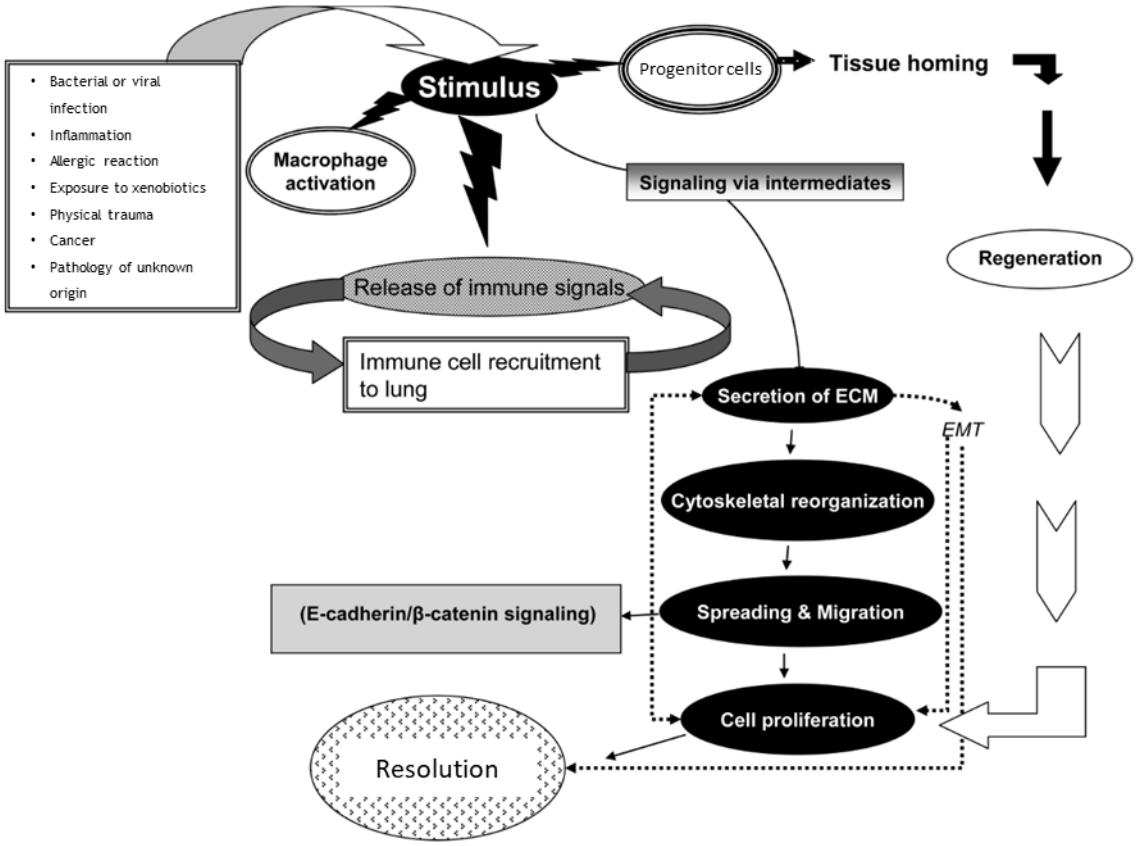

Figure 1.2. The process of normal wound healing in the lung. A flow diagram describing the sequence of events following injury to the lung epithelium; cell-cell signalling via cytokines, growth factors and matrikines; immune cell recruitment; and regeneration via epithelial-to-mesenchymal transition (EMT), extracellular matrix (ECM) secretion and cell proliferation (Adapted from Crosby & Waters, 2010).

This repair process involves a plethora of cell types, including airway Clara cells or alveolar type II epithelial progenitor cells, fibroblasts, endothelial cells, and immune cells (Mason & Williams, 1977; Zahm et al., 1991; Zahm et al., 1992; Zahm et al., 1997; Puchelle et al., 2006; Stripp et al., 2008; Crosby & Waters, 2010). The underlying ECM is also involved in this process to ensure the airways are structurally supported, vascularised, free from infection, and undergoing repair appropriately (Crosby & Waters, 2010).

1.1.3 Aging, inflamm-aging and senescence

The aging human lung is associated with a progressive decline in lung structure and function associated with genetic and epigenetic alterations; stem cell exhaustion; loss of protein homeostasis; senescence; inflamm-aging and dysfunction of the mitochondria, nutrient sensing apparatus and ECM (Mahler et al., 1986; Panda et al., 2009; Lowery et al., 2013; Meiners et al., 2015; Meyer, 2018). Inflamm-aging describes the chronic activation of the innate and adaptive immune response in the absence of injury or immunologic threat (Verbeken et al., 1992; Lowery et al., 2013; Brandsma et al., 2017; Meyer, 2018). The term senescence describes the accumulation of dysfunctional, non-replicative cells (including immune cells) that are suspended in a state of cell cycle arrest but remain metabolically active and secrete a senescence-associated secretory phenotype (SASP) consisting of cytokines, growth factors and proteases (Kortlever et al., 2006; Panda et al., 2009; Lowery et al., 2013; Baker et al., 2016).

Both inflamm-aging and the SASP of senescent lung cells are characterised by elevated proinflammatory cytokines, including interleukin (IL)-1β, IL-6, tumour necrosis factor-α (TNF-α); growth factors, such as transforming growth factor-β (TGF-β); and ECM-degrading matrix metalloproteinases (MMPs), such as MMP9 and MMP12, that act in a vicious cycle to further increase immune system activation and accelerate cellular senescence (Kovacs et al., 2002; Ershler & Keller, 2000; Debacq-Chainiaux et al., 2005; Gomez et al., 2006; Liu & Hornsby, 2007; Panda et al., 2009; Gomez et al., 2009; Carlson et al., 2009; Senturk et al., 2010; Minagawa et al., 2011; Sueblinvong et al., 2012; Lowery et al., 2013; Baker et al., 2016; Papageorgis, 2017; Zhang et al., 2017; Vitenberga & Pilmane, 2018; Hudgins et al., 2018).

1.1.3.1 TGF-β regulates cell cycle arrest and SASP

TGF-β is a key regulator of the cell cycle that, under normal conditions, communicates pro-senescent signals to reduce fibroblast activation and limit the progression of fibrosis as the site of lung injury resolves (Krizhanovsky et al., 2008; Jun & Lau, 2010; Meyer et al., 2016; Parimon et al., 2021). However, aging dysregulates this process promoting non-resolving senescence. Although this

mechanism is not fully understood, inhibiting senescence in models of lung fibrosis has been shown to ameliorate lung remodelling (Hecker et al., 2014; Schafer et al., 2017; Hohmann et al., 2019; Parimon et al., 2021).

1.1.3.2 Hallmarks of age-related remodelling

The primary hallmarks of age-related lung remodelling include reduced airway epithelial and mucus-producing cells; impaired mucociliary clearance; increased senescent fibroblasts; reduced ECM elastin and lamin content; and a fibrotic, collagen-rich ECM (D'Errico et al., 1989; Fulop et al., 2001; Quirk et al., 2016; Godin et al., 2016). Furthermore, in the lung parenchyma alveolar epithelial cells become senescent and apoptotic causing alveolar spaces to increase and lose elasticity without alveolar wall destruction, this is termed senile emphysema (Cho & Stout-Delgado, 2020). Aging also has severe implications for susceptibility, poor disease prognosis and mortality in chronic lung diseases, such as asthma, chronic obstructive pulmonary disease (COPD) and idiopathic pulmonary fibrosis (IPF) (Busse et al., 2017).

1.2 Lung pathophysiology and remodelling

Pathophysiological lung remodelling can manifest in several different ways. Asthma, COPD and IPF are primary examples of diseases where region-dependent lung remodelling is a key characteristic that leads to breathing difficulties, reduced quality of patient life and mortality without option for effective treatment using current therapeutics. While these diseases are distinct in terms of aetiology, they share key mechanistic characteristics of lung remodelling.

1.2.1 Asthma

Asthma is a chronic inflammatory lung disease characterised by reversible wheezing asthma attacks, inflammation and airway remodelling (**Figure 1.3**) often induced by inhalation of otherwise innocuous substances. Asthma is expected to exceed 400 million sufferers worldwide by 2025 (Payne et al., 2003; Rajanandh, 2015). It is estimated that 3-10% of these patients experience severe disease and globally there are approximately 250,000 to 450,000 asthma-related deaths annually (Chung et al.,

2014; Maslan & Mims, 2014; Hekking et al., 2015; Soriano et al., 2017; Vos et al., 2020).

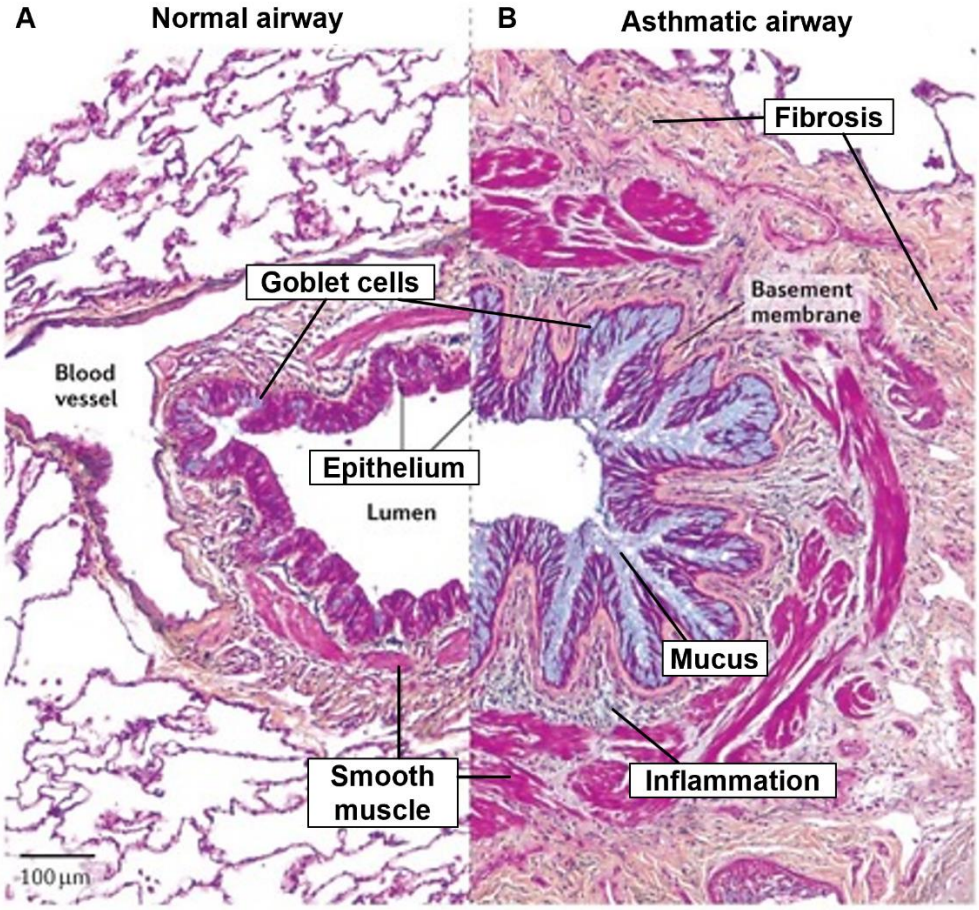

Figure 1.3. Comparison of normal human (left) and severe asthmatic patient (right) airway. The asthmatic airway is narrowed by epithelial changes, smooth muscle hypertrophy and inflammation. It is also obstructed by the mucus produced by an increased number of goblet cells (blue staining). The surrounding functional architecture is destroyed by fibrosis (subject age, gender and post-mortem unknown; Movat's stain; adapted from Wadsworth et al., 2011). Graticule = 100 µm.

1.2.1.1 Pathogenesis

Asthma is recognised as a syndrome of variable disease endotypes where the primary subtypes are IgE/Th2 (allergic) asthma and alarmin-driven (non-allergic) asthma. IgE/Th2 asthma is thought to be triggered by allergens and release of cytokines, such as thymic stromal lymphopoietin (TSLP), IL-25 and IL-33 at the airway epithelium. This activates type 2 innate lymphoid (ILC2) cells and subsequently the adaptive immune response. This immune response is characterised by Th2 cell and

eosinophil activation; IgE production by B cells; histamine release by activated mast cells; and production of Th2-associated cytokines such as IL-4, IL-13 and TGF-ß from a range of cell types (Lambrecht & Hammad, 2015; Israel & Reddel, 2017).

Alarmin-driven asthma is triggered by injury to the airway epithelium which releases alarmins (also known as damage-associated molecular patterns), such as IL-33, to activate both the adaptive and innate immune response as well as the NLRP3 inflammasome (Simpson et al., 2014). The innate immune response is characterised by activation of Th17 cells, neutrophils and bronchial epithelial cells and the release of cytokines such as IL-1ß, IL-6, IL-17, TNFα and TGF-ß from a range of cell types (Burgess et al., 2004; Doherty & Broide, 2007; Halwani et al., 2010; Israel & Reddel, 2017; Boonpiyathad et al., 2019).

1.2.1.2 Asthmatic airway remodelling

Although the endotypes of asthma are discrete, both IgE/Th2 and alarmin-driven asthma exhibit the same manifestations of remodelling (Pillai et al., 2011; Polosa & Thomson, 2013). As shown in **Figure 1.3**, loss of epithelial barrier integrity; epithelial metaplasia; mucociliary dysfunction; goblet cell metaplasia; mucus hypersecretion; smooth muscle thickening; subepithelial and peribronchial fibrosis; and angiogenesis are the hallmarks changes in asthma which narrow, obstruct, constrict and stiffen the larger and smaller airways (Jeffery et al., 1989; Roche et al., 1989; Brewster et al., 1990; Aikawa et al., 1992; Carroll et al., 1993; Li et al., 1997; Ordoñez et al., 2001; Johnson et al., 2001; Jenkins et al., 2003; Bergeron et al., 2010).

1.2.1.3 Treatment of asthma

Treatment consists of a combination therapy using an inhaled corticosteroid for immunosuppression and an additional short-acting or long-acting $ß_2$-agonist bronchodilator to relax smooth muscle during an asthma attack (Fitzgerald et al., 2017; GINA guidelines, 2018). However, antigen-specific biologics are also now approved for asthma treatment and are used to target specific antigens, including type 2 cytokines (e.g. interleukin-4, -5 and -13) or immunoglobulins (e.g. IgE) (Santamaria et al., 2021; Reddel et al., 2021; Busse & Kraft, 2022). Although current

treatments show some benefits against remodelling, particularly in combination (Roth et al., 2002), they do not prevent asthma nor target the root cause of disease, which remains incompletely understood (Lambrecht & Hammad, 2015; Israel & Reddel, 2017).

1.2.1.4 Models of asthma pathophysiology

Several models are predominantly used to recapitulate the endotypes and phenotypes of human asthma in mice. Ovalbumin (OVA), a poultry-derived phosphoglycoprotein, is commonly used as an allergen to induce variations of IgE/Th2 asthma using OVA sensitisation, to ensure an IgE response, and short-term and chronic OVA challenge to produce a range of eosinophil-dominated inflammatory profiles. Using this approach, OVA exposure induces epithelial hypertrophy, goblet cell hyperplasia, hyperresponsive and hypertrophied smooth muscle and subepithelial/peribronchial fibrosis in mouse airways as well as increased cytokine production, including IL-4, IL-13 and IL-33 (Ellis et al., 2003; Hayakawa et al., 2007; Kumar et al., 2008; Kurowska-Stolarska et al., 2008; Hamzaoui et al., 2013; Tang et al., 2014).

Inhaled IL-33 challenge has also been used to induce characteristics of alarmin-driven asthma without an increase in systemic allergic response, including immune cell infiltration; increased Il-4, IL-6, IL-13 and TGF-ß expression; goblet cell hyperplasia; airway smooth muscle hypertrophy; subepithelial and peribronchial collagen deposition; and angiogenesis (Li et al., 2015). Although shorter exposures increase lung immune cells, including neutrophils, and goblet cell remodelling by day 24, smooth muscle and vascular remodelling is only observed by day 36 and ECM remodelling characteristics are visible by day 48 (Li et al., 2015).

1.2.2 Chronic obstructive pulmonary disease

COPD is also considered a chronic inflammatory lung disease characterised by alarmin-driven inflammation, bronchoconstriction, airway remodelling and emphysema. COPD is currently the third leading cause of death worldwide with approximately 3.1-3.2 million annual deaths largely due to lack of effective treatment (Soriano et al., 2017; World Health Organisation, 2020). Although this

disease is strongly associated with cigarette smoking there are several other known causes, such as air pollution and indoor cooking in the non-western world (Brandsma et al., 2017).

1.2.2.1 Pathogenesis

Repeated damage to the airway epithelium by pollutants, such as cigarette smoke, drives COPD by alarmin-driven activation of the innate immune response and NLRP3 inflammasome (Willemse et al., 2005a; Saetta et al., 2006; Hogg & Timens, 2009). This recruits immune cells, including eosinophils, neutrophils, cytotoxic $CD8^+$ T cells, and alveolar macrophages, and upregulates inflammatory cytokines, such as IL-6, IL-8, chemokine C-X-C motif ligand (CXCL) 1, TNFα and TGF-ß (Pizzichini et al., 1998; Kim et al., 2008; Morty et al., 2009; Tashkin & Wechsler, 2018; Hikichi et al., 2019).

1.2.2.2 Remodelling in COPD

The immune response in COPD is thought to be central in driving airway remodelling, including loss of barrier integrity; epithelial metaplasia; mucociliary dysfunction; goblet cell metaplasia; mucus hypersecretion; smooth muscle thickening; peribronchial ECM remodelling; and arteriole thickening (Hogg et al., 1968; Vlahovic et al., 1999; Hogg et al., 2004; Postma & Timens, 2006; Kranenburg et al., 2006; Annoni et al., 2012; Lugade et al., 2014; Tjin et al., 2014; Gohy et al., 2015; Jones et al., 2016; Brandsma et al., 2017; Rose et al., 2018;).

Emphysema is unique to COPD and characterised by a net destruction of alveolar walls reducing scope for gaseous exchange. This is thought to be caused by dysfunction of senescence, apoptosis, autophagy and repair mechanisms leading to increased oxidative stress, proteinase imbalance and an altered ECM where primarily elastin content is reduced (Young & Narita, 2010; Wright et al., 2011; Hikichi et al., 2019). **Figure 1.4** shows a comparison of airways from a case of fatal asthma and severe COPD to highlight that, despite important clinical differences, severe asthma and COPD share several remodelling characteristics including smooth muscle and ECM remodelling (Maselli & Hanania, 2018). The similarity of remodelling characteristics exhibited by these two aetiologically different diseases suggests the mechanisms by which they occur may overlap.

Table 1.1. Comparison of airway remodelling characteristics in asthma and COPD. Asthmatic airways share some key pathophysiological features with chronic obstructive pulmonary disease (COPD) airways, including airway smooth muscle thickening and fibrosis; however, basement membrane thickening and emphysematous alveolar disruption are not shared by these diseases. (Adapted from Barnes, 2011).

Feature	Asthma	COPD
Epithelium	Often shed	Pseudostratification
Goblet cells	Increased	Increased
Basement membrane	Increased	Normal
Airway smooth muscle	Increased	Minimal increase
Airway vessels	Increased	Not increased
Fibrosis	Increased, subepithelial & peribronchial	Increased, predominantly peribronchial
Alveolar disruption	Not increased	Increased

1.2.2.3 Treatment of COPD

Treatment usually involves long-acting β2-adrenoceptor agonists (LABAs) or muscarinic antagonists (LAMAs) to control bronchoconstriction as well as corticosteroids to control inflammation. However, due to the association of inhaled corticosteroid (ICS) treatment with an increased risk of pneumonia the 2020 GOLD guidelines contra-indicates glucocorticosteroid use alone in favour of triple inhaled therapies (combination of ICS/LAMA/LABA) (Liapikou et al., 2015; Halpin et al., 2020). Phosphodiesterase 4 (PDE4) inhibitors, mucolytic agents and xanthines are also available as emerging treatment options (Page & Cazzola, 2016). Episodes of worsening COPD symptoms, called exacerbations, are treated with a combination of bronchodilators, systemic corticosteroids and antibiotics (Halpin et al., 2020). Although these treatments provide much needed symptom relief, these treatments do not target the root cause of disease or reverse the progressive remodelling observed in COPD.

1.2.2.4 Models of COPD pathophysiology

There are three main models of COPD, including cigarette smoke, elastase, and lipopolysaccharide (LPS) exposures using mice, guinea pigs and rats (Ghorani et al.,

2017). A major limiting factor in the investigation of COPD is the lack of small-animal models that can accurately reproduce the characteristics of COPD pathophysiology in a specific timeframe (Beckett et al., 2013). Due to the strong association of cigarette smoke in the pathogenesis of COPD, many consider it to be the ideal choice for inducing COPD-like characteristics in animal models of disease; however, the characteristics induced by cigarette smoke are reversible and return to normal following exposure cessation unlike human disease. These models are also costly and labour intensive.

Alternatively, LPS is a major component of the outer cell wall of gram-negative bacteria and a key contaminant in cigarette smoke, air pollution and organic dusts (Hasday et al., 1999; Rylander, 2006; Pera, 2011; Pera et al., 2011; Ghorani et al., 2017). LPS exposure has been shown to induce immune cell recruitment, including eosinophils, macrophages, neutrophils, CD8 and CD4 T cells; increased cytokine production, including IL-1β, IL-6, IL-8 and TNF-α; and persistent remodelling characteristics, including epithelial thickening, goblet cell hyperplasia, increased airway smooth muscle mass (mice only), peribronchial ECM remodelling, and emphysema that closely resembles COPD (Ulich et al., 1991; Vernooy et al., 2001; Vernooy et al., 2002; Toward & Broadley, 2002; Savov et al., 2002; Brass et al., 2003; Savov et al., 2003; Brass et al., 2004; Savov et al., 2005; Brass et al., 2007a; Brass et al., 2007b; Puljic et al., 2007; Pera, 2011).

Furthermore, Toward & Broadley (2001) observed histological evidence of oedema, epithelial disruption, leukocyte infiltration, and goblet cell metaplasia but no evidence of irreversible emphysematous lung tissue destruction that had been previously observed in a similar protocol using chronic intratracheal LPS installations in hamsters (Stolk et al., 1992).

1.2.3 Idiopathic pulmonary fibrosis (IPF)

IPF is an interstitial lung disease characterised by its unknown aetiology and rapid fibrotic destruction of the lung parenchyma following diagnosis. Due to the extended period of time taken for this disease to present, the mean age of patients with this disease is 65-70 years and, due to the rapid progression of fibrotic remodelling,

patients live a median survival of 2-3 years from diagnosis if left untreated (Sharif, 2017). The primary hallmarks of IPF are epithelial cell metaplasia; goblet cell hyperplasia; increased fibroblast proliferation; hypertrophy and hyperplasia of alveolar epithelial cells; interstitial fibrosis and endothelial cell apoptosis (Katzenstein et al., 2008; Hansell et al., 2008; Bingle 2011; Farkas et al., 2011; Knudsen et al., 2017).

IPF is not considered to be an inflammatory lung disease; however, inflammatory cationic proteins and growth factors play a central role in IPF pathogenesis, including eosinophilic cationic protein (ECP) and TGF-β (Bringardner et al., 2008). Furthermore, accelerated aging is highly implicated in the pathogenesis of IPF and failure of the alveolar epithelium, including processes such as mitochondrial dysfunction; shortened telomeres; mutations to telomerase or surfactant proteins; and less efficient or reliable protein folding in the endoplasmic reticulum (ER), (Armanios et al., 2007; Alder et al., 2008; Naidoo, 2009; Waters et al., 2017; Schuliga et al., 2021). Furthermore, enzymes such as lysyl oxidases are thought to contribute to collagen cross-linking which results in a stiffened ECM and subsequently a pro-fibrotic microenvironment (Wipff et al., 2007; Shi et al., 2011; Tjin et al., 2016; Burgess et al., 2016; Tjin et al., 2017).

1.2.3.1 Models of IPF pathophysiology

The predominant model used to recapitulate characteristics of IPF is bleomycin-induced lung fibrosis in aged male mice. Intratracheal administration of bleomycin induces epithelial cell death, inflammatory infiltration and subsequently fibroblast activation, increased extracellular matrix deposition, and fibrosis, in 2-3 weeks and closely resembles the acute phase of IPF in humans (Peng et al., 2013; Tashiro et al., 2017). *In vitro* models have also been developed to replicate key features of IPF disease, such as myofibroblast differentiation (Balestrini et al., 2012; Mondrinos & Huh, 2015; Surolia et al., 2017), TGFβ signalling (Booth et al., 2012; Mondrinos & Huh, 2015; Surolia et al., 2017) and epithelial-fibroblast crosstalk to investigate anti-fibrotic treatments either isolating specific cell types (e.g. fibroblasts) or reproducing cross-talk between specific cells or tissues (Waghray et al., 2005; Prasad et al., 2014; Epa et al., 2015). Plastic and glass substrates as well as hydrogels are

the potential platforms on which single cell type responses are investigated. These models can utilise treatment with recombinant TGF-β1, bleomycin or TGF-β signalling agonists to induce an IPF-like phenotype for the determination of proliferation, viability, and cytokine production markers (Promchainant, 1975; Breen et al., 1992; Hamilton Jr et al., 1995; Gon et al., 2000; Surolia et al., 2017). However, it is important to acknowledge the differences between the effects of 2D and 3D cultures on cell behaviour (Matera et al., 2020) and more importantly the differences in gene and protein expression of immortalised cell lines compared to primary human cells (Burgess et al., 2018).

1.3 TGF-β in remodelling

It is well known that cytokines and growth factors play a central role in mediating lung remodelling of which TGF-β is a principle example. TGF-β is known to be a potent regulator of growth and apoptosis under physiological conditions (Hu et al., 2018) and plays a central role in both normal and aberrant lung remodelling (Liotta et al., 1986; Coker et al., 1997; Gharaee-Kermani et al., 2009; Halwani et al., 2011; Fernandez & Eikelberg 2012;). Although the effects of TGF-β are cell type-specific and developmental stage-dependent, the signalling pathways remain consistent (Tzavlaki & Moustakas, 2020). TGF-β is one of the most potent inducers of ECM production and its expression is elevated in fibrotic human lungs where it precedes collagen synthesis and deposition in animal models of lung fibrosis (Hoyt & Lazo, 1988; Phan & Kunkel, 1992; Eunhee et al., 1996; Yue et al., 2010). TGF-β can be used to induce fibrosis in animals (Sime et al., 1997; Warshamana et al., 2002; Lee et al., 2004) and inhibition of TGF-β signalling can attenuate TGF-β or bleomycin induced fibrosis (Zhao et al., 2002; Bonniaud et al., 2004).

1.3.1 TGF-β signalling

Active TGF-β1 is the most potent mammalian TGF-β isoform, herein referred to as TGF-β, and elicits its effects by activation of TGF-β receptor (TGF-βR) heterooligomers (Coker et al., 1997; Liu et al., 2021). As shown in Figure 1.4, activation of a TGF-βR heterooligomer complex formed of a TGF-βRI and TGF-βRII is typically associated with activation of the canonical Smad 2/3 signalling pathway or the non-canonical signalling cascade that includes the MAPK cascades, JNK, ERK and p38; PI3K/Akt; mechanistic target of rapamycin (mTOR); and Ras homolog (Rho);

and Wnt signalling, including the β-catenin, phospholipase C (PLC)/inositol triphosphate (IP_3)/calcium (Ca^{2+}) and planar cell polarity pathways (Underwood et al., 2000; Madala et al., 2012; van der Velden et al., 2016; Knipe et al., 2018; Finnson et al., 2020). This plethora of signalling cascades allows TGF-β to mediate a diverse range of cellular remodelling processes, such as cell adhesion, secretion, growth, proliferation, differentiation, migration, apoptosis and ECM remodelling (McCartney-Francis et al., 1998; Leask & Abraham, 2004; Shi-wen et al., 2007; Gharaee-Kermani et al., 2009;). Furthermore, bidirectional TGF-βR-receptor tyrosine kinase (RTK) and TGF-βR-GPCR transactivation has also been demonstrated which further increase the repertoire of cellular responses that can be activated by TGF-β (Uchiyama-Tanaka et al., 2002).

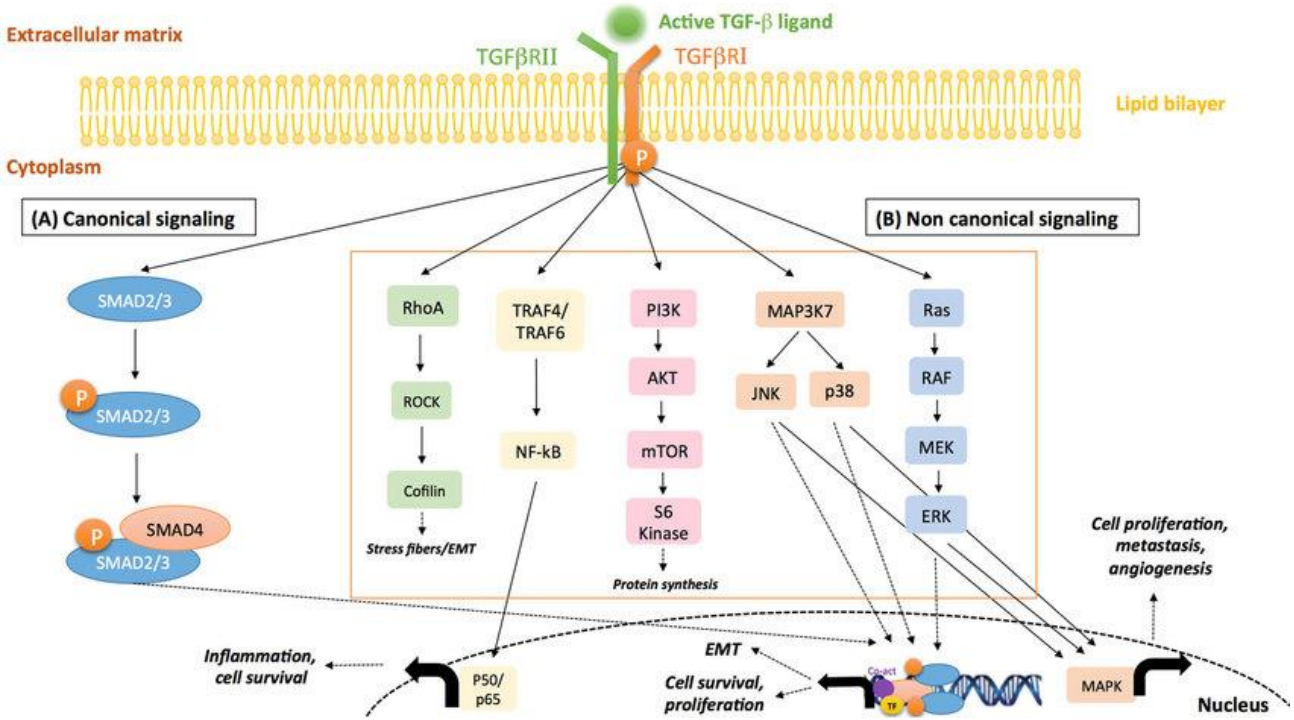

Figure 1.4. Canonical and non-canonical TGF-ß signalling in remodelling. Active TGFß ligands activate (A) Canonical Smad-dependent TGFß signalling or (B) non-canonical Smad-independent signalling via interaction with a TGF-ß receptor (TGFß-R) heterooligomer complex formed of a TGF-BRI and TGF-ßRII. Non-canonical TGF-ß signalling is associated with the susequent activation of a plethora of downstream signalling pathways with known roles in cellular remodelling, such as MAPK cascades, JNK, ERK and p38; PI3K/Akt; mechanistic target of rapamycin (mTOR); and Ras homolog (Rho); and indirectly Wnt signalling (not shown), which includes the ß-catenin, phospholipase C (PLC)/inositol triphosphate (IP_3)/calcium (Ca^{2+}) and planar cell polarity pathways (figure from Costanza et al. (2017)).

TGF-β signalling is positively regulated by accessory proteins, such as betaglycan (TGF-βRIII) and endoglin, that enhance TGF-β complex binding affinity (Blobe et al., 2001; Derynck & Zhang, 2003). However, in some types of cancer, TGF-βRIII has been shown to inhibit TGF-β signalling (Elderbloom et al., 2014). Smad2/3 signalling is also negatively regulated by inhibitory Smads, including Smad7 and Smad6, that inhibit their activation by the TGF-βR and inhibit formation of the Smad2/3/4 complex, respectively (Zhao et al., 2000). TGF-β signalling is also regulated at the transcriptional level where transcription factor complexes, such as AP1, that interact with Smads in the regulation of c-jun and MMP1 expression (Zhang et al., 1998; Wong et al., 1999; Massagué et al., 2005).

1.3.1.1 Canonical Smad2/3 signalling

TGF-β activates Smad2/3 by interacting with a TGF-βR complex containing TGFBRI and TGF-βRII, typically within 1 hour of TGF-β exposure (Baugé et al., 2011). Accessory proteins, such as TGF-βRIII (betaglycan) and endoglin, typically promote TGF-β binding affinity (Renzoni et al., 2004; Bauge et al., 2011; Elderbloom et al., 2014). Smad2/3 then forms a complex with Smad4 chaperoned by the TGF-βR associated protein 1 (TGF-βRAP1), a process negatively regulated by Smad6. The Smad2/3/4 complex then translocates to the nucleus to influence gene transcription. The Smad2/3/4 complex also targets Smad7 that competitively binds the TGF-βR and negatively regulates Smad2/3 activation.

1.3.1.2 Non-canonical Ras signal transduction activation

TGF-β also influences cell behaviour via a plethora of non-Smad signalling cascades such as the MAPK (ERK, JNK, p38), PI3K/Akt, mTOR, and Rho signalling pathways. To do this, the activated TGF-βR recruits molecules such as the growth factor receptor binding protein 2 (Grb2)/Sos complex by binding the substrate Src homology 2 domain-containing protein (Shc) to bring Son of sevenless (Sos) to the plasma membrane. Sos then catalyses the activation of the multifunctional Ras protein by exchanging Ras-bound GDP for GTP (Zhang et al., 2009).

1.3.1.3 Non-canonical MAPK (ERK, JNK, p38) signalling

Activation of Ras recruits Raf and the intermediate activator of ERK1/2 signalling, MEK1/2. ERK1/2 then influences cell adhesion, proliferation and differentiation as well as gene transcription by interaction with transcription factors, such as ELK1 that plays a central role in calcium metabolism and growth signalling; MSK1 (RPS6KA5) that is involved in the epidermal growth factor receptor (EGFR) pathway; and inflammation *via* NFκB (Janknecht et al., 1993; Deak et al., 1998; Davies et al., 2005; Kim et al., 2007a; Vicent et al., 2009; Thiel et al., 2012; Carpenter & Wu, 2014; Šmerdová et al., 2014). ERK is also thought to be central in the interaction with AP-1 transcription factor complex (comprised of FOS, FOSB, FOSL1, FOSL2 and JUN) to upregulate actin cytoskeletal components such as αSMA (Hu et al., 2006).

TGF-β, as well as OVA and IL-33, can also activate MAPK JNK via Ras/Rac1 and either MEKK1/JNK or activation of the JNK-interacting protein (JIP) scaffold kinases, including MLK3, MKK4/7 and finally JNK. JNK then translocates to the nucleus to influence gene transcription via a range of transcription factors, such as JUN, to regulate key cellular processes such as differentiation, proliferation, apoptosis, survival and gene expression such as the remodelling mediator connective tissue growth factor (CTGF) (Spencer, 2007; Kumar et al., 2015; Zhang et al., 2019). CTGF alone has been implicated in the regulation of remodelling processes such as cell adhesion, migration, cell activation and ECM remodelling (Wang et al., 2022). Pharmacological inhibition of JNK signalling has been shown to ameliorate airway remodelling *in vivo* using pre-clinical models of asthma in mice and *in vitro* using human lung fibroblasts (Zhang et al., 2019).

TGF-β also activates p38 MAPK via TAK1 and MKK3 that has been shown to regulate remodelling processes such as proliferation, migration, differentiation, and actin cytoskeleton remodelling (Kim et al., 2007b; Liu et al., 2009a; Chen et al., 2015). In human prostate cancer cells, Smad7 has also been shown to act as an adaptor protein to facilitate non-canonical TGF-β signalling, including p38 and JNK signalling (Edlund et al., 2003; Heldin et al., 2009; Landström, 2010). The importance of these signalling cascades is highlighted by the investigation of MAPK inhibitors for the treatment of asthma and COPD. Although p38 or JNK inhibitors have not shown

efficacy or adequate safety in clinical trials, less toxic mitogen-activated protein kinase activated protein kinase-2 (MAPKAPK-2) inhibitors may overcome these issues (Singh & Najmi, 2019; Defnet et al., 2020).

1.3.1.4 Non-canonical PI3K/Akt signalling

The TGF-βR is also thought to activate lung remodelling via class I PI3K/Akt signalling directly or via Ras (Le Cras et al., 2010; Conte et al., 2011; Mercer et al., 2016). PI3K/Akt signalling has been implicated in cellular remodelling processes, such as apoptosis, senescence, differentiation (e.g. EMT), and ECM remodelling (Wang et al., 2022). PI3K/Akt inhibitors have also shown efficacy in pre-clinical models of bleomycin-induced lung fibrosis (Hsu et al., 2017). Recently, inhaled PI3K inhibitors have shown promising results, including pre-clinical efficacy of the pan-PI3K prodrug CL27c for the treatment of asthma and fibrosis (Campa et al., 2018) and the PI3K inhibitor GSK2269557, also known as nemiralisib, that completed phase IIb clinical trials for the treatment of COPD (Cahn et al., 2017; Wilson et al., 2019). However, no improvement in lung function was observed following treatment with nemiralisib in patients with moderate or severe acute exacerbations of COPD in phase IIb studies (Fahy et al., 2021).

1.3.1.5 Non-canonical mTOR signalling

PI3K/Akt signalling is a key regulator of the two mTOR signalling complexes, mTORC1 and mTORC2. Akt activates mTORC1 by inhibiting the tuberous sclerosis complex 1 and 2 (TSC1/2) GTPase that converts mTORC1-activating $Rheb^{GTP}$ into non-activating $Rheb^{GDP}$. In other words, inhibition of TSC1/2 by Akt results in accumulation of $Rheb^{GTP}$ and activation of mTORC1. Furthermore, Akt or Ras is thought to directly activate complex 2 (mTORC2). Both mTORC1 and 2 are comprised of the catalytic component mTOR, disheveled/Egl-10/pleckstrin (DEP) domain containing mTOR interacting protein (Deptor), and the GTPase ß-subunit like protein gßL, mLST8; however, the scaffolding protein regulatory-associated protein of TOR (Raptor), proline-rich AKT substrate of 40 kDa (PRAS40) are specific to the mTORC1 complex whereas mammalian stress-activated protein kinase (SAPK)-interacting protein (mSIN1), rapamycin-insensitive companion of TOR (Rictor) and proline-rich protein 5 (Protor) are specific to mTORC2 (Roux & Topisirovic, 2012). mTORC1 has been

shown to play a central role in amino acid synthesis pathways, such as 4E-binding protein 1 (4E-BP1); regulation of autophagy via ULK1; and senescence via p70-S6K (Platé et al., 2020). On the other hand, mTORC2 is central to gene targets that regulate senescence via secreted protein acidic and rich in cysteine (SPARC) and cytoskeletal rearrangement via protein kinase C (PKC) (Chang et al., 2014; Platé et al., 2020).

1.3.1.6 Non-canonical Rho signalling

Ras-homologous (Rho) signalling regulates Rho kinases (RhoK), including Rho associated coiled-coil containing protein kinase (ROCK) I and II isoforms, are typically activated by Ras or Rac1 and finally the monomeric G-protein, RhoA. Rho signalling is also regulated by three main groups of proteins, including guanine nucleotide exchange factors (GEFs), GTPase-activating proteins (GAPs) and guanine nucleotide dissociation inhibitors (GDIs) in response to cytokines, growth factors, ECM proteins and GPCR activation (Kjøller & Hall, 1999; Schaafsma et al., 2008).

Rho is known to regulate fundamental cellular functions such as contractile force, adhesion and migration as well as differentiation in smooth muscle cells, fibroblasts, epithelial cells, endothelial cells and immune cells (Goffin et al., 2006; Wipff et al., 2007; Olsen, 2008; Liu et al., 2010a; Hallgren et al., 2012). Genetic or pharmacological inhibition of Rho signalling has been shown to prevent bleomycin-induced lung fibrosis and remodelling (Knipe et al., 2018). Additionally, Rho signalling is central to apoptosis in alveolar epithelial cells as well as endothelial barrier function (Knipe et al., 2018). Although Rho inhibitors show potential in pre-clinical models of lung disease, they are only being evaluated clinically for ocular diseases (Tanna & Johnson, 2018).

1.3.1.7 Wnt signalling

Wnt signalling consists of three distinct pathways, canonical Wnt/β-catenin signalling, non-canonical Wnt/Ca^{2+} signalling and the planar cell polarity pathway. TGF-β can also upregulate Wnt ligands, such as WNT5A and WNT5B, to activate Wnt signalling in an autocrine or paracrine manner via the extracellular Frizzled (FZD) receptor (Działo et al., 2018). In canonical Wnt/β-catenin signalling, this interaction

activates the canonical Wnt/ß-catenin signalling pathway by recruiting Dishevelled (DVL) proteins to the low-density lipoprotein receptor-related proteins 5 and 6 (LRP5/6) co-receptor. Activation of DVL proteins then inhibits the ß-catenin destruction complex, composed of adenomatous polyposis coli (APC), axin, casein kinase-1 (CK-1) and the primary kinase glycogen synthase kinase-3 (GSK-3), to promote accumulation of ß-catenin that directly influences gene expression by interacting with T cell factor (TCF) and lymphoid enhancer factor (LEF) transcription factors (Baarsma & Königshoff, 2017).

RTK and GPCR activation is known to activate Ca^{2+} signalling, directly or via non-canonical Wnt signalling. Binding of Wnt ligands to the FZD receptor and subsequent activation of $G_{q/11}$ subsequently activates the phospholipase C (PLC) and phosphatidylinositol 4,5-bisphosphate (PIP2). PIP2 then activates PKC via diacylglycerol (DAG) or calcineurin (CaN) and calmodulin (CaMKKß) via inositol 1,4,5-trisphosphate (IP_3) pathway and activation of the IP_3 receptor (IP_3R), and finally augmentation of intracellular free ionised Ca^{2+} (Ca^{2+}_i) by Ca^{2+} release from the sarcoplasmic reticulum and store-operated Ca^{2+} channels (SOCC). This process also inhibits ß-catenin signalling (Liu et al., 1999; Nusse, 2012; Baarsma & Königshoff, 2017).

Ca^{2+}_i augmentation itself is an important signalling mechanism that has been implicated in loss of epithelial barrier integrity, epithelial cell adhesion, goblet cell mucus secretion via $G_{q/11}$; airway smooth muscle cells contractility and cell migration (So et al., 1986; Denecker et al., 1997; Huang et al., 2005; Gerthoffer, 2007; Mahn et al., 2009; Mahn et al., 2010; Tu et al., 2011; Riccardi & Kemp, 2012; Yang et al., 2014a; Yang et al., 2014b; Abdulnour-Nakhoul et al., 2015; Yarova et al., 2015; Oppenheimer & Kelly, 2017; Cazzola et al., 2019). Intracellular calcium may also play a role in airway smooth muscle (ASM) remodelling via mitochondrial biogenesis (Trian et al., 2007). Inhibition of extracellular Ca^{2+} influx, using calcium channel blockers, has been shown to reduce the pro-fibrotic response in normal human lung fibroblasts and bleomycin-induced lung fibrosis (Mukherjee et al., 2015), highlighting the importance of intracellular Ca^{2+} in lung fibrogenesis; however, the

efficacy of these therapeutics has been limited (Barnes, 1985; Oppenheimer & Kelly, 2017).

Finally, the Wnt planar cell polarity pathway is associated with regulation of migration, cytoskeletal changes and is activated by Wnt ligands, G_o and $G_{12/13}$ activation, and subsequently JNK and Rho signalling, respectively (Kühl et al., 2000; Pandur et al., 2002; Bikkavilli et al., 2008; Arthofer et al., 2016; Schulte & Wright, 2018).

1.3.2 TGF-ß-mediated remodelling

TGF-ß, by the signalling pathways described above, then mediates lung remodelling by several cellular processes, including cell adhesion, apoptosis, secretion, exocytosis, mitochondrial function, growth, autophagy, proliferation, differentiation, amino acid synthesis, senescence and ECM remodelling. Some of these processes and examples of the remodelling they contribute to are described in more detail below.

1.3.2.1 Apoptosis

Apoptosis is a key process in lung repair as it allows the control of programmed cell death in the resolution of inflammation and fibrosis (Dos Santos, 2008). However, loss of airway epithelial barrier integrity can be caused by mitochondrial dysfunction and apoptosis. Exposure to OVA, IL-13, and TGF-ß has been shown to increase Ca^{2+}_i via the PLC/IP_3 pathway (Sebag et al., 2018; Ray et al., 2020). Due to the negative potential of the mitochondrial matrix (-180mV), mitochondria absorb this intracellular calcium, aided by the chaperon protein glucose regulated protein 75 (Grp75), which is regulated by mitochondrial calcium uptake (MICU), to aid ATP production. However, if Ca^{2+} uptake exceeds a threshold the mitochondrial permeability transition pore (mPTP), containing translocator protein (TSPO) and cyclophilin-D (PPID), and voltage dependent anion channel (VDAC)1/2 open and overload the mitochondria with Ca^{2+}. This accelerates ROS production and causes mitochondrial swelling that ultimately results in cytochrome c-induced apoptosis (Baines et al., 2005; Šileikytė et al., 2011; Sebag et al., 2018; Ray et al., 2020).

1.3.2.2 Secretion

Secretion via exocytosis is a key mechanism in a cells ability to influence its extracellular microenvironment by exporting substances such as inflammatory cytokines, pro-collagens and mucus (Kagan, 2000; Stow & Murray, 2013). Increased mucus secretion, often termed mucus hypersecretion, is another process that contributes to obstruction of the airways of chronic lung disease sufferers. Mucus secretion is actioned by a process called exocytosis which involves trafficking of secretory granules via PLC/DAG/PKC signalling where Ras-related protein (RAB)-27 (RAB27), melanophilin (MLPH), myristoylated alanine rich protein kinase c substrate (MARCKS) and RAB3 aid recruitment of secretory granules to the actin cytoskeleton and PLC/IP3/Ca^{2+} signalling mediates docking of the secretory granule with the plasma membrane aided by soluble N-ethylmaliemide sensitive factor attachment receptor proteins, such as vesicle associated membrane proteins (VAMPs), syntaxins (STXs) and accessory molecules, such as MUNC13 and MUNC18 (Li et al., 2001; Hammer III & Wu, 2002; Singer et al., 2004; Südhof, 2004; Hong, 2005; Ehre et al., 2005; Williams et al., 2006).

1.3.2.3 Growth

Cell growth is also a key contributor to epithelial and goblet cell metaplasia as well as smooth muscle hypertrophy, particularly in severe asthmatics (Benayoun et al., 2003; Innes et al., 2006; Weng et al., 2022). Cell growth occurs when the rate of cellular biosynthesis is greater than the rate of cellular degradation and is regulated independently of proliferation (Conlon & Raff, 1999; Grewal et al., 2003; Thompson, 2010). Furthermore, TGF-ß regulates cell growth, largely via the PI3K/Akt/mTOR pathway. Cell growth is characterised by increased total cell mass or diameter; ribosome biogenesis; increased mRNA translation via RNA polymerase and inhibition of cell degradation processes, such as autophagy (Schmelzle & Hall, 2000; Iadevaia et al., 2014; Platé et al., 2020).

To regulate mRNA translation, mTORC1 activates Maf1 and subsequently RNA polymerase III (POLR3) for the transcription of 5S ribosomal RNA (rRNA). mTORC1 also activates the multifunctional p70-S6 kinase 1 (S6K1) to upregulate RNA polymerase II (POLR2) activity and subsequently the ribosomal biogenesis

transcriptional programme, which includes genes such as Gar1 and Rrp9 (Chauvin et al., 2014). S6K1 also activates the RNA polymerase I (POLR1)/ upstream binding transcription factor (Ubf)/ transcription intermediary factor 1-alpha (TIF1A)/SL1 complex to upregulate transcription of 47S rRNA. Finally, alongside 4E-BP1, S6K1 upregulates cap-dependent translation. Although the primary substrate for S6K is RPS6, it is not the only function of S6K1 and the role of RPS6 in cell growth is unclear. Lastly, mTORC1 activation also activates pro-autophagy genes such as autophagy related 5 (ATG5) that supports autophagic vesicle forming as well as Unc-51 like autophagy activating kinase 1 (ULK1) which both activates or inhibits autophagy in a context-dependent manner (Laplante & Sabatini, 2012; Jhanwar-Uniyal et al., 2019; Platé et al., 2020).

1.3.2.4 Proliferation

Cell proliferation is another key cell process that contributes to lung remodelling in a range of cell types, including epithelial, goblet cell, smooth muscle (particularly in mild asthmatics), fibroblasts and vascular endothelial cells (central in angiogenesis) (Woodruff et al., 2004; Makinde et al., 2007). Proliferation is actioned by progression through the cell cycle, which is known to be regulated by non-canonical TGF-ß signalling, such as ERK MAPK, PI3K/Akt/mTOR and Rac1/RhoA signalling, Wnt signalling, increased Ca^{2+}_i, reduced cyclic adenosine monophosphate (cAMP) levels by adenyl cyclase inhibition and increased cAMP-quenching phosphodiesterase expression (Kim et al., 2018). LPS-containing cigarette smoke extract also promotes cell proliferation in airway smooth muscle cells via calcium signalling which involves calreticulin (CALR), orosomucoid-like 3 (ORMDL3) and increased Ca^{2+}_i (Wylam et al., 2015; Guan et al., 2017; Chen et al., 2018). Furthermore, members of the cyclin family, such as PCNA and cyclin E, and cyclin-dependent kinases (CDKs), such as CDK4, CDK5, and CDK7 are crucial for progression of a cell through the four phases of the cell cycle (Wylam et al., 2015; Qin et al., 2020). TGF-ß also promotes growth factor expression, such as fibroblast growth factor-2 (FGF-2), platelet-derived growth factor (PDGF), and CTGF via ERK MAPK signalling that positively regulate proliferation in an autocrine or paracrine fashion (Kay et al., 1998; Strutz et al., 2001; Bartram & Speer, 2004; Leask & Abraham, 2004; Leask, 2009; Fagone et al., 2011; Xiao et al., 2012; Kim et al., 2018).

Lastly, cell proliferation is also highly resource demanding and thus needs to be supported by processes such as nutrient and amino acid uptake, including glucose (via Solute carrier (SLC) 2A1) and cystine (via SLC3A2) uptake, as well as amino acid synthesis, such as serine synthesis via the 4E-BP1 pathway and asparagine synthesis via upregulation of asparagine synthetase (ASNS) (Zhu & Thompson, 2019).

1.3.2.5 Senescence

The term senescence, describes the accumulation of dysfunctional, non-replicative cells that are still metabolically active. Senescence is a key age-related process that can also be accelerated by TGF-β. Inflamm-aging and the SASP of senescent cells is also associated with increased TGF-β production. Senescent cells also contribute to lung remodelling directly by imparting susceptibility or resistance to apoptosis in epithelial cells, goblet cells and fibroblasts.

TGF-β is known to play a central role in senescence via Smad, p38 MAPK, PI3K/Akt and Wnt signalling to activate cyclin-dependent kinase inhibitors (CDKN) 1A (CDKN1A), CDKN1B, CDKN2A, CDNK2B and TP53 or SPARC, that upregulates the uPA system. The plasminogen activator urokinase (PLAU) (also known as uPA) system consists of PLAU; the cell surface PLAU receptor (PLAUR); the substrate plasminogen (Plg); and the plasminogen activator inhibitor-1 (SERPINE1). Both the activation of CDKNs or the uPA system results in prevention of normal cell cycle progression by inhibiting retinoblastoma protein (Rb); the protective senescence regulator, sirtuin-1 (SIRT1); and the essential cell cycle progression transcription factors, E2F1, E2F2 or E2F3 (Salminen et al., 2012; Warburton et al., 2013; Martínez- Muñoz-Espín et al., 2014; Salama et al., 2014; Wong & Sukkar, 2017; Zamudio et al., 2017; Rashid et al., 2018; Parikh et al., 2019; Gulati & Thannickal, 2019; Lehmann et al., 2020; Parimon et al., 2021).

1.3.2.6 ECM remodelling

Of the ~300 unique ECM proteins, collagen is the most abundant and of these an increased presence of type I collagen is most associated with tissue stiffness and scarring (Maffulli et al., 2002; Hynes & Naba, 2012; Naba et al., 2012; Asgari et al.,

2017; Liu et al., 2021). TGF-β primarily targets collagen encoding genes using the Smad 2/3 complex that binds directly to DNA or in association with other factors that contain a Smad-binding element, such as AP1 and the p300/CBP complex, or SP1 that binds Smad to a CC(GG)-rich element to promote COL1A1, COL1A2, COL3A1, COL5A1, COL6A1 and COL6A3 expression (Chen et al., 1999; Ghosh et al., 2000; Rossert et al., 2000; Zhang et al., 2000; Poncelet & Schnaper, 2001; Verrecchia et al., 2001; Ellis et al., 2003b; Sysa et al., 2009). Additionally, Smad-independent pathways can be activated by TGF-β to modulate collagen gene expression. For example, collagen I expression is known to be modulated by MAPK (JNK and p38), PI3K/Akt and mTOR pathways (Varela-Rey et al., 2002; Wang et al., 2002; Reif et al., 2003; Runyan et al., 2004; Tsukada et al., 2005; Shi et al., 2012; Rozen-Zvi et al., 2013; Ricard-Blum et al., 2018).

To meet the increased demands of collagen biosynthesis during fibrosis, it is essential to also increase production of the two principle amino acid components of collagen, glycine and proline (Kadler et al., 1996; Hamanaka et al., 2019). To achieve increased glycine production, TGF-β is known to activate the mTORC1 via PI3K/Akt activation and subsequent inhibition of the RAS homologue enriched in brain $(Rheb)^{GTP}$ to $Rheb^{GDP}$ converting enzyme, TSC1/2 (Saito et al., 2017; Platé et al., 2020). This process accumulates $Rheb^{GTP}$ for the activation of mTORC1 and ultimately the activating transcription factor 4 (ATF4) that promotes the transcription of solute carrier 2A1 (SLC2A1) and the enzymes required for the 4E-BP1 pathway, such as phosphoglycerate dehydrogenase (PHGDH), phosphoserine aminotransferase 1 (PSAT1), phosphoserine phosphatase (PSPH), and serine hydroxymethyltransferase 2 (SHMT2). To achieve increased proline production, TGF-β is thought to reprogramme metabolic pathways, via upregulation of aldehyde dehydrogenase 18A1 (ALDH18A1)/Δ1-pyrroline-5-carboxylate synthetase (P5CS), to influence the conversion of glutamine-derived glutamate to pyrroline-5-carboxylate (P5C) and finally proline via the P5C reductases (PYCR) 1, PYCR2 and PYCR3 (Phang et al., 2015; Hamanaka et al., 2019).

A number of other ECM components are directly upregulated by TGF-β exposure. For example, elastin, the protein responsible for giving the ECM elasticity, is

upregulated via PI3K/Akt and p38 MAPK activation (Kuang et al., 2007). Similarly, fibronectin expression is upregulated following activation of ERK and p38 MAPK (Uchiyama-Tanaka et al., 2002). CTGF is another molecule with potent remodelling effects in the lung. In fibroblasts, CTGF is known to increase ECM component synthesis as well as reduce adhesion in favour of a more migratory phenotype (Khalil et al., 2005; Xie et al., 2005; Makinde et al., 2007). TGF-ß is known to upregulate CTGF expression via the c-Jun transcription factor and AP-1 promoter which is downstream of JNK in the non-canonical TGF-ß pathway (Utsugi et al., 2003).

MMPs, and their inhibitors called tissue inhibitors of matrix metalloproteinases (TIMPs), comprise a family of proteolytic enzymes that play a central role in regulating cytokine activity to mediate a wide range of cellular functions such as adhesion, proliferation, differentiation, migration and apoptosis in addition to their primary role as mediators of ECM degradation and turnover (Elkington & Freidland, 2005; Pardo et al., 2016). The pathophysiological role of MMPs has been identified in asthma and COPD. In asthma, reduced expression of MMPs and increased expression of TIMPs has been associated with the aberrant ECM remodelling mediated by airway fibroblasts (Vignola et al., 1998; Lemjabbar et al., 1999; Suzuki et al., 2001; Prikk et al., 2002; Bergeron et al., 2003; Bergeron et al., 2010). Specifically, imbalance of MMP-9 and TIMP-1 in ECM remodelling (Atkinson & Senior, 2003; Chen et al., 2008; Zhou et al., 2010; Churg et al., 2012); MMP-1 and MMP-2 in airway obstruction in asthma (Rogers et al., 2014) and COPD (Chen et al., 2008); MMP-1 in the inflammatory phase of IPF (Zhou et al., 2010); and loss of MMP-14 in promotion of bleomycin-induced fibrosis (Placido et al., 2021). Regulation of their transcription is thought to occur by integrin-mediated MAPK signalling (Rogers et al., 2014) and by PI3K/Akt activation in response to TGF-ß, primarily identified in various types of cancer (Zhu et al., 2011; Qin et al., 2016; Hung et al., 2021).

Although several treatments are approved for the treatment of asthma and COPD by targeting inflammation, inflammatory cytokines and smooth muscle relaxation, asthma and COPD remain leading causes of breathing difficulties related to lung remodelling (Liu et al., 2021). Anti-fibrotic drugs, pirfenidone and nintedanib, have also been approved to treat lung remodelling directly by inhibiting growth factor

signalling to reduce fibroblast proliferation; however, despite the slowed decline in lung function and extended patient survival, the associated adverse effects offer no significant improvement to the quality of patient life (Ley et al., 2017; van Manen et al., 2017; Galli et al., 2017; Liu et al., 2021). Although these symptom relieving treatments are crucial for patient care, none of these treatments target the root cause of disease or offer curative treatment, hence the need for novel therapeutics to target lung remodelling.

1.4 The calcium-sensing receptor

The calcium-sensing receptor (CaSR) is a family C GPCR that has a well-established role in extracellular calcium ion (Ca^{2+}_o) homeostasis and parathyroid hormone regulation. It is expressed ubiquitously throughout the body and its expression is highest in tissues involved in calcium ion homeostasis, namely the parathyroid gland, kidney and bone. Here, systemic activation of the receptor by its physiological ligand, Ca^{2+}_o, suppresses parathyroid hormone secretion and inhibits renal Ca^{2+} reabsorption, to maintain physiological Ca^{2+}_o in the 1.1 – 1.3 mM range (Riccardi and Brown 2010). In the parathyroid, activation of the CaSR suppresses parathyroid hormone (PTH) at a half-maximal inhibitory concentration (IC_{50}) of 1.1-1.2 mM Ca^{2+}, the physiological human serum Ca^{2+} concentration. The CaSR also regulates blood calcium ion homeostasis in the kidney, intestine and bone by mediating the production and secretion of Ca^{2+}-regulating hormones, parathyroid hormone, calcitonin, FGF23 and the active form of vitamin D ($1,25(OH)_2D_3$) (Brown, 2013). Furthermore, mammals maintain hypercalcaemic serum calcium levels during fetal development that, acting via the CaSR, regulate tissue and organ development, including skeletal and lung development (Riccardi et al., 2013; Roesler et al., 2019).

1.4.1 CaSR expression and function

Although CaSR expression is most abundant in the parathyroid gland and kidney, CaSR expression has been identified in tissues not associated with Ca^{2+}_o homeostasis, namely the lung and immune cells, where its physiological role remains unclear (Riccardi & Kemp, 2012; Uhlén et al., 2015; Yarova et al., 2015; Hannan et al., 2019). In the lung it is primarily expressed in ciliated cells and alveolar epithelial cells (type I and II) as well as airway smooth muscle, fibroblasts, club cells,

endothelial cells and immune cells, including resident macrophages and T cells but not circulating immune cells (Braga et al., 2019; Karlsson et al., 2021).

The CaSR has an overall affinity for Ca^{2+} in the range of 1.1–1.3 mM and responds to changes in Ca^{2+} lower than 100 µM (Brown, 1983; Brown, 1991; Ramirez et al., 1993). However, unlike typical GPCRs, this receptor is not only activated by its physiological ligand but can also be activated by other divalent and trivalent inorganic cations (e.g. Mg^{2+}, Zn^{2+}, Mn^{2+}, Fe^{2+}, Sr^{2+}, Ba^{2+}, Cd^{2+}, Co^{2+}, Ni^{2+}, Pb^{2+}, Tb^{3+}, Gd^{3+}, Eu^{3+}, and Y^{3+}); organic polycations (e.g. polyamines such as spermine, spermidine and putrescine); and cationic peptides (e.g. ECP, poly-L-arginine, protamine, and aminoglycoside antibiotics such as neomycin, tobramycin, and gentamicin) (Conigrave & Ward, 2013; Leach et al., 2020). These endogenous CaSR-agonists are called type I calcimimetics.

As shown in **Figure 1.5**, the CaSR signals via activation of the three main groups of heterotrimeric Gα proteins, including $G_{q/11}$, $G_{i/o}$, $G_{12/13}$ as well as G_s in some cases and release of the $G_{\beta\gamma}$ subunit (Brown et al., 1993; Chang et al., 1998; Brown et al., 1990; Kifor et al., 2001; Hofer & Brown, 2003; Huang et al., 2004; Mamillapalli et al., 2008; Mamillapalli & Wysolmerski, 2010; Conigrave & Ward, 2013; Liu et al., 2015b; Leach et al., 2020). These G-proteins are encoded by the genes GNAI1-3, GNAQ, GNAS, GNA11-13, GNB1-5, GNG2-14, respectively and interact with signalling pathways independently in a cell-type specific and context-dependent manner. To elicit their effects these G-proteins activate the MAPK (ERK, JNK, p38), PI3K/Akt, mTOR and Rho; augment $Ca^{2+}{}_i$ via PLC; and breakdown cAMP via adenyl cyclase inhibition (Brown & MacLeod, 2001; Tu et al., 2011; Conigrave & Ward, 2013; Yarova et al., 2015; Yarova et al., 2016). Specifically, G_i is associated with Ras activation as well as inhibition of protective cAMP-producing adenyl cyclase (de Jesus Ferreira et al., 1998; Brennan et al., 2016).

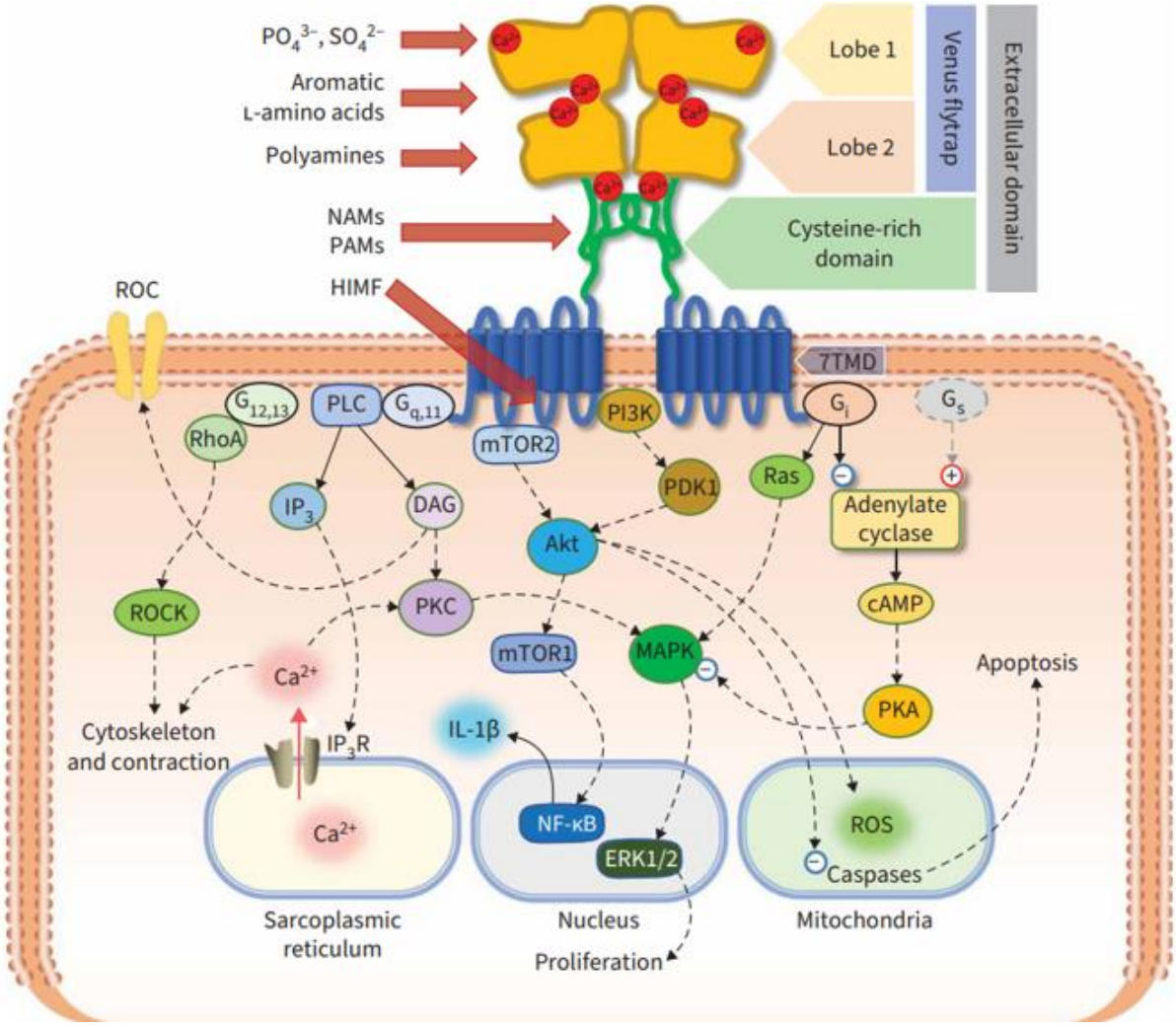

Figure 1.5. A model of the CaSR homodimer conformational structure and downstream cell signalling. The class C G-protein coupled receptor (GPCR) called the calcium-sensing receptor (CaSR) consists of the two lobes of the orthosteric venus flytrap binding site; the cysteine-rich domain; and seven transmembrane domains (7TMD). The activity of the CaSR is influenced by a number of orthosteric or allosteric binding molecules, such as its physiological ligand calcium, polyamines and negative or positive allosteric modulators (NAMs/PAMs). The CaSR elicits its response on cell behaviour by activating or inhibiting a plethora of downstream signalling pathways Ras, mitogen-activated protein kinase (MAPK), phosphatidylinositol 3-kinase (PI3K), mechanistic target or rapamycin (complex) 1 and 2 (mTOR1/2), Rho, protein kinase C (PKC), inositol 1,4,5-trisphosphate (IP_3), nuclear factor kappa-light-chain-enhancer of

activated B cells (NFκB) and adenyl cyclase via the G-proteins coupled to the receptor in a ligand-biased manner (figure from Riccardi et al. (2022)).

It is important to acknowledge that signalling downstream of the CaSR is biased, where distinct orthosteric ligands (ligand-biased signalling) or allosteric modulators (biased allosteric modulation) stabilise different signalling states, and cell-type-specific depending on expression of guanine nucleotide-binding protein (G protein) isoforms and enzymes such as adenyl cyclase (Brennan et al., 2013; Liu et al., 2015b).

1.4.2 Allosteric modulators of the CaSR

Allosteric modulators also exist that increase (positive; PAMs or type II calcimimetics) or decrease (negative; NAMs or calcilytics) the activity of the CaSR, by conformational change, upon binding to a site topographically distinct from the orthosteric "venus flytrap" (VFT) binding site, as shown in **Figure 1.5**. A number of endogenous positive allosteric modulators exist that mimic the action of Ca^{2+} or potentiate the potency of Ca^{2+}, including L-amino acids (e.g. L-Phe, L-Trp, L-histidine), g-glutamyl peptides (e.g. glutathione) and large changes in pH (>0.2 AU) that have been observed in chronic kidney disease-associated acidosis (Leach et al., 2020). Additionally, anions such as phosphate and sulphate are known to inhibit the CaSR (Geng et al., 2016; Centeno et al., 2019; Leach et al., 2020).

Exogenous positive allosteric modulators of the CaSR (CaSR-PAM), also known as type II calcimimetics, have been developed, including compounds such as arylalkyl-amines (e.g. cinacalcet and evocalcet), benzothiazole PAMs (e.g. AC265347), trisubstituted urea compounds (e.g. benzothiazole trisubstituted urea (BTU) compound 13) and peptides (e.g. etelcalcetide). These compounds potentiate the affinity of Ca^{2+} and other CaSR-agonists. Currently, CaSR-PAMs such as cinacalcet, evocalcet and etelcalcetide are currently approved for the treatment of hyperparathyroidism by lowering the concentration of Ca^{2+} required to suppress PTH release (Akizawa et al., 2020; Leach et al., 2020).

Negative allosteric modulators of the CaSR (NAM), also called calcilytics, decrease the activity of the CaSR in the presence of an orthosteric ligand. NAMs are small molecule, mostly amino-alcohols, such as NPS2143, NPSP795 (also known as SHP635), NPS89636, ronacaleret and JTT-305, but also include quinazolinones (e.g. ATF936 and AXT914), pyridines (e.g. BMS compound 1), 3H-quinazoline-4-ones, 3H-pyrimidine-4-ones and benzimidazoles. Furthermore, NPSP-795, ronacaleret, JTT-305, and AXT-914 were assessed in phase I and II clinical trials for treatment of osteoporosis and described as safe and well tolerated when delivered systemically (Kumar et al., 2010; Caltabiano et al., 2013; Halse et al., 2014; John et al., 2014). Furthermore, NPSP-795 is currently under clinical investigation for its therapeutic potential in the treatment of autosomal dominant hypocalcaemia type I (Roberts et al., 2019). Several NAMs have also shown efficacy in pre-clinical models of asthma for suppression of inflammatory cell recruitment and airway hyperresponsiveness (Yarova et al., 2015; Yarova et al., 2021).

Like all allosteric modulators, NAMs offer several advantages as therapeutics: 1) they are non-competitive and do not alter plasma concentrations of endogenous ligands; 2) they enhance or inhibit endogenous physiological responses only and do not activate supra-maximal or non-physiological responses; and 3) NAMs are maximally active at the receptor-ligand half maximal effective concentration (EC_{50}), demonstrating no effect at maximal or minimal ligand concentrations (Christopoulos & Kenakin, 2002; Ward & Riccardi, 2012).

1.4.3 Current understanding of the role of the CaSR in the lung

The CaSR plays a central role in regulating fetal lung development and tissue morphogenesis. Fetal lung development occurs in a relatively hypercalcaemic environment of 1.6–1.7 mM free-ionised Ca^{2+} which is maintained through the regulation of parathyroid hormone-related peptide secretion (Kovacs et al., 1998). In this environment the CaSR suppresses the branching pattern by negatively controlling cell proliferation via PLC-dependent Ca^{2+}_i release and activation of the PI3K/Akt pathway. The CaSR also promotes growth by driving fluid-driven lung

expansion through the cystic fibrosis transmembrane conductance regulator (CFTR) (Finney et al., 2008; Riccardi et al., 2013; Brennan et al., 2016; Chanda et al., 2019).

A number of endogenous and exogenous CaSR agonists (type I and II calcimimetics) have also been associated with inflammatory lung diseases, such as asthma and COPD. These include pollutants, such as Mg^{2+}, Cd^{2+} and Ni^{2+}; upregulation of polycationic compounds, such as polyarginine, eosinophilic cationic protein (ECP) and major basic protein (MBP); increased production of arginase-derived polyamines (spermine, spermidine, putrescine); and increased extracellular Ca^{2+} (Kurosawa et al., 1992; Uchida et al., 1993; Gibson et al., 1998; Koller et al., 1999; Lonkvist et al., 2001; Brown & MacLeod, 2001; Bartoli et al., 2004; Pégorier et al., 2006; Rossol et al., 2012; North et al., 2013; Yarova et al., 2015; Yarova et al., 2016).

Furthermore, upregulation of the CaSR has been observed in asthmatic airways (Yarova et al., 2015). As shown in **Figure 1.6**, evidence suggests the CaSR is central to inflammatory activation in the lung, including regulation of NLRP3 inflammasome activation; recruitment of inflammatory cells, including macrophages, eosinophils, lymphocytes and neutrophils; and production of inflammatory mediators, such as IL-5 and IL-13 (Lee et al., 2012a; Rossol et al., 2012; Yarova et al., 2015; Yarova et al., 2016; Yarova et al., 2021). The CaSR has also been shown to drive airway hyperresponsiveness in pre-clinical models of asthma via suppression of cAMP production and elevation of PLC/IP_3 signalling (Mahn et al., 2010; Riccardi & Kemp, 2012; Koopmans et al., 2014; Yarova et al., 2015; Yarova et al., 2021). NAMs are also consistent with the plethora of emerging or existing asthma drugs that target signalling pathways dependent on MAPK (ERK and p38) and PI3K/Akt activation (Burgess et al., 2008; Page & Cazzola, 2014).

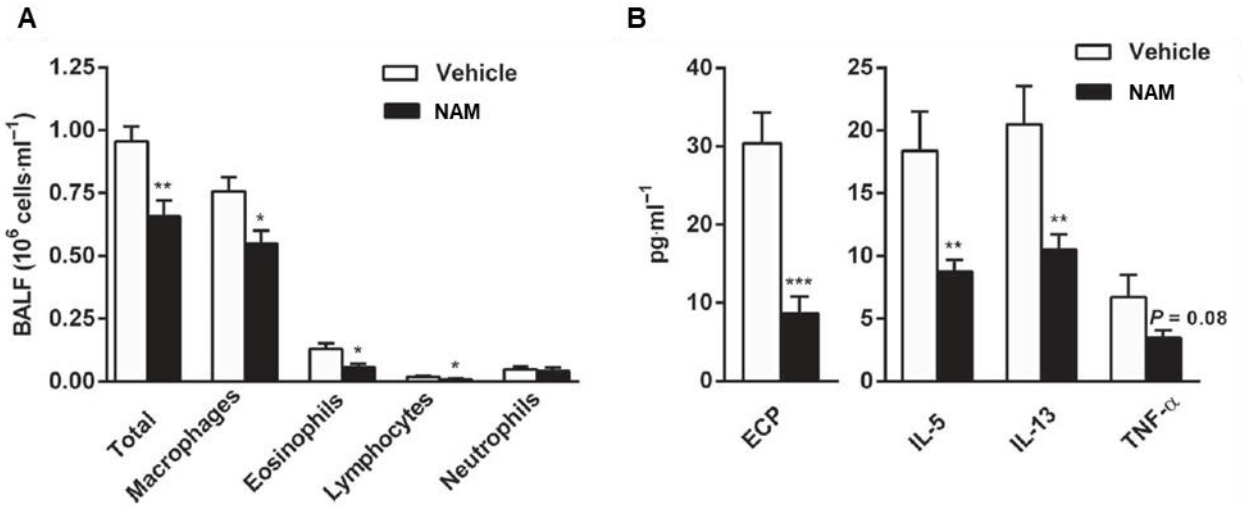

Figure 1.6. Evidence indicating the CaSR plays a central role in inflammation. NAM treatment reduced (**A**) inflammatory cell infiltration and (**B**) ECP levels as well as inflammatory cytokines IL-5 and IL-13 in the bronchoalveolar lavage fluid (BALF) in a model of IgE/Th2 asthma induced by inhaled OVA sensitisation and challenge (Yarova et al., 2015). ECP: eosinophilic cationic protein; IL: interleukin; TNFα: tumour necrosis factor-alpha; NAM: negative allosteric modulator of the CaSR.

CaSR expression can be upregulated by inflammatory cytokines, such as IL-1ß, IL-6, IL-13, TNFα and TGF-ß as demonstrated in the lung or other tissues. Specifically, Canaff & Hendy (2005) demonstrated that IL-1ß and IL-6 upregulate CaSR mRNA expression in human thyroid and kidney cell lines as well as CaSR mRNA and protein expression *in vivo* in rat parathyroid (mRNA only), thyroid, and kidney tissue (Canaff & Hendy, 2005; Hendy & Canaff, 2016). Furthermore, IL-6 was shown to upregulate CaSR expression in Caco2/AQ cells and TNFα was shown to upregulate CaSR expression in Coga1A cells (Fetahu et al., 2014). Lastly, TNFα and IL-13 were also shown to upregulate CaSR mRNA and protein expression in airway smooth muscle cells (Yarova et al., 2015).

Some evidence suggests the CaSR may also play a central role in remodelling. Specifically, the CaSR has been implicated in several cellular remodelling processes in the lung or in other tissues and cell types outside the lung, such as cell-adhesion,

mucus production, proliferation, differentiation, migration and ECM remodelling (Aggarwal et al., 2015; Tharmalingam & Hampson, 2016). For example, the CaSR was shown to mediate hypoxia-induced ASM proliferation, via ERK and PI3K pathways (Li et al., 2011), and extracellular calcium induced ovarian epithelial cell proliferation via ERK (Hobson et al., 2000). The CaSR has also been implicated in hypoxia-induced mucus hypersecretion in bronchial epithelial cells, via $G_{q/11}$, PLC/IP_3 and intracellular Ca^{2+} as well as ERK signalling (Yang et al., 2014a; Yang et al., 2014b).

Targeted CaSR deletion from SM22α-positive cells was also shown to reduced age-related cardiac fibrosis in aging mice (Schepelmann et al., 2016; **Figure 1.7**) and interstitial wall thickening was reduced by NAM treatment in a guinea pig model of LPS-induced COPD-like neutrophilic exacerbation (Yarova et al., 2016). Furthermore, the CaSR was also shown to mediate IL-1ß-induced collagen expression in mouse collecting duct cells (Wu et al., 2019). In addition, known CaSR activating polycations have been shown to enhance epithelial permeability (Meurs et al., 1999; Brown & MacLeod, 2001; Yarova et al., 2015), possibly leading to loss of epithelial cell integrity and reduced protection against insult by inhaled particles (Courtney & Spafford, 2017).

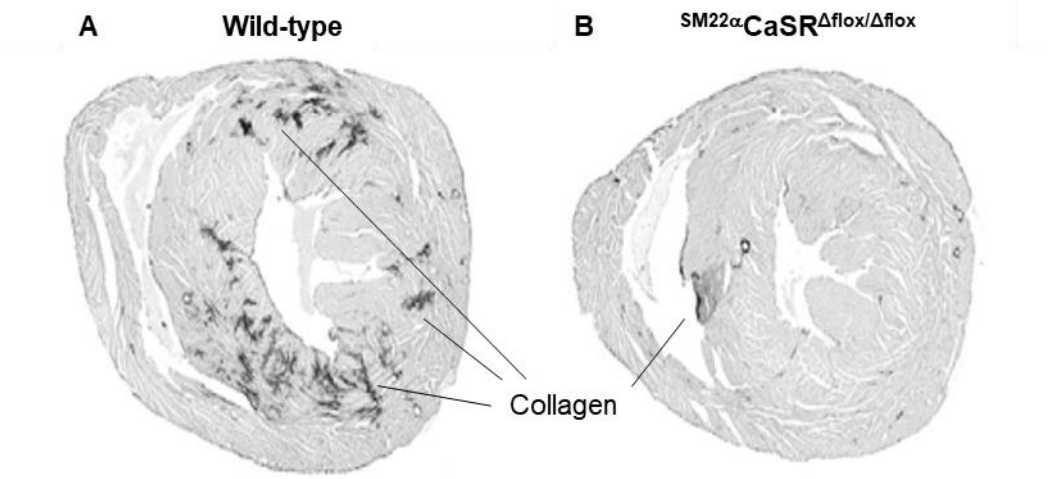

Figure 1.7. Cardiac fibrosis was reduced in middle-aged $^{SM22\alpha}CaSR^{\Delta flox/\Delta flox}$ mice with targeted CaSR deletion from SM22α-positive cells. Comparison of picrosirius red staining of 8 µm cryosections of paraformaldehyde fixed heart

sections from 14-month old (**A**) wild-type and (**B**) $^{SM22\alpha}CaR^{\Delta flox/\Delta flox}$ mice showing reduced collagen staining following genetic ablation of the CaSR (adapted from Schepelmann et al., 2016).

1.5 Hypothesis

Here I propose that a chronic age- or disease-related increase in CaSR activation, by elevated extracellular CaSR agonist concentrations and/or increased CaSR expression, drives lung remodelling by aberrantly activating CaSR-mediated tissue remodelling in a cell-type-specific manner across a variety of lung cell types via signalling cascade activation, such as MAPK (p38, ERK and JNK), PI3K/Akt, mTOR, Rho, Wnt, Ca^{2+}_i augmentation and suppression of cAMP production; and subsequent activation of cellular remodelling mechanisms, such as cell-adhesion, apoptosis, secretion, growth, proliferation, migration, differentiation, autophagy, and ECM remodelling, as shown in **Figure 1.8**.

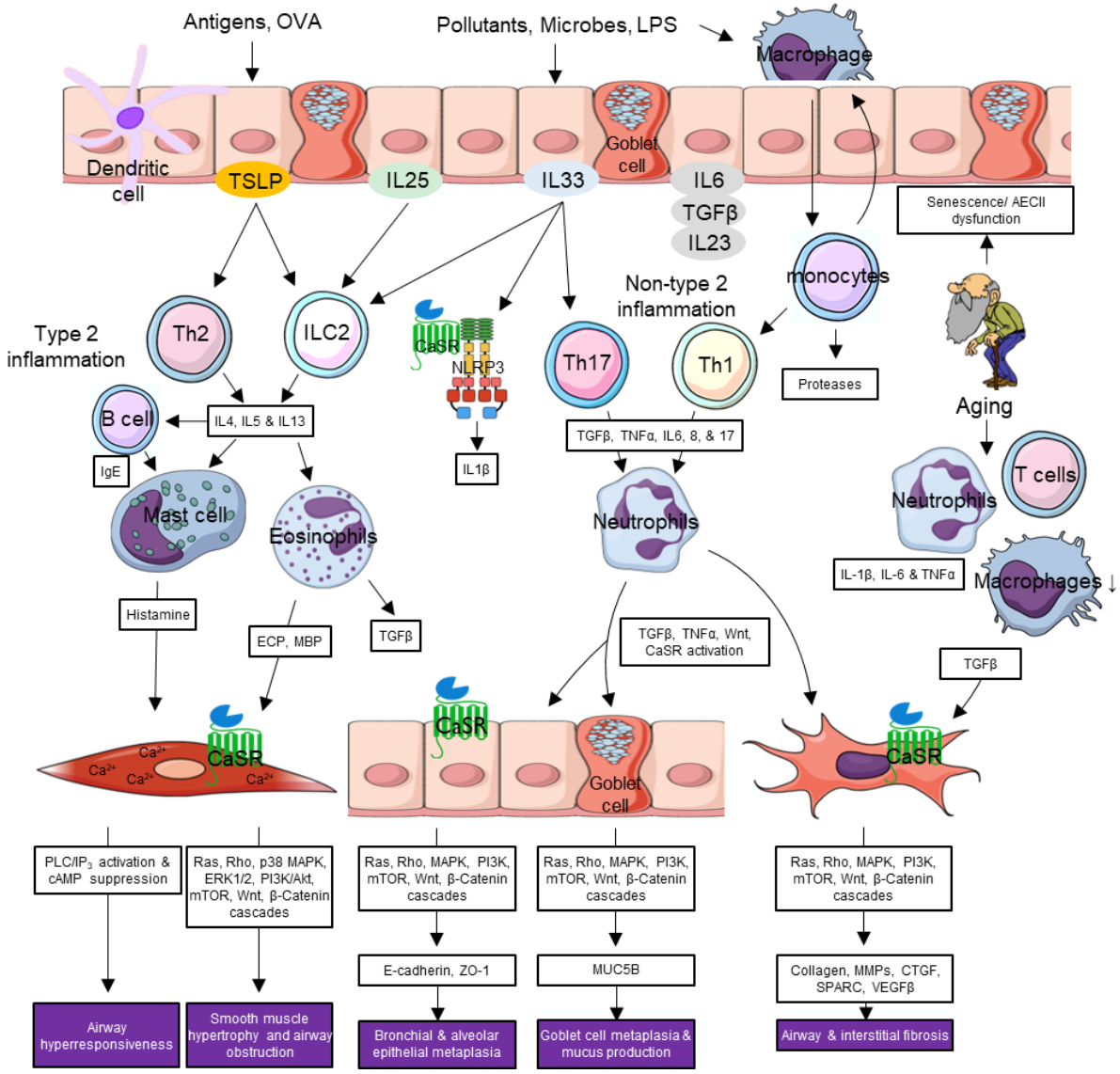

Figure 1.8. Hypothesised role of the CaSR in lung remodelling. Inhaled antigens and pollutants activate IgE/Th2 or alarmin-driven inflammation through the release of inflammatory cytokines and alarmins at the airway epithelium, many of which upregulate CaSR expression. I hypothesise that the CaSR plays a central role in mediating airway and interstitial lung remodelling in a range of different cell types, including epithelial, goblet, smooth muscle cells and fibroblasts via G-protein associated signalling cascades, including Ras, Rho, MAPK (p38, JNK, ERK), PI3K/AKT, mTOR and Wnt/ß-catenin, and subsequent activation of cellular remodelling processes, such as loss of barrier integrity, apoptosis, secretion, , growth, autophagy, proliferation, gene expression, senescence and ECM remodelling. This figure was drawn myself but

referenced information from Yarova et al. (2015) and Israel & Reddel (2017). ECP: eosinophilic cationic protein; IL: interleukin; TNFα: tumour necrosis factor-alpha; NAM: negative allosteric modulator of the CaSR; MBP: major basic protein; IgE: immunoglobulin E; TGF-ß: transforming growth factor-beta; LPS: lipopolysaccharide; CaSR: calcium-sensing receptor; MMP: matrix metalloproteinase; ZO-1: tight junction protein 1; MAPK: mitogen-activated protein kinase; PI3K: phosphatidylinositol 3-kinase; PLC: phospholipase C; IP_3: inositol 1,4,5-trisphosphate; cAMP: cyclic adenosine monophosphate; ERK: extracellular signal-regulated kinase; mTOR: mechanistic target of rapamycin; CTGF: connective tissue growth factor; SPARC: secreted protein acidic and rich in cysteine; VEGFB: vascular endothelial growth factor B; Wnt: Wingless-related integration site.

1.6 Aims & objectives

This thesis aimed to investigate the role of the CaSR in lung remodelling. To do this, the project objectives were to:

1. Develop novel quantitative image analysis methodologies, to determine airway and alveolar interstitial remodelling *in vivo* using specialised (StrataQuest, TissueGnostics, AT) or open-source (FIJI, ImageJ) image analysis software.

2. Determine the effect of genetic ablation of the CaSR on age-related airway and alveolar interstitial lung remodelling *in vivo* using 15-month old mice with targeted CaSR knock-out from SM22a positive cells.

3. Determine the effect of pharmacological ablation of the CaSR, using inhaled NAM treatment, on pathophysiological airway and alveolar interstitial remodelling *in vivo* using three models of inflammatory lung disease, namely shorter-term IgE/Th2 asthma, alarmin-driven asthma and longer-term IgE/Th2 asthma.

4. Determine the effect of pharmacological ablation of the CaSR, using NAM treatment, NPS2143, on cell signalling and cellular mechanisms of lung remodelling *in vitro* using human fibroblasts exposed to a remodelling mediator, TGF-β.

CHAPTER 2: METHODOLOGY

2.1 Animal experiments

In total, five rodent models were used to investigate the role of the calcium-sensing receptor (CaSR) in lung remodelling, including chronic obstructive pulmonary disease (COPD)-like neutrophilic exacerbation in guinea pigs; targeted CaSR-deletion from SM22α-positive cells in aging mice; shorter-term immunoglobulin (Ig)E/ T helper 2 (Th2) asthma in mice; alarmin-driven asthma in mice; and longer-term IgE/Th2 asthma in mice. All animal procedures were performed in accordance with the regulations of the Animals (Scientific Procedures) Act 1986 and Declaration of Helsinki conventions for the use and care of animals and were approved by the Home Office (UK) and a local ethics committee.

2.1.1 LPS-induced COPD-like neutrophilic exacerbation (guinea pigs)

Picrosirius red stained lung sections, that had been generated as part of a previous study, were obtained from a model of COPD-like neutrophilic exacerbation in guinea pigs (Yarova et al., 2016). These lung sections chosen to develop novel methodologies to complete objective 1 (**Section 1.6**) because a professional histopathologist scoring previously performed at AstraZeneca was available to validate my findings. To generate this model, 24 male Dunkin-Hartley guinea pigs were obtained from Harlan Laboratories Ltd (UK) and kept in a room with a 12-hour dark/light cycle and *ad libitum* access to food and water. Using adaptions from protocols by Toward & Broadley (2001) and Kaneko et al. (2007), animals were exposed to 30 μg/ml nebulized lipopolysaccharide (LPS) in saline delivered by a Pulmostar nebulizer (DeVilbiss, Sunrise Medical) at 0.3 mL/min and driven by a constant pressure air supply at 20 psi (gauge) into a Perspex exposure chamber for one hour on alternating days over an 18-day period. Animals received vehicle (0.03% dimethyl sulfoxide (DMSO) in saline) or negative allosteric modulator of the CaSR (NAM) treatment (3 μM NPS89636 and 0.03% DMSO in saline) daily for 30 minutes following the fifth LPS exposure and this continued for 9 days using the same aerosol delivery technique, as shown in **Figure 2.1**. Yarova et al. (2016) observed leukocyte infiltration in the bronchoalveolar lavage fluid (BALF) of LPS-treated guinea pigs on day 18 of the protocol that was suppressed by NAM treatment without changes in systemic free ionized calcium.

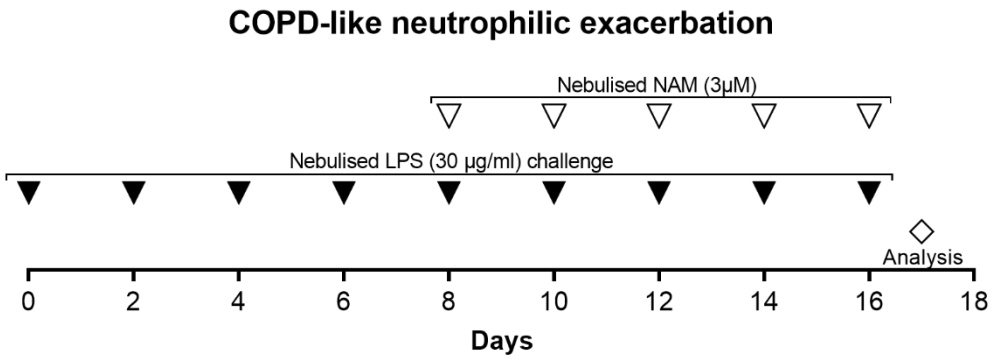

Figure 2.1. Experimental timeline for therapeutic model of COPD-like neutrophilic exacerbation in guinea pigs. 24 guinea pigs were challenged with 30 μg/ml nebulised lipopolysaccharide (LPS) in saline every other day for 18 days. Nebulised vehicle (0.03% DMSO in saline) or NAM treatment (3 μM NPSP89636 and 0.03% DMSO in saline) was delivered every other day from day 9, 30 minutes prior to the LPS exposure (Yarova et al., 2016). DMSO: Dimethyl sulfoxide; NAM: Negative allosteric modulator of the calcium-sensing receptor; LPS: Lipopolysaccharide.

2.1.2 Age-related fibrosis in 15-month-old mice with targeted CaSR deletion from SM22α-positive cells (mice)

The novel quantitative image analysis methods developed in the previous experiment were then used, alongside existing methods, to determine the role of the CaSR in age-related lung remodelling using seven 15-month-old cre-positive $^{SM22\alpha}CaSR^{\Delta flox/\Delta flox}$ mice with targeted CaSR deletion from smooth muscle protein 22α (SM22α)-positive cells and 5 Cre-negative (wild-type (WT)). This model of targeted CaSR ablation from SM22α-positive cells was previously generated by Dr Martin Schepelmann (Schepelmann et al., 2016) by crossing commercially available SM22α-Cre^{+} mice (Jackson Immunoresearch Laboratories, Bar Harbor, ME) (Lepore et al., 2005) with exon7-LoxP CaSR mice, generated by blastocyst injection of floxed CaSR-containing embryonic stem cells (ES) (Chang et al., 2008), and inbreeding for at least three generations. The resulting CaSR-LoxP SM22α-Cre mice were then used for experiments with Cre-negative mice available as WT controls. LoxP sites flanking exon 7 of *CaSR* gene enables the deletion of the seven transmembrane domains and four intracellular loops of the CaSR in cells expressing the SM22α promoter region

without alteration to SM22α expression, as shown in **Figure 2.2** (Chang et al., 2008; Schepelmann et al., 2016). This resulted in a 75 % reduction in CaSR protein expression in the lung and significantly reduced function in airway smooth muscle cells (Yarova et al., 2015; Schepelmann et al., 2016). CaSR expression and function was not directly assessed in fibroblasts from these mice; however, human and mouse lung fibroblasts are known to express the CaSR (Zhang et al., 2014, also see chapter 6) as well as SM22α, also known as transgelin (Lawson et al., 1997). Therefore, the cell types targeted with CaSR deletion were lung fibroblasts, airway smooth muscle cells, and lung vascular cells. Genotyping for CaSR-LoxP sites and Cre was also performed by Dr Martin Schepelmann as shown in **Figure 2.2B-C** (Holtwick et al., 2002; Chang et al., 2008; Yarova et al., 2015). Lungs were harvested from these mice at approximately 15-months of age.

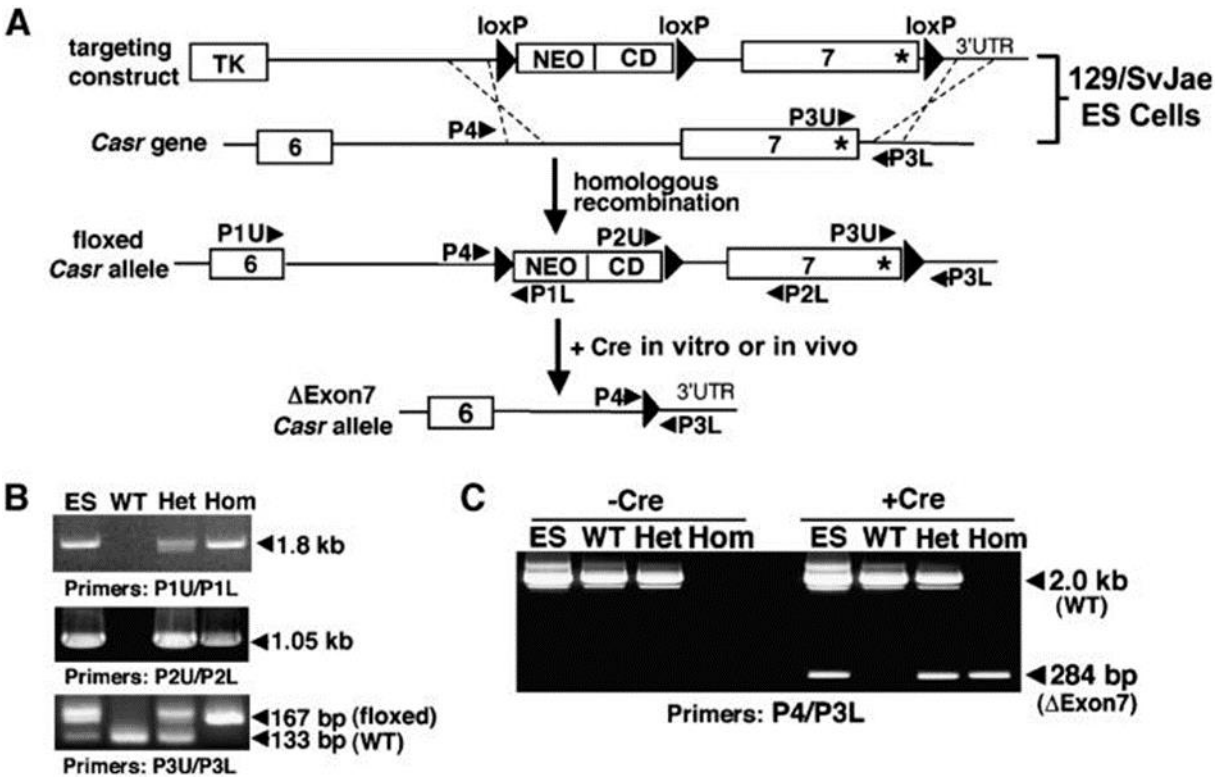

Figure 2.2. Breeding protocol for targeted CaSR deletion from SM22α-positive cells in $^{SM22\alpha}CaSR^{\Delta flox/\Delta flox}$ mice. (**A**) Graphical representation of the gene targeting strategy used to introduce loxP sequences to flank exon 7 of CaSR to obtain heterozygous ($CaSR^{WT/flox}$) and homozygous ($CaSR^{flox/flox}$) mice, published in Chang et al. (2008). (**B**) To confirm integration of the targeting

sequences PCR genotyping was performed on genomic DNAs from floxed CaSR-containing embryonic stem cells (ES) before blastocyst injection as well as from the tails of $CaSR^{wt/wt}$ (WT), heterozygous $CaSR^{wt/flox}$ (Het), and homozygous $CaSR^{flox/flox}$ (Hom) mice. (**C**) polymerase chain reaction (PCR) genotyping was also performed on genomic DNA after incubation with (+Cre) or without (−Cre) bacteriophage P1 Cre recombinase *in vitro* for 30 min. The 284-bp band represents the DNA fragment due to excision of exon 7 of the CaSR (ΔExon7). Breeding programmes and genotyping experiments were performed by Martin Schepelmann in collaboration with Wenhan Chang (University of California, San Francisco, USA) and described in more detail in Chang et al. (2008) and Schepelmann et al., (2016) (adapted from Chang et al., 2008). BP: Base pair; Het: heterozygous; Hom: homozygous; PCR: Polymerase chain reaction; DNA: Deoxyribonucleic acid; ES: embryonic stem cells; CaSR: Calcium-sensing receptor; WT: wild-type.

2.1.3 Shorter-term IgE/Th2 asthma delivered by intranasal instillation (mice)

To investigate the role of the CaSR in IgE/Th2 asthma-like lung remodelling, a model of shorter-term IgE/Th2 was performed using intraperitoneal (IP) ovalbumin (OVA) sensitisation and intranasally instilled (IN) OVA challenge, as shown in **Figure 2.3**. Here, 18 female Balb/c mice (approximately 6-8 weeks old) were sensitised with two intraperitoneal injections of 100 µg/mouse OVA (Sigma-Aldrich, Missouri, United States) emulsified with 10 % aluminium hydroxide ($Al(OH)_3$ (50 µg/mouse) in phosphate-buffered saline (PBS) solution at days 1 and 13 to evoke an allergic response that was confirmed by determining IgE levels. Sensitised mice were then randomly distributed into three treatment groups: vehicle (VEH), ovalbumin + vehicle (OVA+VEH) and ovalbumin + NAM + vehicle (OVA+NAM). Although previous power analysis calculations performed by my colleague, Miss Ping Huang, suggested an optimum sample size of 8 animals, only 6 mice from each group exhibited signs of OVA-sensitisation and were qualified to continue in the experiment. Mice were then challenged with intranasal instillations of 50 µg of OVA in vehicle daily from day 21 until day 26. Inhaled vehicle (50 µl of 0.05% tween-80 and 0.3% DMSO in saline) or NAM treatment (50 µl of 200 µg NPSP795, 0.05% tween-80 and 0.3% DMSO in saline) was then delivered by intranasal instillation twice daily from day 22 until

day 26. At day 27, the mice were euthanised and organs were harvested. This experiment was performed by Miss Ping Huang.

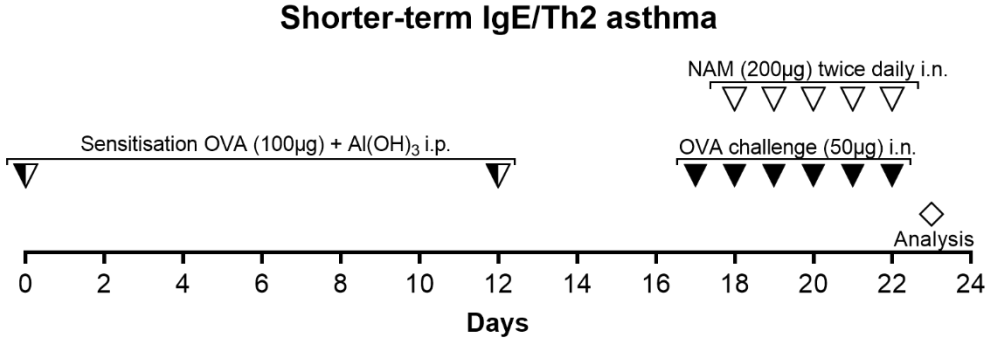

Figure 2.3. Experimental timeline for therapeutic model of shorter-term IgE/Th2 asthma delivered by intranasal instillation in Balb/c mice. 18 female Balb/c mice were sensitised two intraperitoneal injections of OVA (100 µg) and 10 % $Al(OH)_3$ (50 µg/mouse) in PBS solution at days 1 and 15 to induce an allergic response. Animals were then challenged from day 21 with intranasal instillations of 50 µg of OVA in saline daily for 6 days. Intranasal vehicle (50 µl of 0.05% tween-80 and 0.3% DMSO in saline) or NAM (50 µl of 200 µg NPSP795, 0.05% tween-80, 0.3% DMSO in saline) treatment occurred twice daily from day 22 until day 26 and organs harvested at day 27. This experiment was performed by a colleague Miss Ping Huang. DMSO: Dimethyl sulfoxide; NAM: Negative allosteric modulator of the calcium-sensing receptor; OVA: Ovalbumin; PBS: Phosphate buffered saline; IP: intraperitoneal; IN: Intranasal; IgE: Immunoglobulin.

2.1.4 Alarmin-driven asthma (mice)

To investigate the role of the CaSR in alarmin-driven asthma-like lung remodelling, an alarmin-driven asthma model was generated using interleukin (IL)-33 challenge in non-sensitised mice, as shown in **Figure 2.4**. Here, 18 female 6- to 8-week-old Balb/c mice were challenged with intranasal instillation of 30 ng IL-33 (R&D Systems, Minneapolis MN, USA) in 50 µl saline for 6 days. From day 2, inhaled treatment with vehicle (50 µl of 0.05% tween-80 and 0.3% DMSO in saline) or NAM (50 µl of 200 µg/mouse NPSP795, 0.05% tween-80 and 0.3% DMSO in saline) was delivered by intranasal instillation twice daily, 2h before IL-33 administration. Mice were then

euthanised and organs harvested on day 7. This experiment was also performed by Miss Ping Huang.

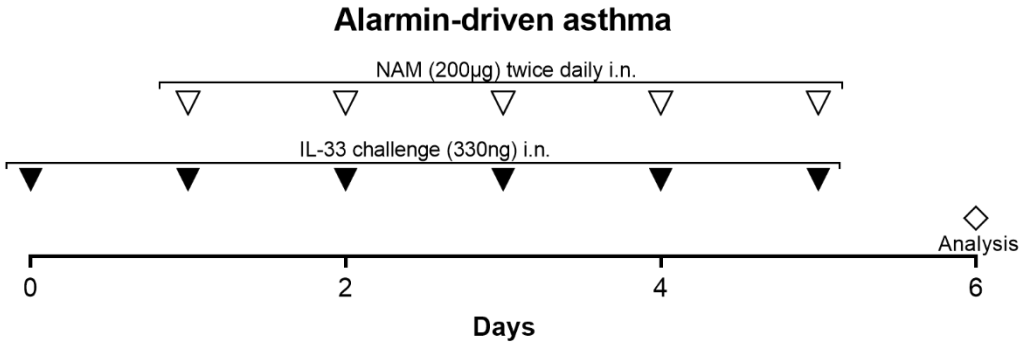

Figure 2.4. Experimental timeline for therapeutic model of alarmin-driven asthma in Balb/c mice. This model of alarmin-driven asthma was developed in parallel with the intranasal IgE/Th2 asthma model excluding the sensitisation stage. 18 female Balb/c mice were challenged intranasally with IL-33 daily for 6 days. Intranasal instillations of vehicle (50 µl of 0.05% tween-80 and 0.3% DMSO in saline) or NAM treatment (50 µl of 200 µg NPSP795, 0.05% tween-80 and 0.3% DMSO in saline) occurred twice daily from day 2. Mice were then euthanised and organs harvested on day 7. This experiment was performed by a colleague Miss Ping Huang. DMSO: Dimethyl sulfoxide; NAM: Negative allosteric modulator of the calcium-sensing receptor; IL-33: Interleukin-33; IN: Intranasal.

2.1.5 Longer-term IgE/Th2 asthma delivered by nebulisation and head-to-head comparison with NAM and an inhaled corticosteroid (mice)

The final model used to investigate the role of the CaSR in asthmatic lung remodelling, named the longer-term IgE/Th2 asthma model, was generated by delivering nebulised OVA challenge and inhaled NAM treatment in OVA sensitised mice. Here, 30 female Balb/c mice (approximately 6-8 weeks old) were obtained from Envigo (UK) and maintained under standard conditions with food and water ad libitum. Female mice were used in this experiment due to their association with a heightened inflammatory response compared to males (Melgert et al., 2005; Blacquiere et al., 2010). A colleague Polina Yarova performed *a priori* F test power calculation for one-way analysis of variance (ANOVA) (where $\alpha = 0.05$, power = 0.8 and effect size = 0.7) and six mice were suggested as suitable for each treatment

group (G*Power v.1.3.9.6). They were sensitised with two intraperitoneal injections of OVA (50 µg) and aluminium hydroxide $Al(OH)_3$ (50 mg) in phosphate-buffered saline (PBS) solution at days 0 and 10 of the experiment where subsequent IgE measurements were used to confirm sensitisation. Again, sensitised mice were then randomly distributed into treatment groups with 6 mice assigned to each group. Mice were then challenged from day 21 every other day with 0.5 % OVA aerosol until day 29. Treatment with nebulised NAM (6µM of NPSP795), fluticasone propionate (FP) (0.25 mg) or vehicle (0.01 % Tween-80/0.03 % DMSO) occurred twice daily from day 25 until day 30. At day 32, the mice were euthanised and organs were harvested (**Figure 2.5**). The following analyses were performed with the experimenter blinded to the experimental conditions. This protocol is now published in Yarova et al. (2021).

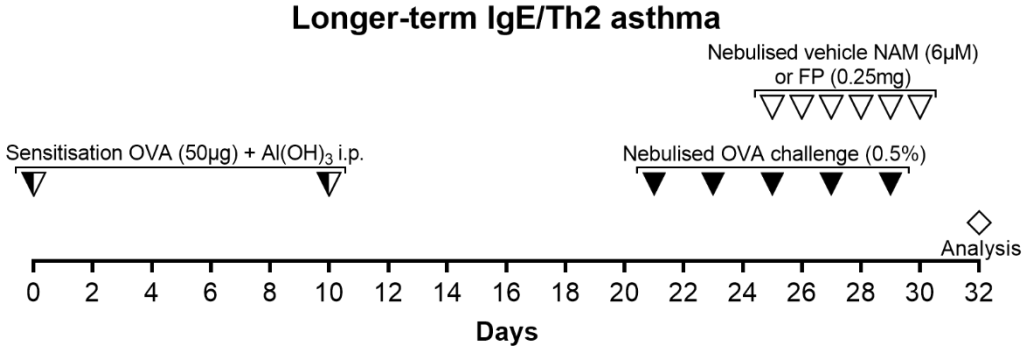

Figure 2.5. Experimental timeline for therapeutic model of longer-term IgE/Th2 asthma delivered by nebulisation in Balb/c mice. 18 female Balb/c mice were sensitised two intraperitoneal (IP) injections of OVA (50 µg) and 50 mg aluminium hydroxide ($Al(OH)_3$) in phosphate-buffered saline (PBS) solution at days 0 and 10 to induce an allergic response. Animals were then challenged from day 21 to 29 with five nebulised instillations of 0.5 % OVA aerosol every other day for one hour for 9 days. Aerosolised treatment with vehicle (0.01 % Tween-80 and 0.03% DMSO in saline), NPSP795 (6 µM, 0.01 % Tween-80 and 0.03% DMSO in saline) or fluticasone propionate (FP) (0.25 mg FP, 0.01 % Tween-80 and 0.03% DMSO in saline) was delivered twice daily for 15 min, 1 hour prior to and 7 hours after each OVA challenge for six days. At day 32, the mice were euthanised and organs were harvested. This experiment was performed by Miss

Ping Huang and Dr Polina Yarova (Yarova et al., 2021). DMSO: Dimethyl sulfoxide; NAM: Negative allosteric modulator of the calcium-sensing receptor; OVA: Ovalbumin; PBS: Phosphate buffered saline; IP: intraperitoneal; IN: Intranasal; IgE: Immunoglobulin; FP: Fluticasone propionate.

2.1.6 Ethics

All animal procedures were approved by local ethical review and conformed to the regulations of the United Kingdom Home Office according to the Animals (Scientific Procedures) Act 1986. All animal experiments were carried out by colleagues following ethical review, in accordance with UK legislation and ARRIVE guidelines (Kilkenny et al., 2013), independently reviewed and approved by the UK Home Office (Home Office Project License 30/3007) and conformed to the guidelines from directive 2010/63/EU of the European Parliament on the protection of animals used for scientific purposes. Euthanasia for tissue collection was performed by cervical dislocation or intraperitoneal injection of pentobarbital overdose according to UK legislation [A(SP)A 1986, Schedule 1].

2.1.7 Histology

Lungs from these animals were harvested and promptly fixed in neutral buffered formalin for 24 hours before being mounted in a paraffin block for sectioning. Syringe injection to inflate the lung was only performed on lungs from $^{SM22\alpha}CaSR^{\Delta flox/\Delta flox}$ mice.

2.1.7.1 Picrosirius red and Periodic Acid-Schiff (PAS) staining

Formalin-fixed paraffin-embedded (FFPE) 5µm thick sagittal lung cross-sections were taken from the three larger lobes of the right lung of all 12 female Dunkin-Hartley guinea pigs used to simulate COPD-like neutrophilic exacerbation, deparaffinised, rehydrated and stained with Picrosirius Red and periodic acid Schiff (PAS) for the identification of collagen and mucosubstances, respectively. These experiments were carried out by Dr Polina Yarova (Yarova et al., 2016)) using a Leica Autostainer XL (Leica Microsystems, Milton Keynes, UK) according to the manufacturer's protocol, as published in Yarova et al. (2016). Reagents purchased from Sigma-Aldrich (Dorset, UK). Imaging was performed by myself at a later date

using an Olympus BX40 slide scanner and individual airways and regions of distal lung parenchyma were identified at random with the experimenter blinded to the experimental conditions.

2.1.7.2 Masson's trichrome staining

FFPE 5µm thick sagittal plane lung cross-sections were taken from the left lung of all animals from the models of age-related fibrosis in $^{SM22\alpha}CaSR^{\Delta flox/\Delta flox}$ mice and shorter-term IgE/Th2 asthma, alarmin-driven asthma, and longer-term IgE/Th2 asthma in Balb/c mice. Additionally, following sagittal sectioning of lungs from the longer-term IgE/Th2 asthma model, these lungs were re-orientated for sectioning in the transverse plane for the identification of more consistent larger airway cross-sections. All sections were mounted on glass slides and embedded in paraffin wax for tissue preservation. To remove the paraffin wax for histological staining the lung sections were immersed twice in xylene (Atom Scientific, UK) for 4 minutes. This was followed by submerging slides twice in 100 % ethanol for two minutes, once in 90 % ethanol for two minutes, once in 70 % ethanol for two minutes and finally in distilled water for five minutes to remove the paraffin. Masson's trichrome staining was then performed in accordance with the manufacturer's kit guidelines (Polysciences Inc., DE) by submerging slides in Bouin's solution for 1 hour at 60˚C in a water bath. Slides were then washed for 5 mins under running tap water and transferred to Weigert's iron haematoxylin working solution (1:1 ratio of solution A and B) for 10 mins. This was followed by a wash in running tap water for 5 minutes and rinse with ddH_2O. Then slides were placed in Biebrich scarlet - acid fuchsin solution for 5 minutes and subsequently washed in ddH_2O. Slides were then incubated in 5% phosphotungstic/phosphomolybdic acid for 10 minutes before slides were drained and transferred to aniline blue for 5 minutes before three consecutive washes in ddH_2O. Slides were subsequently placed in 1% Acetic acid for 1 minute before a final rinse in ddH_2O and dehydration of tissue back to xylene. Sections were then mounted with a xylene-based mounting medium (Distryene plasticiser xylene (DPX); Atom Scientific, UK). This staining was carried out by myself for the age-related fibrosis in $^{SM22\alpha}CaSR^{\Delta flox/\Delta flox}$ mice, shorter-term IgE/Th2 asthma and alarmin-driven asthma models but Masson's trichrome staining for the longer-term IgE/Th2

asthma model was performed by the Cardiff university bioimaging hub using a Leica Autostainer XL (Leica Microsystems, Milton Keynes, UK).

2.1.7.3 Quality control

Due to obtaining pre-stained or autostainer stained lung sections for some of my experiments, implementation of a staining quality control step was not always possible. Instead, only images where markers could be identified successfully with StrataQuest image analysis software were included in these studies, which is described in more detail later in this chapter. In some instances, overstained sections were still permitted to be included in my studies where identification of the markers is undisrupted; however, in future controlling the quality of staining in these experiments should be included to ensure accurate component identification.

2.1.7.4 Brightfield imaging

With the experimenter blinded to the experimental conditions, imaging of the whole lung section was performed using the 20x objective of an Olympus BX40 slide scanner (Olympus, Southend-on-Sea, UK) before suitable airways were selected at random for analysis. Suitable airways were defined as those of a suitable size, larger (> 50,000 μm^2) and smaller (< 50,000 μm^2), with a closed circular shape and little or no elongation, indicating cross-section error. Consistency was maintained within these size limits by ensuring all airways occupied approximately 40% of the total image area for images taken with the 10x objective lens (larger airways) or 20x objective lens (smaller airways).

Areas of distal lung parenchyma were selected at random providing they lacked interfering airways or vasculature and were not adjacent to the exterior wall of the lung where artifacts are more common. Ashcroft et al. (1988) and Hübner et al. (2008) used 10x objective lenses to determine alveolar interstitial remodelling; however, it was not possible to collect more than three 10x objective images (2772 x 2068 px) of the alveolar interstitium per lung section due to interference with airways or vasculature and was deemed unrepresentative; therefore, 12 iterations of 20x objective images (1386 x 1034 px) were obtained instead, totalling the same

area of lung but less susceptible to interference. The number of images (aka regions of interest; ROI) per experiment are detailed in **Table 2.1**.

Table 2.1 Summary of in vivo image analysis information. This table summarises the number of animals; number of technical repeats; total regions of interest (ROIs); and range of ROI's per animal for the quantitative image analysis experiments performed in this thesis.

Model	Experimental Group	Animals per group (N)	Technical repeats (n)	Total ROI	ROI animal^{-1}
Larger airways					
COPD-like neutrophilic exacerbation	LPS	6	3	31 (52)	3-7 (5-14)
	LPS + NAM	6	3	23 (33)	2-6 (2-8)
Shorter-term IgE/Th2 asthma	Vehicle	4	3	8	1-3
	OVA	5	3	12	2-3
	OVA + NAM	6	3	18	2-4
Alarmin-driven asthma	Vehicle	5	3	8	1-3
	IL-33	8	3	20	1-5
	IL-33 + NAM	8	3	13	1-3
Longer-term IgE/Th2 asthma	Vehicle	6	3	35	5-6
	OVA	6	3	34	5-6
	OVA + NAM	6	3	26	2-6
	OVA + FP	6	3	34	4-6
	OVA + NAM + FP	4	3	23	5-6
Smaller airways					
COPD-like neutrophilic exacerbation	LPS	12 (6)	3	52 (60)	3-6 (4-19)
	LPS + NAM	12 (6)	3	51 (60)	1-7 (3-13)
Age-related fibrosis	CaSR-KO	7	3	98	13-15
	WT	5	3	64	8-17
Shorter-term IgE/Th2 asthma	Vehicle	5	3	25	3-7
	OVA	6	3	19	1-5
	OVA + NAM	6	3	21	1-7
Alarmin-driven asthma	Vehicle	7	3	24	2-5
	IL-33	8	3	41	2-7
	IL-33 + NAM	8	3	31	1-7
Longer-term IgE/Th2 asthma	Vehicle	6	4	84	9-16
	OVA	6	4	107	10-22
	OVA + NAM	6	4	111	14-22
	OVA + FP	6	4	69	9-14
Interstitium					
COPD-like neutrophilic exacerbation	LPS	6	3	49	3-10
	LPS + NAM	6	3	42	5-7
Age-related fibrosis	CaSR-KO	7	3	84	12
	WT	5	3	60	12
Shorter-term IgE/Th2 asthma	Vehicle	5	3	45	9
	OVA	6	3	54	9
	OVA + NAM	7	3	63	9
Alarmin-driven asthma	Vehicle	7	3	63	9
	IL-33	8	3	72	9
	IL-33 + NAM	8	3	73	9-10
Longer-term IgE/Th2 asthma	Vehicle	3	3	36	12
	OVA	5	3	60	12
	OVA + NAM	6	3	67	10-12
	OVA + FP	6	3	72	12
	OVA + NAM + FP	5	3	60	12

2.1.7.5 Experimental group blinding

Experimental group blinding was achieved using a two-step approach, first by colleagues prior to the imaging process using coded names for each animal, and

secondly by coding the name of each image file using the opensource protocol published by Salters (2016) named blindrename.pl script (Mariani et al., 2016).

2.1.8 *In vivo* image analysis

2.1.8.1 Adaptation of the Ellis et al. (2003) approach

Using a murine model of IgE/Th2 asthma, induced by OVA sensitisation and inhaled OVA challenge, Ellis et al. (2003) developed a novel method of determining the percentage of peribronchial collagen surrounding 1st generation airways. To do this, concentric rings were mapped to Masson's trichrome, or αSMA, stained airway cross-sections from the left superior, right inferior and left inferior lobes and regions of vasculature were excluded from the analysis. Here, the most sensitive region for determining peribronchial collagen was determined as the 20μm for the larger airways; however, significant changes were observed in all regions.

The lobes deemed most suitable, the left superior and inferior lobes, were used to maintain consistency; however, the sample sizes recommended by Ellis et al. (2003) were larger than those that could be accommodated in my experiments due to obtaining lung sections from previous experiments. Instead sample sizes were aligned with previous power analyses performed by my colleague, Dr Polina Yarova, suggesting an optimum sample size of 8 animals (Yarova et al., 2015). Furthermore, the organs used in this thesis had already been harvested, FFPE, mounted, and sectioned in the sagittal plane resulting in the loss of 1st generation airways. Although the longer-term IgE/Th2 asthma model was later reorientated to obtain larger, likely 1st generation, airways; the airway position could not be confirmed. Therefore, adaptation of the Ellis et al. (2003) method was required for sagittal plane cross-sectioning across the range of airway sizes analysed, including larger (> 50,000μm^2) and smaller (< 50,000μm^2) airways, as shown in **Figure 2.6**.

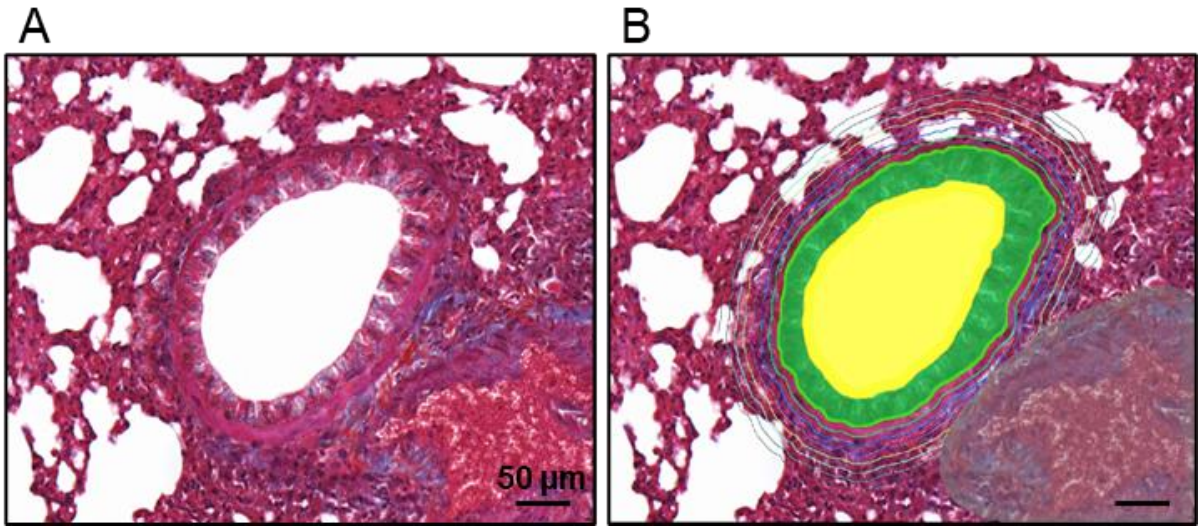

Figure 2.6. Graphical representation of the adaptation to the Ellis et al. (2003) method in StrataQuest. (**A**) Smaller airways were (**B**) manually identified by airway lumen (yellow) and airway epithelium (green). StrataQuest (TissueGnostics, AT) was then programmed to analyse the percentage of positively stained blue pixels with seven peribronchial rings extending away from the airway epithelium in increments of 10 µm. The same method was used for the larger airways except the rings increased in increments of 30 µm. Image shown from Masson's trichrome stained smaller airway from 15-month-old Cre-negative $^{SM22\alpha}CaSR^{flox/flox}$ (Wild-type) mouse. Graticule (A and B) 50 µm. AT: Austria.

In collaboration with Mr Robert Nica at TissueGnostics (Vienna, AT), larger and smaller airways were incorporated into the adapted Ellis et al. (2003) method by adjusting the increment used to produce the concentric ring that would serve as the region for determining peribronchial collagen remodelling. To do this, the airway lumen and epithelium was identified manually and the outer circumference of this region was used to define the airway region, represented as 0µm. The concentric ring used for determining collagen deposition then grew outwards from this point.

Due to the anatomical differences between species and experimental differences in the expected severity of different models of lung remodelling, the size of collagen region used to determine peribronchial collagen was not kept the same. The

rationale for the deviations from Ellis et al. (2003) recommendations are detailed in **Table 2.2**.

Table 2.2. Summary of rationale used to adapt the Ellis et al. (2003) method to different species and experimental models.

Model	Airway size	Increment used	Rationale
COPD-like neutrophilic exacerbation	Larger Smaller	60µm 20µm	Smooth muscle region too large for smaller increments
Age-related fibrosis	Smaller	10µm	Half the recommended size for larger airways and remodelling expected to be mild
IgE/Th2- and alarmin-driven asthma	Larger Smaller	60µm 20µm	Moderate to severe smooth muscle and peribronchial collagen remodelling expected

2.1.8.2 Quantitative Histomorphometry of Airway Cross-section Components (qHACC)

Quantitative image analysis is well suited to determining changes in lung remodelling particularly due to its ability to combine marker location, histology and tissue morphology in a quantitative manner, this is termed histomorphometry. A number of published methodologies to determine characteristics of airway remodelling were found in the literature, including epithelial thickness (Royce et al., 2009); mucus-producing epithelial cells (i.e. goblet cells) (Zeki et al., 2010; Pini et al., 2010); smooth muscle thickness (Pini et al., 2010); and subepithelial/peribronchial collagen (Ellis et al., 2003; Royce et al., 2009).

However, many of these approaches were not applicable to a range of airway sizes as desired and were instead limited to first generation airways which were often unavailable due to the orientation of the pre-cut sections obtained from previous experiments. For example, Zeki et al. (2010) used a "mean goblet cell index" to determine goblet cell remodelling by quantifying the percentage of primary, secondary and tertiary conducting airway PAS-positive cells out of 100 or more epithelial cells over 5 regions of interest. To overcome this problem of unknown airway positioning, Pini et al. (2010) identified airways at random using size as a

control parameter, before manually measuring the thickness of the smooth muscle layer and the percentage of epithelial cells positively stained for mucins. Similarly, Royce et al. (2009) used size as a determinant of airway positioning by only including airways with a lumen diameter of between 150-350μm to determine epithelial and subepithelial collagen thickness.

Therefore, a novel approach was developed using StrataQuest by building on previously described methods and addressing their limitations such as prior knowledge of airway locus; the need for multiple staining protocols for each marker; manual cell counting; and lack of general airway health measurement. To do this, the bronchi and bronchioles were first separated by their size, larger (> 50,000μm^2) and smaller (< 50,000um^2), in a similar manner to the approach described by Hirota et al. (2006) to account for the morphological differences between airways of different sizes and location within the lung. Where pre-stained lung sections were not the only available resource, sections were stained with Masson's trichrome with aniline blue that is capable of staining both mucosubstances and collagen simultaneously. Airways were then imaged with the highest resolution objective that produced a file size suitable for StrataQuest (20x objective). Airway regions were identified manually using StrataQuest with the experimenter blinded to the experimental conditions, as shown in **Figure 2.7**.

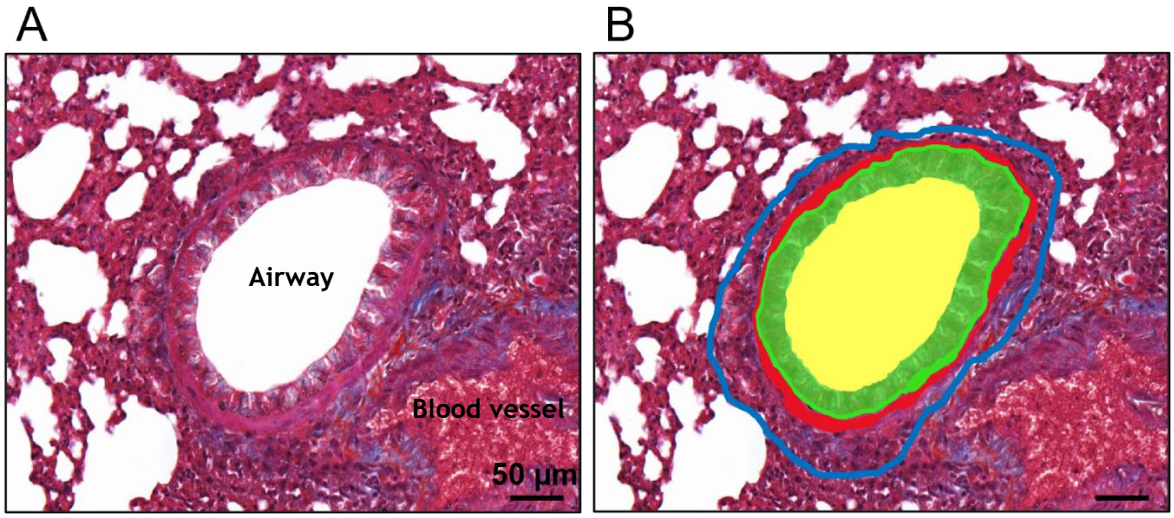

Figure 2.7. Graphical representation of manual region identification for the novel qHACC method using StrataQuest. (**A**) Normal smaller airway stained

with Masson's trichrome. (**B**) In the novel qHACC method airway structures are identified manually including the airway lumen (yellow), airway epithelium (green), RBM/smooth muscle (red) and peribronchial region (blue capsule). This method was also adapted for the larger airways. Image shown from Masson's trichrome stained smaller airway from 15-month-old Cre-negative $^{SM22\alpha}CaSR^{flox/flox}$ (Wild-type) mouse. Graticule (A and B) 50 μm. qHACC: quantitative histomorphometry of airway cross-section components.

Technical input on the StrataQuest programming was obtained from Mr Robert Nica from TissueGnostics (Vienna, AT), specifically to devise a method for determining total tissue, epithelial tissue, goblet cells, smooth muscle and total peribronchial collagen using histomorphometry. To do this, different tissues (mucosubstances, collagen and other tissues) were separated by colour using multiple reference shades for each marker taken from approximately 15 different instances of positive signal from examples of a range of staining intensities irrelevant of treatment group (due to experimenter blinding). This approach controls for inconsistencies in staining colour and intensity by eliminating any staining that does not match the reference shades or intensity threshold for positive signal. This control measure was performed for each individual experiment and was consistent across all experimental groups. In these experiments, Picrosirius Red stains collagen as dark red, nuclei brown and other tissues light red and PAS stains goblet cells purple, other tissues blue and nuclei brown. Alternatively, Masson's trichrome stains collagen dark blue, goblet cells light blue, nuclei brown and other tissues red. Although two shades of blue are present in this stain, that would typically be difficult to distinguish, the region in which the staining was present was also used to differentiate between mucosubstance staining in the airway epithelium and collagen staining in the subepithelial and peribronchial region. Each tissue was then translated into a grey image where the intensity of grey/white is proportional to the staining intensity for that marker. This is comparable to signal strength in a fluorescence image. Providing positively stained pixels surpassed the threshold for positive staining intensity (which was automatically determined by StrataQuest using the reference shades), the pixels were used to generate a positive signal mask. Here, only pixels within the specified regions of interest were included, shown in **Figure 2.8E-H**. These masks

and the known area of each pixel (determined by the Cardiff University Bioimaging Hub; **Table 2.3**) was used for subsequent area measurements. Furthermore, all tissue edges were marked by a blue photo-bleaching artifact, which was caused by the highly contrasting bright white background. To avoid mislabelling this photobleaching as blue staining, any blue colouration immediately adjacent to the white background (up to a distance of 1 pixel) was automatically removed.

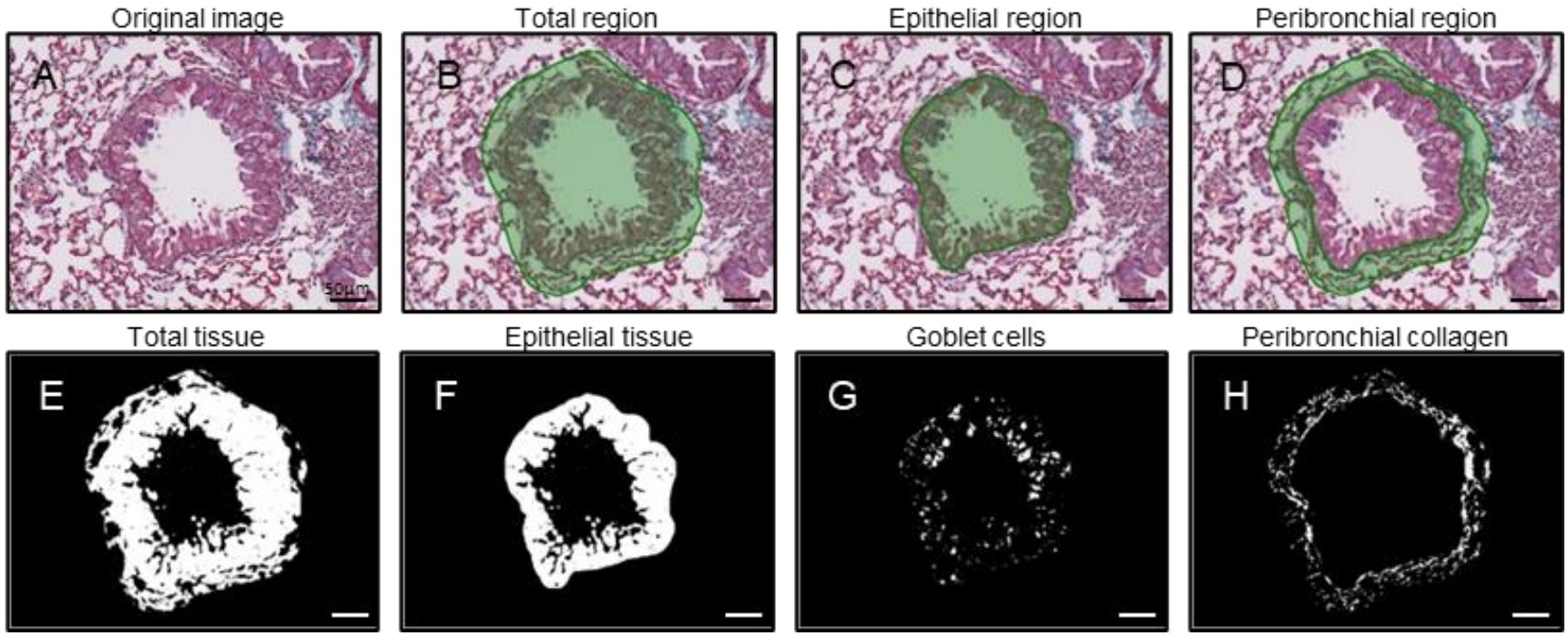

Figure 2.8. Visual representation of positive pixel quantification in qHACC using StrataQuest. Manually identified regions of interest (**B-D**) were used for positive pixel identification and measurements. For masson's trichrome staining, as shown in (**A**), and simiarly for picrosirius red staining (not shown), the tissues of interest, including cytoplasm (red), nuclei (brown), collagen (dark blue) and mucus (light blue), were separated into individual layers based on multiple reference shades and staining intensities for each colour. "Masks" (**E-H**) were then generated from the positive signal layers for each colour and used for subsequent area measurements to determine (**E**) Total tissue, (**F**) Epithelial tissue, (**G**) Goblet cells, smooth muscle (not shown), and (**H**) Peribronchial collagen. All calculations were then normalised to airway size. Image obtained from

Masson’s trichrome stained Balb/c mouse exposed to OVA-sensitisation and –challenge. Graticule (A-D) 50 µm. OVA: ovalbumin; qHACC: quantitative histomorphometry of airway cross-section components (this figure is published in Yarova et al., 2021).

Due to the versatility of manual region identification and the histological identification of mucosubstances, collagen and lung tissue, the quantitative histomorphometry of airway cross-section components (qHACC) approach can be used to determine epithelial thickening, goblet cells, smooth muscle, and peribronchial collagen. These measurements are defined in **Table 2.3**.

Several other markers were evaluated for the potential to be included in the qHACC analysis, including epithelial cell count and goblet cell count, perivascular tissue, perivascular collagen, peribronchial and perivascular tissue, peribronchial and perivascular collagen, as well as peribronchial and perivascular cell count using a combination of nuclei, collagen and/or tissue staining. However, cell identification was poor due to the image resolution of the 20x objective lens and poor nuclear staining intensity. Furthermore, vascular analyses were obstructed by extensive cross-section error and an inability to control for this. Therefore, these measurements were deemed too inaccurate to be included in the qHACC approach without significant improvement and could not be optimised within the timeframe of my PhD.

Table 2.3. Summary of qHACC image analysis measurement definitions.

Measurement	**Definition**
Pixel size	1px = 1.03μm^2
Airway size	Total epithelial region and airway lumen surface area (**Figure 2.8B**).
Positive staining/pixels	Any coloured pixels that exceeds the intensity threshold automatically determined by StrataQuest based on multiple reference shades taken from multiple randomly-selected images.
Total tissue	All positively stained light red, dark red, and brown pixels (Picrosirius red) or red, light blue, dark blue and brown (Masson's trichrome) pixels within the total tissue region (**Figure 2.8A**) divided by the airway size and expressed as a percentage of positive pixels 100μm^{-2}.
Epithelial tissue	All positively stained light red, dark red, and brown pixels (Picrosirius red) or red, light blue, dark blue and brown (Masson's trichrome) pixels within the epithelial region (**Figure 2.8B**) divided by the airway size and expressed as a percentage of positive pixels 100μm^{-2}.
Goblet cells	Only positively stained purple (periodic acid-Schiff) or light blue (Masson's trichrome) pixels located within the goblet cell region (**Figure 2.8C**)

	divided by the airway size and expressed as a percentage of positive pixels $100\mu m^{-2}$.
Smooth muscle	Only positively stained light red (Picrosirius red) or red (Masson's trichrome) pixels within the peribronchial region (**Figure 2.7B**; red) divided by the airway size and expressed as a percentage of positive pixels $100\mu m^{-2}$
Peribronchial collagen	Only positively stained dark red (Picrosirius red) or dark blue (Masson's trichrome) pixels within the peribronchial region (**Figure 2.8D**) divided by the airway size and expressed as a percentage of positive pixels $100\mu m^{-2}$

2.1.8.3 Quantitative Histomorphometry of Interstitial Tissue (qHIT)

Ashcroft et al. (1988) first developed a semi-quantitative scoring approach to determine fibrosis using pre-clinical models of bleomycin-induced fibrosis. This approach is easily accessible and requires only a microscope; however, there are several limitations such as histopathological experience is required to achieve reproducible results; the assignment of scoring is subjective and vulnerable to experimenter bias; and the discontinuous scale (from 0 to 8), designed to score severe bleomycin-induced fibrosis, and is not well suited to models where fibrosis is less severe (i.e. where fibrotic foci are absent).

Grading of the Ashcroft scoring system involves qualitative assessment of the level of thickening to the alveolar or bronchiolar walls, distortion of lung structure and formation of fibrous masses (Ashcroft et al., 1988). Hübner et al. (2008) built upon this method by improving the detail of each definition, separating the alveolar septa from the lung structure and defining the differences between scores in terms of the percentage of the field of view area affected by fibrotic masses (Hübner et al., 2008).

Here, I identified that all these observations will result in a net increase in alveolar interstitial tissue. Therefore, using Fiji image analysis software and the imaging protocol described in **section 2.1.7.4**, regions of alveolar parenchyma were identified at random in picrosirius red or Masson's trichrome stained lung sections with the experimenter blinded to the experimental conditions. Once images were imported into Fiji, the "Huang" thresholding feature was used to create a "mask",

a term describing the generation of a new image where all negatively stained pixels (i.e. the white background) have been removed. The area of the remaining pixels were then calculated as a percentage of the original image size (**Figure 2.9**). Therefore, using the principles of the Ashcroft and modified Ashcroft scoring systems, a novel methodology, termed quantitative histomorphometry of interstitial tissue (qHIT), was built. However, unlike the modified Ashcroft scoring system this approach is non-specific, unbiased and sensitive to changes in lung morphology. Here, the change in tissue area between treatment groups is a surrogate for alveolar interstitial tissue and extracellular matrix (ECM) remodelling as well as cellular remodelling such as alveolar epithelial metaplasia and angiogenesis. Furthermore, a net decrease in tissue area would be indicative of emphysema-like alveolar destruction. However, due to the non-specific nature of this approach, inflammatory cells or is not specifically identified or removed and so is included in the analysis. Therefore, any changes observed are described as a change in interstitial tissue and inflammation until this method can be further developed to identify specific cell types and eliminate non-remodelling characteristics from the analysis.

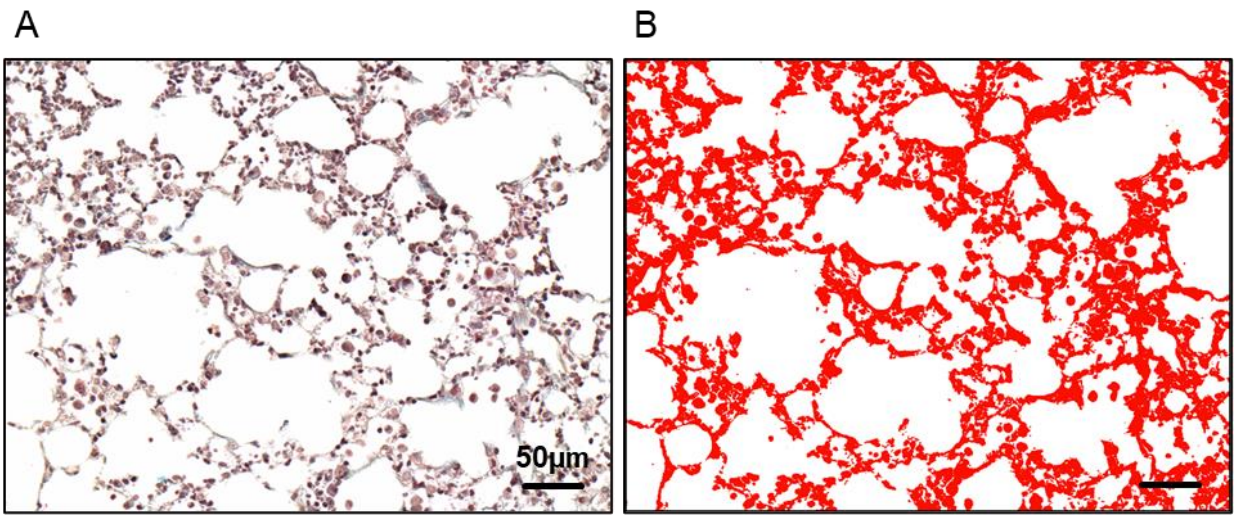

Figure 2.9. Visual representation of qHIT positive signal identification using Fiji. (**A**) The same Masson's trichrome or picrosirius red stain was used to identify regions of tissue lacking airways and vasculature. (**B**) The "Huang" thresholding feature was used to mask positive signal (red) and exclude the background (white) for the quantification of the area of interstitial tissue and

inflammation. Image obtained from Masson's trichrome stained Balb/c mouse exposed to OVA-sensitisation and –challenge. Graticule (A and B) 50 µm. qHIT: quantitative histomorphometry of interstitial tissue; OVA: Ovalbumin.

2.1.8.4 Modified Ashcroft Scale

Although the presence of collagen is not a discrete marker of pathology, collagen is a major component of fibrous extracellular matrix deposited by (myo)fibroblasts and is often used as a marker of ECM remodelling (Redente et al., 2011; Redente et al., 2014). Semi-quantitative scoring systems, such as the modified Ashcroft scale (Hübner et al., 2008), are often used to determine extent of parenchymal fibrosis in severe models of lung fibrosis, such as bleomycin injury, and represents the current industry standard measurement of lung fibrosis. A modified Ashcroft scale (Hübner et al., 2008) was used to determine the severity of fibrosis observed on a grade scale of 0 – 8 using images of the distal lung parenchyma obtained for the qHIT analysis. Example photos provided by Hübner et al. (2008) were used for reference.

2.2 *In vitro* studies

2.2.1 Normal human lung fibroblasts

All consumable and equipment was disinfected with 70% ethanol prior to use. Normal human lung fibroblasts (NHLFs) were purchased from Lonza (Slough, UK) three ethically consented patients, between the ages of 56 and 67, that did not exhibit inflammatory or interstitial lung disease characteristics. These cells were cultured in accordance with the protocol provided by Lonza. Cells were seeded onto 8-chamber Millicell EZ slides (Merck Millipore, Watford, UK) at densities of 0.5×10^3 in Lonza custom fibroblast basal medium-2 (FBM-2) with additional Lonza SingleQuot supplements (FGM-2) containing insulin, recombinant human fibroblast growth factor B (hFGF-B), GA-1000 antibiotics (containing 0.1 % gentamicin and 0.1 % amphotericin B), and fetal bovine serum (FBS) and incubated at 37 °C in a humidified incubator with 5% CO_2. Medium was replaced every other day until the start of the experiment. During the experiment, once cells had reached ~60% confluency, cells were changed to the experimental medium containing 50 ml fibroblast basal medium (FBM)-2, 0.1 % insulin, 0.1 % human fibroblast growth factor (hFGF)-B and 0.1% fetal bovine serum (FBS) but gentamicin and amphotericin (GA)-1000 was ablated as

aminoglycoside antibiotics, such as gentamicin are CaSR activators (McLarnon et al., 2002; Ward et al., 2002). The experimental medium also contained 1.81 mM free ionised Ca^{2+} as measured by my colleague, Dr Kasope Wolffs. Cells were split into four groups once desired confluence had been reached and serum-containing medium had been removed to halt cell cycle progression, including 1) vehicle control: 0.01% DMSO in phosphate-buffered saline (PBS); 2) NAM only: 1 μM NPS2143 and 0.01% DMSO in PBS for 72 hours; 3) transforming growth factor (TGF)-β: recombinant human TGF-β1 (5 ng/ml TGF-β1 and 0.01% DMSO in PBS) in experimental medium for 72 hours; and 4) TGF-β + NAM: a 4-hour pre-incubation with NAM (1 μM NPS2143 and 0.01% DMSO in PBS) followed by treatment with TGF-β1 and NAM (5 ng/ml TGF-β1, 1 μM NPS2143 and 0.01% DMSO in PBS) in experimental medium for 72 hours. **Figure 2.10** shows the experimental timeline for this experiment that was planned and performed by my colleague Dr Kasope Wolffs with my occasional aid.

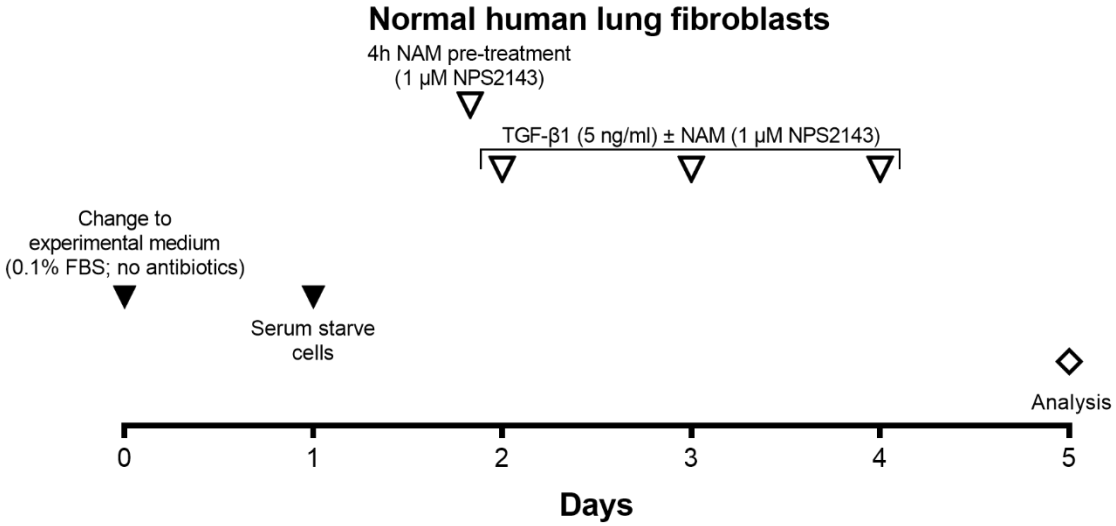

Figure 2.10. Experimental timeline for normal human lung fibroblast experiment. Lung fibroblasts from normal donors (patient CC-2612; Lonza ,UK) were incubated at 37 °C under humidified conditions with 5% CO_2. At 80 - 90% confluence cells were seeded into 8-chamber Millicell EZ slides at densities of $0.5x10^4$ in Lonza custom fibroblast basal medium-2 (FBM-2) with additional Lonza SingleQuot supplements (FGM-2). On day 0, when cells presented 50 - 60% confluency, growth medium was replaced with experimental medium. On the next day the cells were starved (serum-free experimental medium) to halt cell

growth cycle. On day 2, medium was aspirated, and cells were treated with TGF-β1 (5 ng/ml TGF-β1 and 0.01% DMSO in experimental medium) or TGF-β + NAM (0.1 μM NPS2143, 5 ng/ml TGF-β1 and 0.01% DMSO in experimental medium). Pre-treatment involved an incubation with NAM (1 μM NPS2143 and 0.01% DMSO in experimental medium) 4 hours prior to treatment with TGF-β1. NAM: Negative allosteric modulator of the calcium-sensing receptor; DMSO: Dimethyl Sulfoxide; TGF-β1: Transforming growth factor beta 1; FBS: Fetal bovine serum; FBM: Fibroblast basal medium; FGM: Fibroblast growth medium.

2.2.2 Immunofluorescence

2.2.2.1 CaSR and αSMA labelling

CaSR and α-smooth muscle actin (αSMA) immunolabelling was first optimised in human embryonic kidney cells transfected with the CaSR (CaSR-HEK 293) (**Figure 2.11)** using negative primary antibody controls and a non-specific IgG2a isotype control was used to ensure target specificity, as shown in **Figure S9.2**. The antibodies used in these studies are described in more detail in **Table 2.4**. Following optimisation, this protocol was performed on normal human lung fibroblasts fixed with a 20-minute incubation with 2% paraformaldehyde (PFA) solution in PBS. Fixed cells were then incubated in blocking buffer, containing 1% bovine serum albumin (BSA), 3% goat serum and 0.1% triton X100 in filter sterilised PBS (pH 7.4) for one hour before primary antibody co-incubations of the anti-CaSR (ab19347; 1:200) and anti-αSMA (ab5694; 1:300) suspended in blocking buffer solution, at recommended concentrations listed in **Table 2.4** overnight (>12 hours). Next, phosphate-buffered saline (PBS) solution (pH 7.4) washes were performed in three iterations of five-minutes following medium aspiration and antibody incubation steps. Secondary antibody incubation was performed with AlexaFluor488 (ab150077; 1:500) and AlexaFluor594 (A11005; 1:1000) in blocking buffer for one hour. Antibody solutions suspended in blocking buffer were centrifuged for 5 minutes at 15,000 relative centrifugal field (RCF). Mounting was then performed using glycerol based Vectashield (Vector Labs, UK) containing the nuclei stain, 4,6-diamidino-2-phenylindole (DAPI), overnight at 4 ˚C. Nail varnish was then used to seal the glass coverslips to the slide for longevity. Negative control incubations were included to distinguish immunoreactivity from off-target staining and auto-fluorescence. This

was achieved by abrogating the primary antibody incubation step for a blocking buffer only incubation while all other steps and reagents remained the same.

Table 2.4. Summary of antibodies used in immunohistochemical and immunofluorescence experiments. A range of antibodies were used to identify specific protein targets (primary antibodies; unconjugated) or label these targets for detection (secondary antibodies; AlexaFluor488/594) using immunofluorescence or immunohistochemistry. CaSR: Calcium-sensing receptor; αSMA: alpha smooth muscle actin; ROCK1: Rho-associated coiled-coil containing protein kinase 1; IgG: Immunoglobulin G; IgG2a: Immunoglobulin G isotype 2a.

Antibody Target	Antibody No.	Supplier	Species detected	Host	Dilution	Isotype	Conjugation
CaSR (N-terminal)	ab19347	Abcam	Human, Mouse	Mouse (monoclonal)	1:200	IgG2a	Unconjugated
αSMA (N-terminal)	ab5694	Abcam	Human, Mouse	Rabbit (polyclonal)	1:300	IgG	Unconjugated
ROCK1	Cat# 21850-1-AP	ProteinTech	Human, Mouse	Rabbit (polyclonal)	1:500	IgG	Unconjugated
Anti-Rabbit IgG H&L	ab150077	Abcam	Rabbit	Goat (polyclonal)	1:500	IgG	AlexaFluor488
Anti-Mouse IgG H&L	ab150113	Abcam	Mouse	Goat (polyclonal)	1:500	IgG	AlexaFluor488
Anti-Mouse IgG H&L	A11005	Thermofisher	Mouse	Goat (polyclonal)	1:1000	IgG	AlexaFluor594

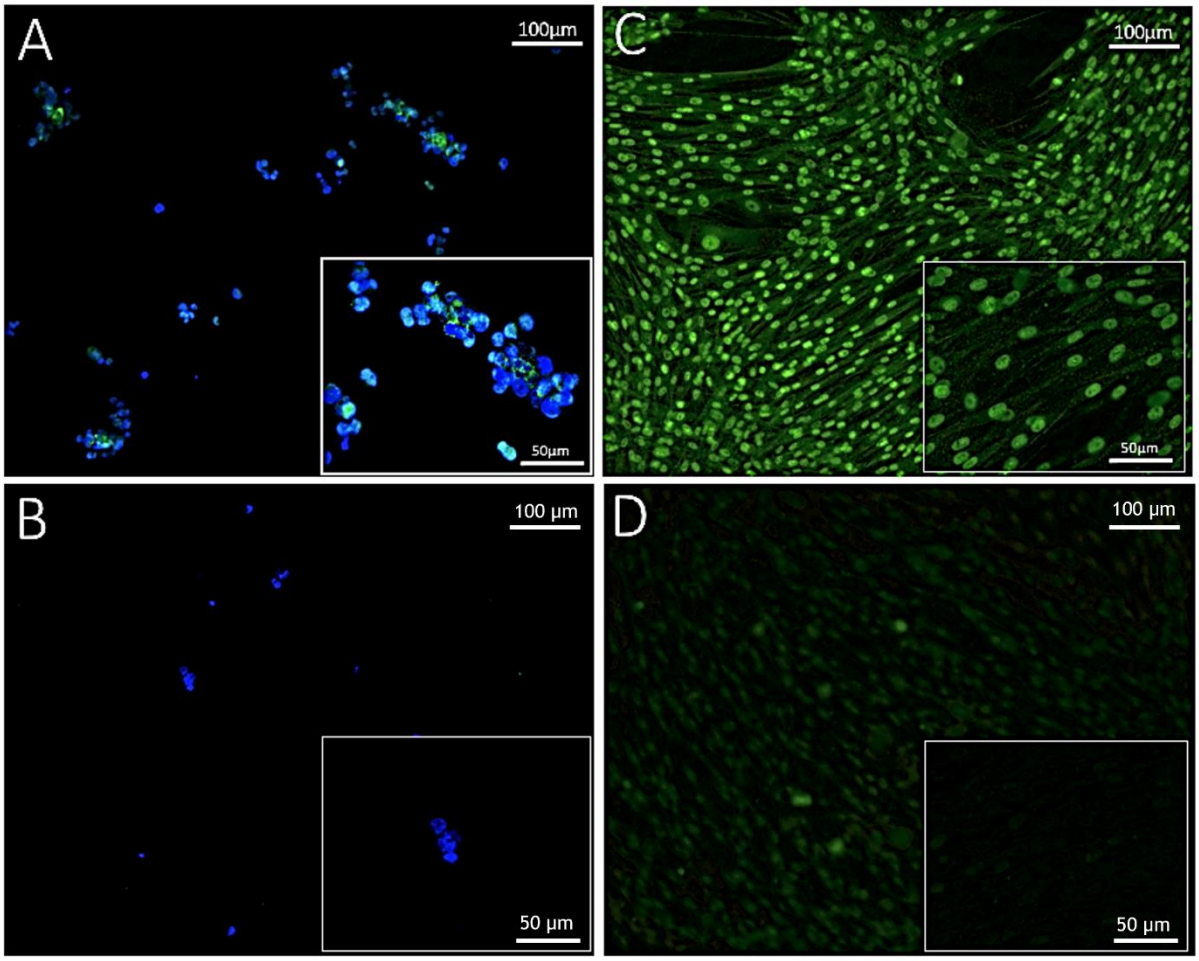

Figure 2.11. Optimisation of CaSR and αSMA immunoreactivity in (A, B) CaSR-HEK293 cells and (C, D) normal human lung fibroblasts, respectively. (**A**) Immunoreactivity was observed using the ab19347 human anti-CaSR antibody [5C10, ADD] (1:200) and (**C**) the ab5694 human anti-αSMA (1:300). (**B, D**) Negative controls. Immunofluorescence was performed on 2% paraformaldehyde fixed HEK-293 cells transfected with the human CaSR. Blocking and permeabilisation was achieved with 1% BSA-PBS, 3% goat serum and 0.1% triton X100. Areas selected at random using the DAPI field. CaSR-HEK293 cells and fibroblasts seeded at different densities. Mag: 10x and 40x. Brightness + 40%; contrast + 40%. Background subtracted using ImageJ ("separate colour"; 50.0 pixels). Graticule 100 µm larger image and 50 µm smaller image. CaSR-HEK293: Human embryonic kidney cells transfected with the calcium-sensing receptor; BSA: Bovine serum albumin; PBS: phosphate buffered saline; CaSR: calcium-

sensing receptor; αSMA: alpha smooth muscle actin; DAPI: 4,6-diamidino-2-phenylindole.

2.2.2.2 ROCK1 protein expression

Rho-associated coiled-coil containing protein kinase 1 (ROCK1) immunostaining was optimised in human embryonic kidney cells transfected with the CaSR (CaSR-HEK 293) cells. Following the 20-minute fixation step using 2% paraformaldehyde (PFA) solution in PBS, cells were incubated in blocking buffer, containing 1% BSA, 3% goat serum and 0.1% triton X100 in filter sterilised PBS (pH 7.4) for one hour before incubation of primary human anti-ROCK1 antibody (Cat# 21850-1-AP; 1:500) suspended in blocking buffer solution, at recommended concentrations listed in **Table 2.4** overnight (>12 hours). Phosphate-buffered saline (PBS) solution (pH 7.4) washes were performed in three iterations of five-minutes following medium aspiration and following antibody incubation steps. Three further iterations of 5-minute PBS (pH 7.4) washes then preceded secondary antibody incubation with anti-rabbit AlexaFluor488 (ab150077; 1:500) in blocking buffer for one hour. Antibody suspensions were centrifuged at 15,000 relative centrifugal force (RCF) for 5 minutes before use. Cells were mounted using phalloidin (1:250) in PBS in 1:1 ratio with glycerol based Vectashield with DAPI (Vector Labs, UK) overnight at 4 °C. Nail varnish was then used to seal the glass coverslips to the slide for longevity. Negative control incubations were included to distinguish immunoreactivity from off-target staining and auto-fluorescence. This was achieved by abrogating the primary antibody incubation step for a blocking buffer step while all other steps and reagents remained the same.

2.2.2.3 Immunofluorescent imaging

An Olympus BX61 fluorescent microscope (CaSR and αSMA) or Zeiss LSM 880 upright confocal microscope (Zeiss, UK) (ROCK1) was used to image NHLFs at wavelengths 358nm (DAPI), 488nm (FITC) and 594nm (TRITC) using the 63x objective lens. Exposure times were optimised automatically using inbuilt surveyor (Objective Imaging Ltd, Cambridge, UK) programming and were maximised without exceeding the point of saturation (approx. 1-5 seconds). Areas of suitable cell density (40 % of the image area) were identified using the DAPI filter. Following imaging the

background was subtracted for analysis using StrataQuest utilising the “separate colour” function in ImageJ (Schneider et al., 2018) set at the default level (50.0 pixels).

2.2.3 *In vitro* immunofluorescent image analysis

The StrataQuest software was also used to determine the mean intensity of CaSR, αSMA and ROCK1 immunolabelling *in vitro* using normal human lung fibroblasts to investigate the effect of NAM treatment on TGF-ß-induced protein. To do this, cells were identified as nuclei-containing areas of positive staining. Therefore, cells without a visible nuclei or cells where the nuclei were outside the image region were excluded. An algorithm was then set to identify positive pixels by increasing in size in all directions (i.e. growing out from the nucleus) until there was a break in the staining or interaction with another cell and the algorithm “growing out” from that nucleus, as shown in **Figure 2.12**. High marker presence is indicated by white and low marker presence indicated by black. All measurements were then normalised to the number of cells in that region of interest. This protocol was also used to determine positive staining surface area.

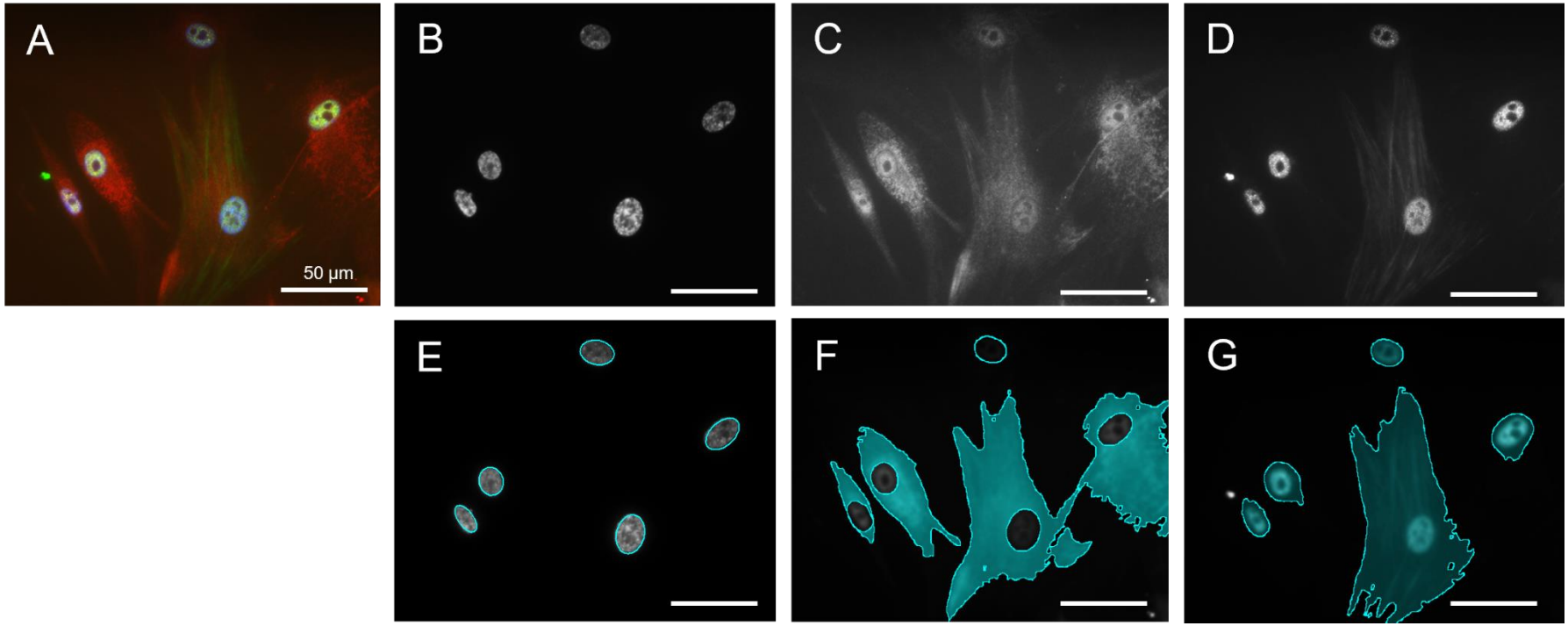

Figure 2.12. Visual representation of immunofluorescent labelling protocol using StrataQuest. (**A**) representative immunoreactivity from all three excitation wavelengths (DAPI, 488, 594) stacked together with artificial colouration. (**B, C, D**) shows representative images from each wavelength without artificial colouration (**B**) nuclei, (**C**) CaSR and (**D**) αSMA staining shown in white on their respective images. Finally, (**E, F, G**) show representative (**E**) nuclei and (**F** and **G**) cell barrier identification and the to determine (**F**) CaSR, (G) αSMA and (not shown) ROCK1 immunoreactivity as a measurement of protein marker expression. Images obtained from normal human lung fibroblasts exposed to 5 ng/ml TGF-ß1; 63x objective; graticule

50 μm. αSMA: alpha-smooth muscle actin; CaSR: calcium-sensing receptor; ROCK1; Rho-associated coiled-coil containing protein kinase 1.

2.2.4 RNA-sequencing

Ribonucleic acid (RNA) was extracted from NHLFs cultured as described in **section 2.2.1** in 6-well plates, using the RNeasy Mini Kit, including the optional on-column DNase digestion (Qiagen, Manchester, UK) according to the manufacturer's protocol for cell culture. This was performed by Dr Kasope Wolffs. Sequencing libraries were prepared at the Genome Hub facility (Cardiff University) using 500 ng total RNA and the Illumina Truseq standard mRNA kit in accordance with the manufacturer's protocols (Illumina, Cambridge, UK). Dual Indexes were made using the Truseq RNA UD indexing plate to ensure accurate library sequencing. The resulting libraries were sequenced on the Illumina NextSeq 500 sequencer platform (Illumina, Cambridge, UK) in 75 bp single end sequencing method, generating approximately 40-42 million reads per sample. Reads in fastq format were aligned to the human reference genome version GRCh38.100 (Ensembl, v.103; Yates et al., 2020) and annotated using Spliced Transcripts Alignment to a Reference (STAR) alignment (STAR/2.7.3a; Dobin et al., 2013). Reads per gene were counted and normalised by the STAR alignment programme in Linux. Finally, differential gene expression was calculated using DESeq2 (Love et al., 2014) using SARTools (v1.7.3; Varet, 2019) in the R Statistical Environment. The changes in gene expression were calculated for pairwise group comparisons, adjusting the p value to account for the false discovery rate (p_{adj}) using the Benjamini-Hochberg correction. This was achieved in collaboration with Dr Daniel Pass in the Genome Hub facility (Cardiff University).

Gene Ontology (GO) enrichment analysis was then performed on these shortlisted differentially expressed genes using the GOnet tool by inputting up- and down-regulated genes in separately to determine the direction of regulation (Pomaznoy et al., 2018). The results of this GO enrichment analysis were analysed manually by cross-referencing known TGF-β signalling pathways and remodelling processes in a hypothesis-driven manner. This was further investigated using a gene-by-gene pathway analysis to investigate the expression of key pathway genes to help determine the direction of pathway regulation.

2.3 Data analysis and statistics

Sample sizes and statistical approaches were decided before the data had been collected and the threshold for significance was set to $\alpha = 0.05$. A Shapiro-Wilk test was used to determine data normality (parametric or non-parametric data). Based on the outcome of this test, a T test (parametric data) or Mann-Whitney U test (non-parametric data) was used to statistically analyse data in experiments where only two treatment groups were used. In experiments with three or more treatment groups a one-way ANOVA with post hoc Holm-Sidak p-value adjusted (p_{adj}) multiple comparisons test (parametric) or Kruskal Wallis with post hoc Dunn's p-value adjusted (p_{adj}) multiple comparisons test (non-parametric) was performed. Unnecessary multiple comparisons tests were also minimised. This was the case for all studies except for the RNA-sequencing experiment that was analysed as described in **section 2.2.3**.

Microsoft Excel was used to collate raw data and make calculations and GraphPad Prism 9 was used to analyse data, perform all statistical analyses and produce figures unless otherwise specified. Data are expressed as median per biological replicate (i.e. per animal or per plate of cells for *in vitro* studies) throughout. Data are presented as medians calculated from the combination of randomly selected regions of interest for each animal or well (i.e. *in vitro* experiments). Truncated violin-plots were used to present the median, upper and lower quartiles as well as variation within the data. Statistical significance between groups is also labelled on each graph. In this thesis, N represents the number of biological replicates (animals *in vivo* or different plate-downs *in vitro*) and n represents the number of technical replicates (e.g. the number of lung sections stained separately for *in vivo* experiments or the number of wells per plate in *in vitro* experiments).

CHAPTER 3: METHOD DEVELOPMENT

3.1 Introduction

Before I could begin to investigate the role of the calcium-sensing receptor (CaSR) in lung remodelling, I had to identify a suitable method of determining molecular, cellular and tissue remodelling in the lung. To my knowledge, no quantitative method existed capable of determining a range of airway remodelling components. Methods involving quantitative image analysis have become a preferred method for determining lung remodelling due to their ability to quantify markers in a loci-specific manner and reduction in experimenter bias and subjectivity.

Inhaled lipopolysaccharide (LPS) challenge is often used in pre-clinical investigations due to its ability to recapitulate many features of chronic obstructive pulmonary disease (COPD) pathophysiology, particularly neutrophilia, increased cytokine (interleukin (IL)-1ß, IL-6, and tumour necrosis factor (TNF)-α) production, goblet cell hyperplasia, increased airway smooth muscle mass, peribronchial collagen deposition, airway and interstitial wall thickening and emphysematous destruction of alveolar walls (Toward & Broadley, 2002; Savov et al., 2002; Vernooy et al., 2002; Savov et al., 2003; Brass et al., 2003; Brass et al., 2004; Willemse et al., 2005a; Savov et al., 2005; Saetta et al., 2006; Brass et al., 2007a; Hogg & Timens, 2009; Pera, 2011). Therefore, this model should be a suitable choice for determining a variety of airway and interstitial lung remodelling characteristics. Furthermore, professional histopathologists at AstraZeneca had already determined that inhaled NAM reduced interstitial wall thickening in these animals (Yarova et al., 2016).

The aim of this study was to to compare quantitative image analysis approaches for determining changes in airway and alveolar interstitial lung remodelling in a model of COPD-like neutrophilic exacerbation on 1) five major COPD-like airway remodelling characteristics in the larger and smaller airways, using the Ellis et al. (2003) and quantitative histomorphometry of airway cross-section components (qHACC) approach, and 2) interstitial remodelling using quantitative histomorphometry of interstitial tissue (qHIT) in direct comparison with existing histopathological analysis performed by AstraZeneca.

3.2 Results

Lung remodelling was induced in this model using nebulised LPS-challenge (30 µg/ml) on alternating days over an 18-day period and inhaled therapeutic treatment with a nebulised negative allosteric modulator of the CaSR (NAM; 3 µM) was provided from day 9. Following organ harvest, fixation and lung sectioning, lung sections were stained with picrosirius red and the larger airways (> 50,000um^2), smaller airways (< 50,000um^2) and alveolar insterstitial regions were imaged for analysis of remodelling characteristics. Previously, this model has been shown to present histological evidence of oedema, epithelial disruption, leukocyte infiltration and goblet cell metaplasia but not emphysematous alveolar disruption (Toward & Broadley, 2001). However, airways from naïve animals were unavailable to confirm the degree of remodelling induced. All statistical analyses were performed using T tests.

3.2.1 COPD-like peribronchial collagen remodelling was unaffected by NAM treatment.

The Ellis et al. (2003) method was used to determine peribronchial collagen in these airways due to its proven effectiveness in determining peribronchial collagen remodelling in murine models of inflammatory lung disease following adaptation to match the altered physiology of guinea pig airways, compared to mouse airways. Using this approach, this study found NAM treatment did not affect peribronchial collagen remodelling in the larger airways (***p* = 0.66, 60µm region**) or the smaller airways (***p* = 0.74, 20µm region**) compared to the LPS-challenged positive control group, as shown in **Figure 3.1**.

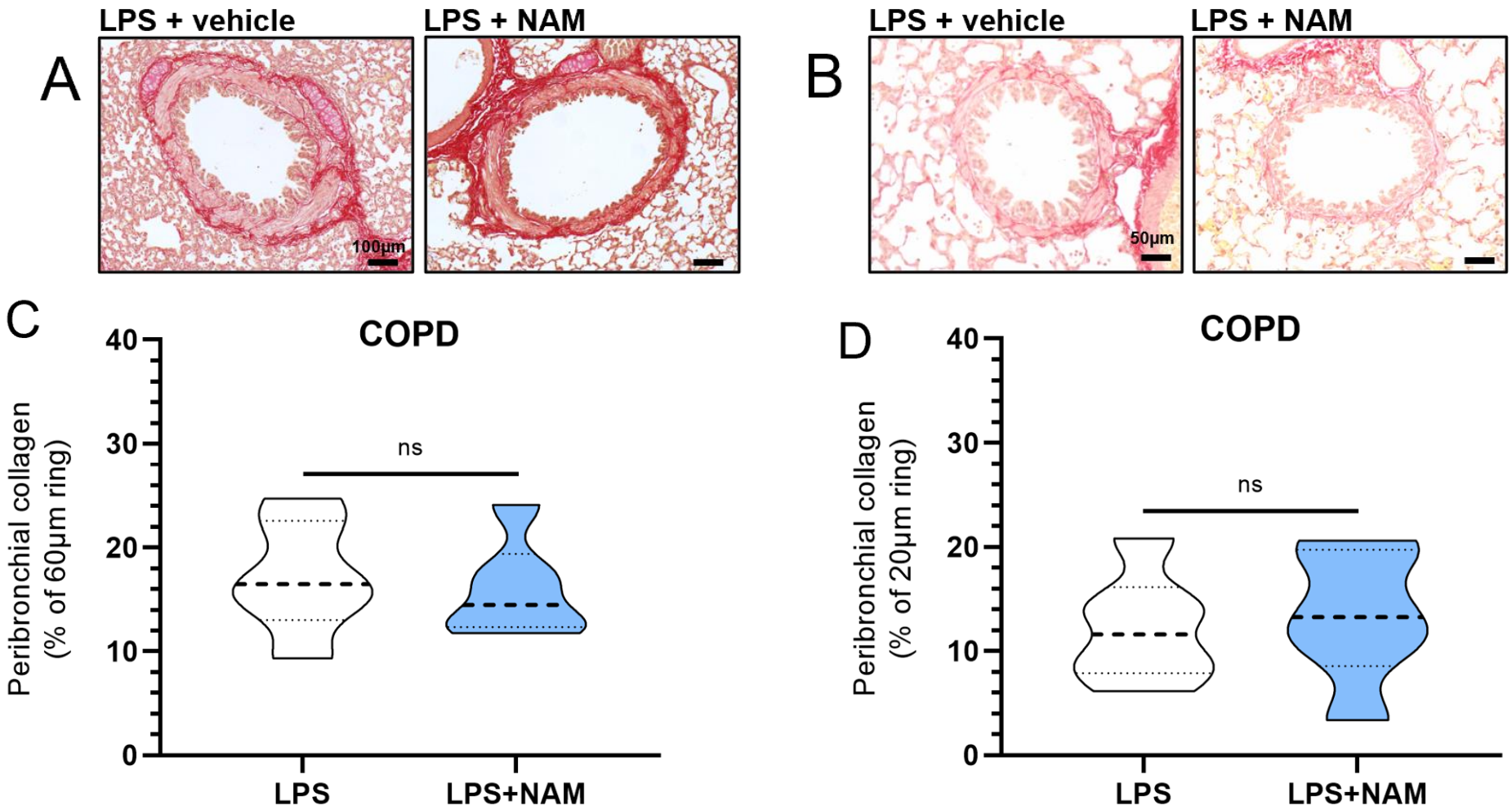

Figure 3.1. No significant differences were observed in larger or smaller airway peribronchial collagen in the COPD-like neutrophilic exacerbation model using the Ellis et al. (2003) method. (**A**) Larger airways (> 50,000 µm^2) and (**B**) smaller airways (< 50,000 µm^2) stained with picrosirius red were analysed for the percentage of collagen in the (**C**) 60µm region or (**D**)

20µm region using the Ellis et al. (2003) method, respectively. Statistical significance identified using a T test. Truncated violin plots were used to demonstrate frequency distribution of the data where dashed lines represent the median and dotted lines represent the upper and lower quartiles, respectively. N = 6, n = 3, ROI = 2-7 (larger airways) and 1-7 (smaller airways), ns ($p > 0.05$). Graticule (A) 100 µm and (B) 50 µm. LPS: lipopolysaccharide; NAM: negative allosteric modulator of the calcium-sensing receptor; COPD: chronic obstructive pulmonary disease.

3.2.2 COPD-like airway remodelling was unaffected by NAM treatment

Here, the novel qHACC approach was used to determine characteristics of airway remodelling not incorporated in the Ellis et al. (2003) method. In this experiment, the measurement of total peribronchial collagen differs from the Ellis et al. (2003) method by incorporating the total presence of collagen in the peribronchial region, opposed to the concentration in a specified region. In the larger airways, NAM treatment had no significant effect on total tissue (***p* = 0.61**), epithelial tissue (***p* = 0.47**), goblet cells (***p* = 0.093**), smooth muscle (***p* = 0.29**) and total peribronchial collagen (***p* = 0.95**) remodelling when compared to inhaled LPS challenge alone, as shown in **Figure 3.2E**. In the smaller airways, NAM treatment had no significant effect on total tissue (***p* = 0.085**), epithelial tissue (***p* = 0.054**), goblet cells (***p* = 0.82**), smooth muscle (***p* = 0.083**) or total peribronchial collagen (***p* = 0.28**), as shown in **Figure 3.2F**. Unfortunately, too few suitable airways from naïve animals could be identified to provide an adequate baseline for the characteristics assessed in the Ellis et al. (2003) and qHACC methods, representing a major limitation.

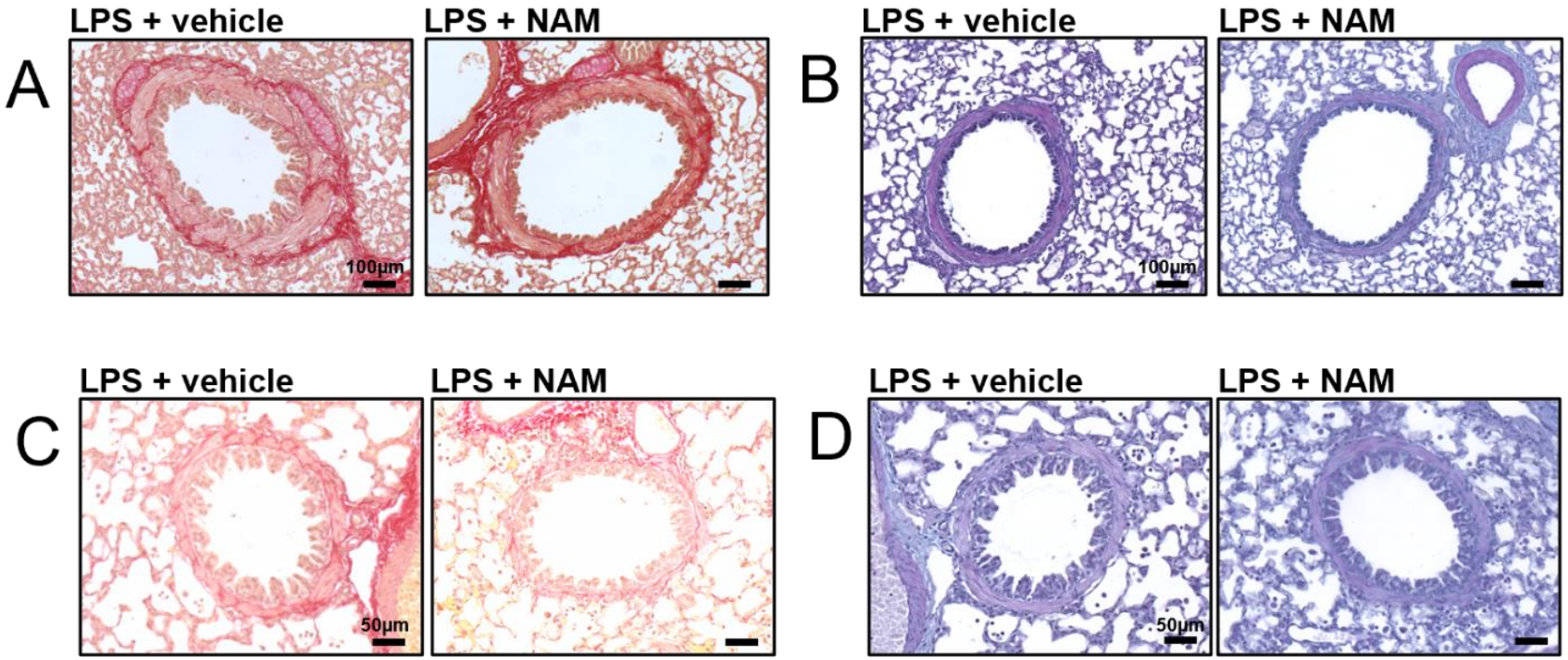
A
LPS + vehicle
LPS + NAM
100μm
B
LPS + vehicle
LPS + NAM
100μm
C
LPS + vehicle
LPS + NAM
50μm
D
LPS + vehicle
LPS + NAM
50μm

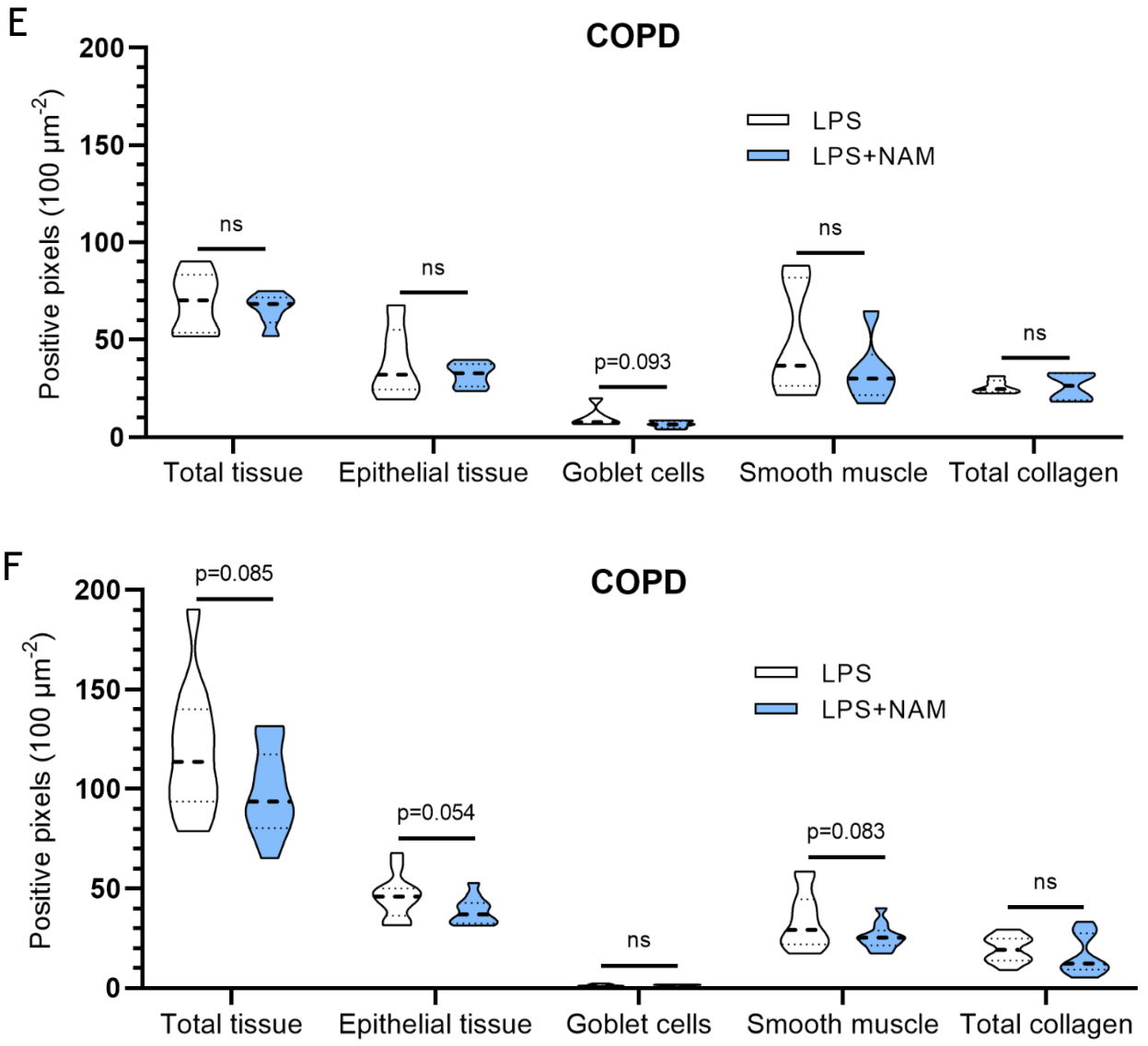
E
COPD
Positive pixels (100 µm-2)
200
150
100
50
0
LPS
LPS+NAM
ns
ns
p=0.093
ns
ns
Total tissue
Epithelial tissue
Goblet cells
Smooth muscle
Total collagen
F
COPD
Positive pixels (100 µm-2)
200
150
100
50
0
LPS
LPS+NAM
p=0.085
p=0.054
ns
p=0.083
ns
Total tissue
Epithelial tissue
Goblet cells
Smooth muscle
Total collagen

Figure 3.2. Inhaled NAM treatment had no statistically significant effect on smaller airway remodelling in a guinea pig model of COPD-like neutrophilic exacerbation. In the (**A, B**) larger airways (> 50,000 μm^2) and (**C, D**) smaller airways (< 50,000 μm^2) (**A, C**) picrosirius red and (**B, D**) PAS stained airways were used to determine the effect of NAM treatment (**E, F**) airway remodelling in LPS-challenged guinea pigs using the qHACC approach. Statistical significance was identified using a T test and truncated violin plots were used to demonstrate the frequency distribution of the data, where dashed lines represent the median and dotted lines represent the upper and lower quartiles. N = 6 (larger airways), 12 (smaller airways) and 6 (smaller airway goblet cells), n = 3, ROI = 2-7 (larger airways), 2-14 (larger airway goblet cells), 1-7 (smaller airways) and 3-19 (smaller airway goblet cells), ns ($p > 0.05$). PAS: periodic acid-schiff; COPD: chronic obstructive pulmonary disease; LPS: lipopolysaccharide; qHACC: quatitative histomorphometry of airway cross-section components; NAM: negative allosteric modulator of the calcium-sensing receptor.

3.2.3 NAM treatment reduced interstitial tissue and inflammation in a guinea pig model of COPD-like neutrophilic exacerbation

In this model of COPD-like neutrophilic exacerbation, inhaled NAM treatment abolished LPS-induced interstitial tissue and inflammation (***p* = 0.037**), as shown in **Figure 3.3**. Here, interstitial tissue and inflammation were determined using the qHIT method and these findings support the previously published professional histopathologist analysis performed at AstraZeneca (Yarova et al., 2016).

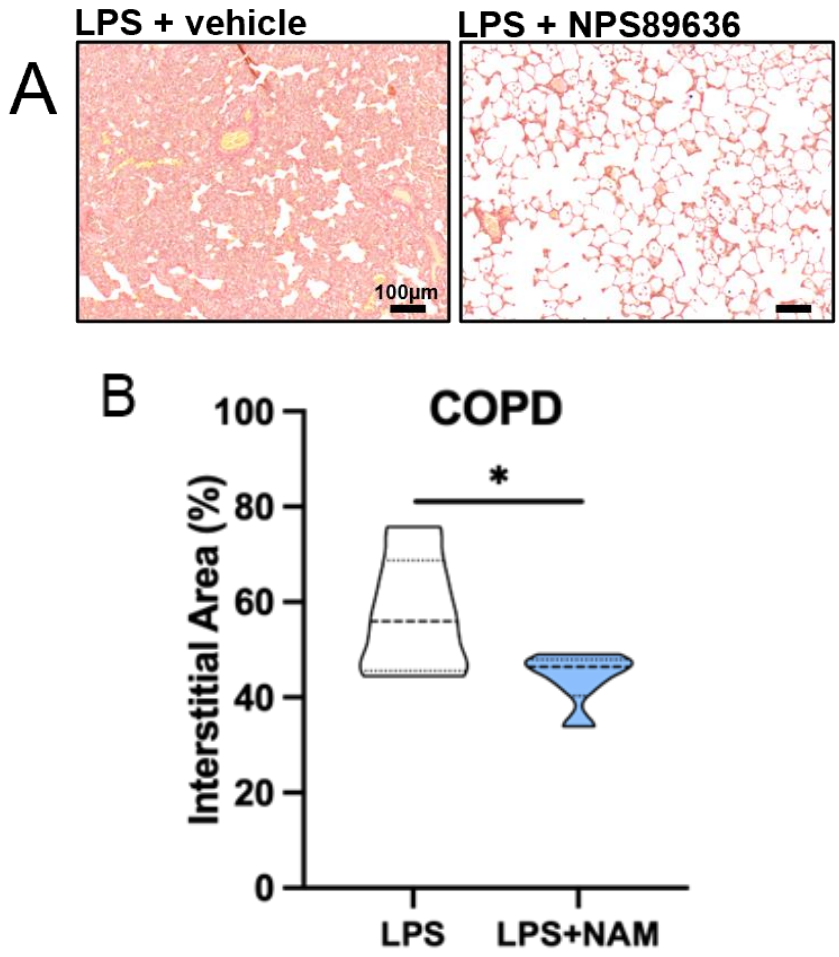

Figure 3.3. Inhaled NAM treatment abolished interstitial remodelling in the guinea pig model of COPD-like neutrophilic exacerbation. In the alveolar interstitium (**A**) picrosirius red staining was used to determine (**B**) interstitial area in LPS-challenged guinea pigs. Here a significant reduction in interstitial tissue remodelling and/or inflammation was observed following inhaled NAM treatment (NPS89636) using the qHIT approach. Statistical significance identified using a T test. Truncated violin plot was used to demonstrate frequency distribution of the data where dashed lines represent the median and dotted lines represent the upper and lower quartiles, respectively. N = 6, n = 3, ROI = 3-10, * ($p < 0.05$). Graticule (A) 100 µm. LPS: lipopolysaccharide; NAM: negative allosteric modulator of the calcium-sensing receptor; COPD: chronic obstructive pulmonary disease; qHIT: quantitative histomorphometry of interstitial tissue.

3.3 Discussion

Prior to my PhD studies, there were no methods capable of quantifying a range of airway remodelling characteristics in pre-clinical models of inflammatory lung disease, particularly if resources are limited or pre-cut lung sections have been obtained. Furthermore, the industry standard method for determining interstitial remodelling, the Ashcroft score, is semi-quantitative and relies heavily on experimenter subjectivity and histopathological experience. Here, I have developed two novel quantitative techniques for determining changes in airway and interstitial lung remodelling, respectively, that address key limitations of previously described methods and maximise the potential research output of novel experiments or lung tissue available from previous experiments.

The qHACC approach was developed to address the current shortfalls of quantifying remodelling in the lung. The qHACC approach is capable of determining four key markers of airway remodelling, epithelial and goblet cell metaplasia, smooth muscle hypertrophy and peribronchial fibrosis, across a range of airway sizes using a maximum of two histological stains. This maintains marker loci-specificity while reducing the resource-demand of conventional quantitative image analysis in the lung. Furthermore, the fifth measurement of total tissue permits the assessment of how multiple remodelling characteristics can have a compounding effect on overall airway health and airflow limitation. The measurement of total peribronchial collagen incorporates both a measurement of concentration and penetration of ECM remodelling into the lung parenchyma, the latter of which is information lost when using the Ellis et al. (2003) approach.

The qHACC approach was also employed on lung tissue obtained from a previous experiment designed to assess the effect of NAM treatment on inflammatory cell infiltration in the lung. Developing methods that can detect remodelling in shorter-term models is desirable for ethical reasons, such as minimising animal suffering, as well as practical reasons, such as increasing the value of previous experiments designed to investigate inflammation, which are usually shorter than those designed to evaluate remodelling. Lastly, the qHACC approach has been peer-reviewed

(Yarova et al., 2021) in addition to the peer-review of the approaches, found in the literature, that it was built upon (Ellis et al., 2003; Royce et al., 2009; Zeki et al., 2010; Pini et al., 2010).

The qHIT approach was also assessed in this study for its ability to determine a net increase in alveolar interstitial tissue and/or inflammation, to build on the analysis performed by professional histopathologists at AstraZeneca. The qHIT approach successfully identified a net change in interstitial tissue remodelling and/or inflammation that was induced by inhaled NAM treatment. This suggests that the qHIT approach may be a suitable method for alleviating labour and histopathological training demands of current approaches. This approach can also be performed on tissue samples from previous experiments with no specific tissue staining constraints. It also requires an open-source software which was used to maintain the accessibility of the current industry standard Ashcroft scoring system. This method could also be used to detect a net loss of interstitial tissue such as the emphysematous destruction of alveolar walls in severe cases of COPD, that usually occurs without obvious fibrosis (Snider et al., 1985; Blundell et al., 2004; Schindelin et al., 2012).

Mechanistically, the reduction of interstitial tissue remodelling and/or inflammation following NAM treatment is interesting in this model. LPS is thought to bind to LPS-binding protein (LBP) and mediate its effects via the toll-like receptor 4 (TLR4), which is itself implicated in the development of COPD in humans (Vogelzang et al., 1998; Brass et al., 2003; Brass et al., 2004; Wang et al., 2005; Brass et al., 2007b; Pera, 2020). Activation of TLR4 is then thought to activate downstream signalling pathways including nuclear factor kappa-light-chain-enhancer of activated B cells (NFκB) and extracellular signal-regulated kinase (ERK) signalling via transforming growth factor-ß (TGF-ß)-activated kinase 1 (TAK1). These signalling pathways are associated with the increased expression of inflammatory cytokines such as IL-1ß, IL-6 and TNF-α which have previously been shown to modulate CaSR expression in the lung or other tissues (Ulich et al., 1991; Vernooy et al., 2001; Vernooy et al., 2002; Brass et al., 2004; Canaff & Hendy, 2005; Brass et al., 2007b; Fetahu et al., 2014; Hendy & Canaff, 2016; Yarova et al., 2015; Pera, 2020). Furthermore, these

signalling pathways are all considered downstream signalling targets of the CaSR which demonstrates considerable overlap between the mechanism of action of LPS and the CaSR. Therefore, there is scope for and evidence to suggest the CaSR is central to the regulation of both remodelling and inflammatory cell infiltration in the lung parenchyma of these animals. However, future studies require more detailed analyses to further investigate these mechanisms to determine if NAM treatment can inhibit LPS-induced lung remodelling in the alveolar interstitium by inhibition of the aforementioned cell signalling pathways.

Evidence suggests there are several temporal factors relevant to COPD in humans. The disease can be present early in 20-45 year olds and develops progressively over a long time period before being detected usually much later following deterioration in lung function (Celli et al., 2003; De Marco et al., 2004). For logistical, as well as biological reasons, animals cannot be used to model the temporal factors of severe or long-term COPD and must be much shorter in duration (Wright et al., 2008; Vlahos & Bozinovski, 2014; Tanner & Single, 2020).

However, the acute phase of COPD exacerbation, ranging from 4 to 15 days in duration, can be modelled in guinea pigs relatively well (Toward & Broadley, 2001; Toward & Broadley, 2002; Miravitlles et al., 2013; Yarova et al., 2016). Acute exacerbation of COPD, often caused by infection, is known to accelerate the rate of remodelling, loss of elasticity and subsequent decline in lung function in COPD patients, especially if the exacerbations are frequent (Stolz et al., 2017; Karakioulaki et al., 2020). LPS may also be a good candidate for modelling acute exacerbation of COPD because it is a component of the cell wall of gram-negative bacteria, such as *Haemophilus influenzae,* that together with gram positive bacterial infections account for approximately 40% of acute exacerbations of COPD (Dimopoulos et al., 2012). LPs is also linked to the pathogenesis of COPD due to its presence in cigarette smoke and the BALF of COPD patients (Tanner & Single, 2020). LPS is also produces an inflammatory cytokine in guinea pigs that is comparable to human disease (Toward & Broadley, 2001; Toward & Broadley, 2002; Patel et al., 2002; Wilkinson et al., 2006; Wright et al., 2008; Tanner & Single, 2020). Furthermore, although the viral infections that account for the other 60% of cases

don't contain LPS, some still contain CaSR-activating polyamines in the viral envelope or produce polyamines in order to replicate, including influenza A (Bachrach, 1970; McCann, 1987). Therefore, the relevance of LPS exposure, for this time period, is an important tool for investigating mechanisms of lung remodelling during acute exacerbations of COPD in humans.

3.4 Study limitations

It is not clear if lung remodelling was induced by LPS-challenge in this model of COPD-like neutrophilic exacerbation due to the lack of naïve or negative control treatment group. Although histological evidence of remodelling has been previously observed using the same protocol in guinea pigs this represents a major limitation of this experiment (Toward & Broadley, 2001; Toward & Broadley, 2002). Future studies should always incorporate a negative control group where possible to establish a baseline level of remodelling. Furthermore, collagen was the only ECM remodelling marker assessed in the airways of this model. Diverse roles for individual ECM components are currently emerging suggesting this approach is limited in detail (Burgess et al., 2016; Burgess et al., 2019). For example, the concentration of collagen subtypes, tenascin, laminin, elastin, fibronectin and versican may be valuable to determine how closely this model resembles exacerbation of human disease (Jones et al., 2016). Although the qHACC and qHIT methods could be adapted to quantify a range of markers, this would incur additional staining, imaging and manual component identification that could not be completed within the timeframe of my PhD.

This model of acute exacerbation, using LPS-challenge, induces several features of COPD-like neutrophilic exacerbation but is limited because it does not induce the key hallmark of COPD, emphysema, in guinea pigs and instead seems to induce characteristics of alveolar interstitial fibrosis (Snider et al., 1985; Toward & Broadley, 2001; Blundell et al., 2004; Schindelin et al., 2012). When interstitial fibrosis is detected in COPD patients it is described as a co-morbidity, such as combined pulmonary fibrosis and emphysema (CPFE), and isn't directly linked to COPD. Therefore, the effects observed in this model may more closely resemble rapid LPS-induced pulmonary fibrosis in mice, thought to occur via the PI3K-Akt-

mTOR/PFKFB3 pathway (Hu et al., 2020b). However, the CaSR has also been shown to play a role in the regulation of fluid secretion which may affect lung edema which is known to occur in this model (Toward & Broadley, 2001; Lazrak et al., 2023). Due to the absence of some key COPD-like features and presence of fibrotic features in this model, the relevance to COPD in this region of the lung must be acknowledged; however, this model may still be valuable for investigating remodelling mechanisms in models of COPD exacerbation.

This study, and others using this protocol, have also failed to assess the persistence of remodelling after the removal of LPS stimulus, a key feature of COPD in humans. Although studies using chronic LPS exposure (12 weeks) found that these features persist for at least 8 weeks after the stimulus is no longer present, it is unclear if these features will persist in shorter-term models like the protocol used in this experiment and therefore, it is unclear how well this represents the remodelling observed in human disease (Vernooy et al., 2002).

It is also important to acknowledge that these animals, like most animal models, lack the underlying pathophysiology that is present in humans with COPD before the onset of acute exacerbation. In future, more complete modelling of acute exacerbation of COPD could be induced in dogs, known to naturally develop features of COPD such as pulmonary emphysema which can be induced using cigarette smoke exposure (Chapman et al., 2008; Williams & Roman, 2016; Ghorani et al., 2017); hamsters, known to develop emphysema and airway remodelling using LPS-challenge (Stolk et al., 1992); or guinea pigs combined with a chronic cigarette smoke-induced model of COPD, known to induce emphysema, to better establish the underlying pathophysiological changes associated with COPD (Wright & Churg, 1990; Ghorani et al., 2017). This could also be investigated using humans cells isolated from COPD patients; however, *in vitro* methods are limited in terms of loss of the immune system and diversity of resident lung cell types that are implicated in lung remodelling processes.

Remodelling in the lung is also not always uniform and can exhibit a degree of localisation (Chung & Adcock, 2008). In this experiment, airways were categorised

by their size due to the differences in morphology and cellular composition between bronchi and bronchioles in humans and guinea pigs (Canning & Chou, 2008). Airway size was also used to normalise airway remodelling measurements because the area occupied by markers of remodelling is proportional to the size of the airway. However, airway size may not be completely reliable as an index of airway comparability due to the potential effect of remodelling on airway size. Although this is difficult to measure directly, remodelling has been observed to reduce the lumen of COPD airways (Hirota & Martin, 2013). For this reason, the region including the airway lumen and epithelial layer (stopping at the reticular basement membrane) was used to determine airway size. Nevertheless, the reticular basement membrane and epithelial region also undergo remodelling in COPD which, to my knowledge, has an unknown effect on airway size (Liesker et al., 2009). The sampling method used in this study could be improved by moving towards approaches that attempt to represent and map the airways in whole lung. To my knowledge this would require a refined sectioning protocol to identify specific generations of airways. Unfortunately, retrospective studies using lung tissue from previous experiments are often unable to incorporate this. However, future studies using approaches similar to those described by Tatler et al. (2023) could achieve this. At the cost of increased time and resource-demands. Advancements in the field of machine learning could also be applied to further alleviate resource demands and move towards better representation of the whole lung during analysis. Additionally, certain types of lung samples, such as those from human lung biopsies, may require a different method of categorising and normalising the analysis where airway size cannot be calculated. In this case, reticular basement membrane length may be a suitable alternative, as proposed by Zeki et al. (2010).

Low power may have impacted the probability of correctly rejecting the null hypothesis in these experiments, particularly where p values were low but did not pass the threshold for significance. For example, the epithelial tissue analysis in the smaller airways had an effect size of 0.4, calculated using Cohen's *d* method, and a power of 0.3, calculated using a power calculation analysis (Statistics Kingdom Statistical Power Calculator). The recommended power for an experiment is at least 0.5 to improve the likelihood of detecting a false null hypothesis (Aktas & Keskin,

2013). This could possibly be improved by adding more lung sections to each slide to increase the number of comparable airways that are available. Ultimately, for more effective hypothesis testing, a negative vehicle control group is required to establish a baseline for the characteristics assessed and ideally resources would allow for optimisation of these novel or adapted methodologies.

The qHIT method benefits from its non-specific approach, incorporating a range of remodelling processes into a single measurement; however, despite the use of an exclusion criteria, this approach did not eliminate some cells that also undergo changes in quantity, such as inflammatory cells, and artifacts, such as red blood cell contamination from organ harvesting, that are not indicators of remodelling. Furthermore, the CaSR has been shown to play a role in inflammatory cell infiltration in the lungs of these animals (Yarova et al., 2016). Due to the effect of NAM treatment on inflammation, it is not possible to distinguish the effects of NAM treatment on remodelling and inflammation as it may have influenced a change in either or both due to the simple marker quantified by qHIT. This inclusion of unwanted components that alter interstitial area could be eliminated using a staining protocol to identify inflammatory cells, such as Congo red staining to identify eosinophils and immunohistochemical identification of neutrophil elastase to identify neutrophils (Dulek et al., 2014; Li et al., 2015). To my knowledge it was not possible to eliminate this using FIJI software so a more sophisticated image analysis software, such as StrataQuest, may be required. However, for the purposes of this study, it is not clear if NAM treatment had any effects on interstitial remodelling, additional to the previously observed decrease in interstitial wall thickening following NAM treatment (Yarova et al., 2016). Therefore, this is a major limitation of the current qHIT approach used in this chapter and following chapters of this thesis.

3.5 Conclusions

In this study, I have demonstrated that the qHACC approach should be further investigated as a method to determine total tissue, epithelial tissue, goblet cell, smooth muscle and peribronchial collagen remodelling in a range of airway sizes using a single analysis, minimal histological staining and negligible experimenter

subjectivity. Furthermore, this study also demonstrates the capability of qHIT to identify interstitial remodelling in a manner comparable to professional histopathologist assessment at AstraZeneca. Lastly, these findings suggest that further studies are required to investigate whether inhaled NAM treatment can reduce characteristics of airway remodelling in pre-clinical models of COPD.

3.6 Future directions

Minimising the number of histological stains used in an experiment is essential to improve the efficiency of quantitative image analysis. In this study, picrosirius red staining was used; however, a more versatile stain, such as Masson's trichrome with aniline blue, a dark blue pan-collagen stain that also stains mucosubstances light blue, has the potential to improve the efficiency of this approach by staining mucosubstances, lung tissue and collagen, simultaneously (Aumann, 1994).

Future experiments could benefit from a more elaborate lung sectioning protocol to improve the availability of comparable larger airways while maintaining the number of smaller airways. To do this, separation of the upper and lower regions of the lung would be required to section them in different orientations. In later chapters of this thesis, I will further test different staining and sectioning protocols as well as the viability of the qHACC approach using a range of experiments aimed at determining the role of the CaSR in lung remodelling using different mouse models of immunoglobulin (Ig)E/ T helper 2 (Th2) asthma and alarmin-driven asthma.

Although NAM treatment had no statistically significant effect on some characteristics of smaller airway remodelling, including total tissue, epithelial tissue and smooth muscle remodelling; the American Statistical Association advises that scientific conclusions should not be entirely based on p value thresholds suggesting further investigation is required to determine if the true effect is consistent with the null hypothesis (Wasserstein & Lazar, 2016).

CHAPTER 4: INVESTIGATING THE ROLE OF THE CASR IN AGE-RELATED LUNG REMODELLING

4.1 Introduction

Increased numbers of activated fibroblasts and an altered airway and interstitial extracellular matrix (ECM) composition are key hallmarks of the aging lung (D'Errico et al., 1989; Fulop et al., 2001; Quirk et al., 2016; Godin et al., 2016; Cho & Stout-Delgado, 2020). Inflamm-aging and senescence are thought to be central to these processes by chronically activating the innate and adaptive immune response and increasing the baseline expression of interleukin (IL)-1β, IL-6, tumour necrosis factor (TNF)-α and transforming growth factor (TGF)-β (Baker et al., 2016; Papageorgis, 2017; Zhang et al., 2017; Vitenberga & Pilmane, 2018; Hudgins et al., 2018).

IL-1β, IL-6 and TNF-α have also previously been shown to upregulate calcium-sensing receptor (CaSR) expression in lung cells and other tissues (Canaff & Hendy, 2005; Fetahu et al., 2014; Yarova et al., 2015; Hendy & Canaff, 2016). Furthermore, a previous study from our lab identified a reduction in cardiac collagen deposition following targeted CaSR deletion from smooth muscle protein 22α (SM22α)-positive cells (fibroblasts, smooth muscle and vascular cells). It was suggested that this was a direct consequence of CaSR deletion on autophagy-related cardiac fibrosis; however, these animals also exhibited a reduced heart rate which may have played a role (Liu et al., 2015a; Schepelmann et al., 2016). Although a role for the CaSR has been described in lung development and tissue morphogenesis, little is known about the physiological role of the CaSR in the aging lung (Riccardi et al., 2013; Brennan et al., 2016; Chanda et al., 2019).

In this study, I aim to investigate the role of the CaSR in age-related lung remodelling by determining the effect of targeted CaSR deletion from SM22α-positive cells, which includes smooth muscle cells, fibroblasts and macrophages on airway and interstitial ECM remodelling in 15-month-old $^{SM22\alpha}CaSR^{\Delta flox/\Delta flox}$ mice. To achieve this, Masson's trichrome stained lung sections were analysed using the adapted Ellis et al. (2003) method to determine peribronchial collagen in the smaller airways.

Quantitative histomorphometry of interstitial tissue (qHIT) and modified Ashcroft scoring was also used to determine interstitial remodelling in the lung parenchyma.

4.2 Results

Targeted CaSR ablation of the CaSR from SM22α-positive cells was achieved in these mice by crossing mice with LoxP-flanked exon 7 of the *CaSR* gene and Cre-recombinase positive mice and subsequent inbreeding for three generations. The resulting CaSR-LoxP SM22α-Cre positive mice (aka $^{SM22\alpha}CaSR^{\Delta flox/\Delta flox}$ or CaSR-KO mice) as well as Cre-negative mice wild-type (WT) controls were then aged to induce age-related fibrosis for the following experiments. Lungs were harvested from these mice when they were 15-months-old to determine the effect of the CaSR in SM22α-positive cells on smaller airway ECM remodelling, using the Ellis et al. (2003) approach, and alveolar interstitial fibrosis, using the qHIT and the industry-standard Ashcroft scoring. All statistical analyses were performed using T tests.

4.2.1 $^{SM22\alpha}CaSR^{\Delta flox/\Delta flox}$ mice are protected from age-related peribronchial collagen deposition

To determine the effect of genetic ablation of the CaSR from SM22α-positive cells on peribronchial collagen in aging mice, the Ellis et al. (2003) method was adapted for the smaller airways using a 10μm ring (half the recommended size for larger airways). Here, a significant reduction in peribronchial collagen (***p* = 0.020**) was identified following targeted CaSR deletion from SM22α-positive cells, compared to WT (Cre-negative) mice, as shown in **Figure 4.1.**

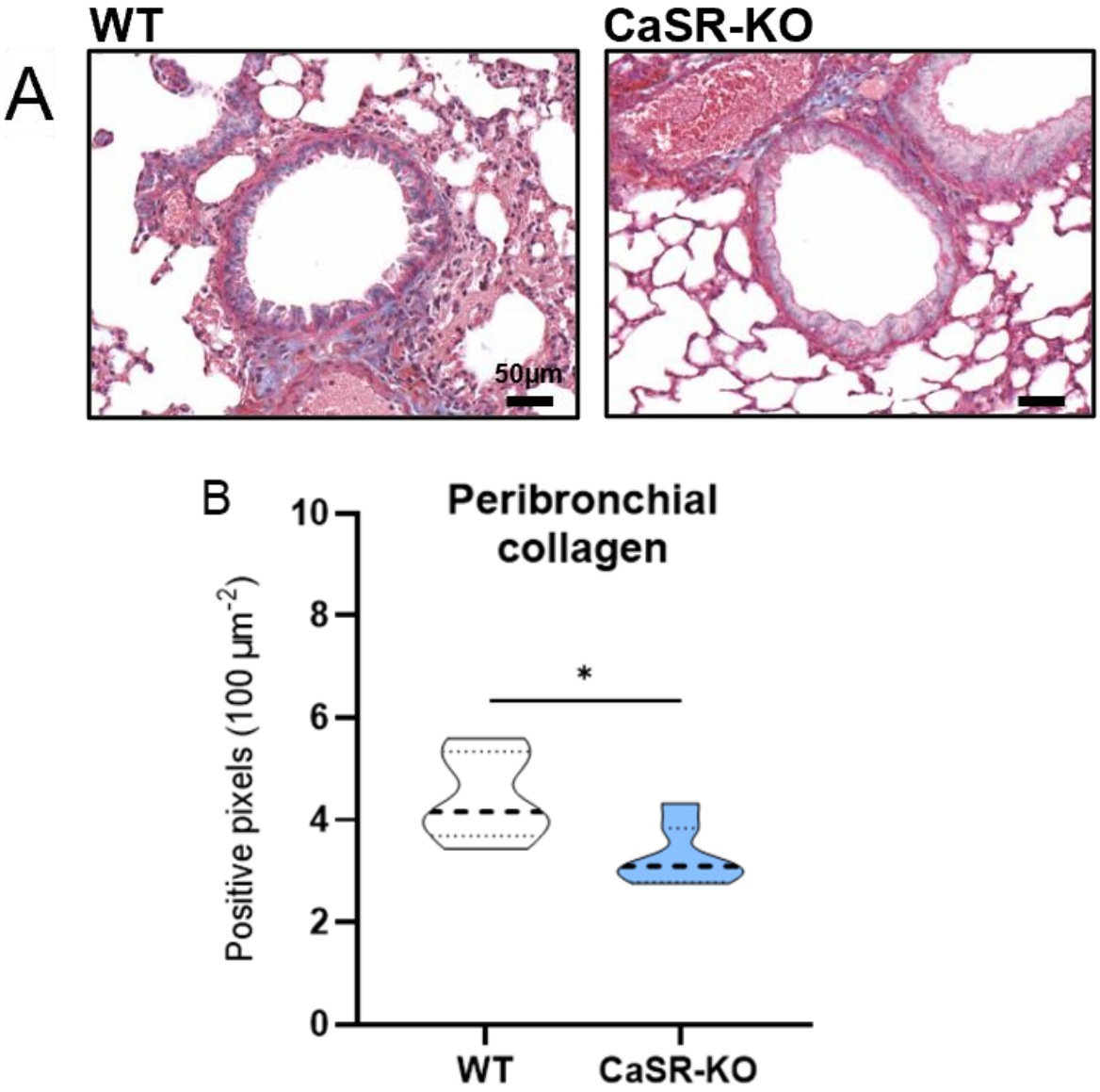

Figure 4.1. Targeted CaSR deletion from SM22α-positive cells protected aging mice from smaller airway peribronchial collagen remodelling. (**A**) Lung sections from 15-month-old mice with targeted CaSR deletion from SM22α-positive cells were stained with Masson's trichrome and analysed using an adaptation to the Ellis et al. (2003) method to determine (**B**) the percentage of pixels stained for collagen per 100µm^2 of tissue in the peribronchial region extending 10µm into the parenchyma away from the basement membrane. Statistical significance identified using T test and data is displayed using a truncated violin plot to demonstrate frequency distribution of the data where dashed lines represent the median and dotted lines represent

the upper and lower quartiles, respectively, N = 5-7, n = 3, ROI = 8-17, * (p < 0.05). Graticule (A) 50 µm. SM22α: transgelin; CaSR: calcium-sensing receptor; CaSR-KO: $^{SM22\alpha}CaSR^{\Delta flox/\Delta flox}$ mice with targeted CaSR deletion from SM22α-positive cells.

4.2.2 $^{SM22\alpha}CaSR^{\Delta flox/\Delta flox}$ mice are protected from age-related interstitial fibrosis

qHIT and modified Ashcroft scoring were used to determine the effect of genetic ablation of the CaSR from SM22α-positive cells on interstitial tissue remodelling in aging mice. Here, qHIT identified a significant reduction in interstitial tissue remodelling and/or inflammation (***p* = 0.0088**) following targeted CaSR deletion from SM22α-positive cells, compared to WT (Cre-negative) mice, as shown in **Figure 4.2**.

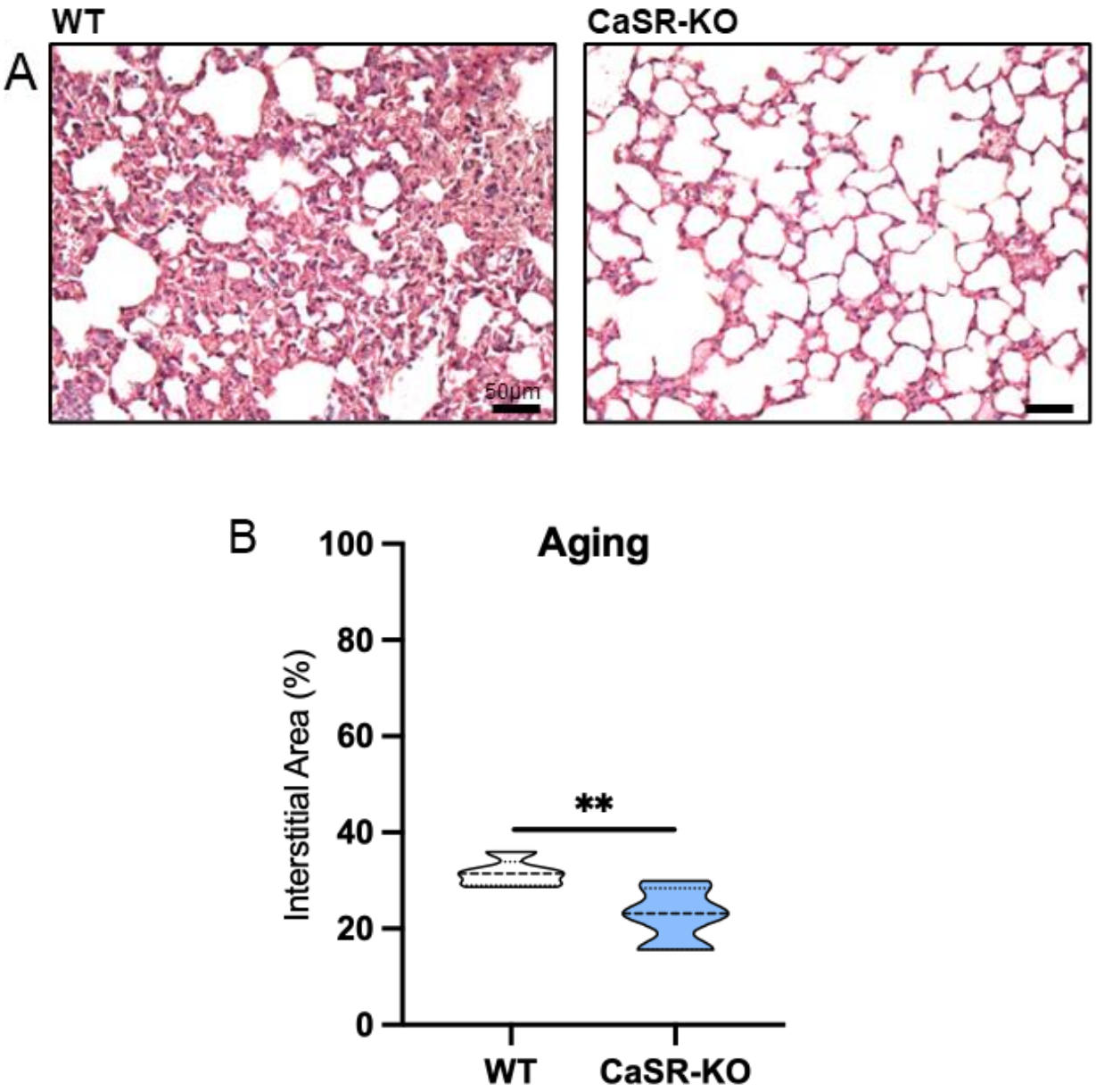

Figure 4.2. Targeted CaSR deletion from SM22α-positive cells protected aging mice from interstitial tissue remodelling and/or inflammation. (**A**) Interstitial regions of Masson's trichrome stained lung sections from 15-month-old mice with targeted CaSR deletion from SM22α-positive cells were analysed to determine (**B**) interstitial tissue area using the qHIT method. Statistical significance identified using a T test. Image size = 1034 x 1386 px. Truncated violin plot, N = 5-7, n = 3, ROI = 12, ** (p < 0.01). Graticule (A) 50 µm. qHIT: quantitative histomorphometry of interstitial tissue; SM22α: transgelin; CaSR: calcium-sensing receptor.

Modified Ashcroft scoring also identified a significant reduction in interstitial fibrosis of grade 4 or above (***p* = 0.027, Figure 4.3B**). Furthermore, a colleague, Dr Kasope Wolffs, repeated this experiment and similarly identified a significant reduction in absolute Ashcroft score values (***p* = 0.013; Figure 4.3C**) following targeted CaSR deletion from SM22α-positive cells.

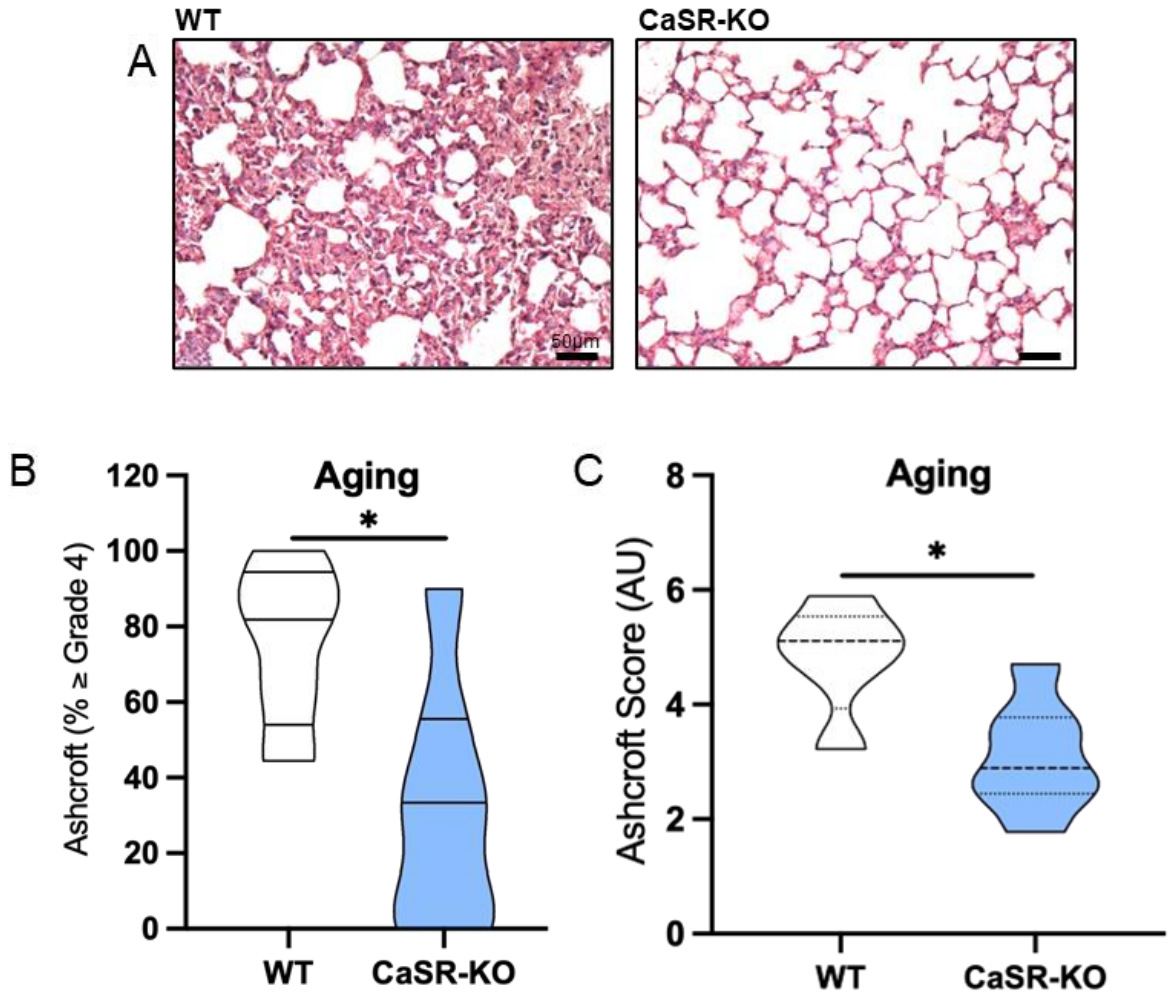

Figure 4.3. Targeted CaSR deletion from SM22α-positive cells protected aging mice from interstitial fibrosis. (**A**) Masson's trichrome stained lung sections from 15-month-old mice with targeted CaSR deletion from SM22α-positive cells were analysed (**B**) by myself and (**C**) by a colleague, Dr Kasope Wolffs, to determine modified Ashcroft scores using two separated methods (**B**) the percentage of grade 4 or above and (**C**) absolute values. Statistical significance identified using a T test. Truncated violin plot, N = 5-7, n = 3, ROI = 12 (B) and

9-11 (C), * ($p < 0.05$). Graticule (A) 50 µm. SM22α: transgelin; CaSR: calcium-sensing receptor; WT: wild-type; CaSR-KO: Targeted CaSR deletion from SM22α-positive cells.

4.3 Discussion

Prior to this study, the mechanisms that drive the age-related progression of airway and interstitial ECM remodelling were not well understood (Lowery et al., 2013). Here, I provide indication that the CaSR, in SM22α-positive cells, plays a central role in age-related peribronchial and interstitial remodelling. This evidence provides a mechanistic link between aging, remodelling and the physiological role of the extracellular cation sensor, CaSR, in the lung. Additionally, I have demonstrated the Ellis et al. (2003) method can be adapted to determine peribronchial collagen remodelling in the smaller airways of aging mice.

4.3.1 Inflamm-aging likely upregulates CaSR expression in the aging lung

The CaSR-activating polycations and damage-associated molecular patterns that are usually upregulated following lung damage, infection and inflammation are not hallmarks of the aging lung. In fact, polyamines have been shown to decrease in the lung with age (Minios et al., 2011). Although molecules associated with lung aging and CaSR activation are still emerging (Ohnishi & Razzaque, 2010); the current body of evidence suggests increased CaSR activation in the aging lung is not likely caused by increased local polycations. In other words, alternative mechanisms must be present to influence the role of the CaSR in the aging lung.

One possible explanation could be that activation of the CaSR is achieved by an increase in receptor expression without alteration to physiological polycation levels. In the aging lung, baseline expression of pro-inflammatory mediators, such as IL-1ß, IL-6, TNF-α and TGF-ß are known to be increased as a consequence of inflamm-aging and cellular senescence (Franceschi et al., 2000; Baker et al., 2016; Kovacs et al., 2017; Papageorgis, 2017; Zhang et al., 2017; Vitenberga & Pilmane, 2018; Hudgins et al., 2018). These cytokines are also known to increase CaSR expression (Fetahu et al., 2014; Leach et al., 2020; also see Chapter 6).

Although cytokine levels were not directly evaluated in these animals, it is possible that age-related increases in pro-inflammatory mediator expression could indirectly increase activation of the receptor by upregulation of CaSR expression. However, physiological polycation levels must at least exceed the threshold for transient receptor activation (1.1 - 1.3 mM free ionised Ca^{2+} for half-maximal response), for this to be the case. Although CaSR expression has not been measured in aging lungs, CaSR expression has been shown to change with age in other tissues including pancreatic islets and keratinocytes (Oh et al., 2016; Celli et al., 2021).

4.3.2 SM22α-positive cells mediate age-related remodelling via the CaSR

Fibroblasts and smooth muscle cells are the predominant producers of ECM components and key mediators of ECM turnover in the lung (Black et al., 2003; White, 2015). Considering both cell types also express SM22α, loss of the fibroblast and smooth muscle cell CaSR expression and function in this experiment likely played a direct role in reducing the production and secretion of ECM components in $^{SM22\alpha}CaSR^{\Delta flox/\Delta flox}$ mice. This may be mediated by signal pathways associated with CaSR activation, such as TGF-ß, mitogen-activated protein kinase (MAPK) (p38, extracellular signal-regulated kinase (ERK) and Jun N-terminal kinase (JNK)), phosphatidylinositol 3-kinase (PI3K)/Akt, mechanistic target of rapamycin (mTOR), Ras homolog kinase (RhoK) and wingless-related integration site (Wnt)/ß-catenin signalling, that have all been associated with ECM remodelling processes in lung fibroblasts and are considered potential therapeutic targets (MacLeod et al., 2003; Tfelt-Hansen et al., 2003; Chattopadhyay et al., 2004; Tu et al., 2011; Rey et al., 2012; Thomsen et al., 2012; Yuan et al., 2019). However, fibroblasts and smooth muscle cells also play a central role in the production and secretion of inflammatory cytokines that directly influence ECM remodelling in the lung so further studies are required to determine the mechanism by which CaSR ablation reduced ECM remodelling in these animals.

However, other cell types, such as vascular cells and macrophages, are also known to express the CaSR and SM22α (Uhlen et al., 2015). These cells may have also played a central role in the observed reduction in lung remodelling in these animals. For example, macrophages are considered regulators of the wound healing process in

combination with fibroblasts (Alber et al., 2012). Furthermore, vascular cells may also play a role due to the high prevalence of hypertension in patients with IPF and COPD (Nadrous et al., 2005; Chaouat et al., 2005; Patel et al., 2007) and their implicated role in IPF pathogenesis (Gaikwad et al., 2020). Although the evidence from this study suggests that the CaSR is central to age-related remodelling in SM22α-positive cells, which include fibroblasts, smooth muscle cells, vascular cells and macrophages; identifying the role of each cell-type in this process was beyond the scope of this experiment.

4.3.3 Morphologically normal $^{SM22\alpha}CaSR^{\Delta flox/\Delta flox}$ mice exhibit cardiac and vascular changes

Lungs from $^{SM22\alpha}CaSR^{\Delta flox/\Delta flox}$ mice were described as morphologically normal and the diameter of internal intralobular bronchi was unchanged (Yarova et al., 2015; Schepelmann et al., 2016). Furthermore, the appearance, litter size, body weights and survival rates were also unchanged. However, $^{SM22\alpha}CaSR^{\Delta flox/\Delta flox}$ mice did exhibit impaired vasoconstriction, systemic hypotension, and bradycardia (Schepelmann et al., 2016). Although pulmonary hypertension is associated with lung remodelling in humans (Lettieri et al., 2006) and aging mice (Caporarello et al., 2020), hypotension has not been associated with increased protection against lung remodelling. Therefore, it is unlikely that the changes observed in this study were the result of unwanted on- or off-target effects on animal physiology.

Furthermore, $^{SM22\alpha}CaSR^{\Delta flox/\Delta flox}$ mice were also hypercalcaemic and exhibited elevated 1,25-dihydroxyvitamin D, parathyroid hormone (PTH) and fibroblast growth factor 23 (FGF23) levels (Schepelmann et al., 2013). Elevated serum calcium (hypercalcaemia), FGF23 and PTH levels have been associated with worsened lung remodelling (Park et al., 2015; Jayakrishnan et al., 2018; Gulati et al., 2019); however, elevated 1,25-dihydroxyvitamin D levels may in fact be protective against lung remodelling (Janssens et al., 2009; Ramirez et al., 2010; Tzilas et al., 2019). However, the extent of protection from this phenomenon requires further investigation.

Finally, in healthy C57BL/6 mice the decline in lung function and structure associated with aging is similar to those observed in humans (Huang et al., 2007); however, NIA's strain survival information indicates 75 % of the C57Bl/6 mice live to approximately 24-months-old. Therefore, the 15-month-old mice used in this experiment are relatively middle-aged for mice of this strain and more severe remodelling would likely be exhibited closer to the end of their lifespan.

4.3.4 Implications for understanding mechanisms of age-related lung disease

Age-related changes to lung structure, cell senescence and inflammation are associated with poor prognosis and mortality in chronic lung disease patients (Thannickal, 2013; Lowery et al., 2013; Raghu et al., 2014). Despite differences in rate and severity, ECM remodelling is also a hallmark of age-related inflammatory lung diseases such as chronic obstructive pulmonary disease (COPD) and idiopathic pulmonary fibrosis (IPF). The CaSR is emerging as a novel therapeutic target for its potential to mediate inflammatory cell recruitment, profibrotic cytokines and airway hyperresponsiveness in murine models of asthma (Yarova et al., 2015) as well as target difficult-to-treat neutrophilic phenotypes and remodelling in COPD (Yarova et al., 2016; see Chapter 3). The evidence presented in this study suggests the CaSR may also be a potential therapeutic target for peribronchial collagen and interstitial remodelling in chronic lung diseases where age is a key risk factor.

It is unclear whether the same mechanisms of age-related remodelling are mediated by the CaSR in the aging lung and chronic lung disease. Although this was not directly investigated, the reduction in cardiac fibrosis observed in $^{SM22\alpha}CaSR^{\Delta flox/\Delta flox}$ mice was hypothesised to be a direct consequence of CaSR deletion from cardiomyocytes and the consequent dampening effect on autophagy via inhibition of the calmodulin (CaMKKß)/AMP-activated protein kinase (AMPK)/mTOR pathway (Schepelmann et al., 2016; Liu et al., 2015a). Autophagy has also been implicated in promoting senescence, a key mediator of remodelling, particularly ECM remodelling, in the aging lung (Slobodnyuk et al., 2019; Zou et al., 2019; Braicu et al., 2019).

Mechanistically, impairment or overactivation of autophagy is thought to promote fibrogenesis, a process highly dependent on increased Ca^{2+}_i (Patel et al., 2012;

Mukherjee et al., 2015). This highlights the importance of Ca^{2+}_i in lung fibrogenesis and Ca^{2+}_i is known to be elevated following CaSR activation in fibroblasts (Wolffs, 2022) as well as airway smooth muscle cells (Yarova et al., 2015). Furthermore, loss of proteostasis and mitochondrial dysfunction in COPD patients have been linked to increased markers of autophagy (Brandsma et al., 2017). This may indicate a plausible role for the CaSR in mediation of fibrogenesis in SM22α-positive cells in the aging lung. However, further studies are required to adequately investigate the role of CaSR-mediated autophagy-related remodelling. This is further addressed in Chapter 6.

4.4 Study limitations

Local CaSR-activating polycation levels, such as polyamine levels, and CaSR expression-altering cytokines and growth factors, such as IL-1ß, IL-6, TNF-α and TGF-ß, were not assessed in these animals. Although the CaSR is central to age-related airway and interstitial ECM remodelling, it is unclear whether CaSR activation drives this process. The effect of targeted CaSR deletion from SM22α-positive cells on larger airway remodelling was also not investigated due to sagittal plane sectioning reducing the availability of suitable larger airways. Therefore, due to the position-dependent differences in cellular composition throughout the airways of the lung, it is not recommended that my results are generalised to other regions of the lung, such as the larger airways, without further analysis.

The absence of lung sections from young WT mice was a limitation of this experiment because it was not possible to determine a baseline for physiological peribronchial collagen. This measurement is important to determine whether the reduction in ECM remodelling was a return to baseline or a reduction below baseline levels. Reducing peribronchial collagen levels around the airways may actually be detrimental to the structural integrity and mechanical microenvironment of the lung, and therefore function of the lung (Narciso et al., 2022). Lastly, as discussed in Chapter 3 (section 3.4), the qHIT analysis observed a reduction in interstitial area suggesting a reduction in interstitial tissue remodelling and/or inflammation; however, because this method does not eliminate inflammatory cells from the analysis it is not capable of distinguishing between tissue remodelling and inflammation. Therefore, either

remodelling, inflammation or a combination of both features may have influenced this result. This methodology should be further improved by eliminating inflammatory cells based on additional staining and more sophisticated image analysis software. It would also be of interest to know if the inflamm-aging in this region of the lung was affected by targeted CaSR deletion from SM22α cells, an additional benefit of incorporating inflammatory cell measurements in this approach. However, for the purposes of this study, Ashcroft scoring remains a more reliable index of interstitial remodelling in this model.

4.5 Conclusions

In conclusion, I have demonstrated the CaSR in SM22α-positive cells is central to age-related ECM remodelling in the airways and parenchymal interstitium. This is likely a direct consequence of CaSR ablation on downstream cell signalling and remodelling processes such as inflamm-aging, autophagy and senescence. Although identifying the specific mechanisms and the cell-types involved is beyond the scope of this study, this evidence has implications for understanding the physiological role of the CaSR in the lung and provides a promising avenue for identifying why age is a key risk factor for the development of chronic lung diseases. Moreover, in addition to previous evidence indicating a role for the CaSR in inflammatory cell recruitment, cytokine production and airway smooth muscle hyperresponsiveness; the CaSR may represent a potential therapeutic target for the treatment of age-related ECM remodelling in the lung.

4.6 Future directions

To test whether CaSR expression is altered in the aging lung future studies should aim to determine CaSR expression *in vivo* using immunohistochemistry or quantitative proteomic analysis techniques using western blotting or ELISA in lung tissue homogenate. Although there is evidence polyamine concentrations are reduced in the aging lung, it is not clear if other CaSR-agonists are upregulated in the aging lung. To investigate this CaSR-transfected HEK293 cells could be treated with the BALF isolated from young and aging mice. Calcium imaging could then be used to determine if the CaSR is activated by determining whether intracellular calcium is released from intracellular stores. Following this, ion chromatography

(ions) and western blotting or ELISA (polycationic proteins) could be used to investigate which known CaSR agonists, if any, are present in the BALF isolated from the aging lung.

In this experiment, it was not clear whether targeted CaSR-deletion from SM22α-positive cells or unwanted effects on animal physiology influenced lung remodelling. Inhaled type I or II calcimimetics could be used to determine the effect of pharmacological CaSR activation on lung remodelling in aging mice. If CaSR activation drives lung remodelling, chronic CaSR activation would enhance remodelling changes in the lung beyond those observed in untreated aging WT mice. However, ligand-biased signalling may diversify the roles of some CaSR activators. Systemic PAMs should be avoided as this is likely to evoke further unwanted effects on animal physiology, such as hypocalcaemia which could affect lung remodelling in an undetermined manner.

Furthermore, in this study I hypothesised that upregulation of CaSR expression in the presence of physiological free ionised Ca^{2+} may indirectly increase CaSR activation in the aging lung. Future studies should aim to quantify the state of CaSR activation in the presence of physiological free ionised Ca^{2+} and inflamm-aging or senescence-associated secretory phenotype (SASP) cytokines known to upregulate CaSR expression. This could be achieved *in vitro* using normal or aging human lung fibroblasts.

Finally, a pan-collagen stain was used in these experiments as a marker to determine total ECM turnover in the peribronchial and alveolar interstitium. However, of the 28 total collagens that are considered fibroblast collagens (fibrillar type I, II, III, V, and VI collagens) only alterations to collagens I, II, IV and V are associated with age (Karsdal et al., 2016; Karsdal et al., 2017). The ECM is also comprised of elastins, proteoglycans, glycoproteins (e.g. fibronectin) and matrix metalloproteinases (MMPs)/ tissue inhibitor of metalloproteinases (TIMPs) that were not investigated in this experiment but have key implications on remodelling processes and lung function. To address this, the role of the CaSR in regulating other ECM components is further investigated in Chapter 6.

These findings have implications for the role of the CaSR in remodelling associated with chronic inflammatory and interstitial lung diseases. A model of more severe fibrosis such as bleomycin challenge in male aging $^{SM22\alpha}CaSR^{\Delta flox/\Delta flox}$ mice could be used to determine the protective effects of targeted CaSR deletion from SM22α-positive cells in a more robust model of age-related lung fibrosis. Additionally, the pharmacological tools exist to inhibit activation of the receptor using inhaled negative allosteric modulators of the CaSR (NAMs). However, this would pharmacologically ablate the CaSR in a greater range of cell types than observed in this experiment, including epithelial and immune cells, and the results would not clarify the role of the CaSR in SM22α-positive cells alone. A more complete CaSR-knock-out (KO) model is not possible due to the non-viable offspring produced and its importance in lung development (Chang et al., 2008; Finney et al., 2008; Brennan et al., 2016). Therefore, investigating the role of the CaSR *in vitro* using normal and aging human lung fibroblasts, smooth muscle cells and vascular endothelial cells exposed to inflamm-aging cytokines such as IL-1β, IL-6, TNFα or TGF-β could be used to determine the role of the CaSR in SM22α-positive cells in ECM remodelling in the lung.

CHAPTER 5: INVESTIGATING THE ROLE OF THE CASR IN ASTHMA-RELATED LUNG REMODELLING

5.1 Introduction

Asthma is expected to exceed 400 million sufferers worldwide by 2025 and although treatment options exist, airway remodelling in asthma is not adequately controlled using current therapeutics (Payne et al., 2003; Rajanandh, 2015). Although the different endotypes of asthmatic disease are aetiologically distinct, the airway remodelling characteristics remain consistent. Here, the irreversibly narrowed, obstructed, constricted and stiffened airways are the direct result of remodelling features such as epithelial thickening, goblet cell proliferation, smooth muscle thickening and peribronchial extracellular matrix (ECM) remodelling (Bergeron et al., 2010).

To investigate these phenomena, features of immunoglobulin (Ig)E/ T helper 2 (Th2) (allergic) asthma can be recapitulated by using sensitisation and challenge with organic dusts, such as ovalbumin. This induces characteristics such as Th2 inflammation; a thickened epithelium; increased numbers of goblet cells; hypertrophied smooth muscle; and peribronchial fibrosis (Ellis et al., 2003; Kumar et al., 2008). Models of alarmin-driven (non-allergic) asthma have also been produced using inhaled challenge to alarmins such as interleukin (IL)-33. This reproduces features such as a T helper (Th)1 and Th2 inflammatory profile; increased goblet cells; smooth muscle hypertrophy, ECM remodelling, angiogenesis; and increased levels of cytokines and growth factors, such as IL-6 and transforming growth factor (TGF)-β after 36 days of exposure (Hamzaoui et al., 2013; Tang et al., 2014; Li et al., 2015).

Previous studies by our lab have demonstrated that the calcium-sensing receptor (CaSR) is central to other features of asthma pathophysiology, including inflammatory cell infiltration, cytokine production and airway hyperresponsiveness in a mouse model of IgE/Th2 asthma (Yarova et al., 2015; Yarova et al., 2021). CaSR expression is also upregulated in asthmatic human and mouse airways, likely due to elevated levels of cytokines known to upregulate the CaSR in airway smooth muscle

cells and other tissues, such as IL-1β, IL-6, IL-13 and tumour necrosis factor (TNF)-α (Canaff & Hendy, 2005; Fetahu et al., 2014; Yarova et al., 2015). Furthermore, systemic and local CaSR agonists, such as eosinophilic cationic protein (ECP), major basic protein (MBP), polyamines and extracellular Ca^{2+} are known to be elevated in asthma (Kurosawa et al., 1992; Gibson et al., 1998; Koller et al., 1999; Lonkvist et al., 2001; Bartoli et al., 2004; Rossol et al., 2012; North et al., 2013; Yarova et al., 2015).

This study aimed to investigate the role of the CaSR in larger airway, smaller airway and interstitial remodelling. To do this, quantitative histomorphometry of airway cross-section components (qHACC) and quantitative histomorphometry of interstitial tissue (qHIT) was employed to determine the effect of pharmacological ablation of the CaSR, using inhaled negative allosteric modulator of the CaSR (NAM) treatment, in three pre-clinical murine models, including shorter-term IgE/Th2 asthma, alarmin-driven asthma and longer-term IgE/Th2 asthma. In the longer-term IgE/Th2 asthma model, NAM treatment was compared head-to-head with the current standard of asthma care, fluticasone propionate (FP).

5.2 Results

To investigate the role of the CaSR in asthma-like lung remodelling, lung sections from three models of shorter-term IgE/Th2 asthma, alarmin-driven asthma, and longer-term IgE/Th2 asthma were obtained from previous experiments and stained with Masson's trichrome for analysis of airway and alveolar interstitial remodelling. The methodology of each animal experiment is briefly described in each respective subsection of the results.

5.2.1 NAM treatment abolished smaller airway remodelling in shorter-term IgE/Th2 asthma

The shorter-term IgE/Th2 asthma model was generated using intraperitoneal (IP) ovalbumin (OVA) sensitisation (100 µg/mouse OVA on day 0 and day 12) that was confirmed by IgE levels. OVA challenge was then intranasally instilled (IN; 50 µg of OVA) for 6 days and inhaled therapeutic treatment performed with IN NAM (200 µg NPSP795) twice daily from the 2nd day of OVA challenge until the end of the

experiment. All statistical analyses were performed using a one-way analysis of variance (ANOVA) with Holm-Sidak post hoc test

In the larger airways of shorter-term IgE/Th2 asthma, OVA induced epithelial tissue and goblet cell remodelling that was unaffected by inhaled NAM treatment, as shown in **Figure 5.1D**. In the smaller airways, OVA induced several features of airway remodelling that were abolished by inhaled NAM treatment, including total tissue remodelling (p_{adj} = **0.048**), goblet cell remodelling (p_{adj} = **0.015**) and total peribronchial collagen remodelling (p_{adj} = **0.019**). NAM treatment also had no effect on epithelial tissue as this result did not pass the threshold for significance (p_{adj} = **0.06**), as shown in **Figure 5.1E**. In the lung parenchyma, no remodelling was induced by OVA (**Figure 5.1F**).

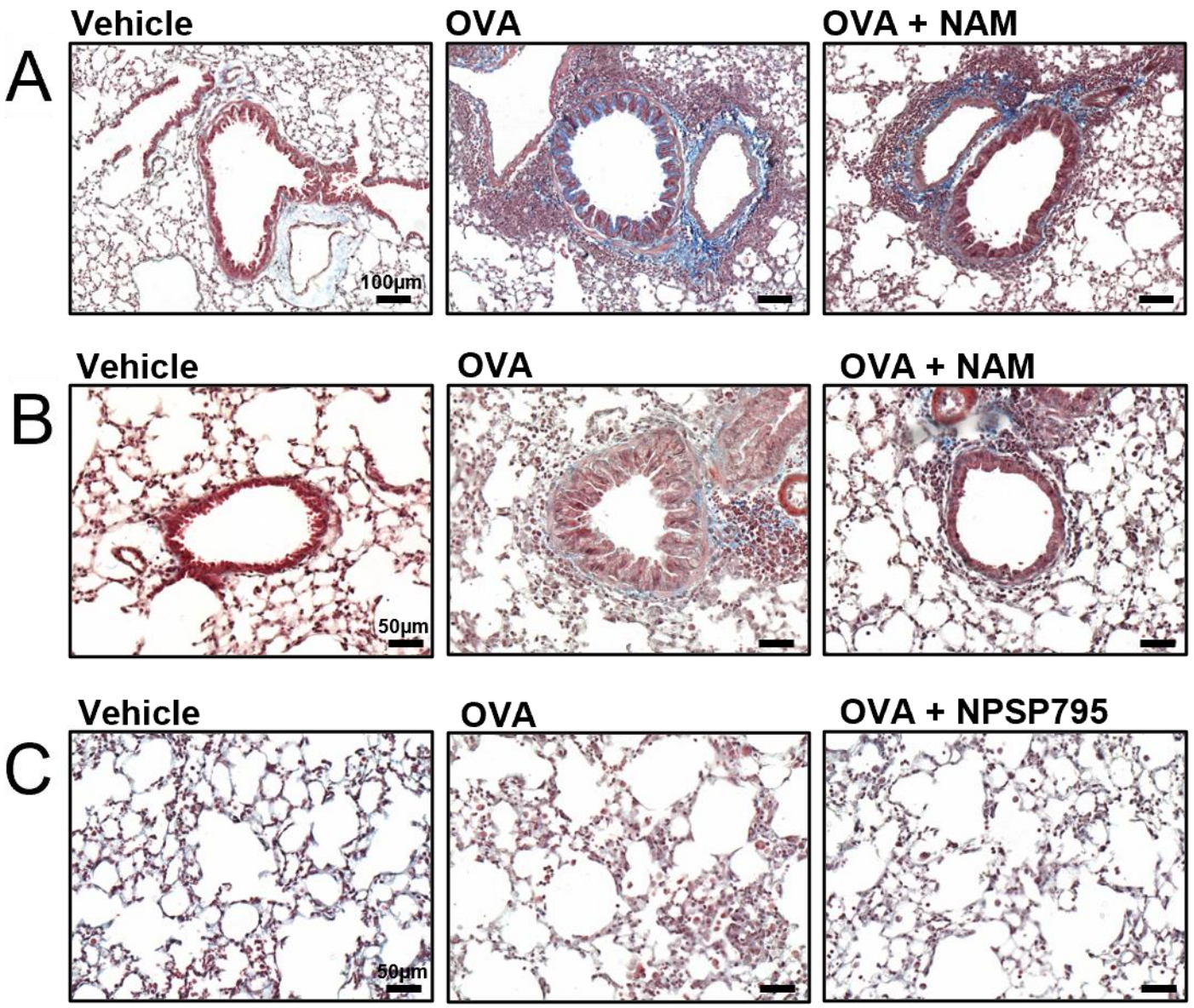
A
Vehicle
OVA
OVA + NAM
100μm
B
Vehicle
OVA
OVA + NAM
50μm
C
Vehicle
OVA
OVA + NPSP795
50μm

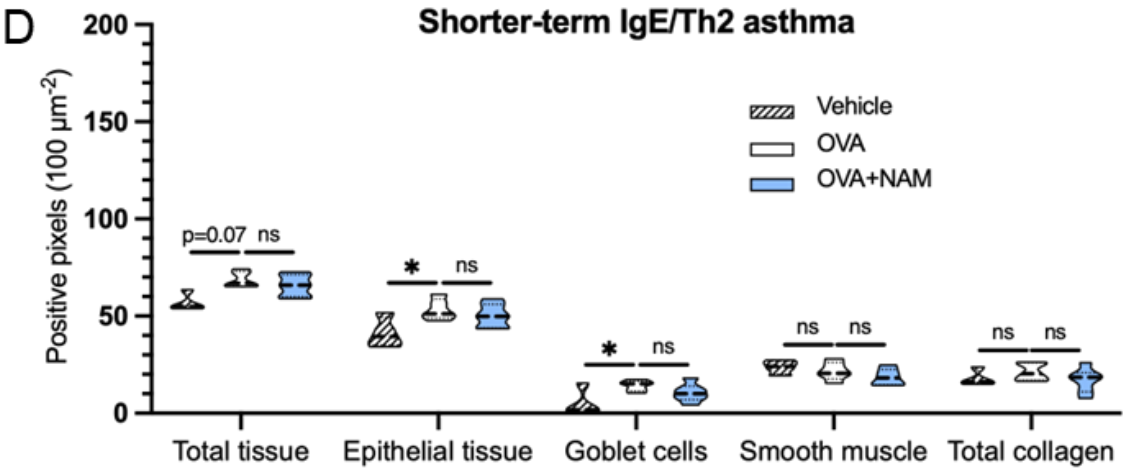
D
Shorter-term IgE/Th2 asthma
Positive pixels (100 µm-2)
200
150
100
50
0
Vehicle
OVA
OVA+NAM
p=0.07
ns
*
ns
*
ns
ns
ns
ns
ns
Total tissue
Epithelial tissue
Goblet cells
Smooth muscle
Total collagen

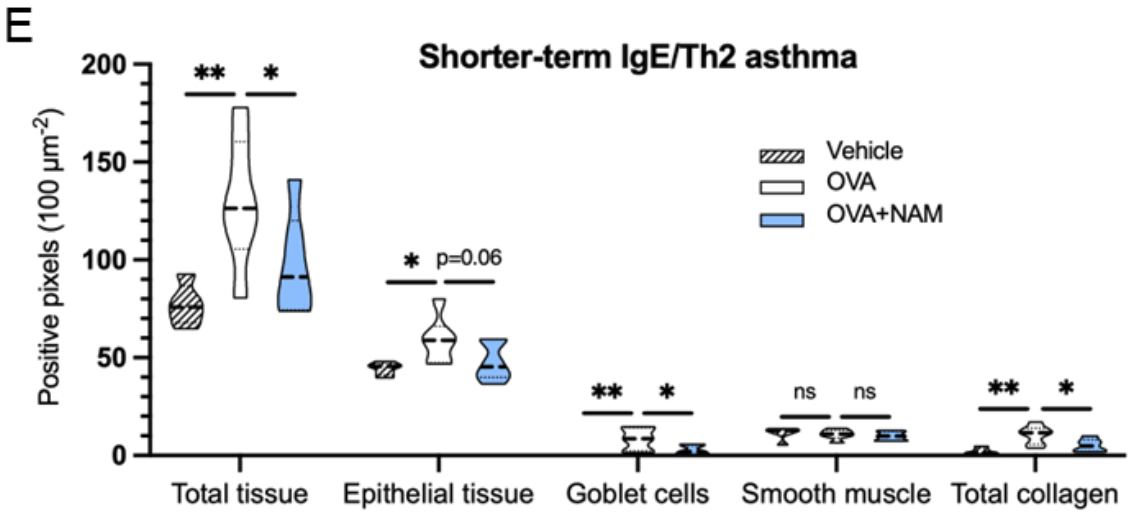
E
Shorter-term IgE/Th2 asthma
Positive pixels (100 µm-2)
200
150
100
50
0
Vehicle
OVA
OVA+NAM
**
*
*
p=0.06
**
*
ns
ns
**
*
Total tissue
Epithelial tissue
Goblet cells
Smooth muscle
Total collagen

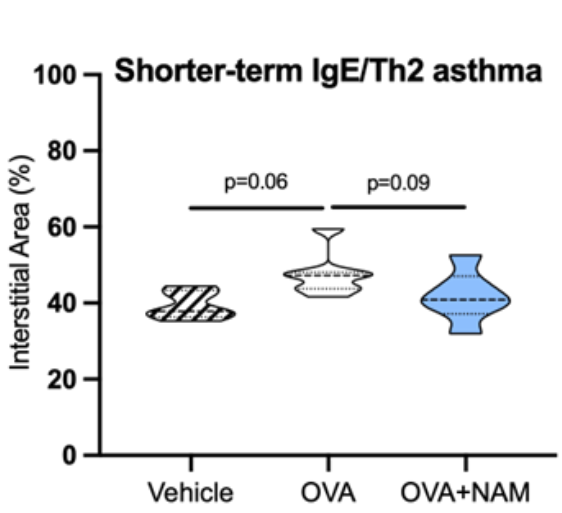
F
Shorter-term IgE/Th2 asthma
Interstitial Area (%)
100
80
60
40
20
0
p=0.06
p=0.09
Vehicle
OVA
OVA+NAM

Figure 5.1. Inhaled NAM treatment abolished smaller airway remodelling in shorter-term IgE/Th2 asthma. (**A**) Larger airways (> 50,000 μm^2), (**B**) smaller airways (< 50,000 μm^2) and (**C**) interstitial regions were identified from Masson's trichrome stained lung sections from the model of shorter-term IgE/Th2 asthma in OVA-sensitised and challenged mice. (**D**) Remodelling was mild in the larger airways and NAM treatment had no effect on reducing larger airway remodelling. (**E**) All components of smaller airway remodelling, apart from epithelial tissue (***p*$_{adj}$ = 0.06**), was significantly reduced by inhaled NAM treatment (***p*$_{adj}$ < 0.05**). (**F**) OVA did not induce interstitial remodelling and/or inflammation in this experiment. Airway remodelling markers were quantified using qHACC and interstitial remodelling and/or inflammation was quantified using qHIT. Statistical significance identified using one-way ANOVA with Holm-Sidak post-hoc test or Kruskal-Wallis with Dunn's post-hoc test. A truncated violin plot was used to demonstrate frequency distribution of the data where dashed lines represent the median and dotted lines represent the upper and lower quartiles, respectively. N = 4-7, n = 3, ROI = 1-4 (larger airways), 1-7 (smaller airways) and 9 (interstitium), ns (p_{adj} > 0.05), * (p_{adj} < 0.05), ** (p_{adj} < 0.01). Graticule (A) 100 μm and (B and C) 50 μm. ANOVA: analysis of variance; IgE: immunoglobulin E; NAM: negative allosteric modulator of the calcium-sensing receptor; OVA: ovalbumin; qHACC: quantitative histomorphometry of airway cross-section components; qHIT: quantitative histomorphometry of interstitial tissue.

5.2.2 NAM treatment abrogated interstitial remodelling and/or inflammation but not airway remodelling in the alarmin-driven asthma model

The alarmin-driven asthma model was generated using IN IL-33 challenge (30 ng per mouse) for 6 days. Inhaled therapeutic treatment with IN NAM (200 µg/mouse) was delivered twice daily, 2h before IL-33 administration, from the 2nd day of challenge to the end of the experiment. All statistical analyses were performed using a one-way ANOVA with Holm-Sidak post hoc test

In the larger airways of alarmin-driven asthma, IL-33 challenge induced total tissue and epithelial tissue remodelling. Here, inhaled NAM treatment had no effect on total tissue as this result failed to pass the threshold for significance (p_{adj} = **0.053**), as shown in **Figure 5.2D**. In the smaller airways, IL-33 only induced goblet cell remodelling and inhaled NAM treatment had no significant effect (p_{adj} = **0.063**) remodelling as shown in **Figure 5.2E**. IL-33 also induced interstitial remodelling and/or inflammation in the lung parenchyma that was significantly abrogated by inhaled NAM treatment (p_{adj} = **0.044**), as shown in **Figure 5.2F.**

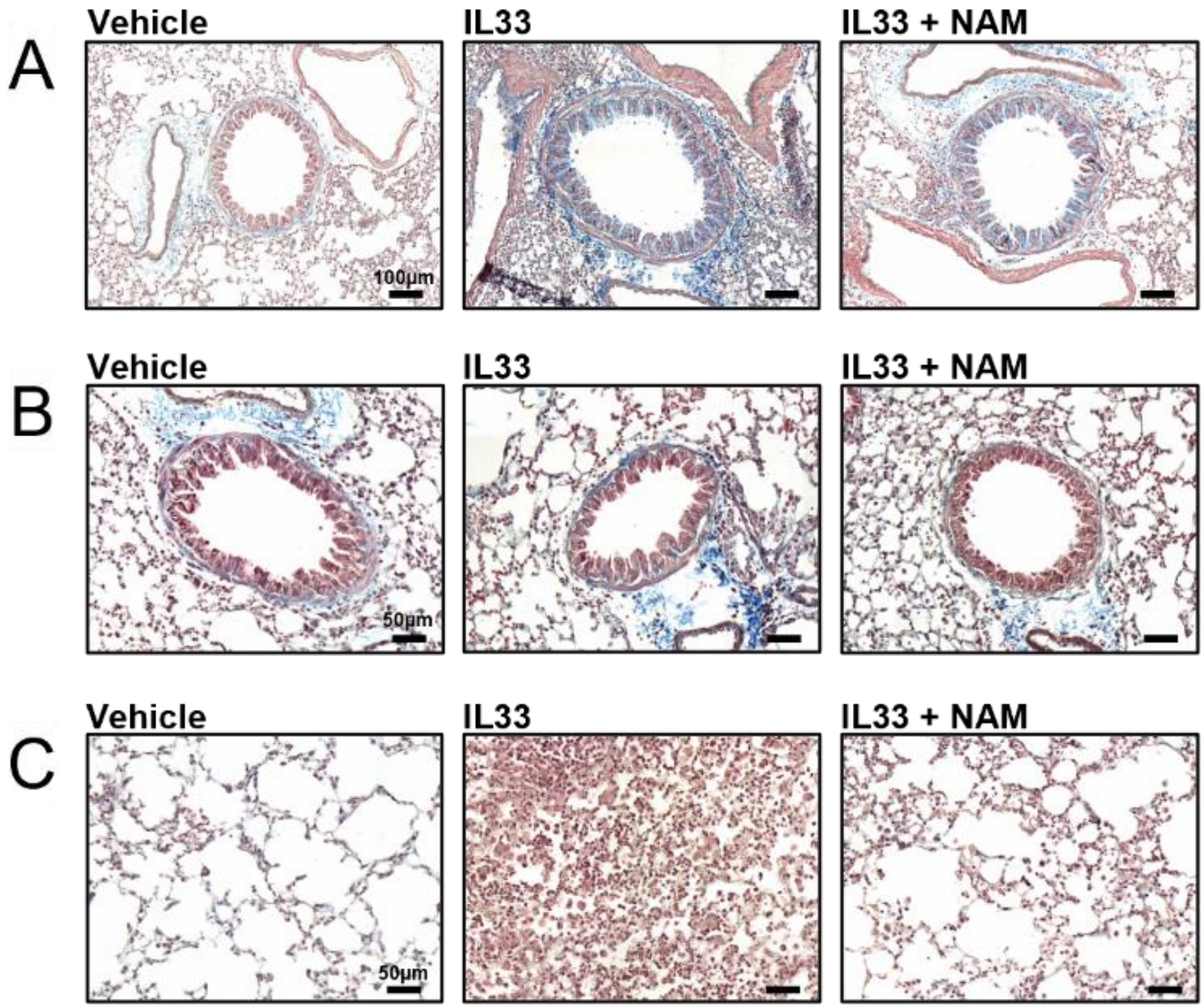
A
Vehicle
IL33
IL33 + NAM
100μm
B
Vehicle
IL33
IL33 + NAM
50μm
C
Vehicle
IL33
IL33 + NAM
50μm

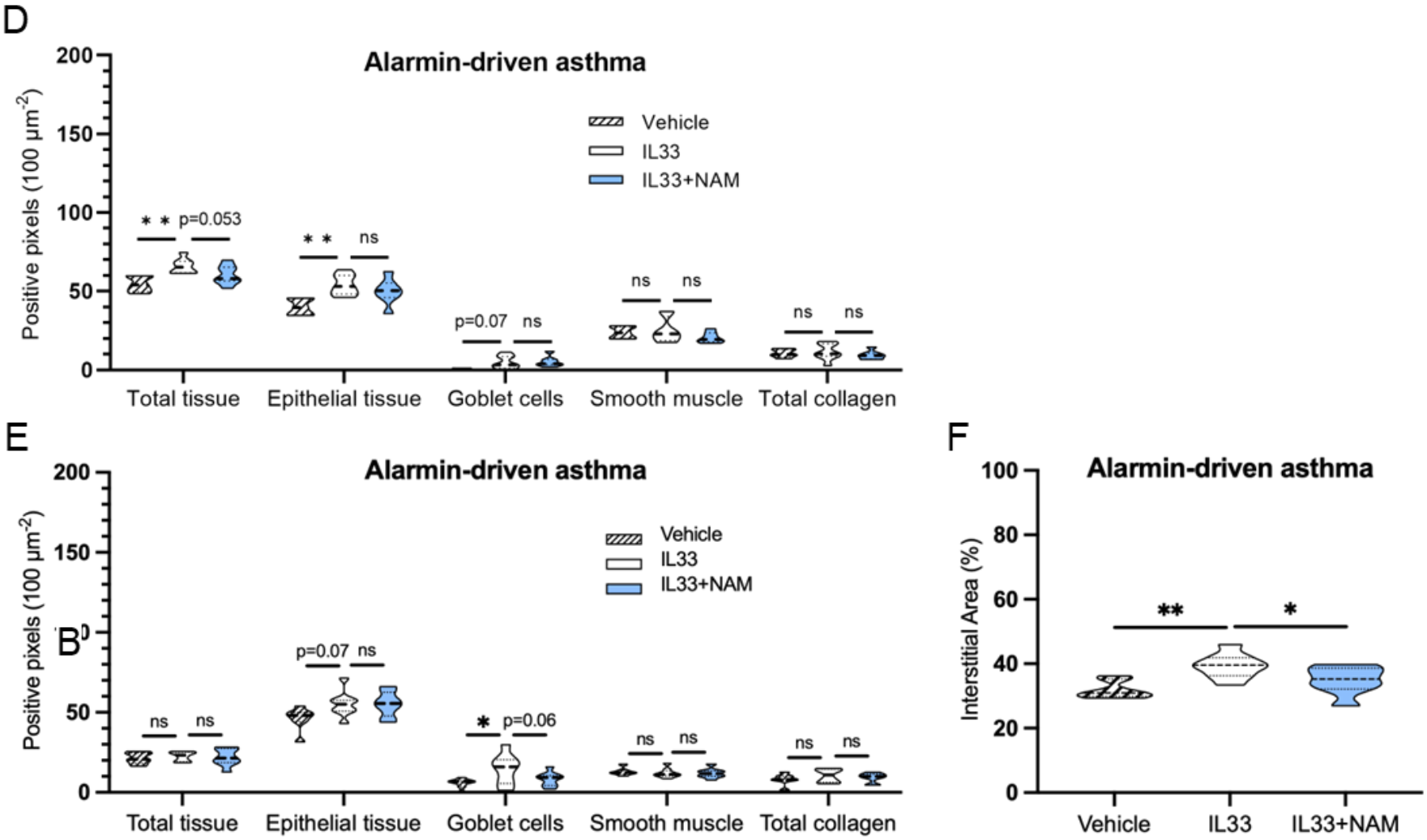
D
Alarmin-driven asthma
Positive pixels (100 µm-2)
Vehicle
IL33
IL33+NAM
* * p=0.053
* *
ns
p=0.07
ns
ns
ns
ns
ns
Total tissue
Epithelial tissue
Goblet cells
Smooth muscle
Total collagen
E
Alarmin-driven asthma
Positive pixels (100 µm-2)
Vehicle
IL33
IL33+NAM
ns
ns
p=0.07
ns
*
p=0.06
ns
ns
ns
ns
Total tissue
Epithelial tissue
Goblet cells
Smooth muscle
Total collagen
F
Alarmin-driven asthma
Interstitial Area (%)
**
*
Vehicle
IL33
IL33+NAM

Figure 5.2. Inhaled NAM treatment abolished interstitial remodelling and/or inflammation in the alarmin-driven asthma model. (**A**) Larger airways (> 50,000 μm^2), (**B**) smaller airways (< 50,000 μm^2) and (**C**) interstitial regions were identified from Masson's trichrome stained lung sections from the model of alarmin-driven asthma in IL-33 challenged mice. (**D**) Only total tissue and epithelial tissue remodelling in the larger airways and (**E**) goblet cell remodelling in the smaller airways was induced by IL-33 challenge, likely due to the short duration of this experiment (Li et al., 2015). Inhaled NAM treatment had no significant effect on larger or smaller airway remodelling. (**F**) Interstitial remodelling and/or inflammation was significantly reduced by inhaled NAM treatment. Airway remodelling markers were quantified using qHACC and interstitial remodelling and/or inflammation was quantified using qHIT. Statistical significance identified using one-way ANOVA with Holm-Sidak post-hoc test or Kruskal-Wallis with Dunn's post-hoc test. A truncated violin plot was used to demonstrate frequency distribution of the data where dashed lines represent the median and dotted lines represent the upper and lower quartiles, respectively. N = 5-8, n = 3, ROI = 2-6 (larger airways, 1-7 (smaller airways) and 9-10 (interstitium), ns (p_{adj} > 0.05), * (p_{adj} < 0.05), ** (p_{adj} < 0.01). Graticule (A) 100 μm and (B and C) 50 μm. ANOVA: analysis of variance; IL-33; interleukin-33; NAM: negative allosteric modulator of the calcium-sensing receptor; qHACC: quantitative histomorphometry of airway cross-section components; qHIT: quantitative histomorphometry of interstitial tissue.

5.2.3 NAM treatment, not FP, abolished smaller airway goblet cell remodelling in longer-term IgE/Th2 asthma

The longer-term IgE/Th2 asthma model, was generated by sensitising mice with two intraperitoneal injections of OVA (50 µg) at day 0 and 10 where IgE measurements were used to confirm sensitisation. Mice were then challenged with nebulised OVA (0.5 %) on alternate days for 9 days, starting from day 21, and inhaled therapeutic treatment with nebulised NAM (6µM) or fluticasone propionate (FP; 0.25 mg) was performed twice daily from the 5th day of OVA challenge for 6 days. All statistical analyses were performed using a one-way ANOVA with Holm-Sidak post hoc test

In the larger airways of longer-term IgE/Th2 asthma, OVA induced total tissue, epithelial tissue and goblet cell remodelling that was unaffected by inhaled NAM, FP or NAM + FP treatment. However, in direct comparison with FP, NAM treatment performed significantly better for peribronchial collagen remodelling ($\boldsymbol{p_{adj}}$ **= 0.0094**), as shown in **Figure 5.3D**. In the smaller airways, OVA induced all features of airway remodelling, with the exception of smooth muscle. Here, NAM treatment significantly abolished goblet cell remodelling ($\boldsymbol{p_{adj}}$ **= 0.013**), where FP did not. In fact, inhaled FP treatment significantly worsened peribronchial collagen remodelling, when compared to vehicle ($\boldsymbol{p_{adj}}$ **= 0.0074**). Furthermore, in direct comparison with FP, NAM exhibited significantly improved total tissue and peribronchial collagen remodelling, as shown in **Figure 5.3E**. OVA also induced interstitial remodelling and/or inflammation in the lung parenchyma. Here, inhaled NAM, FP or co-treatment had no effect on interstitial remodelling and/or inflammation in the lung parenchyma, as shown in **Figure 5.3F**.

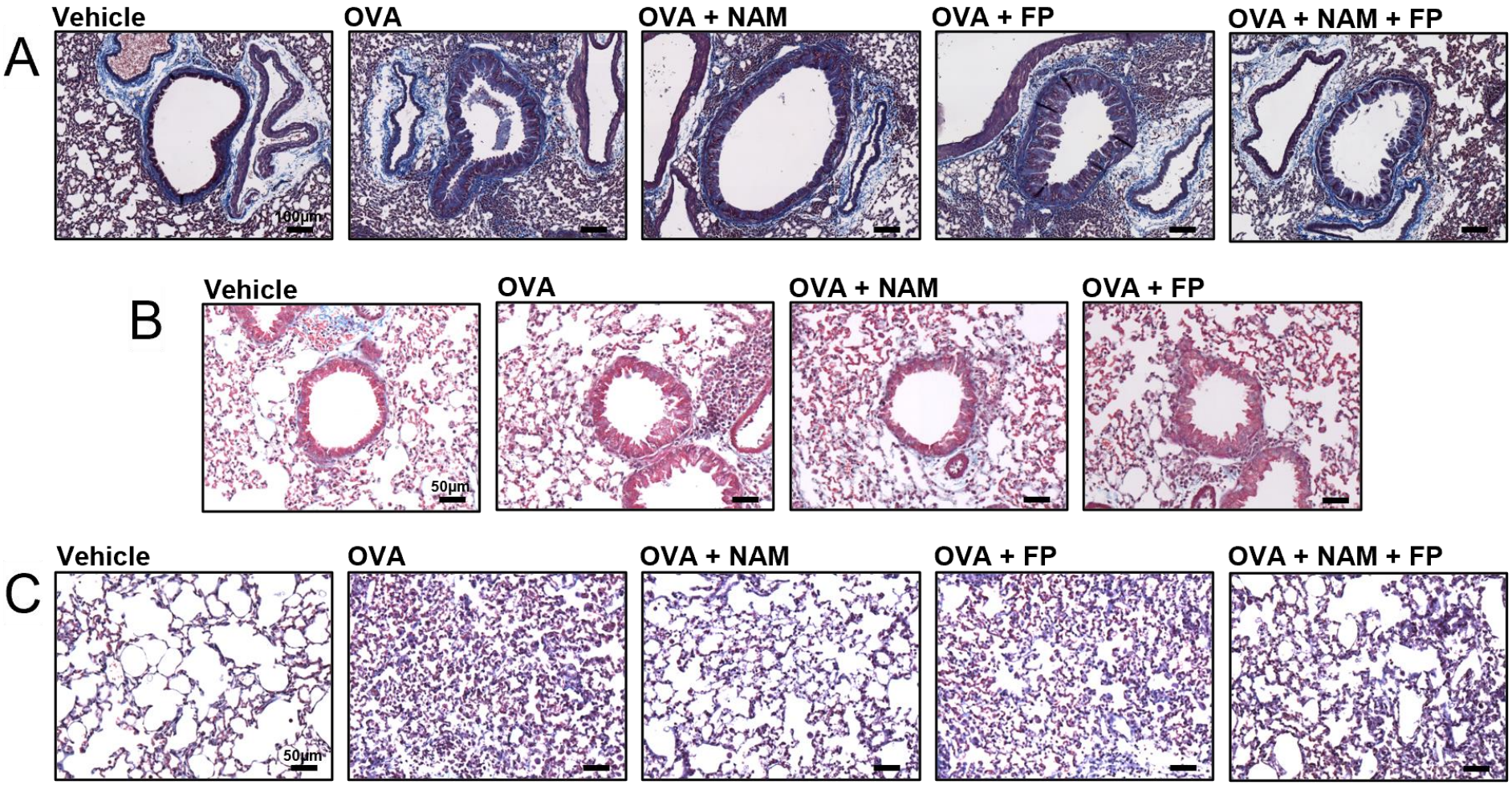
A
Vehicle
OVA
OVA + NAM
OVA + FP
OVA + NAM + FP
100μm
B
Vehicle
OVA
OVA + NAM
OVA + FP
50μm
C
Vehicle
OVA
OVA + NAM
OVA + FP
OVA + NAM + FP
50μm

D

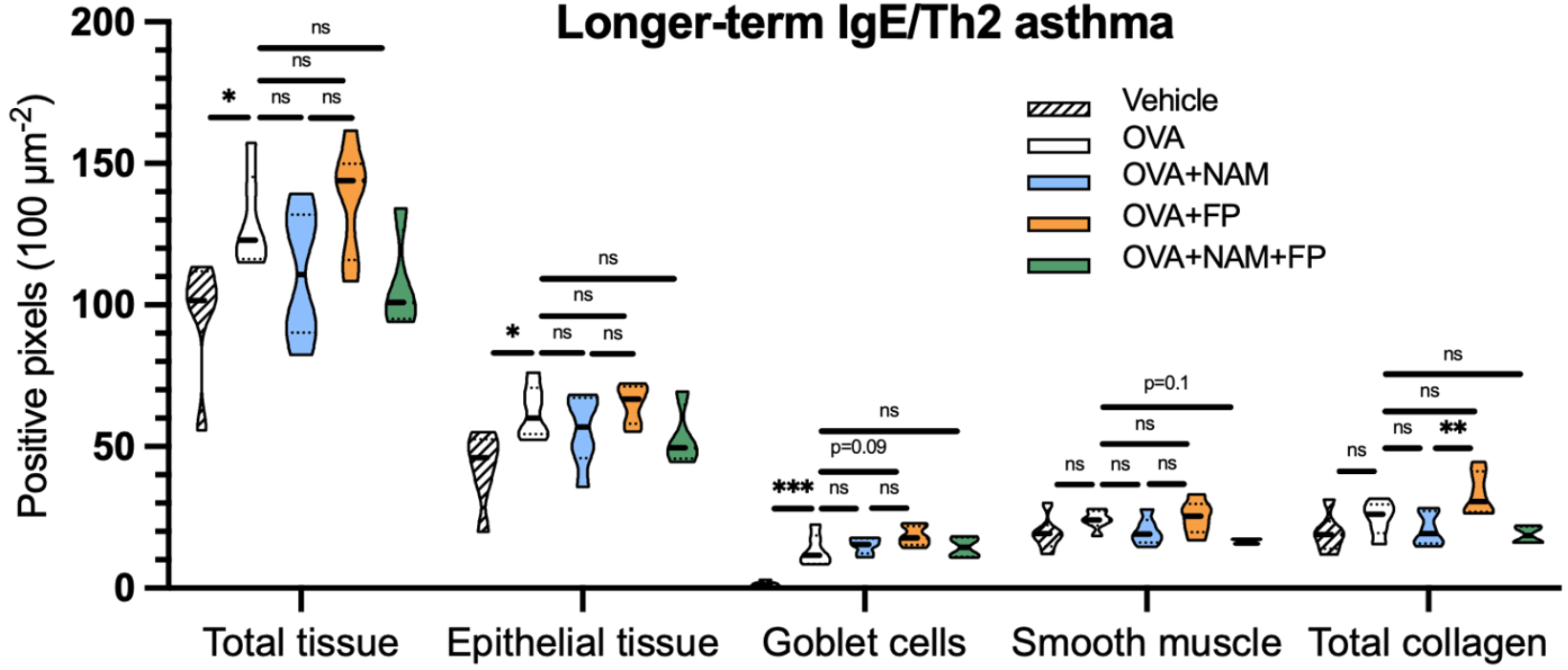
Longer-term IgE/Th2 asthma
Positive pixels (100 µm-2)
200
150
100
50
0
Vehicle
OVA
OVA+NAM
OVA+FP
OVA+NAM+FP
Total tissue
Epithelial tissue
Goblet cells
Smooth muscle
Total collagen
ns
*
***
**
p=0.09
p=0.1

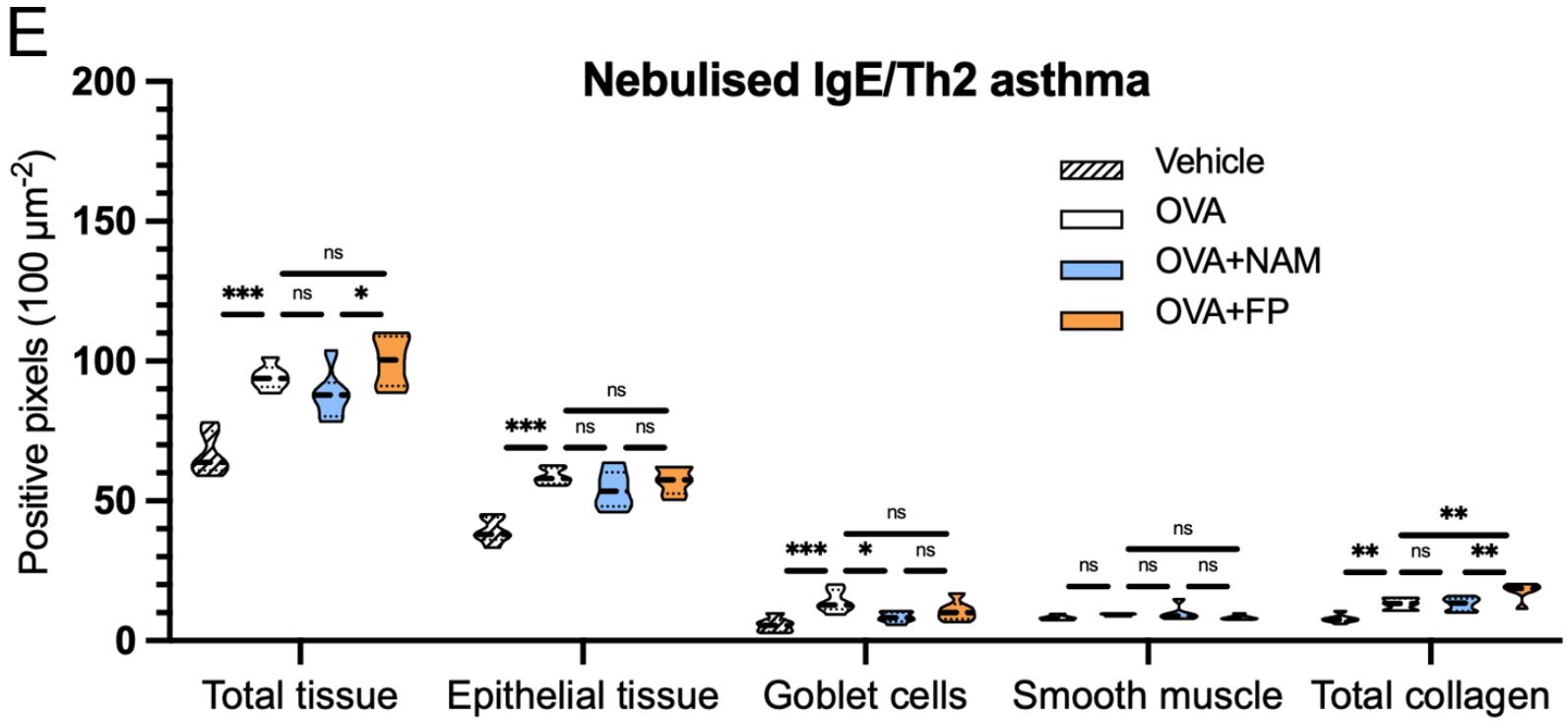
E
Nebulised IgE/Th2 asthma
Positive pixels (100 µm-2)
200
150
100
50
0
Vehicle
OVA
OVA+NAM
OVA+FP
***
ns
*
ns
***
ns
ns
ns
***
*
ns
ns
ns
ns
**
ns
**
Total tissue
Epithelial tissue
Goblet cells
Smooth muscle
Total collagen

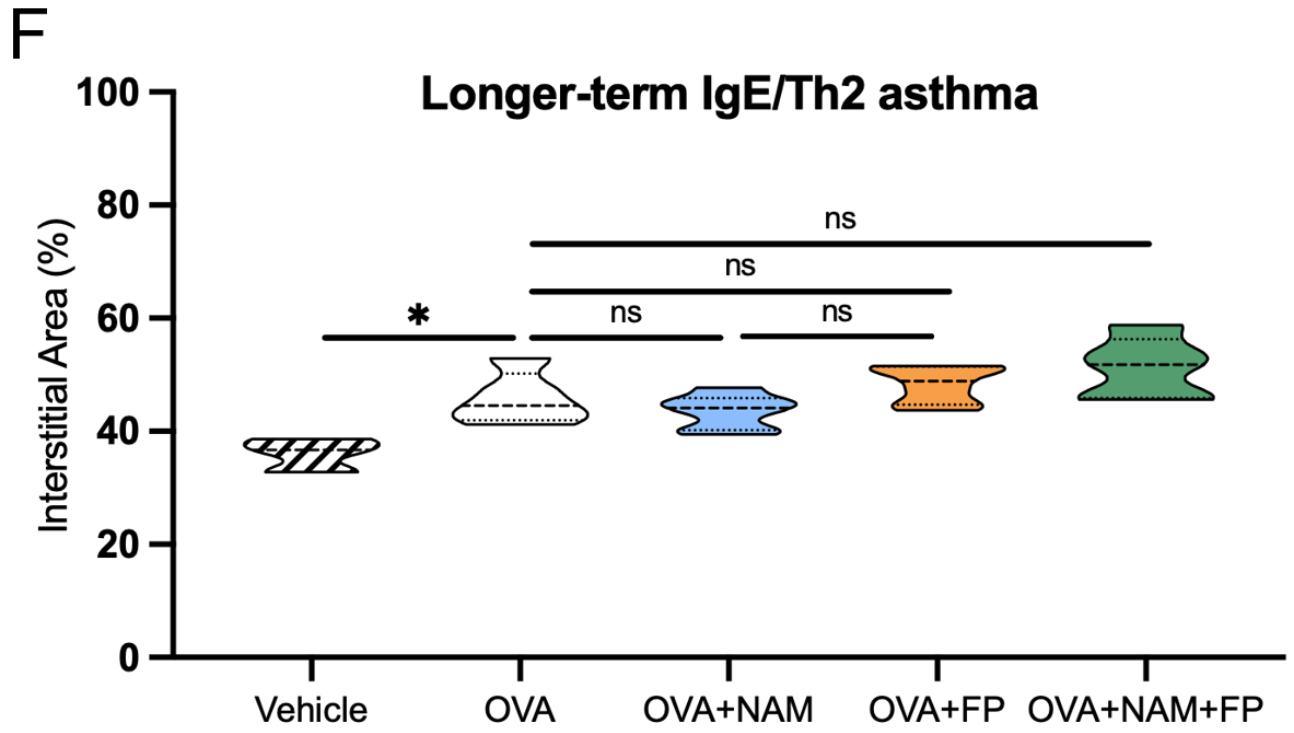

Figure 5.3. Inhaled NAM treatment significantly reduced goblet cell remodelling in the smaller airways of the longer-term IgE/Th2 asthma model. (**A**) Larger airways (> 50,000 μm^2), (**B**) smaller airways (< 50,000 μm^2) and (**C**) interstitial regions were identified from Masson's trichrome stained lung sections from the model of longer-term IgE/Th2 asthma in OVA-sensitised and -challenged mice. (**D**) Inhaled NAM treatment had no effect on total tissue, epithelial tissue and goblet cell remodelling in the larger airways but (**E**) significantly reduced goblet cell remodelling in the smaller airways. (**F**) Inhaled NAM treatment had no effect on interstitial remodelling and/or inflammation. In head-to-head comparison, inhaled NAM treatment out-

performed FP in reducing peribronchial collagen in the larger airways as well as total tissue and peribronchial collagen remodelling in the smaller airways. No significant differences were found between NAM and FP in the interstitial region. Airway remodelling markers were quantified using qHACC and interstitial remodelling and/or inflammation was quantified using qHIT. Statistical significance identified using one-way ANOVA with Holm-Sidak post-hoc test. A truncated violin plot was used to demonstrate frequency distribution of the data where dashed lines represent the median and dotted lines represent the upper and lower quartiles, respectively. N = 3-6, n = 3-4, ROI = 2-6 (larger airways), 9-22 (smaller airways) and 10-12 (interstitium), ns ($p_{adj} > 0.05$), * ($p_{adj} < 0.05$), ** ($p_{adj} < 0.01$), *** ($p_{adj} < 0.001$). Graticule (A) 100 µm and (B and C) 50 µm. ANOVA: analysis of variance; IgE: immunoglobulin E; NAM: negative allosteric modulator of the calcium-sensing receptor; OVA: ovalbumin; qHACC: quantitative histomorphometry of airway cross-section components; qHIT: quantitative histomorphometry of interstitial tissue.

5.3 Discussion

In this study, I aimed to investigate the role of the CaSR in asthma-related lung remodelling. Here, I have presented evidence that suggests inhaled NAM treatment reduces a range of lung remodelling characteristics in the larger and smaller airways as well as the parenchymal interstitium. This evidence suggests a mechanistic link between the CaSR and the previously observed presence of CaSR expression altering cytokines and endogenous polycations in the lung that have been implicated in asthmatic lung remodelling. Furthermore, inhaled NAM treatment may a better alternative for treating lung remodelling, particularly goblet cells, than the current standard of asthma care, FP.

The CaSR is known to be expressed throughout the lung epithelium, including *MUC5AC* expressing cells (Yang et al., 2014a; Yang et al., 2014b; Yarova et al., 2015), airway smooth muscle (Yarova et al., 2015), human lung fibroblasts (see Chapter 6), vascular cells (Schepelmann et al., 2016) and immune cells where NAM treatment has previously been shown to influence cell behaviour (Yarova et al., 2015; Yarova et al., 2016; Yarova et al., 2021). Therefore, it is plausible that inhaled NAM treatment was able to target these cell types in this study.

Interestingly, activation of the receptor is required for NAMs to elicit their effects, as they only bind to the receptor in the presence of an orthosteric ligand. However, the animals in this study were not exposed to exogenous CaSR-agonists. Furthermore, OVA and IL-33 are not known to be direct CaSR activators. Therefore, I hypothesise that CaSR activation was induced by the plethora of extracellular polycations implicated in asthma that are known to activate the CaSR, such as ECP, MBP, extracellular Ca^{2+} or most notably ornithine-derived polyamines (Kurosawa et al., 1992; Gibson et al., 1998; Koller et al., 1999; Lönnkvist et al., 2001; Bartoli et al., 2004; Rossol et al., 2012; North et al., 2013; Yarova et al., 2015).

Furthermore, OVA has been shown to upregulate CaSR expression in the epithelium of mouse lungs and both OVA and IL-33 have been shown to upregulate production of CaSR expression-regulating cytokines, including IL-1ß, IL-6, IL-13, TNF-α and TGF-

β (Canaff & Hendy, 2005; Fetahu et al., 2014; Yarova et al., 2015; Li et al., 2015; see Chapter 6).

The effects of FP observed in this study, causing significant worsening of peribronchial collagen in the smaller airways, have been previously observed. Although these findings are contradictory to suggestions that FP can reduce epithelial thickening, goblet cell metaplasia, smooth muscle and extracellular matrix remodelling in models of asthma and rhinitis (Vanacker et al., 2001; Wakahara et al., 2008; Riesenfeld et al., 2010; Evans et al., 2012; Leclere et al., 2012; Ballone et al., 2017); other studies have found no prevention of airway remodelling at low doses or even worsening of ECM remodelling in the airway wall that support the findings of this study (Vanacker et al., 2002a; Vanacker et al., 2002b; Liu et al., 2009b). This is likely not the cause of incorrect administration as both NAM and FP treatment reduced total leukocyte and eosinophil cell count in the bronchoalveolar lavage fluid (BALF) of these animals suggesting the compound was correctly administered (Yarova et al., 2021). Further studies are required to adequately investigate the effect of FP on peribronchial collagen remodelling. Nonetheless, this evidence may support the hypothesis that inhaled NAMs impart direct protection against airway remodelling, in addition to the previously described effects on inflammation; however, it may also highlight differences in the mechanisms of action between NAMs and FP on inflammation (Yarova et al., 2015; Yarova et al., 2021). This difference in mechanism of action, may relate to the hypothesis that airway hyperresponsiveness drives airway remodelling in the asthmatic lung because NAMs, and not FP, have been shown to play a central role in reducing airway hyperresponsiveness *in vitro* (Yarova et al., 2015). It may also explain why this alteration of lung remodelling was observed in the smaller airways but not the alveolar interstitium in this experiment.

5.3.1 Inhaled NAM treatment reduces interstitial remodelling and/or inflammation

Interstitial remodelling and/or inflammation in the alveolar walls of the distal lung parenchyma is not considered a feature of human asthma; however, there is evidence to suggest the distal lung parenchyma is altered in the asthmatic lung (Dolhnikoff et al., 1998; Angeli et al., 2008; Starling et al., 2009; Boser et al., 2017).

OVA sensitisation and challenge has been shown to induce this remodelling characteristic in guinea pig models of asthma (Possa et al., 2012; Pigati et al., 2015; Fehrenbach et al., 2017). Here I present evidence that may suggest this is also a feature of murine models of IgE/Th2 asthma; however, further studies are required to identify if this is an artefact of parenchymal inflammation. The relevance of this to human asthma is limited but it is important to not overlook these features in models of disease as they may provide insight into the mechanisms of remodelling that have relevance to asthma or other diseases that induce remodelling in the lung parenchyma, such as chronic obstructive pulmonary disease (COPD) or idiopathic pulmonary fibrosis (IPF).

5.3.2 The effects of NAM treatment are not the consequence of unwanted effects of the drug on systemic Ca^{2+} homeostasis

For all experimental animals, the lungs were morphologically normal and no alterations to serum calcium or parathyroid hormone (PTH) levels were observed following NAM treatment (Yarova et al., 2015; Yarova et al., 2021). This suggests the effects of the NAM administered were limited to the lung and did not alter systemic calcium homeostasis and parathyroid hormone regulation. In the models of shorter-term IgE/Th2 asthma and alarmin-driven asthma, serum Ca^{2+} was also unchanged, as measured by my colleague Ping Huang (unpublished). Therefore, any changes to lung remodelling observed in these experiments was unlikely to be mediated by unwanted effects on Ca^{2+} homeostasis.

This study has also demonstrated the suitability of the qHACC approach for determining airway and ECM remodelling in models of IgE/Th2 and alarmin-driven asthma. This is particularly remarkable considering the acute experimental duration used for these experiments that were designed to investigate inflammation and airway hyperresponsiveness. Typically, longer exposure duration or severity is required to investigate lung remodelling (Li et al., 2015).

5.4 Study Limitations

On a number of occasions, such as total tissue in the larger airways of alarmin-driven asthma, epithelial tissue in the smaller airways of shorter-term IgE/Th2 asthma, and

goblet cells in the smaller airways of alarmin-driven asthma, evidence of a net benefit to airway remodelling was not found (p_{adj} > 0.05). However, these experiments all showed a low probability of occurring by chance. Following suggestions made by the American Statistical Association, advising that scientific conclusions should not be entirely based on p value thresholds, further studies are required to determine if the true effect is consistent with the null hypothesis (Wasserstein & Lazar, 2016). To increase statistical power, reducing the variation between airways was a priority; however, the stringent exclusion criteria resulted in a low number of representative airways in some cases. This should be addressed in future studies by increasing the number of lung sections for each animal and therefore increase the likelihood of identifying a greater number of comparable airways per animal. Furthermore, in some models remodelling characteristics remained unchanged from the vehicle control. Where this was the case it was not possible to investigate the effect of NAM treatment on that characteristic of lung remodelling. Therefore, the severity of remodelling induced in the models used in these experiments may have been suboptimal and represents a limitation of these experiments.

As discussed in the Chapter 3 study limitations (section 3.4), the qHIT analysis was also limited by the inability to distinguish lung tissue cells from resident or infiltrating inflammatory cells. Although the magnification is increased from the conventional Ashcroft scoring protocol, permitting identification of these cells that may not have been previously possible, it highlights the presence of inflammatory infiltration into the lung parenchyma that must be removed to permit quantification of alveolar interstitial tissue remodelling alone. Therefore, the inability of qHIT to distinguish remodelling from inflammation is a limitation of this approach.

Further studies are also supported by the findings that CaSR played a central role in many of the same remodelling characteristics in other models or size of airway. Therefore, this may indicate limitations in my methodology. Sample size largely conformed to the power analysis recommendation of 8 animals per treatment group. Therefore, it is more likely that remodelling severity was a limitation in these experiments that were designed for investigating the effects of NAM on

inflammation. Longer challenge exposure duration or severity is typically required to investigate lung remodelling (Li et al., 2015).

Another limitation of this study is that endogenous CaSR agonist levels were not assessed in these animals to confirm activation of the CaSR. To further investigate these phenomena, future studies could aim to increase the severity of remodelling by extending the duration of exposure to inhaled challenge or by co-exposing these animals to an inhaled challenge as well as an exogenous CaSR agonist or PAM.

5.5 Conclusions

In conclusion, this study demonstrates the CaSR is central to asthma-like airway, including epithelial, goblet cell and ECM remodelling, as well as alterations to remodelling and/or inflammation in the lung parenchyma. NAM treatment may also be a better alternative to the current standard of asthma care, FP, for preventing lung remodelling. This evidence, in addition to the previously described effects on inflammatory cell recruitment, cytokine production and airway hyperresponsiveness, further supports the repurposing of inhaled NAMs for the treatment of asthma.

5.6 Future directions

To confirm that CaSR activation drives asthma-related airway and interstitial remodelling, co-exposure of OVA or IL-33 with known CaSR agonists, or positive allosteric modulators of the CaSR (PAMs), could be used to proof of concept to investigate whether increased CaSR activation worsens lung remodelling. Although treatments in these experiments were therapeutic, to mimic the treatment of real world asthma, a time course experiment using normal and asthmatic human lung fibroblasts exposed to mediators of asthmatic ECM remodelling, such as TGFß, could be used to investigate whether NAM treatment has the potential to reverse ECM remodelling, an aspect that was beyond the scope of the studies in this experiment. Hydrogels are also emerging as the best platform from investigating changes ECM remodelling that better represent the mechanical microenvironment of the lung (de Hilster et al., 2020). Furthermore, tight junction protein (ZO)-1 and E-cadherin immunohistochemistry could be used to identify the epithelial barrier and individual

cells to allow the determination of epithelial alterations and distinguish between changes in cell number and cell size (i.e. hyperplasia and hypertrophy). Additionally, providing there is a net change in tissue morphometry or by using additional immunohistochemical staining of tight junction proteins such as E-cadherin and tight junction protein 1, epithelial barrier integrity could be incorporated into the qHACC approach.

Although these markers are informative, the current standard for assessing epithelial barrier integrity is to determine the transepithelial electrical resistance (TEER). It is not possible to implement TEER measurements *in vivo*; however, precision cut lung slices from *in vivo* experiments or *in vitro* human bronchial epithelial cells in air-liquid interface could be analysed using this technique to determine the effect of NAM treatment of models of loss of barrier integrity, as used by Swaby et al. (2023). A combination of these approaches would be most effective to determine the effect and potential mechanism by which this occurs. Lastly, cluster of differentiation (CD)31+ staining could also be used to investigate neovascularisation known to occur in the murine models of IL-33 and OVA challenge (Li et al., 2015).

Lastly, the precise mechanisms of remodelling, such as the cellular signalling cascades downstream of the CaSR, could be investigated *in vitro* using human cells, such as human bronchial epithelial cells or fibroblasts. To investigate the specific pathways associated with CaSR activation in these cell types RNA-sequencing and western blotting could be used to investigate regulation of signalling molecule expression and phosphorylation, respectively.

CHAPTER 6: INVESTIGATING THE ROLE OF THE CASR IN TGF-ß-INDUCED LUNG REMODELLING IN FIBROBLASTS

6.1 Introduction

Transforming growth factor (TGF)-ß is a potent mediator of remodelling implicated in aging, asthma, chronic obstructive pulmonary disease (COPD) and idiopathic pulmonary fibrosis (IPF). To elicit its effects on cell adhesion, secretion, growth, proliferation, differentiation, senescence and extracellular matrix (ECM) remodelling, TGF-ß activates its canonical Smad signalling pathway but also activates non-canonical pathways, including mitogen-activated protein kinase (MAPK) (extracellular signal-regulated kinase (ERK), c-Jun N-terminal kinase (JNK), p38), phosphatidylinositol 3-kinase (PI3K)/Akt, mechanistic target of rapamycin (mTOR), RhoA and Wingless-related integration site (Wnt).

Although TGF-ß is not known to directly activate the calcium-sensing receptor (CaSR), bidirectional transactivation has been demonstrated between the TGF-ß receptor (TGF-ßR) and other G-protein coupled receptors (GPCRs) to greatly expand the repertoire of cellular responses induced by TGF-ß (Burch et al., 2010; Little et al., 2010; Little et al., 2011; Dayati et al., 2018). TGF-ß also upregulates the production of inflammatory cytokines known to increase CaSR expression, such as interleukin (IL)-1ß, IL-6, IL-13 and tumour necrosis factor (TNF)-α, as well as CaSR-activating polycations, such as polyamines via increased arginase activity (Boutard et al., 1995; Canaff & Hendy, 2005; Fetahu et al., 2014; Yarova et al., 2015).

Previous chapters of this thesis or previous studies have demonstrated that genetic or pharmacological ablation of the CaSR can reduce tissue remodelling in the lung or other organs (Yarova et al., 2016; Schepelmann et al., 2016). Coincidentally, the pattern of non-canonical TGF-ß signalling closely resembles elements of CaSR signalling. Although CaSR-mediated activation of MAPK (ERK, JNK, p38), PI3K/Akt, mTOR, RhoA, Wnt and Ca^{2+}_i augmentation has been mechanistically linked to tissue remodelling, the mechanism by which the CaSR mediates lung remodelling is unclear.

This study aimed to investigate the role of the CaSR in mechanisms of TGF-β-induced lung remodelling. To do this, mRNA and protein expression was used to determine the effect of negative allosteric modulator of the CaSR (NAM) treatment on signalling pathway and remodelling process regulation in fibroblasts exposed to the remodelling mediator, TGF-β. In particular the gene enrichment (GO) term enrichment tool was used to connect patterns of differentially expressed genes to terms that describe their biological function within the cell (Pomaznoy et al., 2018). The identified pathways were then further investigated using a hypothesis-driven gene-by-gene approach.

6.2 Results

Normal human lung fibroblasts (NHLFs), from three ethically-consented patients between the ages of 56 and 67, were treated for 72 hours with 1) Vehicle only (0.01% dimethyl sulfoxide (DMSO) in phosphate-buffered saline (PBS)); 2) NAM only (1 μM NPS2143 in vehicle); 3) TGF-β1 (5 ng/ml in vehicle); or 4) a 4-hour pre-incubation with NAM (1 μM NPS2143) followed by treatment with TGF-β1 and NAM (5 ng/ml TGF-β1, 1 μM NPS2143 in vehicle).

6.2.1 NAM treatment ameliorates TGF-β-induced TGF-β, Wnt and CaSR signalling

To determine the effect of NAM treatment on TGF-β-induced cell signalling, GO terms were used to connect patterns of differentially expressed genes to TGF-β- or CaSR-related signalling pathways. These terms, and their direction of regulation, are summarised in **Table 6.1**. As expected, TGF-β exposure upregulated GO terms associated with TGF-β receptor and Wnt signalling. However, TGF-β exposure also downregulated genes associated with MAPK cascade activation and regulation of Ras, stress-activated MAPK, JNK, p38, PI3K and Rho signalling. NAM treatment upregulated the regulation of Ras, stress-activated MAPK, JNK, Rho and specifically upregulated negative regulation of mTOR signalling. NAM treatment also downregulated TGF-β receptor signalling, Ras signal transduction, Wnt signalling and positive regulation of mTOR signalling. This demonstrates that NAM treatment plays a central role in the regulation of TGF-β signalling pathways and provides rationale to further investigate the role of the CaSR in these pathways.

Table 6.1. NAM treatment abrogates the activation or regulation of TGF-β-induced signalling pathways in human lung fibroblasts. This table summarises the differentially expressed GO terms describing biological function within the cell; the direction of regulation; the number of differentially expressed genes that match that term; and the adjusted p value (p_{adj}). Up- and down-regulated genes were input into the GOnet enrichment tool separately to provide the direction of regulation. Here, NAM treatment abrogated activation or regulation of several TGF-β signalling processes, including TGF-βR, Ras, MAPK (JNK, p38), PI3K, mTOR, Rho and Wnt signalling. Statistical significance calculated using a Fisher exact test with Benjamini-Hochberg p value correction. N = 3, n = 6. * (p_{adj} < 0.05), ** (p_{adj} < 0.01), *** (p_{adj} < 0.001), **** (p_{adj} < 0.0001). TGF-βR: Transforming growth factor beta receptor; MAPK: Mitogen activated protein kinase; JNK: Jun N-terminal kinase; PI3K: Phosphatidylinositol 3-kinase; mTOR: Mechanistic target of rapamycin; Wnt: Wingless-related integration site; NAM: Negative allosteric modulator of the calcium-sensing receptor.

Gene Ontology (GO) term	TGFβ			TGFβ + NAM		
Signalling processes	**Direction**	**Genes**	**p_{adj}**	**Direction**	**Genes**	**p_{adj}**
Regulation of TGFβ receptor signaling pathway	UP	33	***	DOWN	25	*
Ras protein signal transduction				DOWN	49	*
Positive regulation of mTOR signaling				DOWN	13	*
Wnt signaling pathway	UP	73	***	DOWN	73	***
MAPK cascade	DOWN	55	*			
Regulation of Ras protein signal transduction	DOWN	52	****	UP	49	***
Regulation of stress-activated MAPK cascade	DOWN	38	*	UP	40	*
Regulation of JNK cascade	DOWN	34	**	UP	34	*
Regulation of p38 MAPK cascade	DOWN	11	*			
Regulation of PI3K activity	DOWN	18	***			
Regulation of Rho signal transduction	DOWN	31	***	UP	29	*
Negative regulation of mTOR signaling				UP	15	**

6.2.1.1 Canonical TGF-β signalling

Here, TGF-β upregulated its own expression (*TGFB1*) as well as *SMAD7* and downregulated the *TGFBRIII* co-receptor, *SMAD3* and *SMAD6* indicating downregulation of Smad2/3 signalling after 72 hours (**$\log_2$ fold change *TGFB1* = 1.39, *SMAD7* = 1.04, *TGFBR3* = -2.39, *SMAD3* = -1.72, *SMAD6* = -0.81; p_{adj} < 0.05; TGF-β vs vehicle**). This is consistent with reports that TGF-β upregulates Smad2/3 signalling within 1 hour and downregulates Smad2/3 signalling after 3 hours which then remains downregulated for at least 72 hours (Baugé et al., 2011). NAM treatment significantly reversed *TGFB1*, *TGFBRIII*, and *SMAD3* but also upregulated the TGF-BR associated protein 1 (*TGFBRAP1*) expression demonstrating that NAM treatment regulates central Smad2/3 signalling components (**$\log_2$ fold change *TGFB1* = -0.56, *TGFBR3* = 0.27, *SMAD3* = 0.37, *TGFBRAP1* = 0.69; p_{adj} < 0.05; TGF-β + NAM vs TGF-β**). When compared to baseline expression, *SMAD4* and *SMAD6* expression was indistinguishable from baseline expression indicating dampening of TGF-β-induced effects on Smad2/3 signalling (**p_{adj} > 0.05; TGF-β + NAM vs vehicle**), as shown in **Figure 6.1**.

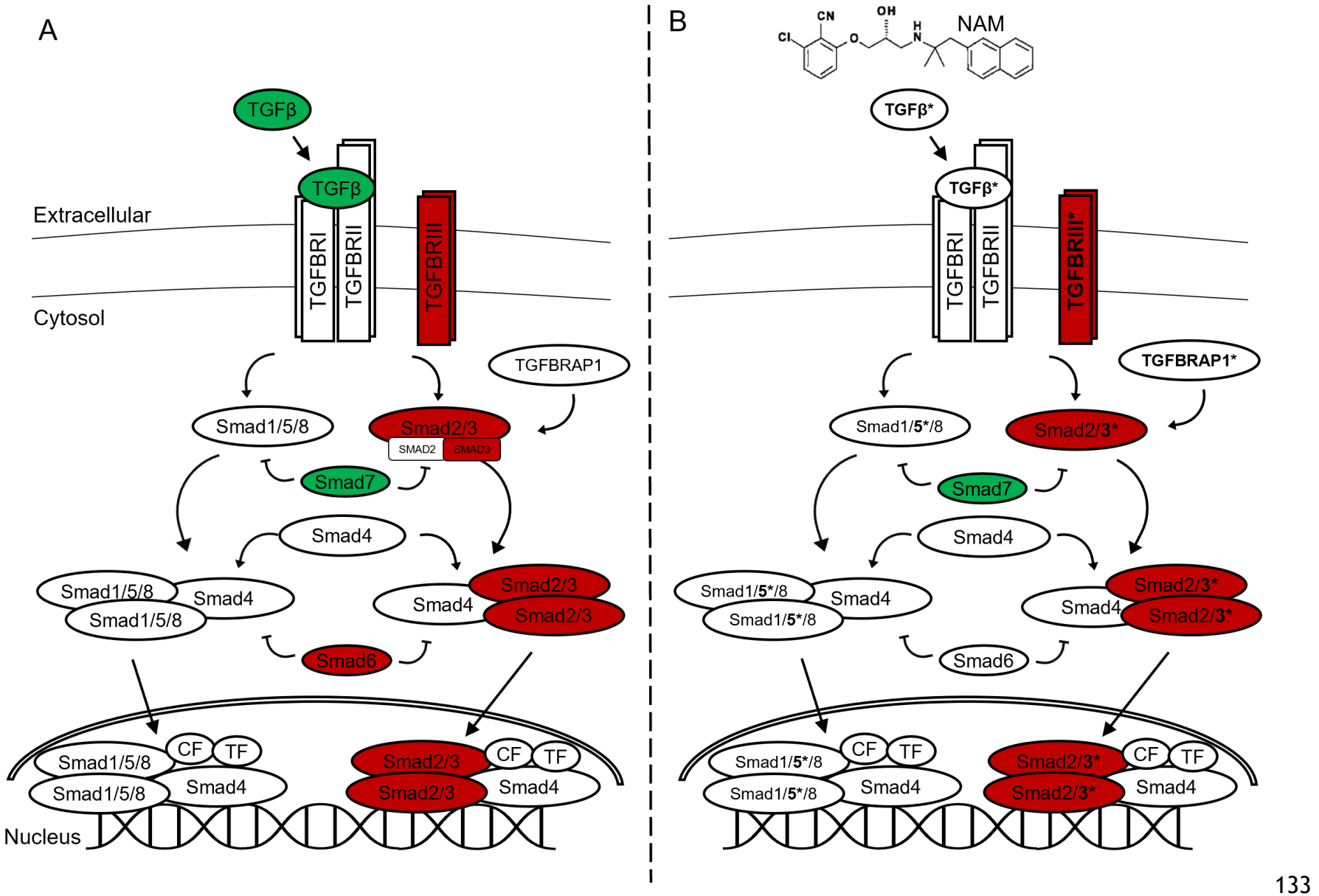
A
B
NAM
TGFβ
TGFβ
Extracellular
Cytosol
TGFBRI
TGFBRII
TGFBRIII
TGFBRAP1
Smad1/5/8
Smad2/3
SMAD2
SMAD3
Smad7
Smad4
Smad6
CF
TF
Nucleus
TGFβ*
TGFBRIII*
TGFBRAP1*
Smad1/5*/8
Smad2/3*

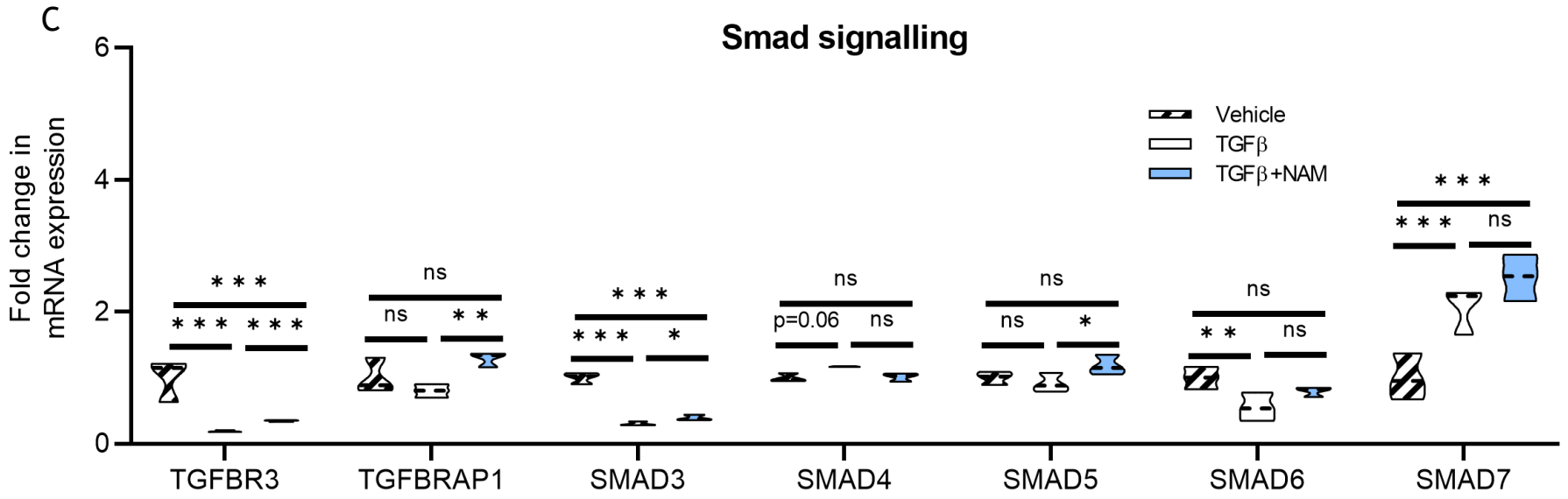

Figure 6.1. NAM treatment differentially regulated TGF-ß-induced Smad signalling components in human lung fibroblasts. (**A**) TGF-ß binds to the TGF-ßR complex activating canonical Smad signalling aided by co-receptors Betaglycan (TGF-ßRIII), adaptor proteins (Grb2, Shc), interacting proteins (SARA) and exchange factors (Sos). TGF-ß down-regulated *TGFBRIII*, *Smad3* and inhibitory *Smad7* (red) indicating Smad signalling was down-regulated after 72 hours. (**B**) NAM treatment reversed the expression of some TGF-ß signalling components (**bold***) but had little overall effect on Smad signalling component expression (green and red), when compared to the vehicle control. (**C**) A truncated violin plot was used to demonstrate frequency distribution of the data where the dashed line represents the median. Differentially expressed signalling pathways and remodelling processes were identified using gene ontology (GO) and further investigation was conducted with a gene-by-gene approach. Statistical significance identified using Deseq2 (Sartools) with Benjamini-Hochberg p-value adjustment. Upregulation compared to vehicle control (green); downregulation compared to vehicle control (red); significant difference

between TGF-β alone and TGF-β + NAM treatment (**bold***). N = 3, n = 6, ns (p_{adj} > 0.05), * (p_{adj} < 0.05), ** (p_{adj} < 0.01), *** (p_{adj} < 0.001). TGF-β: Transforming growth factor beta 1; NAM: Negative allosteric modulator of the calcium-sensing receptor; GO: Gene ontology; Smad: small mother against decapentaplegic; Grb2: Growth factor receptor binding protein 2; Shc: Src homology 2 domain-containing transforming protein C; SARA: Smad anchor for receptor activation; Sos: Son Of Sevenless.

6.2.1.2 Non-canonical Ras signal transduction activation

The GO term "Regulation of Ras protein signal transduction" was downregulated by TGF-β. TGF-β also upregulated genes involved in Ras activation, including *GRB2*, *HRAS, NRAS, RRAS* and *MRAS* expression but downregulated the receptor tyrosine kinase (RTK) substrate Shc isoforms *SHC3* and *SHC4* (**$\log_2$ fold change *GRB2* = 0.26, *HRAS* = 0.70, *NRAS* = 0.43, *RRAS* = 0.52, *MRAS* = 0.86, *SHC3* = -1.26, *SHC4* = -1.33; p_{adj} < 0.05; TGF-β vs vehicle**). NAM treatment downregulated the GO term "Ras protein signal transduction", upregulated "Regulation of Ras protein signal transduction" and reversed the expression of *GRB2, NRAS, RRAS, SOS1* and *SOS2* but not *SHC3* or *SHC4* (**$\log_2$ fold change *GRB2* = -0.32, *HRAS* = -1.00, *RRAS* = -0.73, *SOS1* = 0.64, *SOS2* = 0.58; p_{adj} < 0.05; TGF-β + NAM vs TGF-β**). Following NAM treatment, all Ras signal transduction genes were indistinguishable from baseline levels (**p_{adj} > 0.05; TGF-β + NAM vs vehicle**) indicating that NAM treatment abolished TGF-β-induced Ras signal transduction, as shown in **Figure 6.2**.

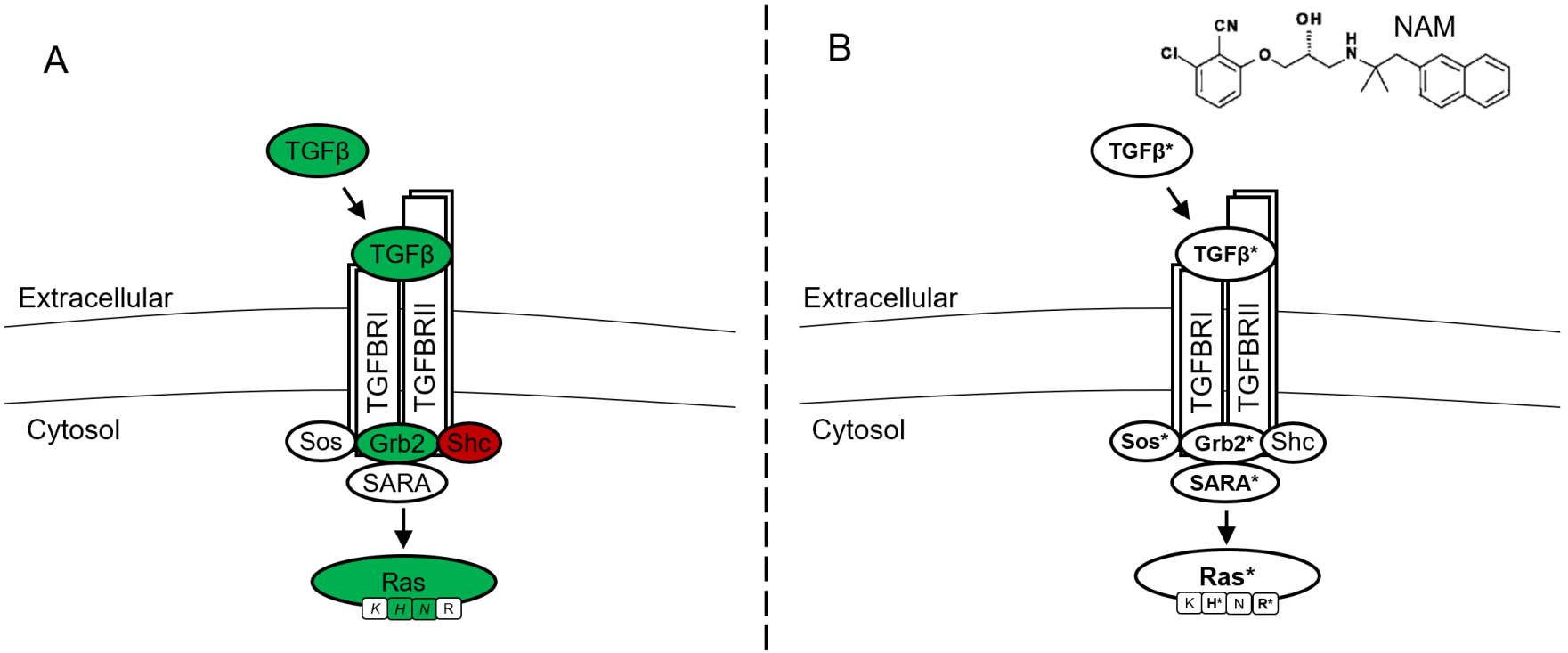
A
TGFβ
TGFβ
Extracellular
TGFBRI
TGFBRII
Cytosol
Sos
Grb2
Shc
SARA
Ras
K H N R
B
NAM
CN
OH
Cl
O
H
N
TGFβ*
TGFβ*
Extracellular
TGFBRI
TGFBRII
Cytosol
Sos*
Grb2*
Shc
SARA*
Ras*
K H* N R*

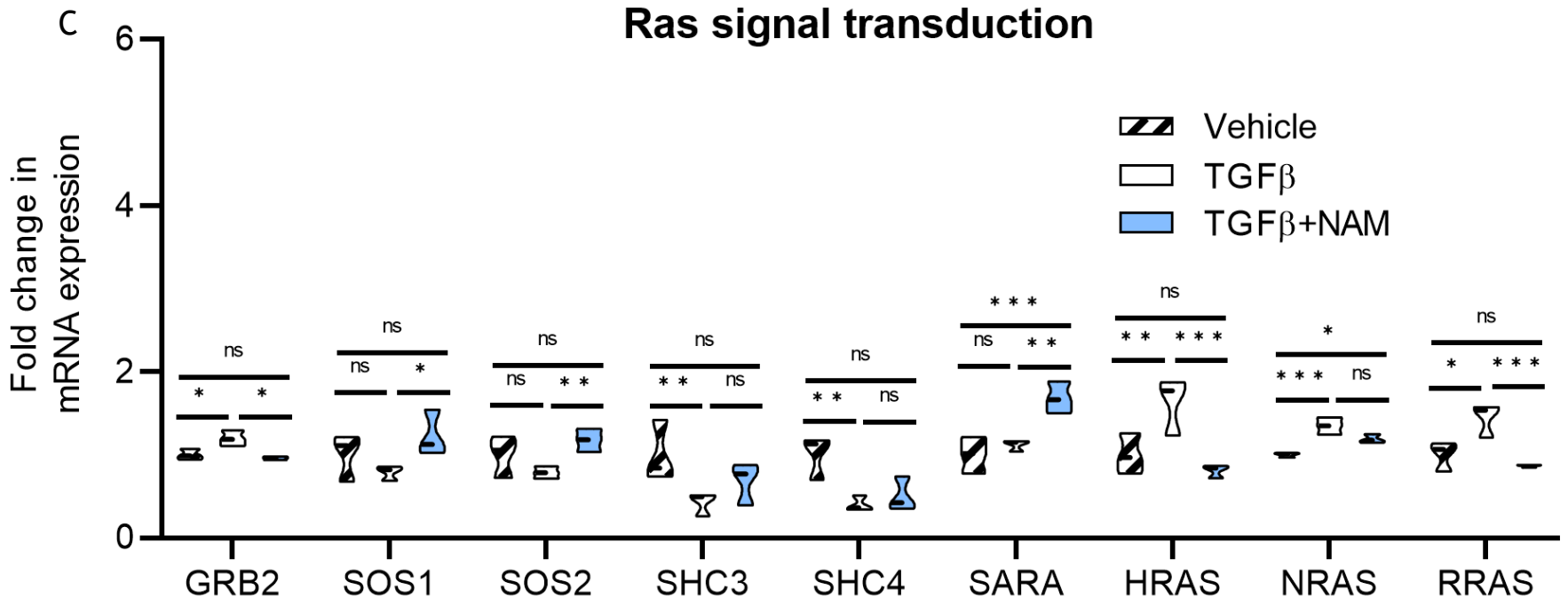

Figure 6.2. NAM treatment abolished TGF-ß-induced Ras protein signal transduction regulation in human lung fibroblasts. (**A**) To activate non-canonical TGF-ß signalling, TGF-ß activates the TGF-ßR to recruit molecules such as the Grb2/Sos complex by binding the substrate Shc to bring Sos to the plasma membrane which subsequently catalyses Ras by exchanging Ras-bound GDP for GTP (Zhang et al., 2009). TGF-ß upregulated *Grb2*, *HRAS* and *NRAS* (green) but down-regulated Shc (red), when compared to vehicle control. (**B**) NAM treatment significantly reversed *Sos*, *Grb2*, *SARA*, *HRAS* and *RRAS* expression (**bold***), when compared to TGF-ß. All of these genes were indistinguishable from baseline levels following NAM treatment (white). (**C**)

A truncated violin plot was used to demonstrate frequency distribution of the data where the dashed line represents the median. Differentially expressed signalling pathways and remodelling processes were identified using gene ontology (GO) and further investigation was conducted with a gene-by-gene approach. Statistical significance identified using Deseq2 (Sartools) with Benjamini-Hochberg p-value adjustment. Upregulation compared to vehicle control (green); downregulation compared to vehicle control (red); significant difference between TGF-β alone and TGF-β + NAM treatment (**bold***). N = 3, n = 6, ns (p_{adj} > 0.05), * (p_{adj} < 0.05), ** (p_{adj} < 0.01), *** (p_{adj} < 0.001). TGF-β: Transforming growth factor beta 1; NAM: Negative allosteric modulator of the calcium-sensing receptor; GO: Gene ontology; Grb2: Growth factor receptor binding protein 2; Shc: Src homology 2 domain-containing transforming protein C; SARA: Smad anchor for receptor activation; Sos: Son Of Sevenless; HRAS: H-Ras isoform; NRAS: N-Ras isoform; RRAS: R-Ras isoform.

6.2.1.3 Non-canonical MAPK (ERK, JNK, p38) signalling

TGF-β upregulated the expression of ERK-activating *MEK2* and the downstream ERK target α-smooth muscle actin (αSMA) (*ACTA2*) but downregulated mitogen- and stress-activated protein kinase (MSK1) (*RPS6KA5*), and the ERK transcription factor targets *NFκB1* and *FOSL2* (**log_2 fold change *MEK2* = 0.46, *ACTA2* = 1.12, *RPS6KA5* = -1.60, *NFKB1* = -0.53, *FOSL2* = -0.63; padj < 0.05**) suggesting TGF-β had a complex effect on ERK signalling regulation. NAM treatment downregulated MEK2 and αSMA (*ACTA2*) as well as *ERK6* but also upregulated *ERK3, ERK5*, and transcription factor targets *ELK1, MSK1* (*RPS6KA5*) and *NFκB1* (**log_2 fold change *MEK2* = -0.63, *ACTA2* = -0.93, *ERK6* = -0.52, *ERK3* = 0.49, *ERK5* = 0.49, *ELK1* = 0.40, *RPS6KA5* = 1.17, *NFKB1* = 0.64; p_{adj} < 0.05; TGF-β + NAM vs TGF-β**). When compared to baseline expression, NAM treatment upregulated *ERK3* and downregulated *ERK6* in the presence of TGF-β (**log_2 fold change *ERK3* = 0.59, *ERK6* = -0.68; p_{adj} < 0.05; TGF-β + NAM vs Vehicle**) but all other genes were indistinguishable from baseline levels (**p_{adj} > 0.05; TGF-β + NAM vs vehicle**) suggesting the CaSR plays a central role in TGF-β-induced ERK signalling regulation, as shown in **Figure 6.3**.

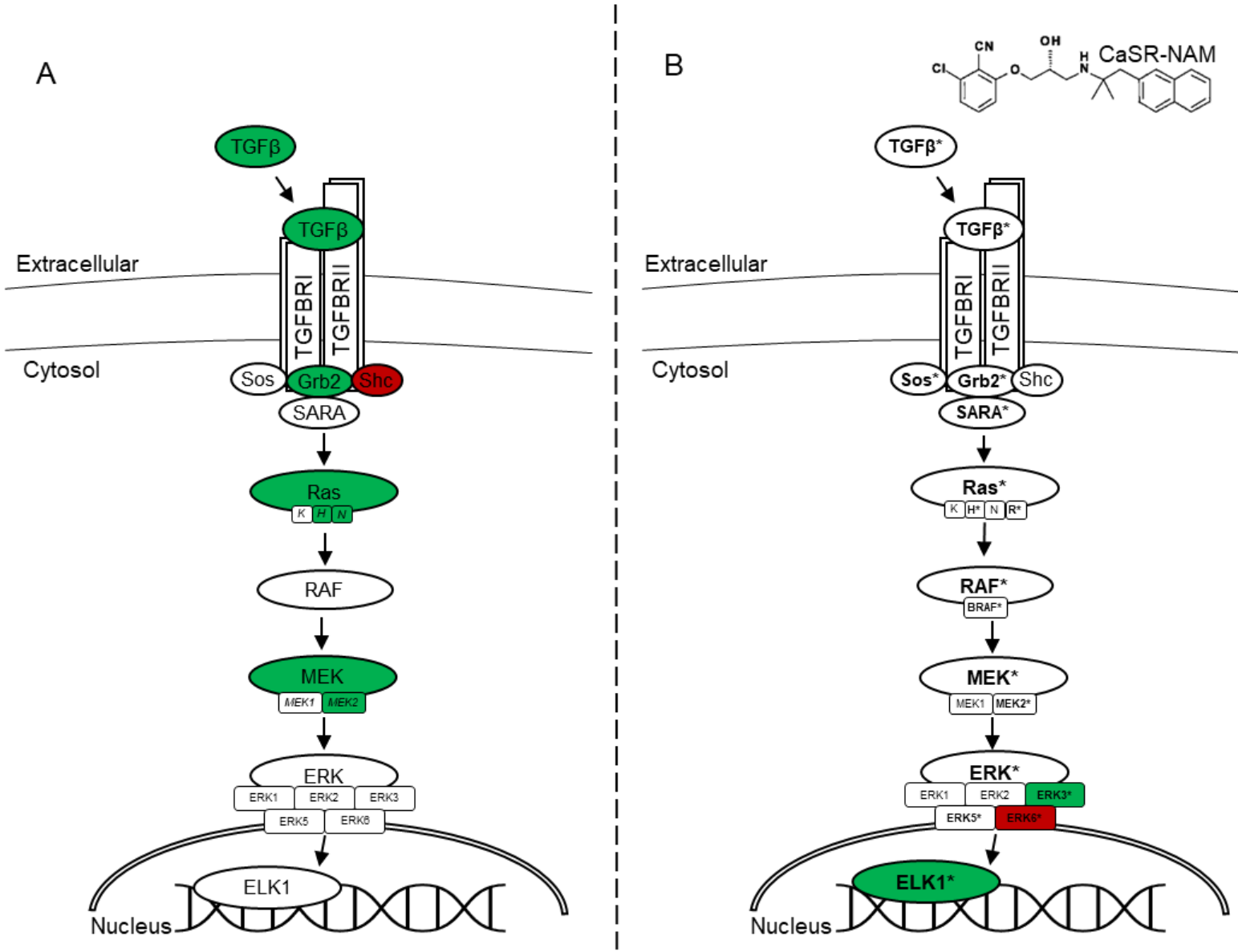
A
TGFβ
TGFβ
Extracellular
TGFBRI
TGFBRII
Cytosol
Sos
Grb2
Shc
SARA
Ras
K H N
RAF
MEK
MEK1 MEK2
ERK
ERK1 ERK2 ERK3
ERK5 ERK6
ELK1
Nucleus
B
CaSR-NAM
TGFβ*
TGFβ*
Extracellular
TGFBRI
TGFBRII
Cytosol
Sos*
Grb2*
Shc
SARA*
Ras*
K H* N R*
RAF*
BRAF*
MEK*
MEK1 MEK2*
ERK*
ERK1 ERK2 ERK3*
ERK5* ERK6*
ELK1*
Nucleus

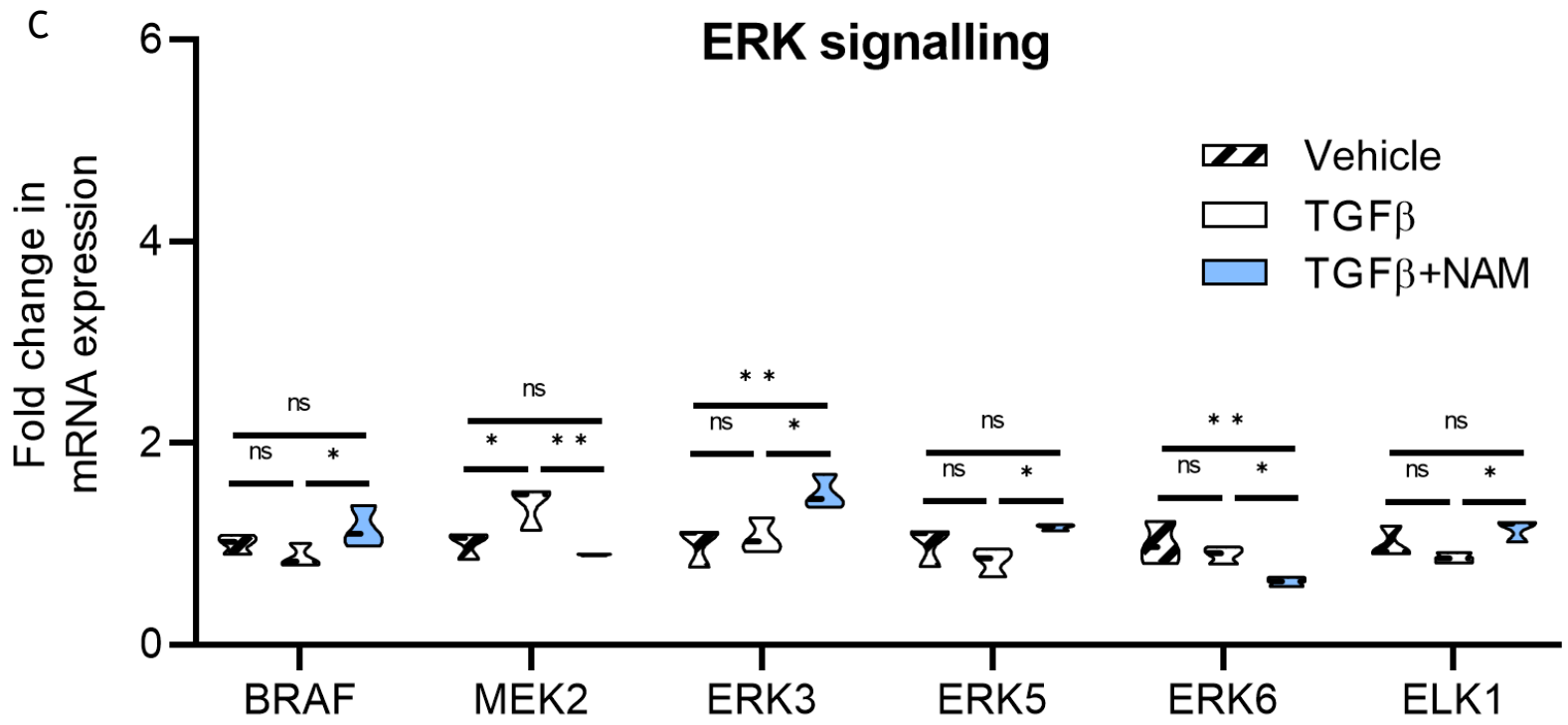

Figure 6.3. NAM treatment had a significant effect on ERK signalling regulation in human lung fibroblasts. (**A**) TGF-β activations non-canonical ERK signalling via Ras, which recruits Raf and subsequently MEK1/2 to activate ERK1/2 which influences processes such as cell adhesion, proliferation, differentiation and gene transcription by interacting with transcription factors, such as the calcium metabolism and growth signalling regulator ELK1; actin cytoskeletal component regulator AP-1 to influence αSMA expression; MSK1 (*RPS6KA5*) that is involved in the epidermal growth factor receptor (EGFR) pathway; and inflammation via NFκB (Davies et al., 2005; Kim et al., 2007a; Thiel et al., 2012; Janknecht et al., 1993; Deak

et al., 1998; Hu et al., 2006; Carpenter & Wu, 2014; Šmerdová et al., 2014; Vicent et al., 2009). TGF-ß upregulated MEK2 (green), when compared to vehicle control. (**B**) NAM treatment significantly reversed TGF-ß-induced *BRAF, MEK2*, and *ERK5* expression (**bold***); upregulated *ERK3* (green); and down-regulated *ERK6* (red), when compared to TGF-ß. All of these genes, except *ERK3, ERK6* and *ELK1*, were indistinguishable from baseline levels following NAM treatment (white). (**C**) A truncated violin plot was used to demonstrate frequency distribution of the data where the dashed line represents the median. Differentially expressed signalling pathways and remodelling processes were identified using gene ontology (GO) and further investigation was conducted with a gene-by-gene approach. Statistical significance identified using Deseq2 (Sartools) with Benjamini-Hochberg p-value adjustment. Upregulation compared to vehicle control (green); downregulation compared to vehicle control (red); significant difference between TGF-ß alone and TGF-ß + NAM treatment (**bold***). N = 3, n = 6, ns (p_{adj} > 0.05), * (p_{adj} < 0.05), ** (p_{adj} < 0.01), *** (p_{adj} < 0.001). TGF-ß: Transforming growth factor beta 1; NAM: Negative allosteric modulator of the calcium-sensing receptor; GO: Gene ontology; Grb2: Growth factor receptor binding protein 2; Shc: Src homology 2 domain-containing transforming protein C; SARA: Smad anchor for receptor activation; Sos: Son Of Sevenless; BRAF: B-Raf isoform; MEK: MAPK/ERK Kinase; ERK: Extracellular signal-regulated kinase; AP-1: Activator protein 1; αSMA: alpha smooth muscle actin; MSK1: Ribosomal protein S6 kinase; EGFR: Epidermal growth factor receptor.

TGF-β can also activate MAPK JNK and subsequently JUN signalling via Ras to influence the expression of remodelling markers such as connective tissue growth factor (CTGF). Here TGF-β increased the expression of *Rac1, JUNB , JUND* and *CTGF* but downregulated *MEKK1* indicating upregulation of JNK signalling (**log_2 fold change *RAC1* = 0.64, *JUNB* = 0.99, *JUND* = 0.51, *CTGF* = 1.16, *MEKK1* = -0.85; p_{adj} < 0.05; TGF-β vs Vehicle**). NAM treatment reversed the expression of *Rac1, JUNB, JUND, CTGF* and *MEKK1* (**log_2 fold change *RAC1* = -0.76, *JUNB* = -0.71, *JUND* = -0.88, *CTGF* = -0.87, *MEKK1* = 0.79; p_{adj} < 0.05; TGF-β + NAM vs TGF-β**) to levels indistinguishable from baseline expression (**p_{adj} > 0.05; TGF-β + NAM vs vehicle**) indicating TGF-β-induced JNK activation was returned to baseline levels by NAM treatment, as shown in **Figure 6.4**.

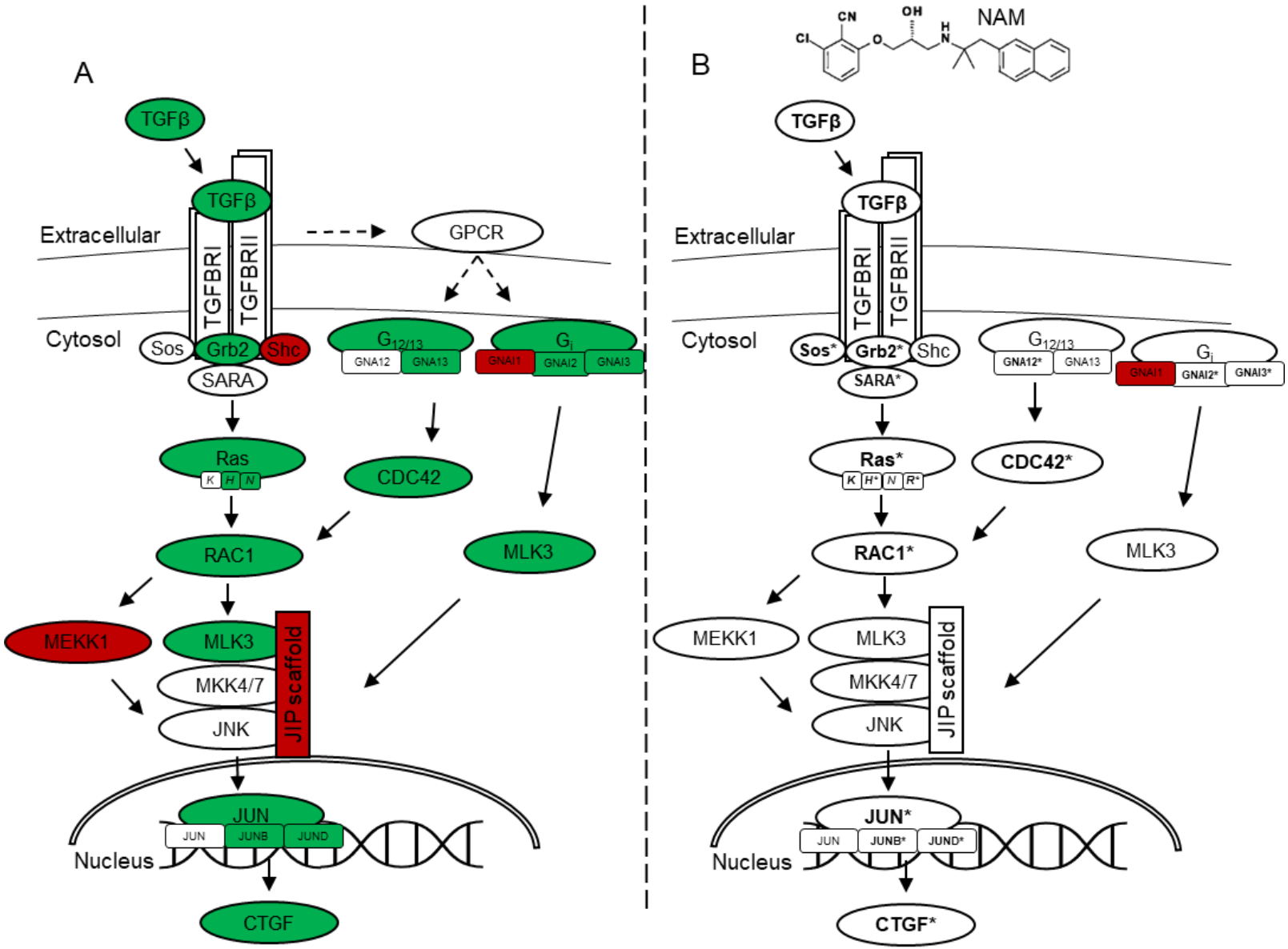
A
TGFβ
TGFβ
Extracellular
TGFBRI
TGFBRII
GPCR
Cytosol
Sos
Grb2
Shc
SARA
G12/13
GNA12
GNA13
Gi
GNAI1
GNAI2
GNAI3
Ras
K H N
CDC42
RAC1
MLK3
MEKK1
MLK3
MKK4/7
JNK
JIP scaffold
JUN
JUN
JUNB
JUND
Nucleus
CTGF
B
NAM
TGFβ
TGFβ
Extracellular
TGFBRI
TGFBRII
Cytosol
Sos*
Grb2*
Shc
SARA*
G12/13
GNA12*
GNA13
Gi
GNAI1
GNAI2*
GNAI3*
Ras*
K H* N R*
CDC42*
RAC1*
MLK3
MEKK1
MLK3
MKK4/7
JNK
JIP scaffold
JUN*
JUN
JUNB*
JUND*
Nucleus
CTGF*

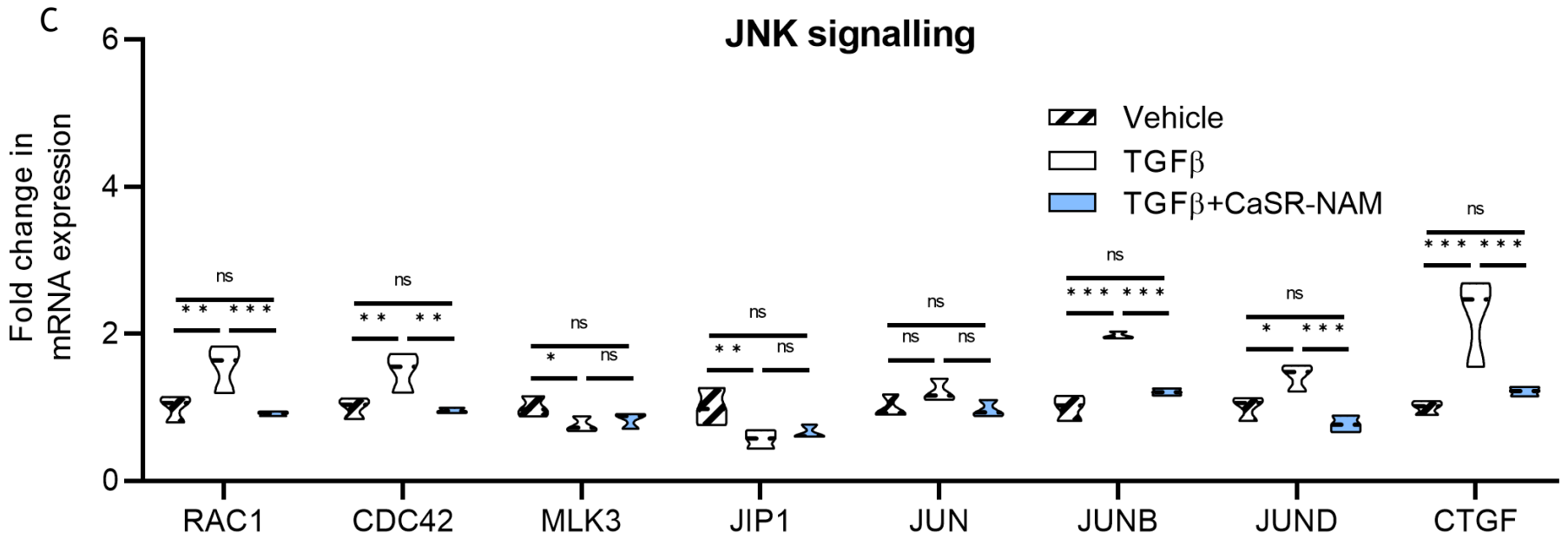

Figure 6.4. NAM treatment abolished TGF-ß-induced JNK signalling regulation in human lung fibroblasts. (**A**) TGF-ß acitvates JNK signalling via Ras, Rac1, as well as by potential GPCR transactivation and G-protein activation of *MEKK1* and *MKK4/7* (dashed arrows), to regulate cell adhesion, migration and ECM remodelling via interaction with JUN transcription factors and subsequent expression of genes such as *CTGF*. TGF-ß upregulated *Rac1, CDC42, GNA13, JUND, JUND* and *CTGF* (green) but downregulated *MEKK1* (red). (**B**) NAM treatment significantly reversed TGF-ß-induced *Rac1, CDC42, GNA12, JUNB, JUND* and *CTGF* expression (**bold***), when compared to TGF-ß. All of these genes were indistinguishable from baseline levels following NAM treatment (white). (**C**) A truncated violin plot was used to demonstrate frequency distribution of the data where the dashed line represents the median. Differentially expressed signalling pathways and remodelling processes were identified using gene ontology (GO) and further investigation was conducted with a gene-by-gene approach. Statistical

significance identified using Deseq2 (Sartools) with Benjamini-Hochberg p-value adjustment. Upregulation compared to vehicle control (green); downregulation compared to vehicle control (red); significant difference between TGF-β alone and TGF-β + NAM treatment (**bold***). N = 3, n = 6, ns (p_{adj} > 0.05), * (p_{adj} < 0.05), ** (p_{adj} < 0.01), *** (p_{adj} < 0.001). TGF-β: Transforming growth factor beta 1; NAM: Negative allosteric modulator of the calcium-sensing receptor; GO: Gene ontology; Grb2: Growth factor receptor binding protein 2; Shc: Src homology 2 domain-containing transforming protein C; SARA: Smad anchor for receptor activation; Sos: Son Of Sevenless; JNK: Jun N-terminal kinase; *CDC42*: Cell division cycle 42; G_{12}: Guanine Nucleotide-Binding Protein subunit alpha (12); G_{13}: Guanine Nucleotide-Binding Protein subunit alpha (13); G_i: Guanine Nucleotide-Binding Protein subunit alpha (i); *JIP*: Jun N-terminal kinase interacting protein; *MLK3*: Mixed lineage kinase 3; MEKK: MAPK/ERK kinase kinase; MKK: Mitogen activation protein kinase kinase; *CTGF*: Connective tissue growth factor; ECM: Extracellular matrix.

TGF-β downregulated the GO term "Regulation of p38 MAPK cascade" as well as the p38δ (*MAPK13*) subunit (**log2 fold change MAPK13 = -0.94; p_{adj} < 0.05; TGF-β vs vehicle**). NAM treatment downregulated p38β (*MAPK11*), p38γ (*MAPK12*) and upregulated p38δ (*MAPK13*) expression but no GO terms were differentially expressed for this pathway (**log_2 fold change MAPK11 = -0.70, MAPK12 = -0.52, MAPK13 = 0.77; p_{adj} < 0.05**). p38δ (*MAPK13*) was the only p38 subunit returned to baseline levels (**p_{adj} > 0.05; TGF-β + NAM vs vehicle**).

6.2.1.4 Non-canonical PI3K/Akt signalling

Class I PI3K complexes are formed of a p110 catalytic subunit (*PIK3C-A, -B, -C, -D* or *-Y*) and a p85 regulatory subunit (*PIK3R1* or *PIK3R2*) which are bound to the PI3K complex by PI3K adaptor protein 1 (*PIK3AP1*). Inhibitors of PI3K activation also exist, such as PIK3 interacting protein 1 (*PIK3IP1*) (Gheyas et al., 2017). The PI3K complex then phosphorylates Akt, enhanced by Akt interacting protein (*AKTIP*), to influence the activity of over 100 downstream substrates (Khalil et al., 2021; Aytenfisu et al., 2022). TGF-β upregulated *PIK3AP1* and AKT1-phosphorylation enhancing *AKTIP* expression as well as downregulated *PIK3R1* and the inhibitory *PIK3IP1* gene indicating upregulation of PI3K/Akt signalling (**log_2 fold change *PIK3AP1* = 3.85, *AKTIP* = 0.60, *PIK3R1* = -0.76, *PIK3IP1* = -0.68; p_{adj} < 0.05; TGF-β vs vehicle**). NAM treatment reversed PIK3R1 expression but also significantly altered expression of PI3K catalytic subunits by upregulating PIK3CA and PIK3CB and downregulating PIK3CD (**log_2 fold change *PIK3R1* = 0.55, *PIK3CA* = 0.44, *PIK3CB* = 0.38, *PIK3CD* = -0.51; p_{adj} < 0.05; TGF-β + NAM vs TGF-β**). When compared to baseline expression, NAM treatment only altered the expression of *AKT3* (**log_2 fold change *AKT3* = 0.64; p_{adj} < 0.05; TGF-β + NAM vs vehicle**) and expression of *PIK3CA, PIK3CB, PIK3CD, PIK3R1, PIK3IP1* and *AKTIP* could not be distinguished from baseline levels (**p_{adj} > 0.05; TGF-β + NAM vs vehicle**). This suggests TGF-β-induced PI3K signalling was returned to baseline levels, with the exception of *AKT3*, following NAM treatment, as shown in **Figure 6.5**.

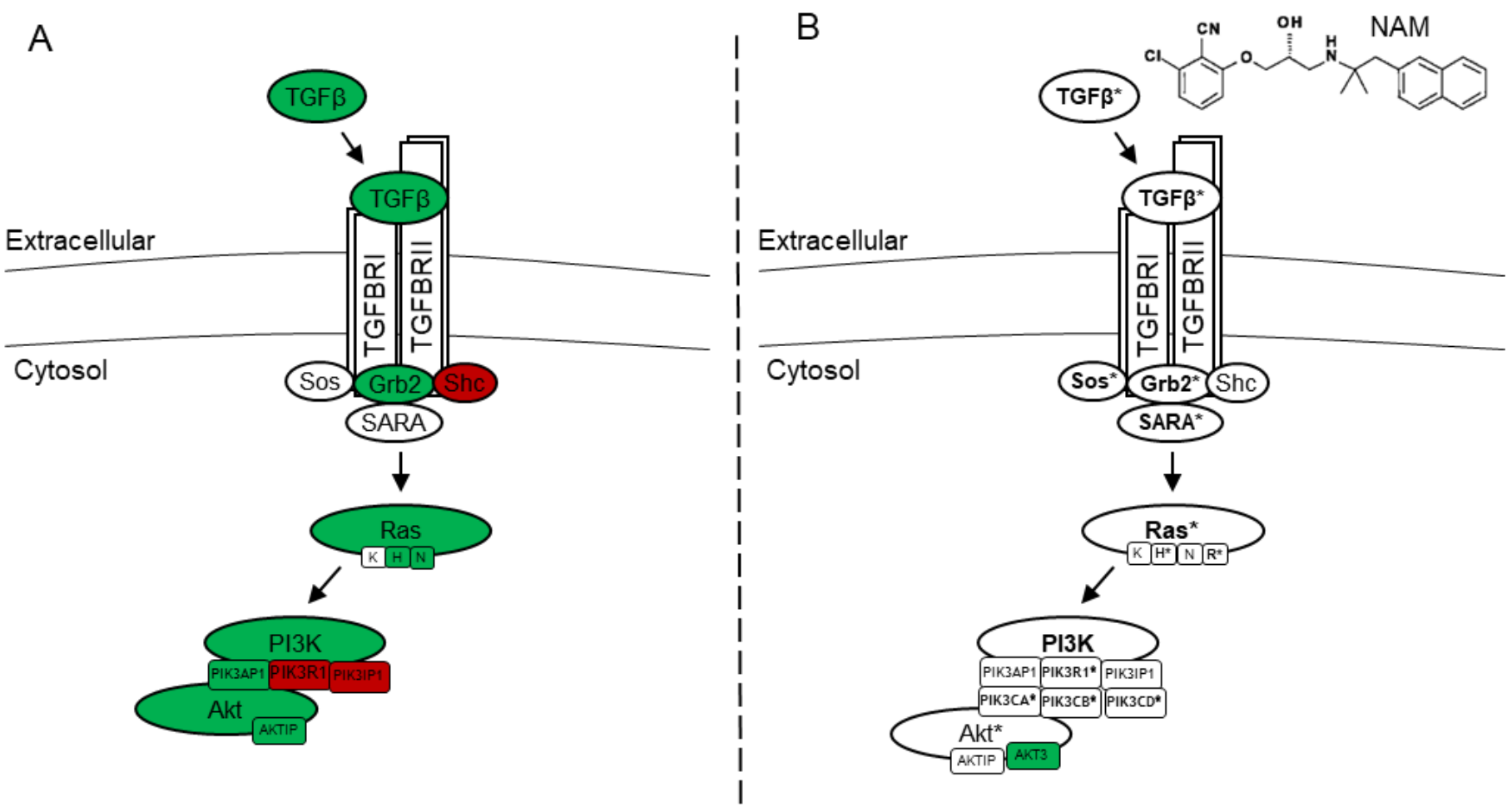
A
TGFβ
TGFβ
Extracellular
TGFBRI
TGFBRII
Cytosol
Sos
Grb2
Shc
SARA
Ras
K
H
N
PI3K
PIK3AP1
PIK3R1
PIK3IP1
Akt
AKTIP
B
NAM
CN
OH
Cl
O
H
N
TGFβ*
TGFβ*
Extracellular
TGFBRI
TGFBRII
Cytosol
Sos*
Grb2*
Shc
SARA*
Ras*
K
H*
N
R*
PI3K
PIK3AP1
PIK3R1*
PIK3IP1
PIK3CA*
PIK3CB*
PIK3CD*
Akt*
AKTIP
AKT3

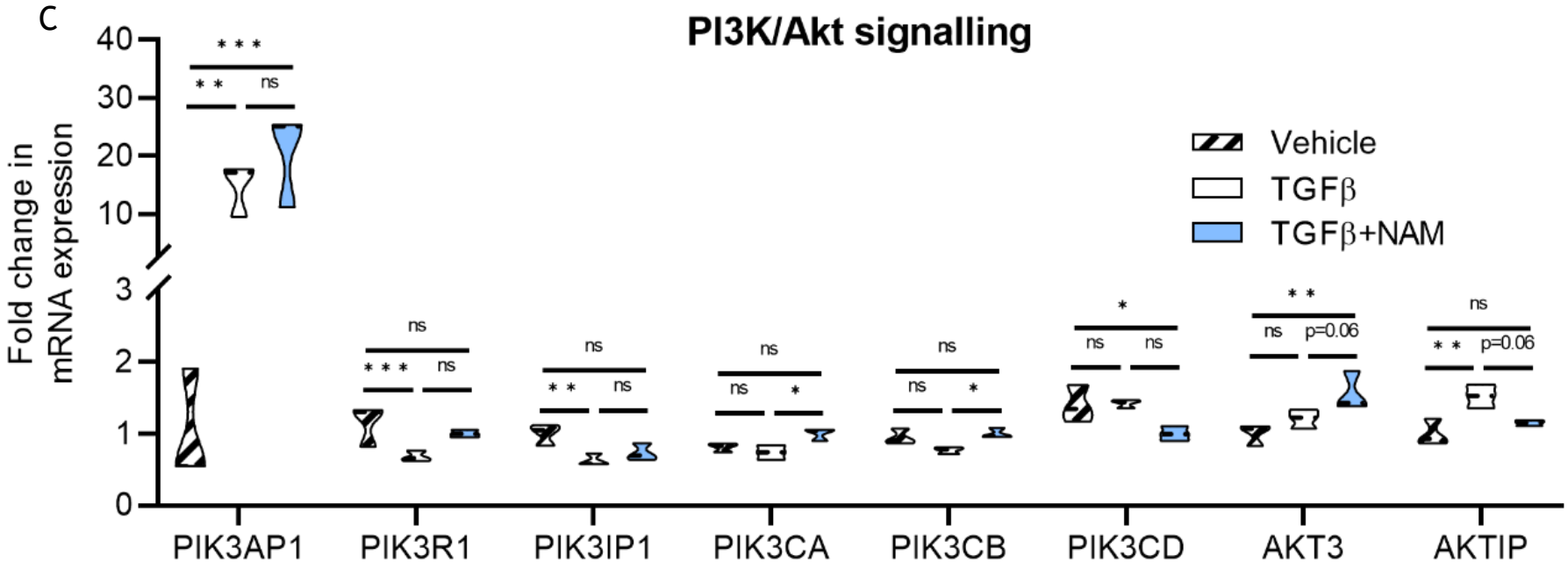

Figure 6.5. NAM treatment abolished TGF-ß-induced PI3K/Akt signalling regulation in human lung fibroblasts. (**A**) TGF-ß activates class I PI3K complexes via Ras and subsequently activation of Akt. TGF-ß upregulated *PIK3AP1* and *AKTIP* (green) and downregulated *PIK3R1* and inhibitory *PIK3IP1* (red) indicating upregulation of PI3K/Akt signalling. (B) NAM treatment significantly reversed TGF-ß-induced *PIK3R1* expression but also up-regulated *PIK3CA, PIK3CB* and *AKT3* (green) and downregulated *PIK3CD* (**bold***), when compared to TGF-ß. All of these genes, except AKT3 were indistinguishable from baseline levels following NAM treatment (white). (**C**) A truncated violin plot was used to demonstrate frequency distribution of the data where the dashed line represents the median. Differentially expressed signalling pathways and remodelling processes were identified using gene ontology (GO) and further investigation was conducted with a gene-by-gene approach. Statistical

significance identified using Deseq2 (Sartools) with Benjamini-Hochberg p-value adjustment. Upregulation compared to vehicle control (green); downregulation compared to vehicle control (red); significant difference between TGF-β alone and TGF-β + NAM treatment (**bold***). N = 3, n = 6, ns (p_{adj} > 0.05), * (p_{adj} < 0.05), ** (p_{adj} < 0.01), *** (p_{adj} < 0.001). TGF-β: Transforming growth factor beta 1; NAM: Negative allosteric modulator of the calcium-sensing receptor; GO: Gene ontology; Grb2: Growth factor receptor binding protein 2; Shc: Src homology 2 domain-containing transforming protein C; SARA: Smad anchor for receptor activation; Sos: Son Of Sevenless; *PIK3AP1*: Phosphatidylinositol 3-kinase adaptor protein 1; *PIK3R1*: Phosphatidylinositol 3-kinase regulatory subunit 1; *PIK3CA*: Class I phosphatidylinositol 3-kinase catalytic subunit alpha; *PIK3CB*: Class I phosphatidylinositol 3-kinase catalytic subunit beta; *PIK3CD*: Class I phosphatidylinositol 3-kinase catalytic subunit delta; *AKT*: Akt isoform 3; *AKTIP*: Akt interacting protein.

6.2.1.5 Non-canonical mTOR signalling

TGF-β downregulated inhibitory *TSC1* and *TSC2* and upregulated *Rheb*, *mLST8*, *Deptor* and *mSIN1* as well as the downstream targets of mTOR complex 1 (mTORC1), such as 4E-binding protein 1 (4E-BP1) (*EIF4EBP1*) and *ULK1*, and downstream targets of mTOR complex 2 (mTORC2), such as *SPARC*, demonstrating clear activation of the mTOR pathway (**log_2 fold change *TSC1* = -0.44, *TSC2* = -0.48, *RHEB* = 0.51, *MLST8* = 0.37, *DEPTOR* = 1.23, mSIN1 (*MAPKAP1*) = 0.30, *EIF4EBP1* = 1.4, *ULK1* = 0.45, *SPARC* = 1.17; p_{adj} < 0.05; TGF-β vs vehicle**). NAM treatment reversed the expression of *TSC1*, *TSC2*, *Rheb*, *mLST8*, *mSIN1* and *SPARC* but also upregulated *mTOR*, *Raptor* and *Rictor* (**log_2 fold change *MTOR* = 0.76, *RPTOR* = 0.76, *RICTOR* = 0.63, *MLST8* = -0.33, mSIN1 (*MAPKAP1*) = -0.27, *SPARC* = -0.91; p_{adj} < 0.05 vs TGF-β**). Importantly, all components of the mTOR pathway, including *mTOR*, *Raptor*, *Rictor*, were indistinguishable from baseline levels (**p_{adj} > 0.05; TGF-β + NAM vs vehicle**); however, unc-51 like autophagy activating kinase 1 (ULK1), an inhibitor of autophagy (Platé et al., 2020), was unaffected by NAM treatment and remained significantly upregulated (**p_{adj} = 0.010, Log2FC = 0.54**). Despite downstream effectors, such as *ULK1*, demonstrating the potential for multiple regulatory mechanisms, this data suggests that TGF-β-induced mTOR signalling was ameliorated by NAM treatment, as shown in **Figure 6.6**.

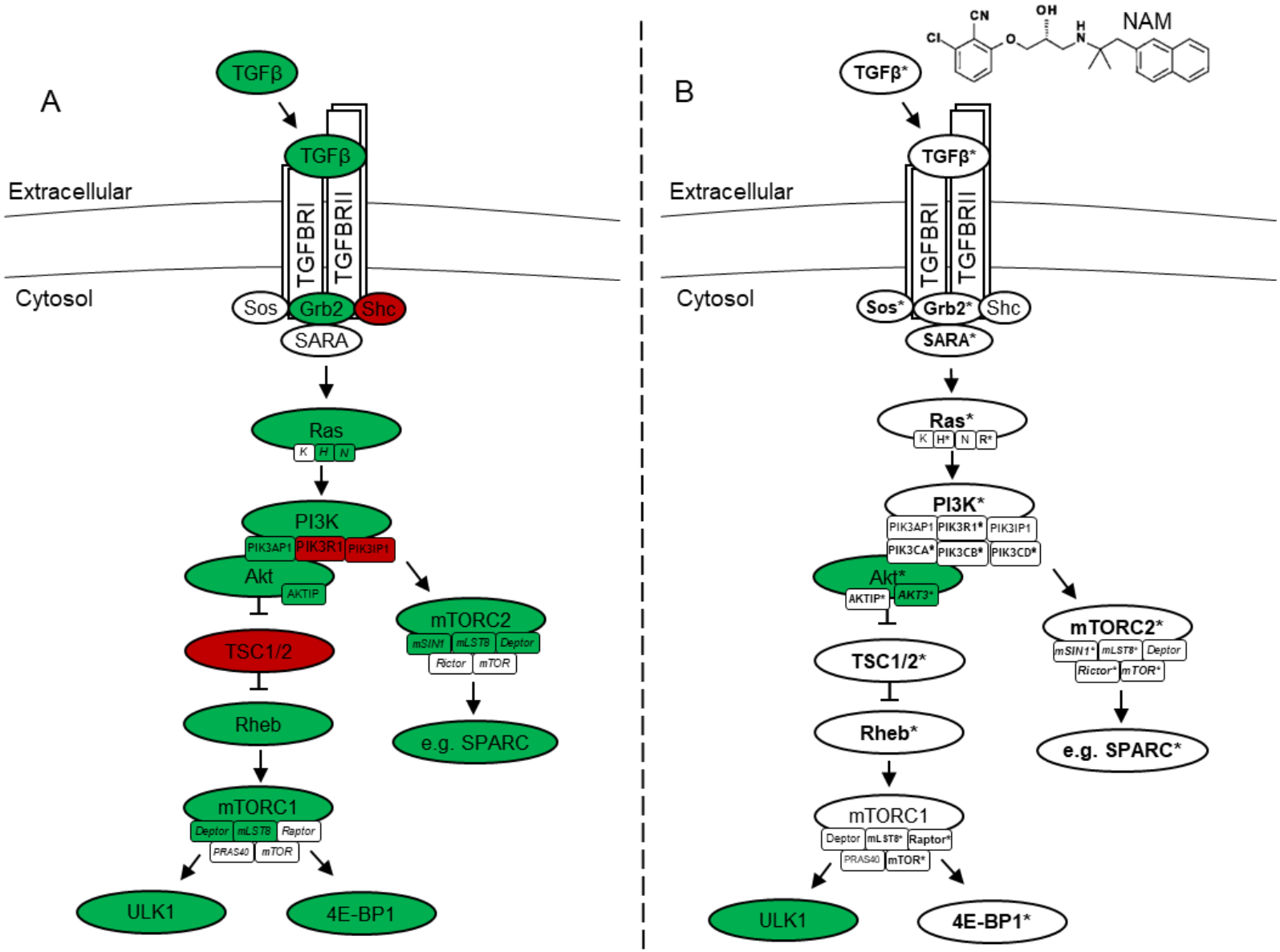
A
TGFβ
TGFβ
Extracellular
TGFBRI
TGFBRII
Cytosol
Sos
Grb2
Shc
SARA
Ras
K H N
PI3K
PIK3AP1 PIK3R1 PIK3IP1
Akt
AKTIP
TSC1/2
Rheb
mTORC1
Deptor mLST8 Raptor
PRAS40 mTOR
ULK1
4E-BP1
mTORC2
mSIN1 mLST8 Deptor
Rictor mTOR
e.g. SPARC
B
NAM
TGFβ*
TGFβ*
Extracellular
TGFBRI
TGFBRII
Cytosol
Sos*
Grb2*
Shc
SARA*
Ras*
K H* N R*
PI3K*
PIK3AP1 PIK3R1* PIK3IP1
PIK3CA* PIK3CB* PIK3CD*
Akt*
AKTIP* AKT3*
TSC1/2*
Rheb*
mTORC1
Deptor mLST8* Raptor*
PRAS40 mTOR*
ULK1
4E-BP1*
mTORC2*
mSIN1* mLST8* Deptor
Rictor* mTOR*
e.g. SPARC*

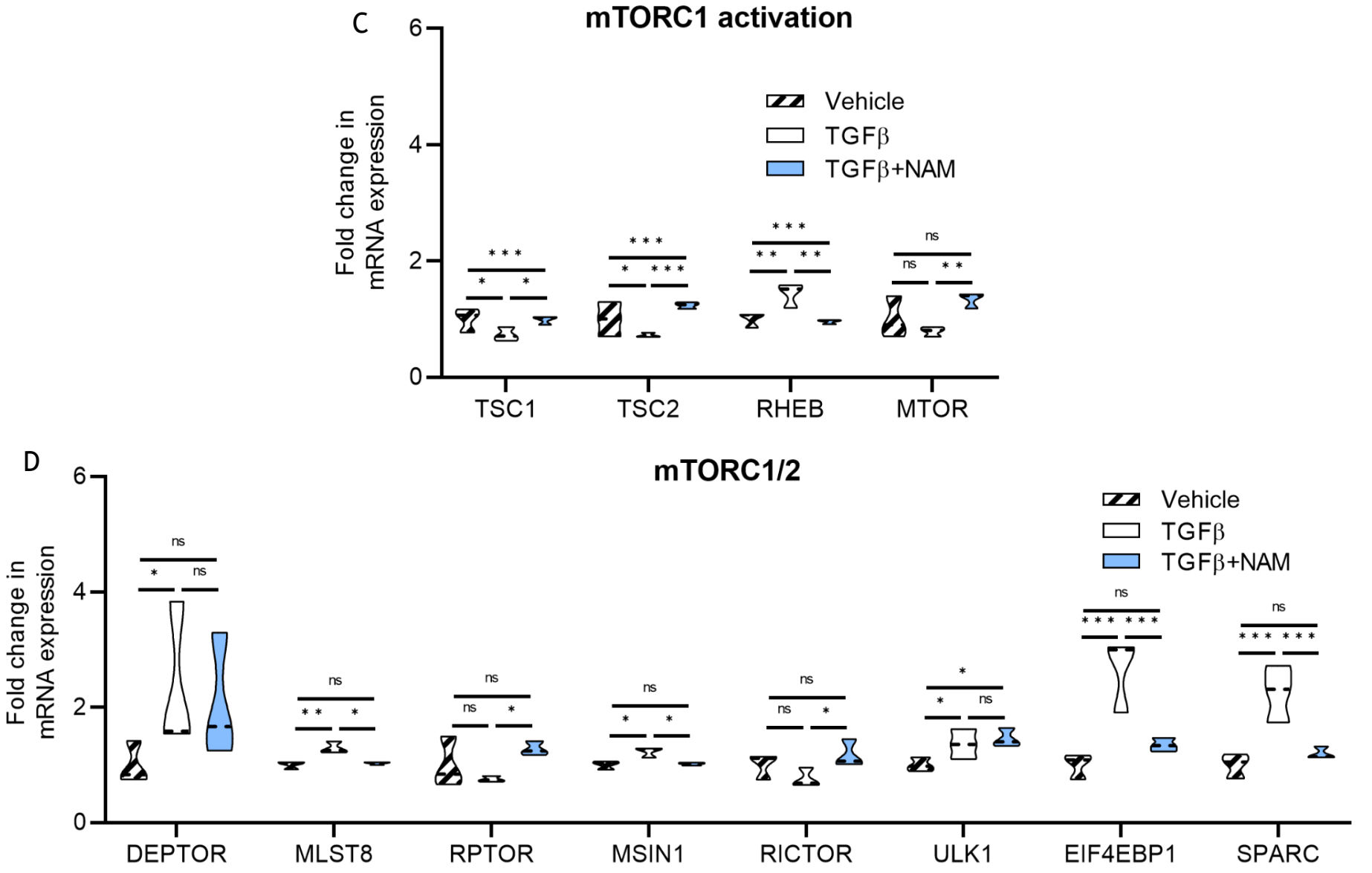
C
mTORC1 activation
Fold change in mRNA expression
Vehicle
TGFβ
TGFβ+NAM
TSC1
TSC2
RHEB
MTOR
D
mTORC1/2
DEPTOR
MLST8
RPTOR
MSIN1
RICTOR
ULK1
EIF4EBP1
SPARC

Figure 6.6. NAM treatment ameliorated TGF-ß-induced mTORC1 and mTORC2 signalling regulation in human lung fibroblasts. (**A**) TGF-ß activates Ras/PI3K/Akt and subsequently mTORC1 by preventing TSC1/2 from converting $Rheb^{GTP}$ to $Rheb^{GDP}$. Accumulation of $Rheb^{GTP}$ then activates mTORC1 that regulates gene targets such as the amino acid synthesis pathway, 4E-BP1 (*EIF4EBP1*) via ATF4 and regulation of autophagy via ULK1 (Nigdelioglu et al., 2016; Selvarajah et al., 2019; Plate et al., 2020). TGF-ß also activates mTORC2 via PI3K/Akt directly to influence gene targets such as SPARC (Chang et al., 2014; Platé et al., 2020). TGF-ß significantly downregulated TSC1 and TSC2 (red) and upregulated Rheb, mLST8, Deptor and mSIN1 (green) as well as the downstream targets of mTORC1, 4E-BP1 (*EIF4EBP1*) and *ULK1*, and downstream target of mTORC2, SPARC indicating activation of the PI3K/Akt/mTOR pathway. (**B**) NAM treatment significantly reversed TGF-ß-induced *TSC1*, *TSC2*, Rheb and mLST8 but also upregulated Raptor and mTOR (**bold***), when compared to TGF-ß. All of these genes, except ULK1, were indistinguishable from baseline levels following NAM treatment. (**C, D**) Truncated violin plots were used to demonstrate frequency distribution of the data where the dashed line represents the median. Differentially expressed signalling pathways and remodelling processes were identified using gene ontology (GO) and further investigation was conducted with a gene-by-gene approach. Statistical significance identified using Deseq2 (Sartools) with Benjamini-Hochberg p-value adjustment. Upregulation compared to vehicle control (green); downregulation compared to vehicle control (red); significant difference between TGF-ß alone and TGF-ß + NAM treatment (**bold***). N = 3, n = 6, ns ($p_{adj} > 0.05$), * ($p_{adj} < 0.05$), ** ($p_{adj} < 0.01$), *** ($p_{adj} < 0.001$). TGF-ß: Transforming growth factor beta 1; NAM: Negative allosteric modulator of the calcium-sensing receptor; GO: Gene ontology; Grb2: Growth factor receptor binding protein 2; Shc: Src homology 2 domain-containing transforming protein C; SARA: Smad anchor for receptor activation; Sos: Son Of Sevenless; ATF4: Activating transcription factor 4; TSC: Tuberous sclerosis; Rheb: Ras homolog enriched in brain; mLST8: GTPase ß-subunit like protein gßL; Deptor: DEP domain containing mTOR interacting protein; mSIN1: Mammalian stress-activated protein kinase (SAPK)-interacting

protein; mTORC: mechanistic target of rapamycin complex; 4E-BP1: 4E-binding protein 1; ULK1: Unc-51 like autophagy activating kinase; SPARC: Secreted protein acidic and rich in cysteine; PI3K: Phosphatidylinositol 3-kinase.

6.2.1.6 Non-canonical Rho signalling

Rho signalling, also activated by Ras or Rac1 and subsequently RhoA is considered as a therapeutic target for lung remodelling due to its contribution to the profibrotic responses of epithelial cells, endothelial cells, and fibroblasts via processes such as actin cytoskeleton rearrangement, differentiation and apoptosis (Knipe et al., 2018). Here, TGF-β upregulated *RHOA* and downregulated *ROCK2* (**$\log_2$ fold change *RHOA* = 0.74, *ROCK2* = -0.51; p_{adj} < 0.05; TGF-β vs vehicle**) but no effect was observed on Rho-associated coiled-coil containing protein kinase 1 (ROCK1) mRNA (**Figure 6.7**) or protein (**Figure 6.8**) expression indicating a separate regulatory mechanism for ROCK signalling but clear upregulation of RhoA signalling. NAM treatment downregulated RhoA (**$\log_2$ fold change *RhoA* = -0.81; p_{adj} < 0.05; TGF-β + NAM vs TGF-β**) but not ROCK1 protein expression (**p_{adj} = 0.13; TGF-β + NAM vs TGF-β**) or ROCK2 mRNA expression. Gene expression following NAM treatment was indistinguishable from baseline levels (**p_{adj} > 0.05; TGF-β + NAM vs vehicle**) suggesting TGF-β-induced RhoA signalling was returned to baseline levels following NAM treatment.

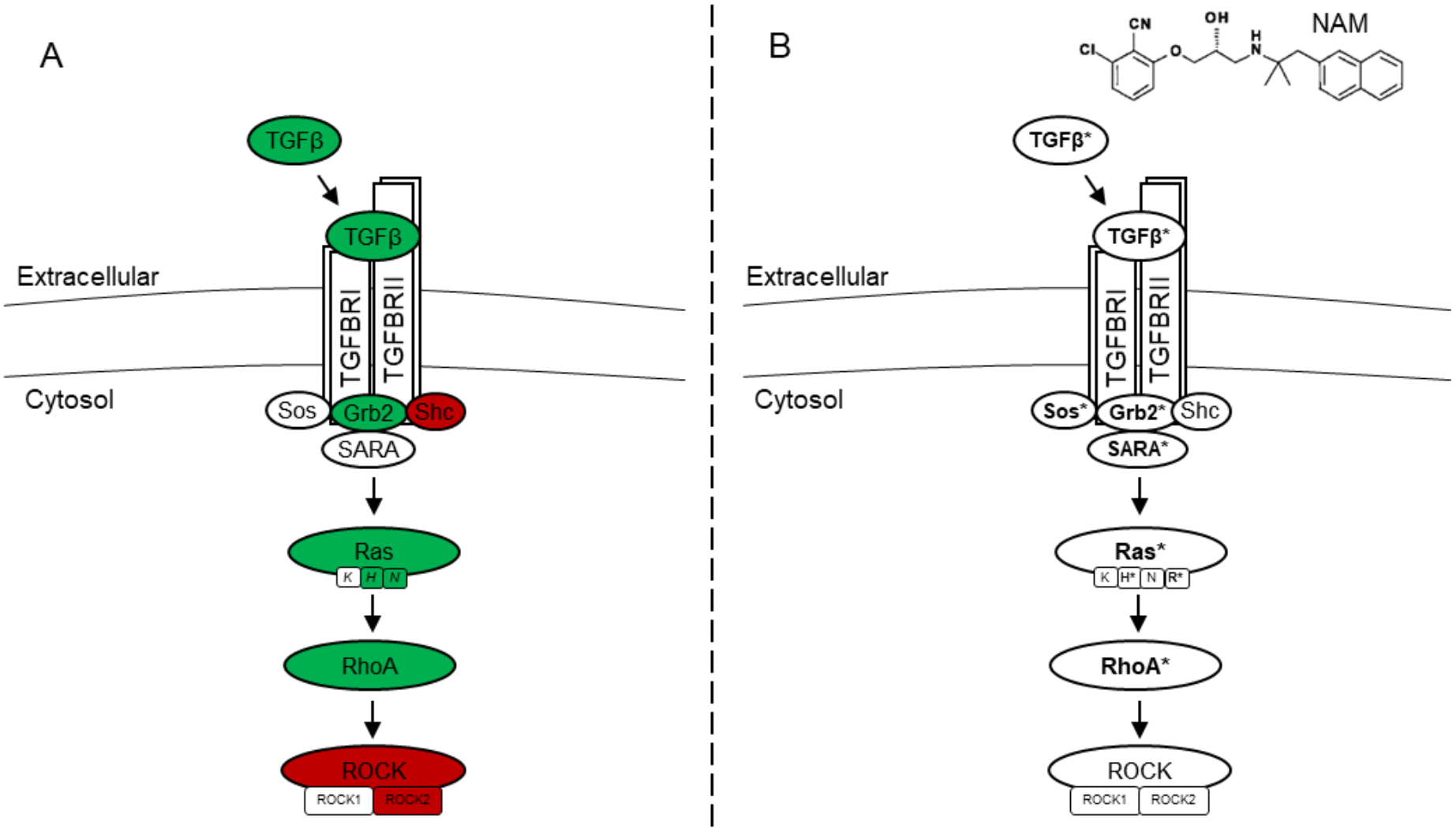
A
TGFβ
TGFβ
Extracellular
TGFBRI
TGFBRII
Cytosol
Sos
Grb2
Shc
SARA
Ras
K H N
RhoA
ROCK
ROCK1 ROCK2
B
NAM
CN
OH
Cl
O
H
N
TGFβ*
TGFβ*
Extracellular
TGFBRI
TGFBRII
Cytosol
Sos*
Grb2*
Shc
SARA*
Ras*
K H* N R*
RhoA*
ROCK
ROCK1 ROCK2

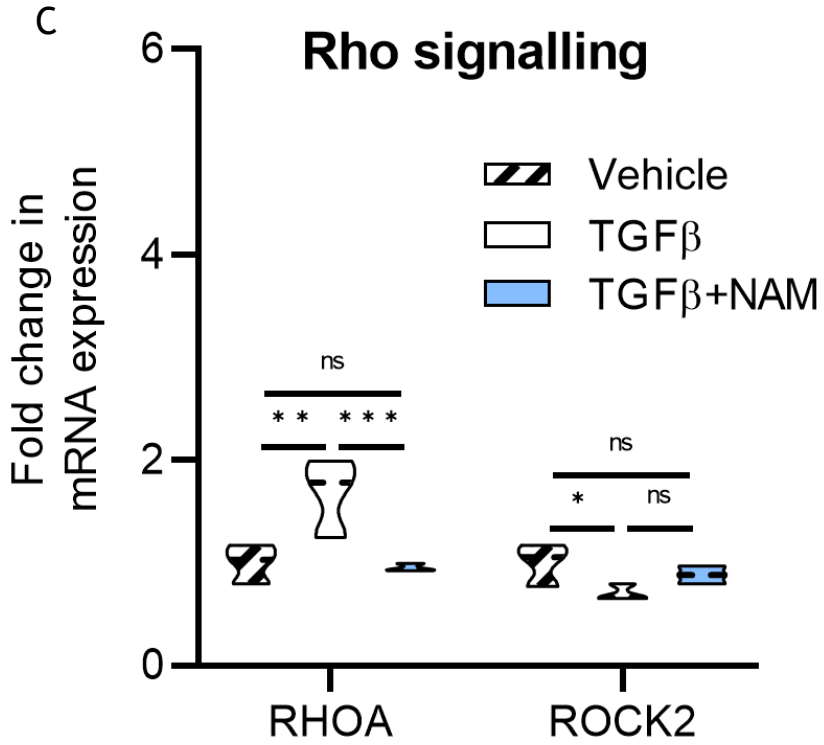

Figure 6.7. NAM treatment ameliorates TGF-ß-induced Rho, but not ROCK, signalling regulation in human lung fibroblasts. (**A**) TGF-ß activates Rho signalling via Ras to target Rho Kinases, such as *ROCK1* and *ROCK2*. TGF-ß significantly upregulated RhoA (green) and downregulated *ROCK2* (red). (**B**) NAM treatment significantly reversed TGF-ß-induced RhoA expression (**bold***), when compared to TGF-ß. All of these genes were indistinguishable from baseline levels following NAM treatment. (**C**) A truncated violin plot was used to demonstrate frequency distribution of the data where the dashed line represents the median. Differentially expressed signalling pathways and remodelling processes were identified using gene ontology (GO) and

further investigation was conducted with a gene-by-gene approach. Statistical significance identified using Deseq2 (Sartools) with Benjamini-Hochberg p-value adjustment. Upregulation compared to vehicle control (green); downregulation compared to vehicle control (red); significant difference between TGF-β alone and TGF-β + NAM treatment (**bold***). N = 3, n = 6, ns (p_{adj} > 0.05), * (p_{adj} < 0.05), ** (p_{adj} < 0.01), *** (p_{adj} < 0.001). TGF-β: Transforming growth factor beta 1; NAM: Negative allosteric modulator of the calcium-sensing receptor; GO: Gene ontology; Grb2: Growth factor receptor binding protein 2; Shc: Src homology 2 domain-containing transforming protein C; SARA: Smad anchor for receptor activation; Sos: Son Of Sevenless; ROCK: Rho associated coiled-coil containing protein kinase.

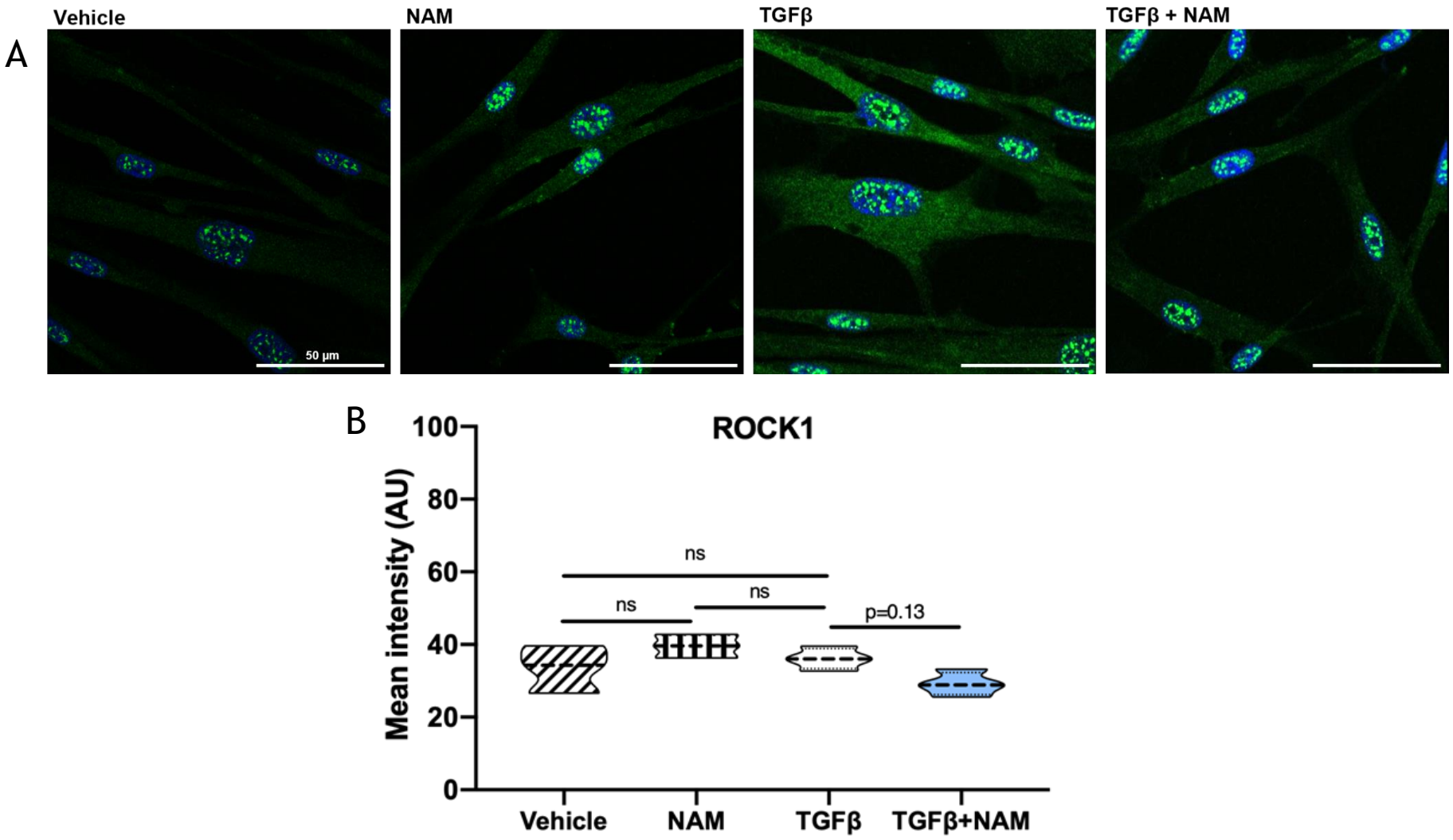

Figure 6.8. TGF-ß induced no changes to ROCK1 protein expression in human lung fibroblasts. (**A**) Primary normal human lung fibroblasts (Lonza, UK) were exposed to a remodelling mediator, TGF-ß, in the presence or absence of NAM (NPS2143).

ROCK1 (green) was identified using anti-ROCK1 antibody (21850-1-AP) and AlexaFluor 488 (Ab150077) secondary antibody. (B) Mean intensity was quantified using StrataQuest and normalised to nuclear cell count (blue). Truncated violin plot to demonstrate frequency distribution of the data where dashed lines represent the median and dotted lines represent the upper and lower quartiles, respectively. 63x objective. Background subtracted using ImageJ ("separate colour"; 50.0 pixels). N = 3, n = 8, ROI = 5, ns (p_{adj} > 0.05). Graticule (A) 50 µm. TGF-ß: Transforming growth factor beta 1; NAM: Negative allosteric modulator of the calcium-sensing receptor; ROCK: Rho associated coiled-coil containing protein kinase.

6.2.1.7 Wnt signalling

As shown in **Table 6.1**, GO enrichment suggested Wnt signalling was upregulated by TGF-ß. As shown in **Figure 6.9**, with the exception of downregulated *DVL2*, TGF-ß upregulated mRNA associated with Wnt/ß-catenin signalling, including *WNT5A, WNT5B, FZD8, CK1a* (*CSNK1A1*) and ß-catenin (*CTNNB1*) as well as target transcription factors, including *TCF3, TCF4, TCF25* and *LEF1*. As shown in **Figure 6.10**, TGF-ß also downregulated mRNA associated with non-canonical Wnt/Ca^{2+} signalling, including phospholipase C (PLC) (*PLCB1, PLCD1, PLCD3, PLCD4*), inositol triphosphate receptor (IP_3R) (*ITPR2, ITPR3*), PKC (*PRKCD, PRKCE*), and calmodulin (*CAMK2A, CAMK2D, CAMK2G, CAMK2N1*) isoforms and upregulated the calcineurin regulatory subunit, PPP3R1 (**log_2 fold change *DVL2* = -0.45, *WNT5A* = 0.63, *WNT5B* = 0.62, *FZD8* = 4.17, *CSNK1A1* = 0.31, *CTNNB1* = 0.49, *TCF3* = 0.29, *TCF4* = 0.88, *TCF25* = 0.39, *LEF1* = 1.01, *PLCB1* = -0.67, *PLCD1* = -0.83, *PLCD3* = -0.40, *PLCD4* = -1.57, *ITPR2* = -0.58, *ITPR3* = -1.12, *PRKCD* = -1.01, *PRKCE* = -1.91, CAMK2A = , CAMK2D = , CAMK2G = , CAMK2N1 = , CAMK2A = -3.53, CAMK2D = -0.75, CAMK2G = -0.26, CAMK2N1 = -0.26, PPP3R1 = 0.50; p_{adj} < 0.05; TGF-ß vs vehicle**). NAM treatment reversed both Wnt/ß-catenin and Wnt/Ca^{2+} signalling by downregulating *WNT5B*, *DVL2*, ß-catenin and *TCF25*; increasing ß-catenin destruction complex components, including *GSK3B* and *APC*; and reversed the expression of genes involved in PLC/Ca^{2+} signalling, including PLC (*PLCD1* and *PLCD4*), IP3R (*ITPR2* and *ITPR3*), protein kinase C (PKC) (*PRKCD* and *PRKCE*), calmodulin (*CAMK2G*) and calcineurin (*PPP3R1* and *PPP3CC*) isoforms (**log_2 fold change *WNT5B* = -0.63, *DVL2* = 0.59, *CTNNB1* = -0.36, *TCF25* = -0.43, *GSK3B* = 0.37, *APC* = 0.55, *PLCD1* = 0.57, *PLCD4* = 0.70, *ITPR2* = 0.81, *ITPR3* = 1.48, *PRKCD* = 0.49, *PRKCE* = 0.90, CAMK2G = 0.35, PPP3CC = 0.30, PPP3R1 = -0.54; p_{adj} < 0.05; TGF-ß + NAM vs TGF-ß**). When compared to baseline expression, NAM treatment upregulated expression of *FZD8*, *CK1a* (*CSNK1G3*), *TCF4*, *PIP4P2* and *PRKCA* but downregulated *PRKCD*, *PRKCE*, *CAM2KA*, *CAM2KD*, *CAMK2N1* and *PLCD4* expression (**log_2 fold change *FZD8* = 3.75, *CSNK1G3* = 0.34, *TCF4* = 1.13, *PIP4P2* = 0.50, *PRKCA* = 0.64, *PRKCD* = -0.52, *PRKCE* = -1.01, *CAMK2A* = -2.62, *CAMK2D* = -0.56, *CAMK2N1* = -0.66, *PLCD4* = -0.87; p_{adj} < 0.05; TGF-ß + NAM vs vehicle**). All other Wnt signalling components were indistinguishable from baseline levels (**p_{adj} > 0.05; TGF-ß + NAM vs vehicle**). This data suggests that although expression had

not been completely returned to baseline levels, the CaSR plays a central role in the regulation of TGF-β-induced Wnt/β-catenin and Wnt/Ca^{2+} signalling.

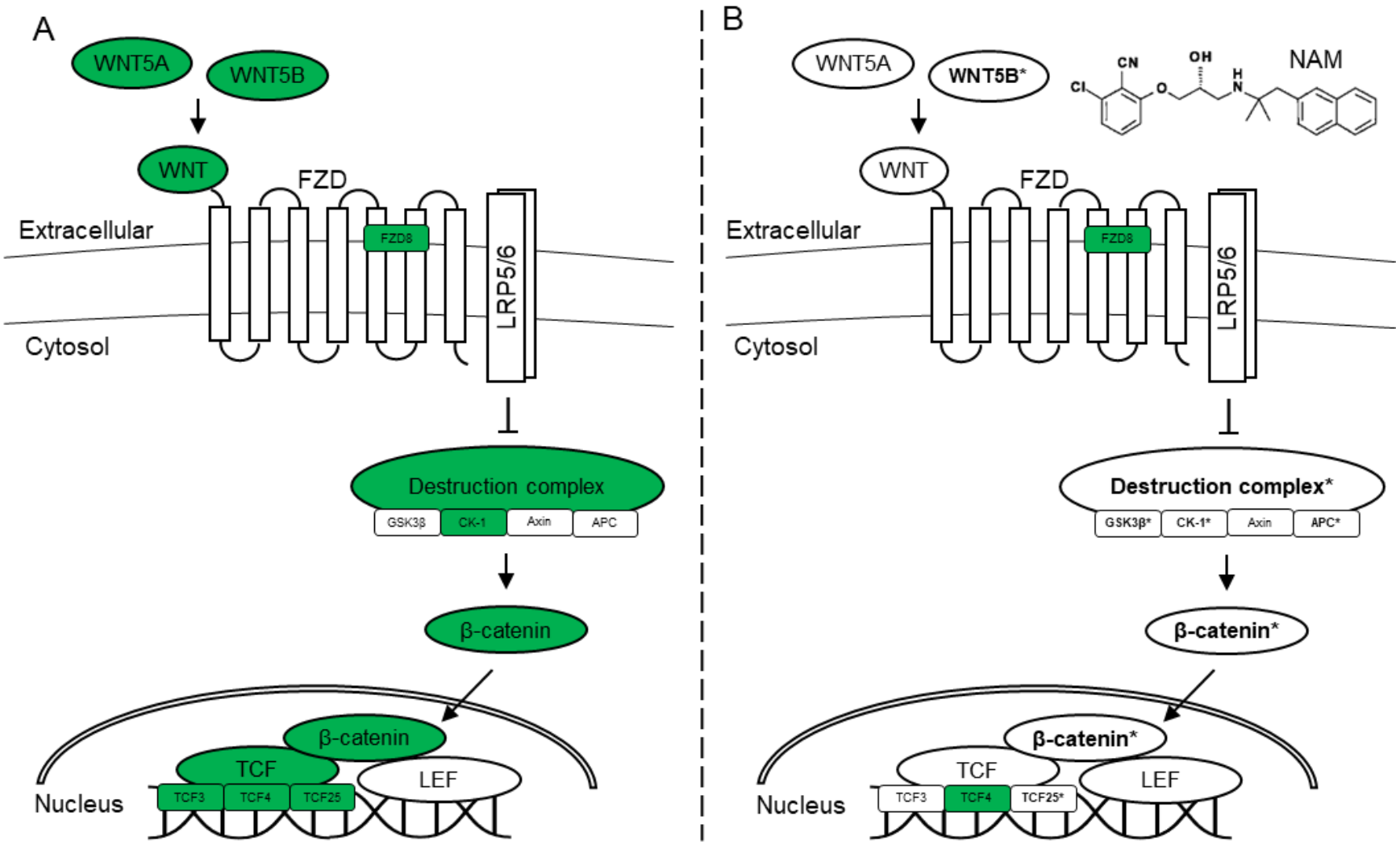
A
WNT5A
WNT5B
WNT
FZD
Extracellular
FZD8
LRP5/6
Cytosol
Destruction complex
GSK3β
CK-1
Axin
APC
β-catenin
β-catenin
TCF
LEF
TCF3
TCF4
TCF25
Nucleus
B
WNT5A
WNT5B*
NAM
CN
OH
Cl
O
H
N
WNT
FZD
Extracellular
FZD8
LRP5/6
Cytosol
Destruction complex*
GSK3β*
CK-1*
Axin
APC*
β-catenin*
β-catenin*
TCF
LEF
TCF3
TCF4
TCF25*
Nucleus

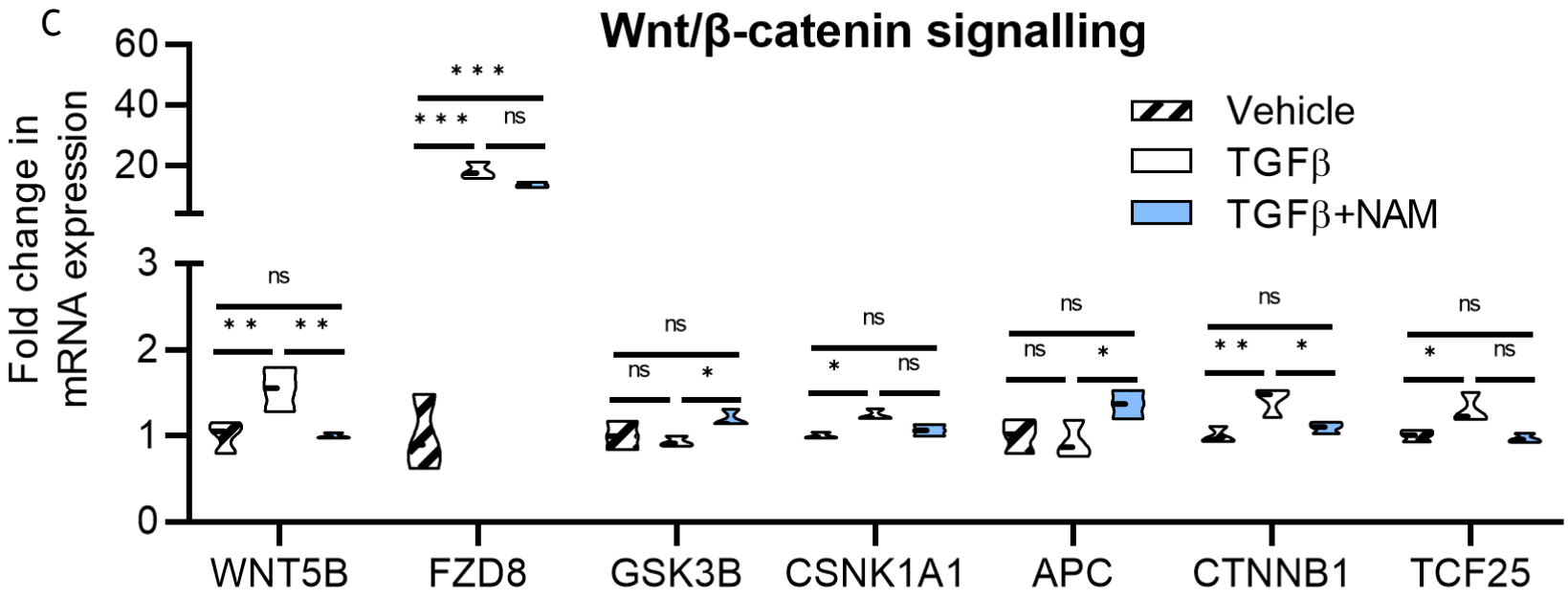

Figure 6.9. NAM treatment abolished TGF-ß-induced Wnt/ß-catenin signalling regulation in human lung fibroblasts. (**A**) Wnt ligands activate the FZD receptor and LRP5/6 co-receptor to inhibit the ß-catenin destruction complex via activation of DVL protein that allows ß-catenin accumulation where it translocates to the nucleus and interacts with TCF and LEF transcription factors to influence gene expression. TGF-ß upregulated *WNT5A*, *WNT5B*, *FZD8*, *CK-1*, ß-catenin and TCFs such as *TCF3*, *TCF4* and *TCF25* (green). (**B**) NAM treatment significantly reversed TGF-ß-induced *WNT5B*, *GSK3B*, *CK-1*, *APC*, ß-catenin and TCF25 expression (**bold***), when compared to TGF-ß. All of these genes, except *FZD8* and *TCF4* (green), were indistinguishable from baseline levels following NAM treatment. (**C**) Truncated violin plots were used to demonstrate frequency distribution of the data where the dashed line represents the median. Differentially expressed signalling pathways and

remodelling processes were identified using gene ontology (GO) and further investigation was conducted with a gene-by-gene approach. Statistical significance identified using Deseq2 (Sartools) with Benjamini-Hochberg p-value adjustment. Upregulation compared to vehicle control (green); downregulation compared to vehicle control (red); significant difference between TGF-β alone and TGF-β + NAM treatment (**bold***). N = 3, n = 6, ns ($p_{adj} > 0.05$), * ($p_{adj} < 0.05$), ** ($p_{adj} < 0.01$), *** ($p_{adj} < 0.001$). TGF-β: Transforming growth factor beta 1; NAM: Negative allosteric modulator of the calcium-sensing receptor; GO: Gene ontology; TCF: Transcription factor; LEF: Lymphoid enhancer binding factor; Wnt: Wingless-related integration site; WNT5A: Wingless-related integration site 5A isoform; WNT5B: Wingless-related integration site 5B isoform; FZD: Frizzled; LRP: Low-density lipoprotein receptor-related protein; GSK3β: Glycogen synthase kinase 3 beta; CK-1: Casein kinase 1; APC: Adenomatosis polyposis coli; DVL: Dishevelled.

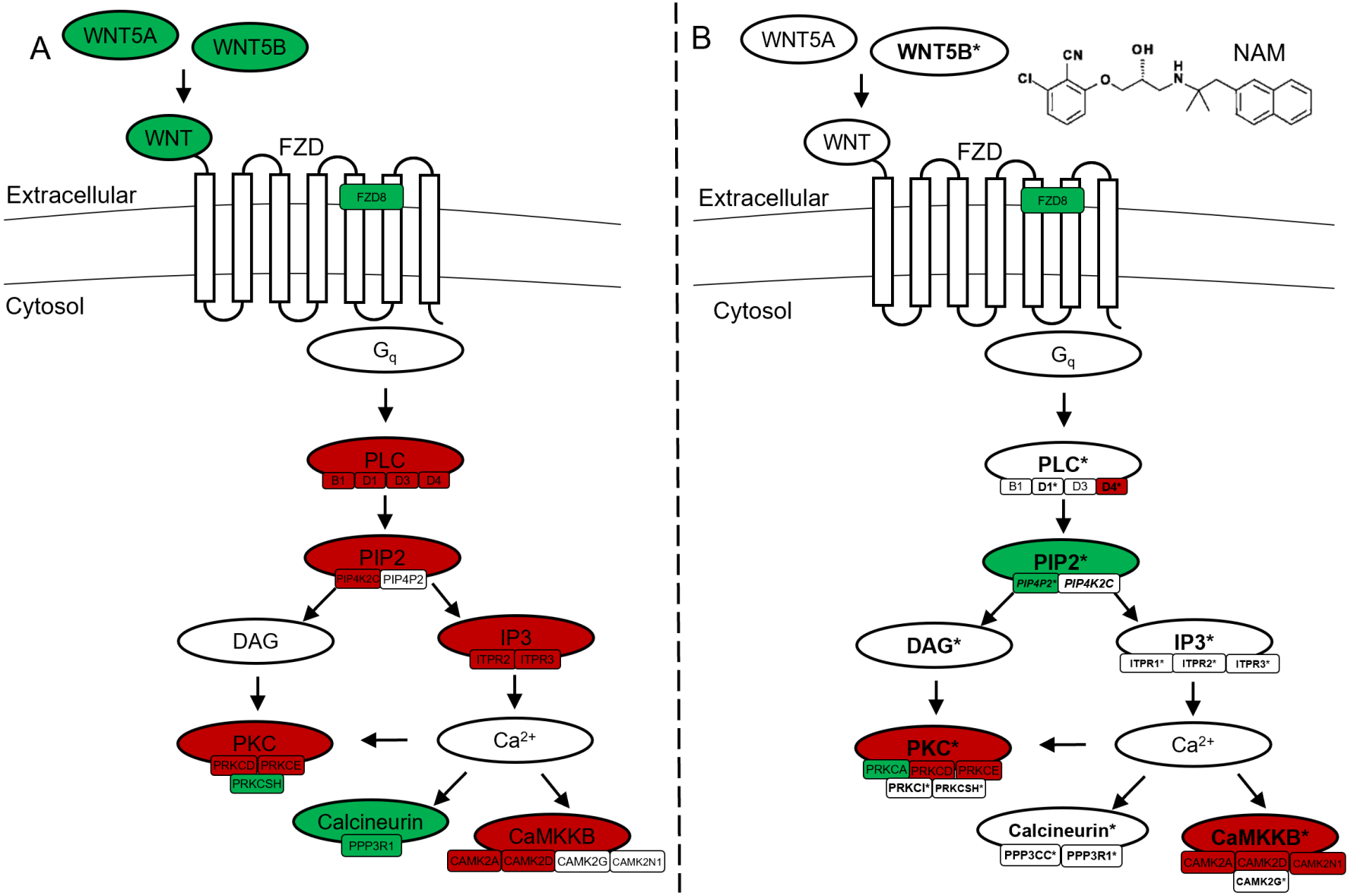
A
WNT5A
WNT5B
WNT
FZD
FZD8
Extracellular
Cytosol
G_q
PLC
B1
D1
D3
D4
PIP2
PIP4K2C
PIP4P2
DAG
IP3
ITPR2
ITPR3
PKC
PRKCD
PRKCE
PRKCSH
Ca^{2+}
Calcineurin
PPP3R1
CaMKKB
CAMK2A
CAMK2D
CAMK2G
CAMK2N1
B
WNT5A
WNT5B*
NAM
CN
OH
Cl
O
H
N
WNT
FZD
FZD8
Extracellular
Cytosol
G_q
PLC*
B1
D1*
D3
D4*
PIP2*
PIP4P2*
PIP4K2C
DAG*
IP3*
ITPR1*
ITPR2*
ITPR3*
PKC*
PRKCA
PRKCD
PRKCE
PRKCI*
PRKCSH*
Ca^{2+}
Calcineurin*
PPP3CC*
PPP3R1*
CaMKKB*
CAMK2A
CAMK2D
CAMK2N1
CAMK2G*

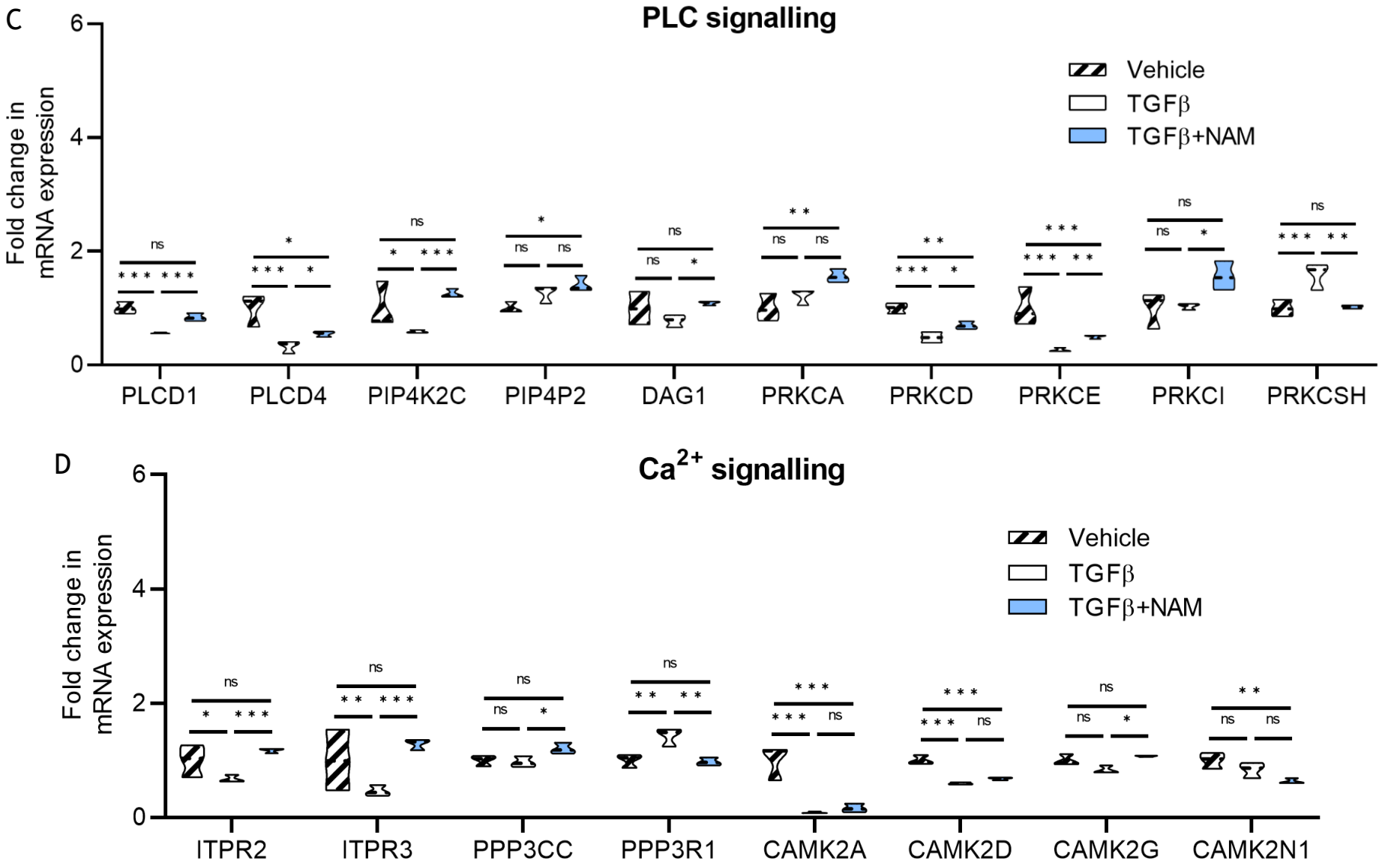
C
PLC signalling
Fold change in mRNA expression
Vehicle
TGFβ
TGFβ+NAM
PLCD1
PLCD4
PIP4K2C
PIP4P2
DAG1
PRKCA
PRKCD
PRKCE
PRKCI
PRKCSH
D
Ca2+ signalling
Fold change in mRNA expression
Vehicle
TGFβ
TGFβ+NAM
ITPR2
ITPR3
PPP3CC
PPP3R1
CAMK2A
CAMK2D
CAMK2G
CAMK2N1

Figure 6.10. NAM treatment ameliorates Wnt/Ca^{2+}/calcineurin signalling regulation. (**A**) Non-canonical Wnt/Ca^{2+} signalling is associated with phospholipase C and the inositol trisphosphate (IP3) receptor and leads to intracellular calcium release, calcineurin activation and calmodulin (CaMKKβ) activation. TGF-β downregulated PLC, PIP2, DAG, IP3, PKC, and CaMKKβ (red) and upregulated Calcineurin (green). (**B**) NAM treatment significantly reversed TGF-β-induced downregulation of PLC, PIP2, IP3, PKC and CaMKKβ as well as upregulation of calcineurin expression, when compared to TGF-β (**bold***). However, when compared to baseline levels, only DAG, IP3 and calcineurin were returned to baseline levels (white). (**C, D**) Truncated violin plots were used to demonstrate frequency distribution of the data where the dashed line represents the median. Differentially expressed signalling pathways and remodelling processes were identified using gene ontology (GO) and further investigation was conducted with a gene-by-gene approach. Statistical significance identified using Deseq2 (Sartools) with Benjamini-Hochberg p-value adjustment. Upregulation compared to vehicle control (green); downregulation compared to vehicle control (red); significant difference between TGF-β alone and TGF-β + NAM treatment (**bold***). N = 3, n = 6, ns (p_{adj} > 0.05), * (p_{adj} < 0.05), ** (p_{adj} < 0.01), *** (p_{adj} < 0.001). TGF-β: Transforming growth factor beta 1; NAM: Negative allosteric modulator of the calcium-sensing receptor; GO: Gene ontology; Wnt: Wingless-related integration site; WNT5A: Wingless-related integration site 5A isoform; WNT5B: Wingless-related integration site 5B isoform; FZD: Frizzled; G_q: Guanine Nucleotide-Binding Protein subunit alpha (q); PLC: Phospholipase C; PIP2: Phosphatidylinositol 4,5-bisphosphate; *DAG*: Diacylglycerol; IP3: inositol trisphosphate; PKC: Protein kinase C; *CaMKKB*: calmodulin; *PLCD*: Phospholipase C delta; *PIP4K2C*: Phosphatidylinositol-5-phosphate 4-kinase type 2 gamma; PRKCA: Protein kinase C alpha; *PRKCD*: Protein kinase C delta; *PRKCE*: Protein kinase C epsilon; *PRKCI*: Protein kinase C iota; *PRKCSH*: Protein kinase C substrate 80Kda H; ITPR: Inositol 1,4,5-trisphosphate receptor; *PPP3CC*: Protein phosphatase 3 catalytic subunit gamma; *PPP3R1*: Protein phosphatase 3 regulatory subunit B alpha; *CAMK2A*: Calcium/calmodulin dependent protein kinase II alpha; *CAMK2D*: Calcium/calmodulin dependent protein kinase II delta;

CAMK2G: Calcium/calmodulin dependent protein kinase II gamma; CAMK2N1: Calcium/calmodulin dependent protein kinase II inhibitor 1.

6.2.1.8 CaSR signalling

Using immunofluorescence, as shown in **Figure 6.11**, cell surface and intracellular CaSR expression was identified in human lung fibroblasts. Furthermore, CaSR protein expression was significantly increased (p_{adj} = **0.0011**) following TGF-β exposure. An effect that was significantly reversed by NAM treatment (p_{adj} < **0.0001**). CaSR mRNA expression could not be confirmed by RNA-sequencing due to low expression. The human protein atlas (Uhlen et al., 2015) also observed undetectable mRNA expression but confirmed CaSR protein expression in the lung. It is possible that CaSR protein recycling and low desensitisation may reduce its reliance on high levels of mRNA translation for CaSR protein expression resulting in below threshold expression (Breitwieser, 2013; Ray, 2015).

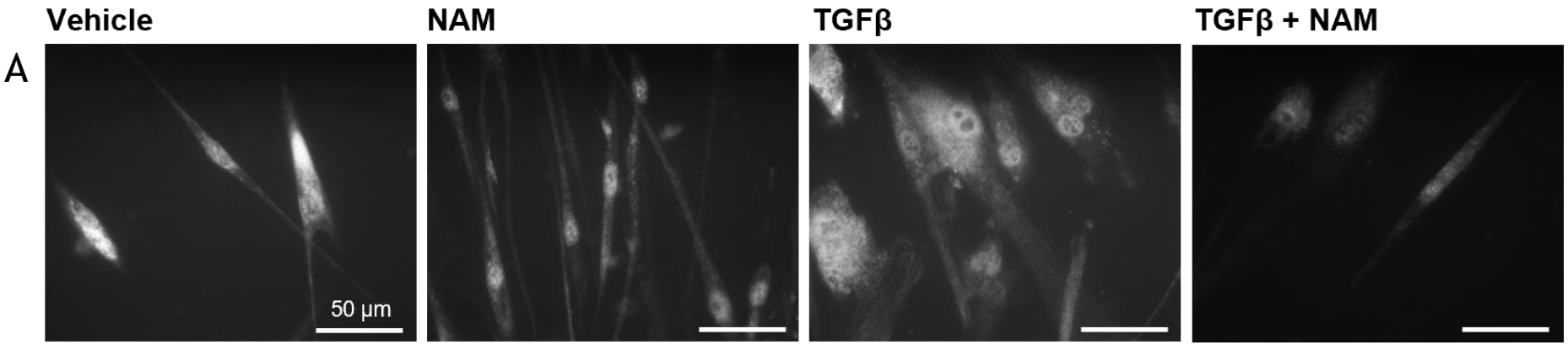
A
Vehicle
NAM
TGFβ
TGFβ + NAM
50 µm

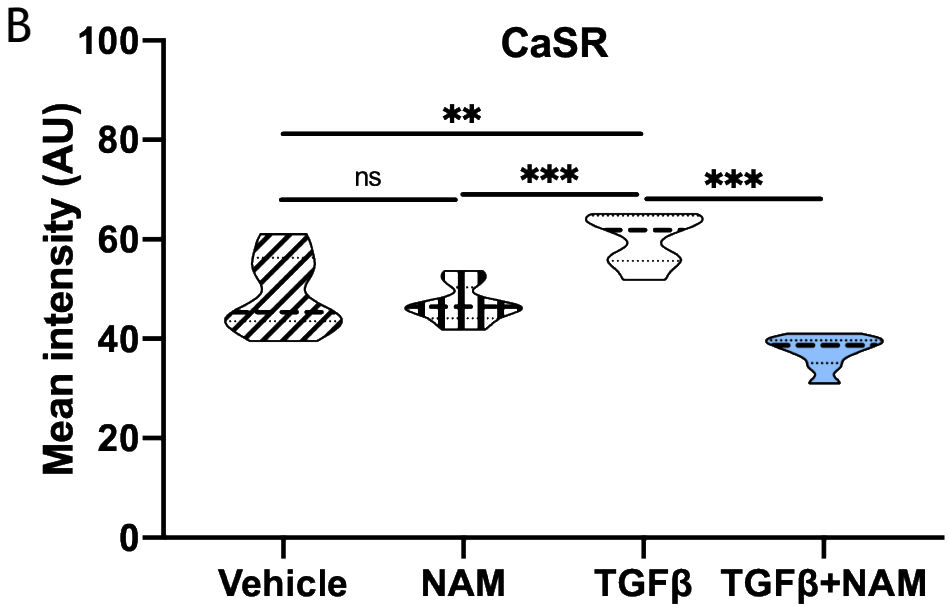
B
CaSR
Mean intensity (AU)
100
80
60
40
20
0
**
ns
***
***
Vehicle
NAM
TGFβ
TGFβ+NAM

Figure 6.11. TGF-ß significantly upregulates CaSR protein expression in human lung fibroblasts, a process abolished by NAM treatment. Primary normal human lung fibroblasts (Lonza, UK) were treated with and without remodelling mediator TGF-ß and/or treated with a NAM (NPS2143). CaSR was identified using anti-CaSR antibody (Ab19347) and AlexaFluor 594 (Ab11005) secondary antibody. Mean intensity was quantified using StrataQuest and normalised to nuclear count (blue). Truncated violin plot to demonstrate frequency distribution of the data where dashed lines represent the median and dotted lines represent the upper and lower quartiles, respectively. 63x objective. Background subtracted using ImageJ ("separate colour"; 50.0 pixels). N = 3, n = 5. ns ($p_{adj} > 0.05$), * ($p_{adj} < 0.05$), ** ($p_{adj} < 0.01$), *** ($p_{adj} < 0.001$). Graticule (A) 50 µm. TGF-ß: Transforming growth factor beta 1; NAM: Negative allosteric modulator of the calcium-sensing receptor; GO: gene ontology; AU: Arbitrary units.

In this experiment, TGF-β upregulated of *GNAI3, GNAS, GNA13, GNB1, GNB4*, and *GNG11* and downregulated *GNAI1, GNG2, ADCY3, ADCY6* and *ADCY9* consistent with activation of Ras and inhibition of adenyl cyclase (**$\log_2$ fold change *GNAI3* = 0.38, *GNAS* = 0.63, *GNA13* = 0.37, *GNB1* = 0.49, *GNB4* = 0.38, *GNG11* = 0.64, *GNAI1* = -0.45, *GNG2* = -0.88, *ADCY3* = -0.97, *ADCY6* = -0.50, *ADCY9* = -0.65; p_{adj} < 0.05; TGF-β vs vehicle**). NAM treatment downregulated *GNAI2, GNAI3, GNAS, GNA12, GNB1* and upregulated *ADCY3, ADCY6, ADCY7* and *ADCY9* indicating downregulation of Ras signalling and restoration of cyclic adenosine monophosphate (cAMP)-producing adenyl cyclase expression (**$\log_2$ fold change *GNAI2* = -0.41, *GNAI3* = -0.41, *GNAS* = -0.60, *GNA12* = -0.62, *GNB1* = -0.45, *GNB2* = -0.53, *ADCY3* = 0.85, *ADCY6* = 0.60, *ADCY7* = 1.46, *ADCY9* = 0.80; p_{adj} < 0.05; TGF-β + NAM vs TGF-β**). When comparing NAM treatment to baseline expression, *GNA13, GNB3* and *GNB4* were upregulated and *GNAI1* and *GNG2* were downregulated (**$\log_2$ fold change *GNA13* = 0.53, *GNB3* = 0.98, *GNB4* = 0.41, *GNAI1* = -0.65, *GNG2* = -0.49; p_{adj} < 0.05; TGF-β + NAM vs vehicle**) but all other G proteins and ADCY genes were indistinguishable from baselines levels (**p_{adj} > 0.05; TGF-β + NAM vs vehicle**). This indicates that NAM treatment ameliorated TGF-β-induced effects on G_i and adenyl cyclase expression but also has implications for other G protein expression with unknown effect, as shown in **Figure 6.12**.

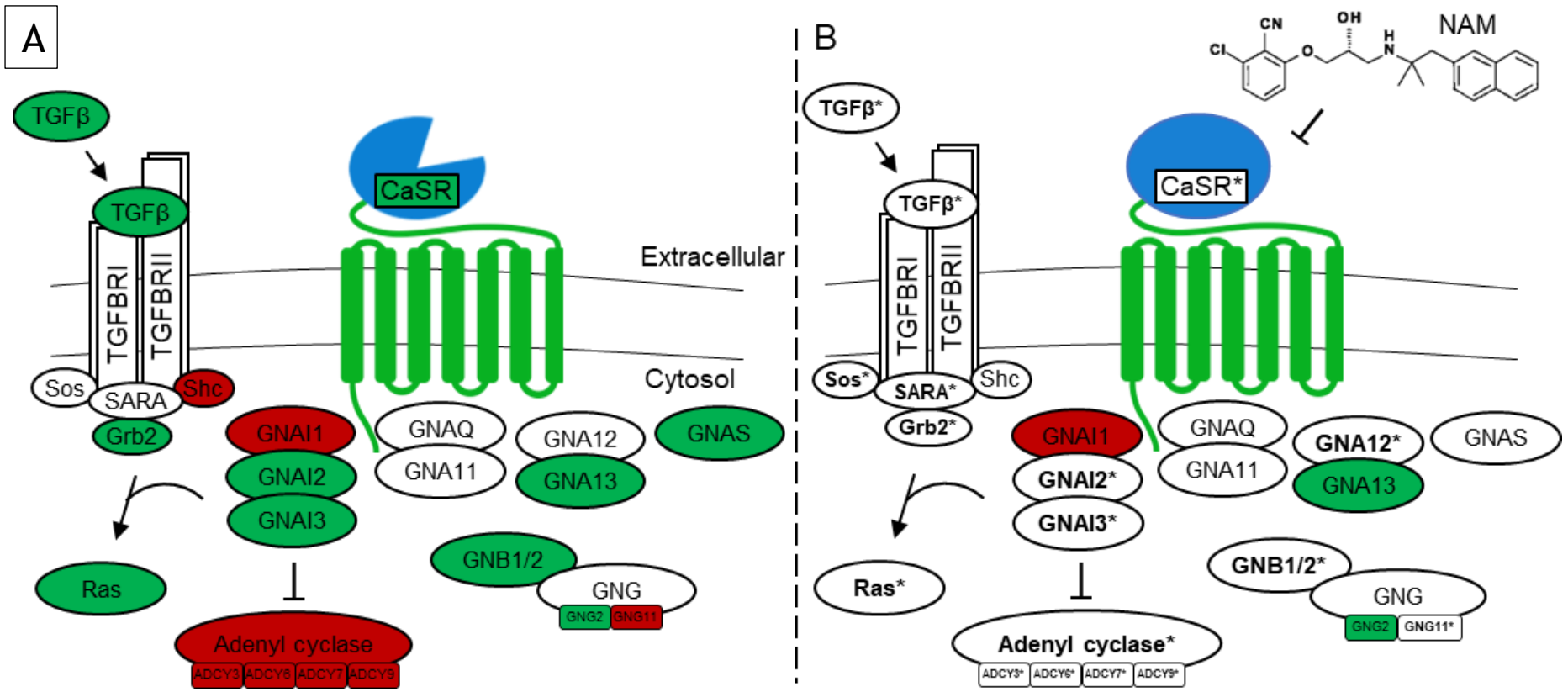
A
TGFβ
TGFβ
TGFBRI
TGFBRII
Sos
SARA
Shc
Grb2
CaSR
Extracellular
Cytosol
GNAI1
GNAI2
GNAI3
GNAQ
GNA11
GNA12
GNA13
GNAS
GNB1/2
GNG
GNG2
GNG11
Ras
Adenyl cyclase
ADCY3
ADCY6
ADCY7
ADCY9
B
NAM
TGFβ*
TGFβ*
TGFBRI
TGFBRII
Sos*
SARA*
Shc
Grb2*
CaSR*
GNAI1
GNAI2*
GNAI3*
GNAQ
GNA11
GNA12*
GNA13
GNAS
GNB1/2*
GNG
GNG2
GNG11*
Ras*
Adenyl cyclase*
ADCY3*
ADCY6*
ADCY7*
ADCY9*

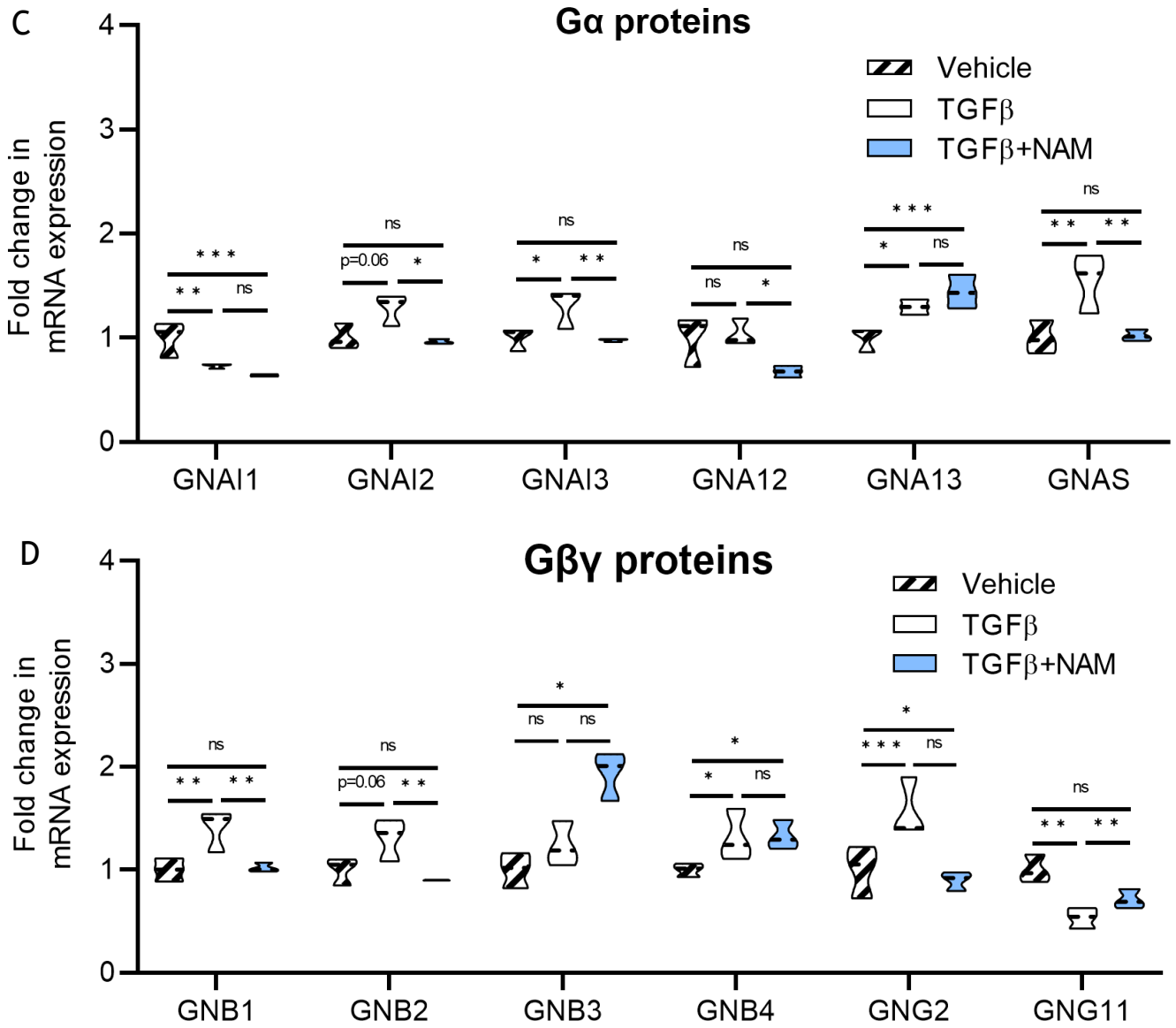
C
Gα proteins
Vehicle
TGFβ
TGFβ+NAM
Fold change in mRNA expression
0
1
2
3
4
GNAI1
GNAI2
GNAI3
GNA12
GNA13
GNAS
D
Gβγ proteins
Vehicle
TGFβ
TGFβ+NAM
Fold change in mRNA expression
0
1
2
3
4
GNB1
GNB2
GNB3
GNB4
GNG2
GNG11

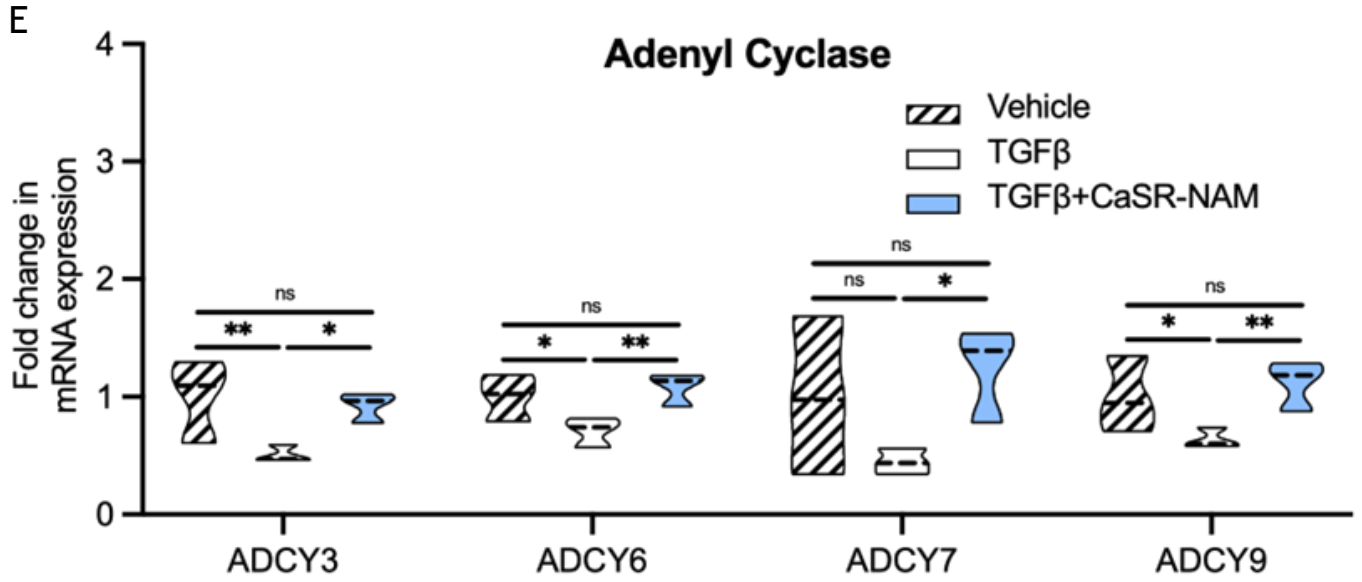

Figure 6.12. NAM treatment ameliorates TGF-ß-induced upregulation of CaSR-related G proteins and downregulation of cAMP-producing adenyl cyclase. (**A**) The CaSR is mainly associated with G_i, $G_{q/11}$, $G_{12/13}$, G_β, and G_γ heterotrimeric G proteins but also G_S in some cases. Specifically, G_i proteins are associated with Ras activation and αßγ adenyl cyclase inhibition which depletes cAMP levels. cAMP is protective against mechanisms of fibrosis, such as proliferation, migration, fibroblast to myofibroblast transition, and the ability to synthesize extracellular matrix (ECM) proteins in lung fibroblasts. TGF-ß significantly upregulated mRNA expression of *GNAI3, GNAS, GNA13, GNB1, GNB4*, and *GNG11* and downregulated *GNAI1, GNG2, ADCY3, ADCY6* and *ADCY9* consistent with activation of Ras and inhibition of adenyl cyclase. (**B**) NAM treatment significantly reversed TGF-ß-induced *GNAI2, GNAI3, GNAS, GNA12, GNB1, ADCY3, ADCY6, ADCY7* and *ADCY9* expression (**bold***), when compared to TGF-ß. All of these genes, except *GNAI1* and *GNA13*, were indistinguishable from baseline levels following NAM treatment. (**C, D and E**) Truncated violin plots were used to demonstrate frequency distribution of the data where the dashed

line represents the median. Differentially expressed signalling pathways and remodelling processes were identified using gene ontology (GO) and further investigation was conducted with a gene-by-gene approach. Statistical significance identified using Deseq2 (Sartools) with Benjamini-Hochberg p-value adjustment. Upregulation compared to vehicle control (green); downregulation compared to vehicle control (red); significant difference between TGF-β alone and TGF-β + NAM treatment (**bold***). N = 3, n = 6, ns ($p_{adj} > 0.05$), * ($p_{adj} < 0.05$), ** ($p_{adj} < 0.01$), *** ($p_{adj} < 0.001$). TGF-β: Transforming growth factor beta 1; NAM: Negative allosteric modulator of the calcium-sensing receptor; GO: gene ontology; Grb2: Growth factor receptor binding protein 2; Shc: Src homology 2 domain-containing transforming protein C; SARA: Smad anchor for receptor activation; Sos: Son Of Sevenless; G_i: Guanine nucleotide-binding protein subunit alpha (i); $G_{q/11}$: Guanine nucleotide-binding protein subunit alpha (q/11); $G_{12/13}$: Guanine nucleotide-binding protein subunit alpha (12/13); G_β: Guanine nucleotide-binding protein subunit beta; G_γ: Guanine nucleotide-binding protein subunit gamma; GNA: Guanine nucleotide-binding protein subunit alpha gene isoform; GNB: Guanine nucleotide-binding protein subunit beta gene isoform; GNY: Guanine nucleotide-binding protein subunit gamma gene isoform; ADCY: Adenyl Cyclase; cAMP: Cyclic adenosine monophosphate.

6.2.2 NAM treatment ameliorates TGF-β-induced cellular remodelling processes

To investigate the role of the CaSR in TGF-β-induced cell remodelling processes, GO enrichment analysis was used to connect differentially expressed genes to "GO terms" that describe the effect of TGF-β on remodelling processes within the cell in the presence or absence of NAM treatment (Pomaznoy et al., 2018). **Table 6.2** summarises the terms, and their direction of regulation, that were shortlisted based on their association with lung remodelling.

Table 6.2. NAM treatment reverses TGF-β-induced signalling pathway activation and regulation in human lung fibroblasts. This table summarises the differentially expressed GO terms that describe biological functions within the cell, the direction of regulation, the number of differentially expressed genes that match that term and the adjusted p value (p_{adj}). Up- and down-regulated genes were input into the GOnet enrichment tool separately to provide the direction of regulation. NAM treatment reversed activation or regulation of several cellular remodelling processes implicated in epithelial, goblet cell, smooth muscle, and ECM remodelling. Statistical significance calculated using a Fisher exact test with Benjamini-Hochberg p value correction. N = 3, n = 6. * ($p_{adj} < 0.05$), ** ($p_{adj} < 0.01$), *** ($p_{adj} < 0.001$), **** ($p_{adj} < 0.0001$). TGF-β: Transforming growth factor beta 1; NAM: Negative allosteric modulator of the calcium-sensing receptor; GO: gene ontology.

	Gene Ontology (GO) term	TGFβ			TGFβ + NAM		
	Physiological processes	**Direction**	**Genes**	p_{adj}	**Direction**	**Genes**	p_{adj}
Apoptosis	Regulation of morphogenesis of an epithelium	UP	49	****	DOWN	47	****
	Regulation of cytochrome c release from mitochondria	UP	14	*	DOWN	15	*
	Apoptotic process	UP	168	****	DOWN	174	****
Secretion	Secretion	UP	206	****	DOWN	211	****
	Exocytosis	UP	159	****	DOWN	176	****
Growth	Regulation of cell growth	UP	73	*			
	Ribosome biogenesis	UP	116	****	DOWN	125	****
	Transcription initiation from RNA polymerase II promoter	UP	37	*	DOWN	39	**
	Autophagy	UP	56	**	DOWN	60	****
Proliferation	Cell population proliferation	UP	74	*			
	Regulation of epithelial cell proliferation	UP	53	**			
	Regulation of smooth muscle cell proliferation	UP	24	*			
	Regulation of fibroblast proliferation	UP	24	**	DOWN	21	*
	Angiogenesis	UP	61	*			
ECM remodelling	Aging	UP	57	**	DOWN	51	*
	Cellular response to stress	UP	354	****	DOWN	359	****
	Actin filament organisation	UP	57	****	DOWN	45	*
	Stress fibre assembly	UP	8	*			
	Extracellular matrix assembly	UP	8	*			
	Collagen biosynthetic process	UP	6	**	DOWN	6	**
	Elastic fibre assembly	UP	5	*			
	Growth	DOWN	66	***	UP	64	**
	Regulation of tissue remodelling	DOWN	18	**			

6.2.2.1 Apoptosis

In this experiment, TGF-ß upregulated the GO terms "Regulation of morphogenesis of an epithelium", "Regulation of Cytochrome c release from mitochondria" and "Apoptotic process". TGF-ß also upregulated mitochondrial calcium regulating genes *MICU2, TSPO, PPID, VDAC2, VDAC3, Grp75* (*HSPA9*) and apoptosis-inducing Cytochrome C (*CYCS*) and downregulated *MICU3* suggesting TGF-ß induced dysfunction of mitochondrial calcium homeostasis and subsequently apoptosis via mitochondrial Cytochrome C release (**log_2 fold change *MICU2* = 0.48, *TSPO* = 0.80, *PPID* = 0.41, *VDAC2* = 0.59, *VDAC3* = 0.37, *HSPA9* = 0.79, *CYCS* = 0.51, MICU3 = -0.92; p_{adj} < 0.05; TGF-ß vs vehicle**). NAM treatment significantly reversed this effect by downregulating the GO terms "Regulation of morphogenesis of an epithelium", "Regulation of Cytochrome C release from mitochondria" and "Apoptotic process" as well as *MICU2, TSPO, PPID, VDAC1, VDAC2, VDAC3, Grp75* (*HSPA9*) and Cytochrome C (*CYCS*) as well as upregulating *MICU3* (**log_2 fold change, *MICU2* = -0.58, *TSPO* = -0.93, *PPID* = -0.43, *VDAC1* = -0.32, *VDAC2* = -0.69, *VDAC3* = -0.44, *HSPA9* = -0.57, *CYCS* = -0.53, *MICU3* = 0.74; p_{adj} < 0.05; TGF-ß + NAM vs TGF-ß**). When compared with baseline levels, gene expression following NAM treatment could not be distinguished from baseline levels (**p_{adj} > 0.05; TGF-ß + NAM vs vehicle**).

6.2.2.2 Secretion

In this experiment, TGF-ß upregulated the GO terms "Secretion" and "Exocytosis". TGF-ß also upregulated the expression of *MARCKS* and *STX10* and downregulated *RAB3A, RAB3D, VAMP1, VAMP4, STX3, STX17, MUNC13* (*UNC13B*) and *MUNC18* (*STXBP1*) but not *RAB27A*, melanophilin (MLPH) or *RAB3* which actually suggests TGF-ß inhibited secretion and exocytosis by this mechanism (**log_2 fold change *MARCKS* = 0.72, *STX10* = 0.36, *RAB3A* = -1.21, *RAB3D* = -2.07, *VAMP1* = -1.12, *VAMP4* = -0.63, *STX3* = -0.58, *STX17* = -0.69, *UNC13B* = -0.43, *STXBP1* = -0.36; p_{adj} < 0.05; TGF-ß vs vehicle**). NAM treatment significantly attenuated *MARCKS*, *STX10*, *RAB3A*, *VAMP1*, *STX3*, *STX17*, *MUNC13* (*UNC13B*) and *MUNC18* (*STXBP1*) expression (**log_2 fold change *MARCKS* = -0.70, *STX10* = -0.64, *RAB3A* = 1.05, *VAMP1* = 0.87, *STX3* = 0.57, *STX17* = 0.61, *UNC13B* = 0.46, *STXBP1* = 0.38; p_{adj} < 0.05; TGF-ß + NAM vs TGF-ß**) reinstating baseline expression (**p_{adj} > 0.05; TGF-ß + NAM vs vehicle**).

Although it is unclear if secretion was up- or down-regulated by TGF-ß; this data shows NAM treatment ameliorated the TGF-ß-induced effects on regulation of secretion and exocytosis, a key process in fibroblast mediation of inflammation via secretion of inflammatory cytokines and extracellular matrix remodelling by secretion of components such as procollagen.

6.2.2.3 Growth

As shown above, TGF-ß upregulated the PI3K/Akt/mTOR pathway as well as the GO terms "Regulation of cell growth", "Ribosome biogenesis" and "Transcription initiation from RNA polymerase II promoter" suggesting TGF-ß induced growth; however, TGF-ß also downregulated the GO term "Growth" and upregulated the GO term "Autophagy". Further investigation found that TGF-ß upregulated *MAF1*, *POLR3D*, S6K1 (*RPS6KB1*), *RPS6*, *POLR2* isoforms, *GAR1*, *RRP9*, Ubf (*UBTF*), *SL1* (*TAF1D*), *4E-BP1* (*EIF4EBP1*), *ULK1* and *ATG5* but not *POLR1* or *TIF1A* (*TRIM24*) which suggests ribosome biogenesis, RNA polymerase expression was upregulated but also indicates that autophagy was upregulated (**log2 fold change *MAF1* = 0.67, *POLR3D* = 0.43, *RPS6KB2* = 0.37, *RPS6* = 0.96, *POLR2C* = 0.35, *POLR2F* = 0.69, *POLR2G* = 0.77, *POLR2H* = 0.38, *POLR2J* = 0.71, *POLR2K* = 0.55, *POLR2L* = 0.53, *GAR1* = 0.81, *RRP9* = 0.71, *UBTF* = 0.37, *TAF1D* = 0.43, *EIF4EBP1* = 1.4, *ULK1* = 0.45, *ATG5* = 0.33; p_{adj} < 0.05; TGF-ß vs vehicle**). NAM treatment downregulated the GO terms "Ribosome biogenesis" and "Transcription initiation from RNA polymerase II promoter" but also upregulated the GO term "Growth" and downregulated the GO term "Autophagy". NAM treatment also reversed the expression of *MAF1*, *RPS6KB2*, *RPS6*, *POLR2* isoforms, *Gar1*, *Rrp9*, *Ubf*, 4E-BP1 (*EIF4EBP1*) and *ATG5* and also upregulated *POLR3A* suggesting growth-supporting RNA polymerase expression and ribosome biogenesis processes were reversed by NAM treatment (**log2 fold change *MAF1* = -0.61, *RPS6KB2* = -0.46, *RPS6* = -1.02, *POLR2E* = -0.30, *POLR2F* = -0.88, *POLR2G* = -0.83, *POLR2H* = -0.65, *POLR2I* = -0.83, *POLR2J* = -0.84, *POLR2K* = -0.55, *POLR2L* = -0.90, *GAR1* = -0.77, *RRP9* = -0.62, Ubf (*UBTF*) = -0.35, *EIF4EBP1* = -0.97, *ATG5* = -0.31, *POLR3A* = 0.52; p_{adj} < 0.05; TGF-ß + NAM vs TGF-ß**). Furthermore, the expression of these genes following NAM treatment was indistinguishable from baseline expression (**p_{adj} > 0.05; TGF-ß + NAM vs vehicle**)

suggesting TGF-β-induced regulation of growth and degradation processes were abolished by NAM treatment.

6.2.2.4 Proliferation

In this experiment, TGF-β upregulated the GO terms "cell population proliferation", "regulation of epithelial cell proliferation", "regulation of smooth muscle cell proliferation", "angiogenesis" and "regulation of fibroblast proliferation". As shown above, TGF-β also upregulated PI3K/Akt/mTOR, Rac1/RhoA and Wnt signalling and downregulated adenyl cyclase expression which are central to cell proliferation. Further investigation found that TGF-β upregulated *CALR*, *ORMDL3*, *PCNA*, *CDK4*, *CDK5*, *CDK7*, *SLC3A2* and *ASNS* and downregulated Cyclin E (*CCNE2*) suggesting upregulation of progression through the cell cycle (**log2 fold change *CALR* = 0.74, *ORMDL3* = 0.60, *PCNA* = 0.52, *CDK4* = 0.52, *CDK5* = 0.58, *CDK7* = 0.41, *SLC3A2* = 1.12, *ASNSD1* = 0.42, *CCNE2* = -1.31; p_{adj} < 0.05; TGF-β vs vehicle**). NAM treatment downregulated the GO term "regulation of fibroblast proliferation" and reversed *CALR*, *ORMDL3*, *PCNA*, *CDK4*, *CDK5*, *CDK7*, *SLC3A2*, *ASNS* and Cyclin E (*CCNE2*) expression as well as downregulation of angiogenic VEGFB expression (**log2 fold change *CALR* = -0.79, *ORMDL3* = -0.51, *PCNA* = -0.67, *CDK4* = -0.50, *CDK5* = -0.59, *CDK7* = -0.59, *SLC3A2* = -0.68, *ASNSD1* = -0.47, *CCNE2* = 1.23, *VEGFB* = -0.58; p_{adj} < 0.05; TGF-β + NAM vs TGF-β**). When compared to baseline, NAM treatment could not be distinguished from baseline expression (**p_{adj} > 0.05; TGF-β + NAM vs vehicle**).

6.2.2.5 Senescence

In this experiment, TGF-β upregulated the GO term "Aging" and "Cellular response to stress" which includes, but is not limited to, the GO term cell senescence. TGF-β also upregulated *CDKN1A*, *CDKN2A*, *CDNK2B*, *SPARC*, *PLAUR* and *SERPINE1/2* suggesting TGF-β induced a senescence-associated phenotype in these cells (**log_2 fold change *CDKN1A* = 0.58, *CDKN2A* = 0.75, *CDNK2B* = 1.32, *SPARC* = 1.17, *PLAUR* = 0.63, *SERPINE1* = 1.19, *SERPINE2* = 1.74; p_{adj} < 0.05; TGF-β vs vehicle**). NAM treatment downregulated the GO terms "Aging" and "Cellular response to stress" and reversed expression of *CDKN1A*, *CDKN2A*, *SPARC*, *PLAUR* and *SERPINE1/2*. NAM treatment also downregulated *PLAU* and upregulated protective *RB1* and *SIRT1*

(**log_2 fold change *CDKN1A* = -0.51, *CDKN2A* = -0.82, *SPARC* = -0.91, *PLAU* = -0.47, *PLAUR* = -0.49, *SERPINE1* = -0.83, *SERPINE2* = -0.79, *RB1* = 0.65, *SIRT1* = 0.41; p_{adj} < 0.05; TGF-β + NAM vs TGF-β**). Furthermore, with the exception of *CDKN2B*, NAM treatment returned the expression of senescence associated genes back to baseline levels (**p_{adj} > 0.05; TGF-β + NAM vs vehicle**). This data indicates that TGF-β-induced regulation of aging and senescence was ameliorated by NAM treatment, a central process in, but not limited to, autophagy-related ECM remodelling.

6.2.2.6 ECM remodelling

Here, TGF-β significantly upregulated GO terms for ECM remodelling processes such as "Actin filament organisation", "Stress fibre assembly", "Extracellular matrix assembly", "Collagen biosynthetic process", "Autophagy" and "Elastic fibre assembly". Collagens are a major component of the ECM that are increased in ECM remodelling (Specks et al., 1995; Keynon et al., 2003). Here, TGF-β upregulated *COL1A1*, *COL1A2*, *COL3A1*, *COL5A1*, *COL6A2*, and *COL16A1* (**log_2 fold change *COL1A1* = 1.29, *COL1A2* = 1.02, *COL3A1* = 0.87, *COL5A1* = 1.60, *COL6A2* = 0.60, *COL16A1* = 1.13; p_{adj} < 0.05; TGF-β vs vehicle; Figure 6.13A**). NAM treatment significantly downregulated the GO term "Collagen biosynthetic process" and "Autophagy" as well as *COL1A1*, *COL1A2*, *COL3A1*, *COL5A1*, *COL6A2* and *COL16A2* expression suggesting collagen expression was significantly downregulated and supports my previous findings of reduced peribronchial collagen remodelling *in vivo* (**log_2 fold change *COL1A1* = -0.86, *COL1A2* = -0.80, *COL3A1* = -0.69, *COL5A1* = -0.53, *COL6A2* = -0.80, *COL16A1* = -0.44; p_{adj} < 0.05; TGF-β + NAM vs TGF-β; Figure 6.13A**).

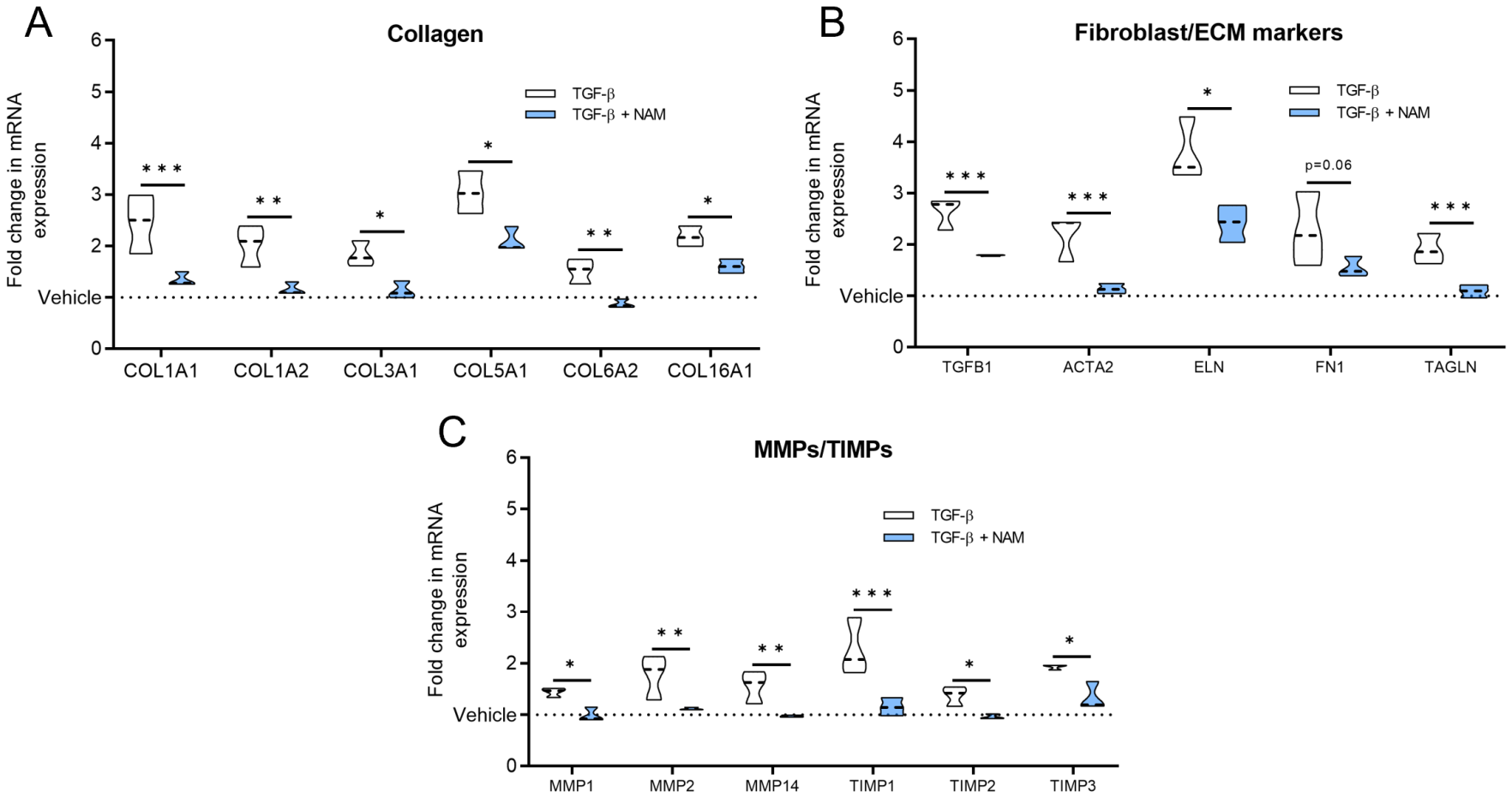

Figure 6.13. NAM treatment abolished TGF-β-induced ECM remodelling in human lung fibroblasts. ECM remodelling in the lung involves (**A** and **B**) synthesis and increased deposition of ECM components such as (**A**) the most abundant component,

collagen; (**B**) other ECM components, such as αSMA (*ACTA2*), elastin (*ELN*), fibronectin (*FN1*) and SM22α (*TAGLN*); and (**C**) turnover of these ECM components by MMPs and TIMPs. NAM treatment significantly reversed TGF-ß-induced upregulation of collagen, other ECM components, such as αSMA (*ACTA2*), elastin (*ELN*) and SM22α (*TAGLN*) and MMP/TIMP genes. Truncated violin plots were used to demonstrate frequency distribution of the data where the dashed line represents the median. Differentially expressed signalling pathways and remodelling processes were identified using gene ontology (GO) and further investigation was conducted with a gene-by-gene approach. Statistical significance identified using Deseq2 (Sartools) with Benjamini-Hochberg p-value adjustment. Upregulation compared to vehicle control (green); downregulation compared to vehicle control (red); significant difference between TGF-ß alone and TGF-ß + NAM treatment (**bold***). N = 3, n = 6, ns (p_{adj} > 0.05), * (p_{adj} < 0.05), ** (p_{adj} < 0.01), *** (p_{adj} < 0.001). TGF-ß: Transforming growth factor beta 1; NAM: Negative allosteric modulator of the calcium-sensing receptor; GO: gene ontology; ECM: Extracellular matrix; COL: collagen gene; αSMA: Alpha smooth muscle actin; *ACTA2*: Alpha smooth muscle actin gene; *ELN*: Elastin; *FN1*: Fibronectin 1; SM22α: Transgelin; *TAGLN*: Transgelin gene; MMP: Matrix metalloproteinase; TIMP: Tissue inhibitor of metalloproteinase.

Furthermore, to meet the amino acid demands of increased collagen production, TGF-β also upregulates synthesis of the two key amino acid components glycine and proline. To upregulate glycine synthesis, TGF-β activates the 4E-BP1 pathway via PI3K/Akt/mTORC1/ATF4 pathway to promote the conversion of the glycolytic intermediate 3-phosphoglycerate (3-PG) to glycine via the serine-glycine converting enzymes, encoded by genes *PHGDH*, *PSAT1*, *PSPH*, and *SHMT2*. Here, TGF-β upregulated *4E-BP1* (*EIF4EBP1*), *ATF4*, *PHGDH*, *PSAT1*, *PSPH*, *SHMT2* and *LDHA* indicating upregulation of glycine synthesis (**$\log_2$ fold change *EIF4EBP1* = 1.40, *ATF4* = 0.95, *PHGDH* = 1.35, *PSAT1* = 1.66, *PSPH* = 1.45, *SHMT2* = 0.91, LDHA = 0.76; p_{adj} < 0.05; TGF-β vs vehicle**). NAM treatment reversed the expression of all members of the 4E-BP1 pathway, including the serine-glycine converting enzymes, *PHGDH*, *PSAT1*, *PSPH and SHMT2* (**$\log_2$ fold change *EIF4EBP1* = -0.97, *ATF4* = -0.90, *PHGDH* = -0.72, *PSAT1* = -0.64, *PSPH* = -0.49, *SHMT2* = -0.49, LDHA = -0.71; p_{adj} < 0.05; TGF-β + NAM vs TGF-β**). However, *PHGDH, PSAT1* and *PSPH* were still expressed above baseline levels following NAM treatment (**$\log_2$ fold change *PHGDH* = 0.63, *PSAT1* = 1.01, *PSPH* = 0.96; p_{adj} < 0.05; TGF-β + NAM vs vehicle**), as shown in **Figure 6.14**.

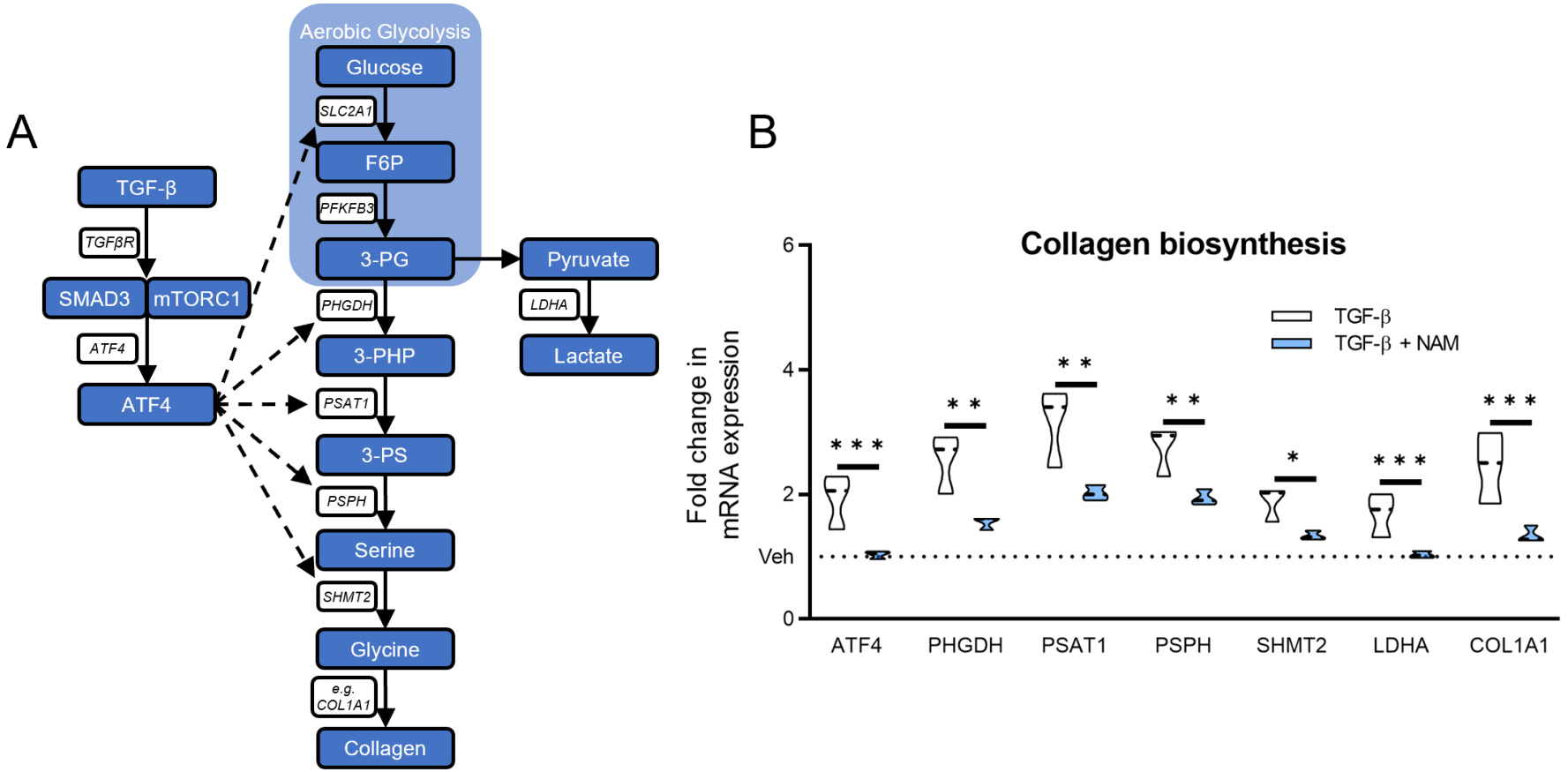

Figure 6.14. NAM treatment ameliorates the TGF-ß-induced serine-glycine pathway. (**A**) In activated (myo)fibroblasts TGF-ß supports the enhanced glycine demand required for collagen production by promoting the conversion of the glycolytic intermediate 3-phosphoglycerate (3-PG) to glycine via Smad3- and mTORC1-dependent increase in ATF4 and subsequent upregulation of serine-glycine pathway enzymes, including PHGDH, PSAT1, PSPH, and SHMT2. (**B**) NAM treatment significantly

reversed TGF-β-induced *ATF4, PHGDH, PSAT1, PSPH*, *SHMT2*, *LDHA* and *COL1A1* expression, when compared to TGF-β. All of these genes, except *PHGDH*, *PSAT1*, and *PSPH*, were indistinguishable from baseline levels following NAM treatment. A truncated violin plot was used to demonstrate frequency distribution of the data where the dashed line represents the median. Differentially expressed signalling pathways and remodelling processes were identified using gene ontology (GO) and further investigation was conducted with a gene-by-gene approach. Statistical significance identified using Deseq2 (Sartools) with Benjamini-Hochberg p-value adjustment. Upregulation compared to vehicle control (green); downregulation compared to vehicle control (red); significant difference between TGF-β alone and TGF-β + NAM treatment (**bold***). N = 3, n = 6, ns (p_{adj} > 0.05), * (p_{adj} < 0.05), ** (p_{adj} < 0.01), *** (p_{adj} < 0.001). TGF-β: Transforming growth factor beta 1; NAM: Negative allosteric modulator of the calcium-sensing receptor; GO: gene ontology; Smad3: Small mother against decapentaplegic 3; mTORC1: Mechanistic target of rapamycin complex 1; ATF4: Activating transcription factor 4; PHGDH: Phosphoglycerate dehydrogenase; PSAT1: Phosphoserine aminotransferase 1; PSPH: Phosphoserine phosphatase; SHMT2: Serine hydroxymethyltransferase 2; COL: collagen gene; F6P: Fructose 6-phosphate; 3-PG: 3-Phosphoglyceric acid; 3-PHP: 3-Phosphohydroxypyruvate; 3-PS: 3-Phosphoserine; LDHA: Lactate dehydrogenase A; PFKFB3: 6-Phosphofructo-2-kinase/fructose-2,6-biphosphatase 3.

To achieve increased proline production, TGF-β is thought to reprogramme metabolic pathways, via upregulation of *ALDH18A1*, to influence the conversion of glutamine-derived glutamate to pyrroline-5-carboxylate (P5C) and finally proline via the P5C reductases encoded by genes *PYCR1*, *PYCR2*, and *PYCR3* (Hamanaka et al., 2019; Phang et al., 2015). Here, TGF-β upregulated *ALDH18A1*, *PYCR1* and *PYCR2* indicating upregulation of proline synthesis (**$\log_2$ fold change *ALDH18A1* = 0.47, *PYCR1* = 0.90, *PYCR2* = 0.53; p_{adj} < 0.05; TGF-β vs vehicle**). NAM treatment had no effect on *ALDH18A1* or *PYCR1* expression but significantly reversed *PYCR2* expression (**p_{adj} = 0.0027; Log2FC = -0.58; TGF-β + NAM vs TGF-β**) to levels indistinguishable from baseline levels (**p_{adj} > 0.05; TGF-β + NAM vs vehicle**) suggesting NAM treatment attenuated TGF-β-induced proline synthesis.

In the presence of profibrotic stimuli, such as TGF-β, fibroblasts mature into a profibrotic contractile myofibroblast phenotype, which is marked by an increase in αSMA and SM22α expression (Hinz et al., 2007; Kato et al., 2020; Malmstrom et al., 2004; Misharin et al., 2018). TGF-β is also known to induce ECM remodelling in fibroblasts, marked by increased expression of ECM components, such as elastin and fibronectin. As shown in **Figure 6.13B**, TGF-β upregulated fibroblast maturation markers αSMA (*ACTA2*) and SM22α *(TAGLN)* as well as ECM components elastin (*ELN*) and fibronectin *)* (**log2 fold change *ACTA2* = 1.12, *ELN* = 1.92, *TAGLN* = 0.92, *FN1* = 1.18; p_{adj} < 0.05; TGF-β vs vehicle**). NAM treatment significantly downregulated *TGFB1, ACTA2, ELN* and *TAGLN* but not *FN1* (**$\log_2$ fold change *TGFB1* = -0.56, *ACTA2* = -0.93, *ELN* = -0.65, *TAGLN* = -0.80; p_{adj} < 0.05; TGF-β + NAM vs TGF-β; Figure 6.13B**). When compared to baseline expression, *ACTA2*, *TAGLN* and *FN1*, but not *ELN*, were indistinguishable from baseline levels following NAM treatment (**p_{adj} > 0.05; TGF-β + NAM vs vehicle**). As shown in **Figure 6.15**, αSMA protein expression was not significantly upregulated by TGF-β (**p_{adj} = 0.083**) when compared to vehicle; however, NAM treatment significantly downregulated αSMA protein expression (**p_{adj} = 0.014**) when compared to TGF-β. This suggests a possible limitation in my methodology, likely due to the dramatic proliferation induced by TGF-β that limited my ability to accurately determine cell boundaries due to overlapping cuboidal-shaped cells, opposed to non-overlapping spindle-like vehicle treated cells.

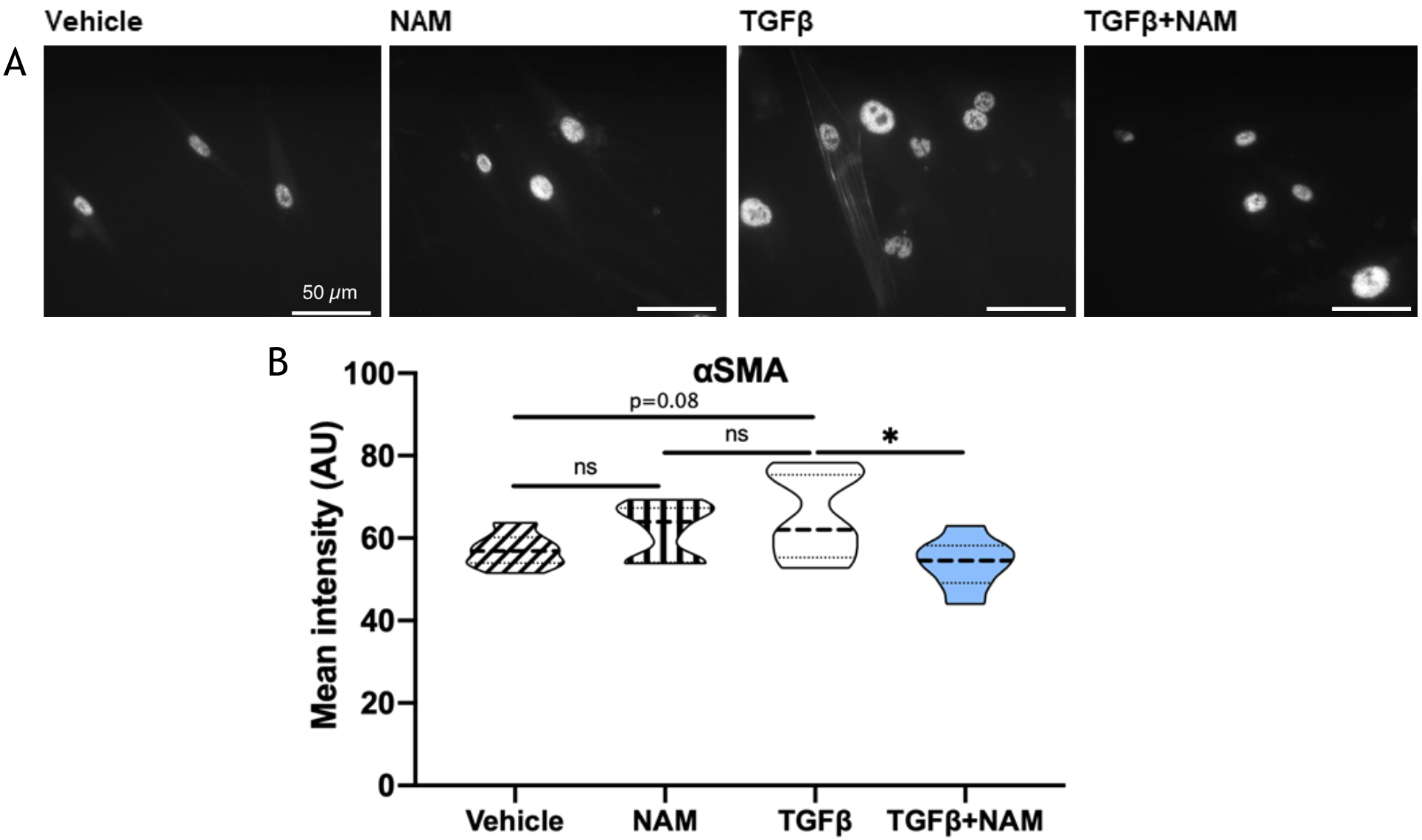
A
Vehicle
NAM
TGFβ
TGFβ+NAM
50 μm
B
αSMA
p=0.08
ns
ns
*
Mean intensity (AU)
100
80
60
40
20
0
Vehicle
NAM
TGFβ
TGFβ+NAM

Figure 6.15. NAM treatment significantly reduced αSMA immunoreactivity in NHLFs exposed to the remodelling mediator TGF-β. (**A**) Primary normal human lung fibroblasts (Lonza, UK) were treated with and without remodelling mediator TGF-β and/or treated with a NAM (NPS2143). αSMA was identified using the anti-αSMA antibody (ab5694; 1:300) and AlexaFluor488 (ab150077; 1:1000) secondary antibody. Quantification of mean intensity was achieved using StrataQuest and normalised to nuclear count (DAPI) as well as cell size. Truncated violin plot to demonstrate frequency distribution of the data where dashed lines represent the median and dotted lines represent the upper and lower quartiles, respectively. 63x objective, background subtracted using ImageJ ("separate colour"; 50.0 pixels). N = 3, n = 5. ns ($p_{adj} > 0.05$), * ($p_{adj} < 0.05$). Graticule (A) 50 µm. TGF-β: Transforming growth factor beta 1; NAM: Negative allosteric modulator of the calcium-sensing receptor; GO: gene ontology; AU: Arbitrary units; αSMA: Alpha smooth muscle actin.

matrix metalloproteinases (MMPs), and their inhibitors tissue inhibitors of metalloproteinases (TIMPs), are central to ECM turnover (Royce et al., 2012; Vitenberga & Pilmane, 2018). As shown in **Figure 6.13C**, TGF-β upregulated *MMP2*, *MMP14*, *TIMP1* and *TIMP3* but not *MMP1* or *TIMP2* indicating upregulation of ECM turnover by TGF-β (**$\log_2$ fold change *MMP2* = 0.82, *MMP14* = 0.64, *TIMP1* = 1.18, *TIMP3* = 0.95; p_{adj} < 0.05; TGF-β vs vehicle**). NAM treatment significantly reversed *MMP1*, *MMP2*, *MMP14*, *TIMP1*, *TIMP2* and *TIMP3* (**$\log_2$ fold change *MMP1* = -0.54, *MMP2* = -0.66, *MMP14* = -0.68, *TIMP1* = -0.97, *TIMP2* = -0.52, *TIMP3* = -0.53; p_{adj} < 0.05; TGF-β + NAM vs TGF-β**) to levels indistinguishable from baseline expression (**p_{adj} > 0.05; TGF-β + NAM vs vehicle**). This indicates NAM treatment ameliorated TGF-β-induced ECM turnover mechanisms in these cells.

6.3 Discussion

TGF-β is known to be a key mediator of age-, asthma- and COPD-related lung remodelling. The results of this study demonstrate that the CaSR is central to the TGF-β-induced upregulation of 1) CaSR expression, 2) RTK and GPCR signalling and 3) a range of cellular remodelling processes and pathways central to remodelling in the lung. Although further investigation is required to elucidate these mechanisms in other cell types, this study indicates the CaSR plays a central role in TGF-β signalling and key cellular remodelling processes in the lung such as loss of epithelial barrier integrity, secretion, growth, proliferation and ECM remodelling to elicit the protective effects observed in previous chapters of this thesis.

TGF-β and CaSR share remarkably similar signal transduction pathways. Physiologically, TGF-β and the CaSR act synergistically to regulate fetal lung development and tissue morphogenesis (Finney et al., 2008; Riccardi et al., 2013; Brennan et al., 2016; Chanda et al., 2019). Furthermore, bidirectional transactivation is well established in RTKs and GPCRs, including the TGF-βR (Burch et al., 2010; Little et al., 2010; Little et al., 2011; Dayati et al., 2018). Coupling of the CaSR with G_i and $G_{q/11}$ allows the CaSR to mediate the activation of ERK and JNK MAPK, PI3K/Akt, mTOR and RhoA pathways (Kifor et al., 2001; Pi et al., 2002; Hofer & Brown 2003; Tfelt-Hansen et al., 2003; Huang & Miller, 2007; Liu et al., 2016b; Rybchyn et al., 2019). The data generated in this study supports the hypothesis that

the CaSR plays a central role in transducing cellular remodelling signals, such as those induced by TGF-β.

TGF-β also activates canonical Wnt/β-catenin signalling which is critical for TGF-β-mediated (Akhmetshina et al., 2012) and age-related tissue remodelling (Hu et al., 2020a). This pathway has also been implicated in lung diseases, such as asthma and COPD (Heijink et al., 2016; Hussain et al., 2017; Shi et al., 2017). There is also considerable overlap between Wnt and CaSR signalling where previous studies, using CaSR knockout models, have suggested the CaSR is a central regulator of Wnt/β-catenin signalling that maintains the E-cadherin/β-catenin complex to prevent epithelial remodelling in other tissues (MacLeod, 2013; Singh et al., 2013: Aggarwal et al., 2015). The CaSR is thought to interact with Wnt signalling via $G_{12/13}$ to modulate β-catenin release from E-cadherins and RTKs, a suggested point of intersection between cAMP, RhoA and Wnt signalling (Conigrave & Ward, 2013).

G_i proteins also inhibit adenyl cyclase, an enzyme responsible for catalysing the conversion of adenosine triphosphate (ATP) to cAMP. cAMP is protective against ECM remodelling (Insel et al., 2012), profibrotic growth factor production (Black et al., 2007; Clancy et al., 2007), apoptosis (Huang et al., 2009), proliferation (Dunkern et al., 2007; Huang et al., 2008; Sandbo et al., 2009; Selige et al., 2010) and ECM remodelling (Liu et al., 2004; Liu et al., 2005; Sachs et al., 2007; Huang et al., 2008; Bauman et al., 2010; Liu et al., 2010b; Wójcik-Pszczoła et al., 2020). Furthermore, G_i has strong links to Ras signalling via the Grb2 adaptor protein (Kranenburg et al., 1997). Grb2 is an adaptor protein critical for interaction between the TGF-βR and Ras activation (Chardin et al., 1993; Zhang, 2017; Finnson et al., 2020), stimulation of MAPK activity via Src-family tyrosine kinases (Luttrell et al., 1996; Luttrell et al., 1997; Kifor et al., 2001) and PI3K recruitment (Haidar et al., 2015). G_i has also been linked with the activation of mixed lineage kinase 3 (MLK3) and subsequently JNK (Sun et al., 2019).

The CaSR also signals by augmenting Ca^{2+}_i (Chang et al., 1998; Brennan & Conigrave, 2009). Ca^{2+}_i augmentation is associated with mitochondrial dysfunction by breakdown of calcium homeostasis, ROS production and subsequent mitochondrial

swelling that induces cytochrome C-mediated apoptosis. This process has been linked to the loss of cell-cell adhesion that is crucial for epithelial barrier integrity (Ray et al., 2018). The CaSR has also been implicated in this process by other mechanisms, such as ERK-mediated tight junction protein dissociation (Ray et al., 2018; Aghapour et al., 2020) or disruption of the E-cadherin/ß-catenin complex by interaction with Wnt/ß-catenin signalling (Tian et al., 2011). Furthermore, the CaSR has previously been shown to regulate E-cadherin expression in a pancreatic beta cell line, MIN6 (Hills et al., 2012; Leach et al., 2020).

Mucociliary clearance is a crucial defence mechanism that is impaired in aging, asthma and COPD airways (Bonzer et al., 2016; Zhou-Suckow et al., 2017; Cho & Stout-Delgado, 2020). In airway epithelial cells, synchronisation of ciliary beat frequency is highly dependent on intracellular calcium (Salathe et al., 2001). Mitochondrial calcium uptake can negatively impact this process by reducing intracellular calcium availability, as demonstrated by acetylcholine-induced mitochondrial calcium uptake (Salathe et al., 2001). Furthermore, dysfunction of mitochondrial calcium homeostasis leads to ROS production, mitochondrial swelling and Cytochrome C-mediated apoptosis which enhances mucociliary dysfunction. This is demonstrated by the increased prevalence of swollen mitochondria in severe asthmatic airways and *in vivo* models of asthma (Mabalirajan et al., 2008; Thomas et al., 2010; Reddy, 2011; Schmid & Salathe, 2011; Ray et al., 2020).

TGF-ß and GPCR activation has previously been shown to mediate mucus secretion in the lung (Kim, 1997; Shale & Ionescu, 2004; Deshpande & Penn, 2006; Makinde et al., 2007; Lee et al., 2012b). The CaSR has also been implicated in this process in gastrointestinal epithelial cells, likely via G_q signalling (Rutten et al., 1999; Geibel & Hebert, 2009). Although this study could not clearly identify the effect of TGF-ß on secretion and exocytosis, the data generated from this study clearly indicates the CaSR is central to the regulation of this process. This provides a rationale to further investigate this mechanism in mucus producing cells.

TGF-ß is also a key mediator of age-, asthma-, COPD- and IPF-related ECM remodelling, where fibroblasts are the key effector cell type. In chapter 3, targeted

ablation of the CaSR from SM22α-positive cells reduced age-related peribronchial ECM remodelling. Schepelmann et al., (2016) hypothesised that the reduction in cardiac fibrosis, observed in the same animals used here, was due to a reduction in autophagy by inhibition of the CaMKKβ/AMPK/mTOR pathway. In this study, NAM treatment downregulated a number of ECM remodelling markers, including collagen expression, glycine and proline synthesis and autophagy; however, based on TGF-β-induced gene expression PI3K/Akt, rather than CaMKKβ, seems to be a more likely candidate for AMPK/mTOR activation. ERK signalling and autophagy have also been implicated in promoting senescence, a key mediator of remodelling, particularly ECM remodelling, in the aging lung (Slobodnyuk et al., 2019; Zou et al., 2019; Braicu et al., 2019). In this study, TGF-β-induced markers of senescence were attenuated by NAM treatment suggesting the CaSR mediates several key ECM remodelling-related processes.

6.4 Study Limitations

RNA-sequencing quantifies mRNA expression to provide insight into what influence NAM treatment was having on the regulation of TGF-β-induced mRNA transcription. Although differentially expressed mRNAs often correlate well with their protein product, particularly compared to non-differentially expressed mRNAs, it does not take into account the potential for post-transcriptional or post-translational modifications that would also modulate protein expression or activity (Koussounadis et al., 2015). Furthermore, altered expression of genes encoding signalling kinases does not confirm whether these proteins are phosphorylated, and thus activated, following TGF-β exposure. My findings should be confirmed using techniques that can determine protein phosphorylation, such as Western blotting.

Another key limitation is that this experiment was performed with normal human lung fibroblasts in isolation, without influence of a number of key regulatory systems present in the lung, such as inflammatory cells, matrikines or input from other resident cell types. Therefore, future studies should aim to recapitulate a more complete system to further investigate the role of the CaSR in remodelling mechanisms. Furthermore, exogenous TGF-β is not a real-world scenario, lung remodelling mediators are released in humans following injury or dysregulation of

physiological repair processes due to other environmental or genetic factors. However, this experiment provides key insight into how TGF-ß mediates remodelling via the CaSR as a basis for future experiments.

Although some appropriate cytoskeletal staining was observed using immunofluorescence in this experiment, nuclear staining of αSMA was also observed. Although Arora & McColloch (1994) previously described co-distribution of αSMA and G-actin in the perinuclear cytoskeleton of fibroblasts, it is unlikely that αSMA would be present surrounding, or potentially within, the nucleus in these cells. This suggests this could be the result of non-specific reactivity of the primary antibody due to similarities between the αSMA antigen and components of the nucleus which represents a major limitation in this experiment. Future studies could manipulate the StrataQuest algorithm to remove this nuclear staining; however, it is not possible to determine the extent to which the staining is non-specific. Therefore, an isotype control experiment could be used to determine whether this staining is non-specific. Furthermore, 3D imaging could identify the location of this staining within or around the nucleus. Following this a more suitable antibody should be identified and this experiment repeated to re-evaluate TGF-ß-induced αSMA expression following NAM treatment in these cells.

Lastly, due to the effect of TGF-ß on increased cell proliferation, 2-dimensional immunofluorescence imaging may not be the most appropriate technique for quantifying protein expression in this experiment. Increased cell confluency and overlapping cells limited the accuracy of individual cell barrier identification and lead to selection of cells in more sparsely populated areas of the slide. This is a key limitation of the approach and future studies should reduce the number of cells seeded into each well. This may have also had a dramatic effect on the comparability of TGF-ß exposed cells with cells that had not been treated with TGF-ß, such as the vehicle or NAM only treatment groups. This may be supported by the finding that TGF-ß induced a significant increased in αSMA expression compared to the TGF-ß + NAM group but not the vehicle or NAM only groups. In future, single cell flow cytometry may be a more appropriate method of determining protein expression in these cells using immunofluorescent protein staining.

6.5 Conclusion

In conclusion, this study has demonstrated that the CaSR plays a central role in TGF-ß-induced fibroblast apoptosis, differentiation, migration, growth, actin filament organisation, collagen biosynthesis, cell activation, aging, autophagy, proliferation which may provide insight into the mechanisms involved in other cell types. TGF-ß influences these processes by activating downstream signalling such as Ras, mTORC1, MTORC2, ERK, RhoA, JUN and Wnt signalling to regulate effector molecules such as MMPs, TIMPs, collagen, elastin, vascular endothelial growth factor B (VEGFB), secreted protein acidic and rich in cysteine (SPARC) and CTGF in a manner dependent on the CaSR. Here I have shown that inhibition of the CaSR, using a NAM, reverses non-canonical TGF-ß-signalling and mostly re-establishes baseline expression. Pharmacological ablation of the CaSR also influenced a shift from Wnt/ß-catenin signalling towards non-canonical Wnt/Ca^{2+} signalling as well as reduced G_i inhibition of the protective cAMP-producing enzyme adenyl cyclase. To my knowledge, this is the first evidence mechanistically linking TGF-ß and Wnt signalling with the extracellular cation sensing CaSR in the lung. This direct implication of the CaSR in processes of remodelling further supports the repurposing of NAMs as a treatment for the prevention of lung remodelling resulting from age-related fibrosis and diseases such as asthma as well as potentially COPD and IPF, where TGF-ß-induced fibrosis is a key pathophysiological characteristic. Furthermore, this study highlights the safety of NAMs having no adverse on-target effects on human lung fibroblast gene expression in the absence of TGF-ß.

6.6 Future Directions

The results of this chapter have identified a number of signalling pathways differentially regulated by TGFß and the CaSR; however, the regulation of mRNA expression does not demonstrate the true expression or activation of the proteins encoded by the mRNA analysed here. Western blotting could be used to determine the protein expression and phosphorylation status of the signalling molecules identified in this study to validate the hypothesis-driven inferences made in this study.

NAMs non-competitively reduce CaSR activation only in the presence of an orthosteric ligand. Although NAM treatment had a significant effect on the profibrotic fibroblast phenotype induced by TGF-β in this study, implying a reduction in CaSR activation, CaSR activation was not directly induced. Therefore, treatment with known CaSR agonists or calcimimetics could be used in a future study to confirm that CaSR activation is central to the TGF-β-induced changes observed in these cells. Although therapeutic benefits were presented in Chapter 5 of this thesis, fibroblasts were pre-treated with a NAM in this study. Future studies may benefit from a therapeutic treatment strategy to better mimic real world treatment of lung disease. In particular, investigating the ability of NAM treatment to reverse an established fibrotic ECM is of upmost relevance to the therapeutic potential of NAM treatment in patients with established lung remodelling or fibrosis.

Many of the processes of remodelling investigated in this study also apply to other cell types in the lung, such as epithelial, goblet and smooth muscle cells. Repeating this experiment using other cell types would help elucidate whether the role of the CaSR extends to other cell types involved in lung remodelling, such as epithelial cells and goblet cells. Lastly, to investigate the therapeutic potential of NAMs, cells isolated from patients with the remodelling lung diseases, such as IPF, could be used to identify differences in this mechanism where the underlying pathophysiology of the cells more completely replicates human disease, including predisposing environmental and genetic factors.

Lastly, the protein expression findings of this study could be validated using flow cytometry, a single cell immunofluorescent labelling technique, to avoid inaccuracies associated with fibroblast proliferation *in vitro* and eliminate the problems associated with overlapping cells in two-dimensional immunofluorescent imaging.

CHAPTER 7: GENERAL DISCUSSION

7.1 Advantages and limitations of the novel qHACC method

The evidence presented in this PhD thesis demonstrates that the novel quantitative histomorphometry of airway cross-section components (qHACC) methodology is capable of determining a range of airway remodelling characteristics, including epithelial thickening, goblet cell metaplasia and peribronchial ECM remodelling in models of immunoglobulin (Ig)E/T helper (Th)2 asthma and alarmin-driven asthma, the only models where vehicle control groups were present. Although epithelial-based measurements were consistent across both the larger and smaller airways, qHACC was only capable of determining peribronchial collagen remodelling in the smaller airways of these models.

The novel total (airway) tissue measurement also demonstrated that the airway as a whole consistently undergoes a net increase in tissue quantity in these models, which may have implications for future clinical and pre-clinical markers of lung remodelling. The qHACC approach did not successfully identify any smooth muscle thickening. Although short experimental duration was likely a key contributing factor, this suggests there are still some limitations to overcome in future studies (Li et al., 2015).

The evidence presented in this thesis also demonstrates that the quantitative histomorphometry of interstitial tissue (qHIT) approach is capable of detecting changes in interstitial tissue remodelling and/or inflammation in a range of models. However, further analyses or previously published findings, using more specific markers, were required to identify the cause of these changes and distinguish remodelling from a change in inflammatory cell infiltration. Although this method has potential for further development, sophisticated image analysis software, such as StrataQuest, will be required at the cost of open-source accessibility. Once this method has been further developed I recommend the alveolar interstitium of the alarmin-driven asthma model be reanalysed to determine whether negative allosteric modulation of the calcium-sensing receptor (NAM) reduced interstitial tissue remodelling, inflammation or both characteristics in these animals.

These methodologies were required to address the current resource-demand limitations of image analysis in the lung. Several lung remodelling markers are often required to effectively represent the state of remodelling in the lung, particularly in the ECM due to the large number of functional components (Asgari et al., 2017; Liu et al., 2021). However, the tools did not exist to effectively investigate them without increasing the resource demand of a single experiment exponentially (i.e. iterations of staining, microscopy and manual airway component identification). Adaptation of the conventional Masson's trichrome stain, using aniline blue, proved to be a consistent and reliable method of identifying goblet cell remodelling in conjunction with markers of tissue and ECM remodelling while dramatically reducing resource demands. Further innovations of this kind will allow researchers to redistribute resources and move towards a greater diversity of lung remodelling markers. For example, additional histological or immunohistochemical stains could be used to investigate a greater portion of the ~300 components of the ECM that may undergo remodelling in the lung (Asgari et al., 2017; Liu et al., 2021).

Other innovations could be attempted, such as the use of machine learning to alleviate the researcher-dependence during the time-consuming airway component identification phase of the qHACC analysis. Unfortunately, this could not be completed within the timeframe of my PhD. Nevertheless, innovations to permit the redistribution of resources is an important step towards incorporation of 1) more specific and diverse approaches to determining changes in lung remodelling markers and 2) better representation of the localisation of lung remodelling using a larger number of images or lung regions.

Together, the evidence generated in this thesis suggests the qHACC and qHIT approaches are key methodological tools for investigating the mechanisms that underpin lung remodelling across the three main compartments of the lung, including the larger airways, smaller airways and alveolar interstitium. Although they begin to address current limitations, these approaches should be further developed to redistribute more resources towards remaining methodological obstacles.

7.2 Evidence supporting a role for the CaSR in regulation of smaller airway goblet cell metaplasia

The evidence presented in this thesis, as summarised in **Table 7.1**, demonstrates that the calcium-sensing receptor (CaSR) is a mediator of goblet cell and extracellular matrix (ECM) remodelling. These findings are novel and further elucidate the role of the CaSR in the lung as a local environment sensor and regulator of lung remodelling. It also demonstrates that NAMs may be suitable for treating lung diseases where remodelling is a key characteristic.

Table 7.1. Summary of the effect of genetic or pharmacological ablation of the CaSR on lung remodelling in the larger airways, smaller airways and alveolar interstitium. Changes in airway remodelling, including total tissue, epithelial tissue, goblet cells and peribronchial collagen, using qHACC and interstitial remodelling using Fiji image analysis software is summarised below following pharmacological or genetic ablation of the CaSR using data presented in Chapters 3-5. Statistical comparison compared to positive control (inhaled challenge or aged wild-type mice) by one-way ANOVA with Holm-Sidak *post-hoc* test or Kruskal-Wallis with Dunn's post-hoc, where appropriate. Columns and rows containing non-statistically significant or relevant results, or where no changes were determined compared to vehicle controls, have been removed for clarity. N = 4-12, n = 3, ROI = 1-15, * ($p < 0.05$), ** ($p < 0.01$).

Model	Alarmin-driven asthma	COPD	Aging	Shorter-term IgE/Th2 asthma	Longer-term IgE/Th2 asthma	Alarmin-driven asthma
Region	Larger airways	Smaller airways				
Total tissue	*p=0.053*	*p=0.08*		*		
Epithelial tissue		*p=0.054*		*p=0.06*		
Goblet cells		*p=0.08*		*	*	*p=0.06*
Peribronchial collagen			*	*		

Model	COPD	Aging	Alarmin-driven asthma
Region	Alveolar interstitium		
Interstitial remodelling and inflammation	*	**	*
Interstitial wall thickening	*		
Fibrosis (Ashcroft score)		*	

Goblet cell remodelling is a characteristic of asthma, COPD and idiopathic pulmonary fibrosis (IPF) (Bergeron et al., 2010; Brandsma et al., 2017; Knudsen et al., 2017; Rose et al., 2018). Mucociliary clearance is also impaired in the aging lung (Quirk et al., 2016; Godin et al., 2016). Transdifferentiation of ciliated to mucus-producing goblet cells is thought to be the primary mechanism of goblet cell remodelling in the human lung (Tyner et al., 2006). Transdifferentiation of Clara cells is also the primary mechanism underpinning goblet cell metaplasia in rodent and guinea pig lungs (Boucherat et al., 2013). This is thought to be triggered by inflammatory mediators and growth factors, such as IL-4, IL-13, epidermal growth factor (EGF) and tumour necrosis factor alpha (TNFα), that subsequently activate signalling pathways such as STAT6, EGFR/ERK, PI3K/Akt/mTOR, Wnt/ß-catenin and NFκB signalling (Gagliardo et al., 2003; Chen et al., 2003; Broide et al., 2005; Lora et al., 2005; Mushaben et al., 2011; Boucherat et al., 2013; Hussain et al., 2017; Ma et al., 2021; Xu et al., 2023).

In this thesis, goblet cell remodelling was abolished using inhaled NAM treatment in the smaller airways of the shorter- and longer-term IgE/Th2 asthma models. This suggests the CaSR plays a central role in the development of goblet cell metaplasia; however, the mechanism by which this occurs is not clear. The CaSR has been previously shown to regulate hypoxia-induced mucin production in human bronchial epithelial cells, a marker of goblet cell phenotype, as well as key cell differentiation processes in other cell types via ERK, PI3K/Akt/mTOR, Wnt/ß-catenin and NFκB signalling (Chapter 6; Conte et al., 2011; Aggarwal et al., 2015; Tharmalingam & Hampson, 2016). There is also scope for the CaSR to regulate STAT6 indirectly via Rho signalling (Xie et al., 2015).

There is also evidence to suggest the local microenvironment in the lung is primed for CaSR activation. For example, in other similar IgE/Th2 asthma models, allergen challenge upregulates IL-4, IL-5 and IL-13 (Kumar et al., 2008; Li et al., 2015; Yarova et al., 2015). Although IL-4 and IL-13 are not considered direct CaSR-agonists, IL-13 has been shown to upregulate arginase I and subsequently increase the production of CaSR-activating polyamines via the arginase pathway as well as upregulate CaSR expression in the lung (Hesse et al., 2001; Zimmermann et al., 2003; Wills-Karp,

2004; Yarova et al., 2015). Furthermore, a positive feedback loop exists in models of IgE/Th2 asthma to maintain this microenvironment by upregulation IL-13, TNFα and CaSR-activating eosinophilic cationic protein (ECP) in a CaSR-dependent manner (Yarova et al., 2015).

Contrastingly, NAM treatment did not prevent goblet cell metaplasia in the model of COPD-like neutrophilic exacerbation or alarmin-driven asthma suggesting a CaSR-independent mechanism may exist in these models. However, the only evidence that supports this is the increase in goblet cell remodelling cytokines IL-5 and IL-25 in the alarmin-driven asthma model where no clear link to the CaSR exists (Justice et al., 2002; Grubek-Jaworska et al., 2012; Li et al., 2015; Yarova et al., 2015; Li et al., 2020). All other differentially expressed cytokines were comparable between the IgE/Th2 and alarmin-driven asthma models (Justice et al., 2002; Li et al., 2015; Yarova et al., 2015).

The inflammatory cytokine profile in the COPD-like neutrophilic exacerbation model is also consistent with increased CaSR expression or activation which should support the existence of a CaSR-dependent mechanism in these models. For example, similar albeit longer-term models of LPS-induced COPD exhibit increased expression of cytokines associated with increased CaSR expression, such as IL-1β, IL-6, IL-8 and TNFα (Canaff & Hendy, 2005; Pera, 2011; Fetahu et al., 2014; Yarova et al., 2015; Hendy & Canaff, 2016). Although there is scope for IL-5 and IL-25 to mediate CaSR-independent goblet cell metaplasia, it remains possible that limitations in my methodology influenced this result. Further investigations into the role of the CaSR in mechanisms of goblet cell metaplasia beyond IgE/Th2 asthma are therefore recommended. Together, the evidence produced in this thesis suggests the CaSR plays a central role in goblet cell remodelling in models of IgE/Th2 asthma and that NAM treatment should be further investigated as a novel therapeutic strategy for preventing goblet cell metaplasia and mucus dysfunction.

7.3 Evidence supporting a role for the CaSR in regulation of lung ECM remodelling

The evidence presented in **Table 7.1** also demonstrates that, in the smaller airways, the CaSR plays a central role in peribronchial ECM remodelling in the aging lung and IgE/Th2 asthma. This was demonstrated using genetic or pharmacological ablation of the CaSR *in vivo* and *in vitro* and identified that the CaSR is central to physiological and pathophysiological models of ECM remodelling. This likely occurs via interaction of the CaSR with signalling pathways already implicated in lung remodelling, such as the TGF-β pathway. Here I also demonstrated that TGF-β upregulates CaSR expression.

Remodelling mediators, such as IL-6, IL-13, TNFα and TGF-β, are thought to drive peribronchial and interstitial ECM remodelling in the aging and diseased lung. To do this, the activate cell surface receptor and subsequently signalling pathways such as Ras, mTOR, ERK, Rho, JUN and Wnt/β-catenin. These pathways regulate a plethora of effector molecules, including matrix metalloproteinases (MMPs) and tissue inhibitors of metalloproteinases (TIMPs), as well as cellular processes such as fibroblast proliferation, growth, nutrient uptake, metabolic reprogramming, senescence, apoptosis and ECM component production to mediate ECM remodelling (Crosby & Waters, 2010; Milara et al., 2010; Bergeron et al., 2010; Chang et al., 2014; Pardo et al., 2016; Meyer et al., 2016; Baker et al., 2016; Papageorgis, 2017; Zhang et al., 2017; Vitenberga & Pilmane, 2018; Hudgins et al., 2018; Platé et al., 2020).

The evidence generated in this thesis demonstrates a CaSR-dependent mechanistic link between age- and IgE/Th2 asthma-related ECM remodelling. Furthermore, I have demonstrated how central remodelling mediators, such as TGF-β, require the CaSR to regulate key cellular signalling and remodelling processes in key cell types. IL-13, TNFα and TGF-β are upregulated in humans and the animal models of ECM remodelling used here and have been shown to contribute to a lung microenvironment primed for CaSR activation (Li et al., 2011; Morimoto et al., 2011; Vitenberga & Pilmane, 2018; Hudgins et al., 2018; Wolffs, 2022; Chapter 6). Therefore, this evidence suggests the CaSR is a central mediator of ECM remodelling

in the lung. This theory is also supported by evidence that asthmatic lungs exhibit increased CaSR expression and rare genetic variants affecting CaSR function (Yarova et al., 2015; Carey et al., 2016; Dershem et al., 2020; Riccardi et al., 2022).

NAM treatment also seemed to exhibit localised effects. Peribronchial ECM remodelling was not affected by NAM treatment in the model of COPD-like neutrophilic exacerbation or the larger airways of the IgE/Th2 asthma models. Ablation of the CaSR also had differential effects on interstitial remodelling in COPD-like neutrophilic exacerbation, where it reduced interstitial wall thickening, opposed to a reduction in fibrosis in age-related fibrosis (Yarova et al., 2016). This phenomenon may be explained by the proposed role of the CaSR in lung edema, via regulation of fluid secretion, which is known to be induced in this model (Toward & Broadley, 2001; Lazrak et al., 2023). However, it is also possible that the localisation of CaSR-mediated effects were influenced by limitations in my methodologies, such as the restricted numbers of comparable larger airways that were suitable for analysis. Therefore, further investigations are required to determine whether CaSR-dependent and CaSR-independent mechanisms exist in ECM remodelling in the lung.

7.4 Implications for the physiological and pathological role of the CaSR in the lung

The concept that CaSR mediates lung repair and tissue remodelling is further supported by its central role in the regulation of branching pattern and tissue morphogenesis during fetal lung development (Brennan et al., 2016). The CaSR also utilises PLC and ERK signalling to regulate non-calcitropic processes such as wound repair in human bronchial epithelial cells and keratinocytes, a process dependent on ECM remodelling for regulation and structural support (Crosby & Waters, 2010; Milara et al., 2010; Oda et al., 2017; Tu et al., 2019). Together this evidence suggests that the physiological role of the CaSR is not limited to calcium ion homeostasis and plays a central regulatory role in normal repair and remodelling processes.

Dysregulated, uncontrolled or maladaptive defence and repair mechanisms can also lead to pathological outcomes, such as tissue fibrosis (Wynn & Vannella, 2016).

Recent evidence suggests the CaSR is a central mediator of inflammatory cell infiltration, cytokine production and airway hyperresponsiveness in pre-clinical models of asthma and human cells (Yarova et al., 2015; Yarova et al., 2021). Inflammation in the lung is a key defence process that leads to pathological outcomes when unknown mechanisms prevent it from resolving. Exogenous inflammation-inducing factors that have been linked to the pathogenesis of chronic lung diseases, such as viral infection and air pollution, have also been linked to CaSR activation in the lung (Bachrach, 1970; McCann, 1987; Yarova et al., 2015; Singh & Singh, 2021; Mansfield, 2022).

Whether the CaSR mediates lung remodelling in a physiological or pathological manner, the potential of NAM treatment to target key features of lung disease is multi-faceted. However, the reason the CaSR can potentially target multiple features of lung disease is due to its ubiquitous expression. Targeting such a central physiological component could have unwanted consequences on physiology, such as impairment of systemic calcium homeostasis and parathyroid hormone regulation. However, studies have previously monitored the systemic effects of inhaled NAM treatment and found that systemic calcium homeostasis was unaffected (Yarova et al., 2016; Yarova et al., 2021). This suggests that NAM inhalation is a suitable delivery method that has no measurable unwanted on-target effects on systemic calcium ion homeostasis or parathyroid hormone regulation. Furthermore, NAMs offer several advantages as therapeutics to modulate CaSR function in the lung. All NAMs are non-competitive, meaning they lower the ligand binding affinity at the orthosteric site to ensure only physiological responses are inhibited. NAMs also require the presence of an orthosteric ligand to bind to the receptor, meaning they evoke no effect at minimal ligand concentrations (Christopoulos & Kenakin, 2002; Ward & Riccardi, 2012). In other words, these compounds are ineffective unless extracellular cation concentrations rise in a pathological manner. Under these circumstances alone NAMs will elicit a concentration-dependent effect, dampening the hypothesised mechanisms that drive remodelling in the lung.

7.5 Implications for the translation of these findings to human scenarios

Animal models are key tools for researchers to investigate mechanisms that relate to human scenarios; however, animal models, particularly temporal factors in rodent and guinea pig models, are not always complete representations of human scenarios. The experimental duration used in the model of COPD-like neutrophilic exacerbation (18 days) actually mimics acute exacerbation of COPD relatively effectively, which ranges from 4 to 15 days in duration in humans (Toward & Broadley, 2001; Toward & Broadley, 2002; Miravitlles et al., 2013; Yarova et al., 2016). Although evidence suggests the underlying pathophysiology of COPD is present long before symptoms are exhibited, COPD then develops progressively over a long time period which is not well represented by the animal models used here (Celli et al., 2003; De Marco et al., 2004). However, for logistical and biological reasons, animals cannot be used to model the time-dependent factors underpinning severe or long-term COPD (Wright et al., 2008; Vlahos & Bozinovski, 2014; Tanner & Single, 2020). These differences must therefore be accounted for when drawing conclusions from relatively short-term models of COPD.

The model of age-related fibrosis used in this thesis also has limitations regarding its representation of human scenarios. Age-related fibrosis developed over a timeframe of 15 months which, while short compared to advanced human age, is a considerable portion of the animals 24 month lifespan. The inflammatory cytokine profile in the lungs of aging C57Bl/6 mice also mimics human inflamm-aging relatively effectively. Here, expression of IL-1ß, IL-6, IL-13, TNFα and TGF-ß has been shown to be upregulated (Li et al., 2011; Morimoto et al., 2011; Vitenberga & Pilmane, 2018; Hudgins et al., 2018). Furthermore, decreased elastin content, increased type I and III collagen as well as age-related ECM alterations, called advanced glycation end products (AGEs), are also a feature of both the elderly human lung and lungs from 15-month-old C57Bl/6 mice (D'Errico et al., 1989; Huang et al., 2007; Sueblinvong et al., 2012; Rolewska et al., 2013; Roman, 2014). Although the inflammatory cell, cytokine and ECM profile is more complex than stated above, this model of age-related fibrosis encapsulates several key features of the aging human lung with links to altered CaSR function.

The duration of the IgE/Th2 and alarmin-driven asthma models is also considerably shorter than human disease; however, some studies suggest remodelling of the epithelial-mesenchymal trophic unit in children is actually an early event in the aetiology of asthma, termed pre-modelling (Fedorov et al., 2005; Boxall et al., 2006). There is also evidence to suggest temporal factors are central to the severity of asthmatic lung remodelling, such as the rate by which inflammation resolves (Chernyavsky et al., 2014). Although based on a mathematical model, this study suggests even a series of mild exacerbation events can result in significant lung remodelling. This is further supported by observations of rapid-onset angiogenesis in the asthmatic lung that is slow to resolve (Walter et al., 2008). Although these animals lack the underlying pathophysiology of asthma, and do not naturally develop asthma, the models used in these experiments also exhibit key features of asthmatic lung remodelling that are relevant to human remodelling processes.

Although these models represent key features of human disease, it is important to establish these effects in human scenarios, such as primary human cells, to further elucidate the mechanisms of remodelling in the human lung. For example, humans possess a substantially different bronchial Clara cell population compared to rodents, therefore, the role of the CaSR in regulation of goblet cell remodelling, via transdifferentiation of Clara cells, must be further investigated in human cells (Kling, 2011; Boucherat et al., 2013). The ECM remodelling findings have been confirmed in human cells exposed to the remodelling mediator TGF-ß.

Lastly, systemic NAM treatment was described as safe and well tolerated in phase I and II clinical trials for treatment of osteoporosis (Kumar et al., 2010; Caltabiano et al., 2013; Halse et al., 2014; John et al., 2014). The evidence presented in this thesis also supports the safety of NAM treatment *in vivo* in a range of animal models and *in vitro* using cultured human fibroblasts. For example, NAM treatment did not induce cytotoxicity in human lung fibroblasts and in the absence of TGF-ß, and theoretically the absence of CaSR ligand, NAM altered the expression of 0 genes (**Figure S9.4**). There were also no confirmed negative effects of NAM treatment *in vivo* in these studies.

7.6 Limitations

The primary limitation in this thesis is that genetic or pharmacological ablation of the CaSR was used to demonstrate the effect of reduced CaSR activity, implying a reduction in CaSR activation; however, CaSR activation was not directly induced in any of these experiments. Therefore, it is not clear if CaSR activation drives these changes in the lung. This represents a key limitation in my studies and future experiments should investigate the effect of direct CaSR activation on remodelling, with particular attention to ligand-biased effects.

In Chapter 3 and 4, no negative control tissues were available to determine the baseline level of remodelling induced by LPS challenge or aging. Therefore, in the event of a non-significant effect it was not possible to distinguish between 1) no remodelling was induced in that model or 2) CaSR ablation had no effect on remodelling in that model. Future studies always require a negative control to determine a baseline for remodelling and represents a major limitation in this thesis. This information is also important to determine the effectiveness of the novel qHACC and qHIT methodologies. However, as performed by Ellis et al. (2003), future studies should aim to investigate the sensitivity and efficacy of the qHACC approach using a more complete approach, preferably using tissue from previous experiments.

Although resolution of lung fibrosis has been observed in humans and animals the remodelling observed in asthma, COPD and IPF is considered irreversible due to the lack of effective therapeutics (Mittermayer et al., 1978; Degryse & Lawson, 2011; Skeoch et al., 2018; Atabai et al., 2020; Terbuch et al., 2020; Zhang et al., 2020; George et al., 2020; Yu & Tang, 2022). However, the therapeutic treatment strategy and single time-point of analysis was not well designed to investigate the potential of NAM treatment to reverse ECM remodelling. In the model of IgE/Th2 asthma, therapeutic NAM treatment reduced peribronchial ECM remodelling after 6 days; however, it is not clear whether 1) ECM remodelling was induced after the first day and returned to baseline levels by NAM or whether 2) NAM treatment prevented further remodelling after day 1. The lack of efficacy in longer-term IgE/Th2 asthma model suggests NAMs do not reverse remodelling; however, evidence from human lung fibroblasts studies suggests it may be possible, due to regulation of MMP and

TIMP levels, for example. Future studies should aim to determine whether NAM treatment has the potential to reverse remodelling in the lung as this is a key unmet medical need. This could be investigated using NAM treatment in models where spontaneous fibrotic resolution does not occur, such as bleomycin-induced fibrosis in young or old mice (Yu & Tang, 2022).

The remodelling markers used to determine lung remodelling *in vivo* also lacked specificity in order to maximise the markers included in each analysis, such as the pan-mucus and pan-collagen stain aniline blue. However, particularly for ECM remodelling, not all components of remodelling are affected in the same way. For example, elastin can be down-regulated as a result of ECM remodelling resulting in a loss of ECM elasticity and the ratio of collagen subtypes (e.g. I, III and IV), fibronectin, tenascin and laminin, can affect ECM stiffness (Liu et al., 2021; Ramis et al., 2022). Therefore, not knowing exactly which components of remodelling were affected by ablation of the CaSR limits the understanding of its role in lung remodelling. Future studies should incorporate more specific markers of remodelling to further investigate the role of the CaSR in lung remodelling.

Finally, as discussed above, the models of lung remodelling used in these experiments demonstrate a reasonable degree of relevance to human scenarios. Furthermore, animal models are the key pre-clinical tool for investigating mechanisms of lung remodelling because they offer a homogenous aetiology; accelerated lifespan; similar lung physiology and gene expression to humans; and a comparable immune system (Takahashi et al., 2007; Alessandrini et al., 2020; Bates et al., 2009; Bates, 2017). However, there are also important dissimilarities between animal and human lung physiology. Rodents are obligate nasal breathers with dissimilar airway branching patterns, lobe structure, and proportionally larger airways (Kling, 2011). Although guinea pig lungs most closely resemble the human lung compared to other small animal species, the Clara cell, serous cell and submucous gland populations are different (Brewer and Cruise, 1997; Canning & Chou, 2008; Hargaden & Singer, 2012).

Mice also demonstrate physiological differences such as a high respiratory rate to accommodate their metabolism and an increased rate of reactive oxygen species production (Rydell-Törmänen & Johnson 2019). There are also differences in cellular composition, such as an altered epithelial Clara cell, club cell and submucosal gland population (Kling, 2011; Danopoulos et al., 2019). Furthermore, the progenitor and smooth muscle cell population display different transcriptomic profiles, where a total of 348 unique genes were observed in human lung tips compared to mice (Danopoulos et al., 2018; Danopoulos et al., 2019). Due to these differences, the role of the CaSR in lung remodelling may differ in humans.

In vitro studies using human cells are therefore important to provide physiological and genetic aetiological similarities to human scenarios; however, *in vitro* studies lack a range of important physiological systems in the lung, such as the immune system and resident cell type diversity and function. Although these approaches are important tools for pre-clinical investigations, their relevance should not be overstated in human scenarios. These approaches, in addition to novel approaches, such as a human lung-on-a-chip, may provide the necessary tools to further investigate these hypotheses in the future (Shrestha et al., 2020).

7.7 Conclusion

The key findings presented in this thesis are: 1) qHACC and qHIT are key tools for researchers to investigate mechanisms of lung remodelling; 2) the CaSR plays a central role on IgE/Th2 asthma-mediated goblet cell remodelling; 3) the CaSR plays a central role in age- or IgE/Th2 asthma-related ECM remodelling, via CaSR-dependent facilitation of TGF-β-induced signalling and cellular remodelling processes; and 4) inhaled NAM treatment represents a potential novel therapeutic strategy for preventing lung remodelling, in addition to previously described effects on inflammation and airway hyperresponsiveness.

7.8 Future Directions

7.8.1 Elaborate on the qHACC and qHIT methodologies using specific markers and machine learning

Image analysis is an effective tool for determining lung remodelling; however, this thesis highlighted that there are still some limitations to over come. Most notably, negative control treatment groups are always required to determine whether changes in remodelling have been induced and an increased sample size is required to identify a suitable number of larger airways for analysis. However, the field is also moving towards more specified markers of lung remodelling. For example, specific subtypes of collagen are dysregulated in the aging lung, including collagen IV, VI, XIV, XVI (Onursal et al., 2021). Furthermore, collagen I, collagen III and decorin expression as well as fibrillar collagen I packaging is dysregulated in the asthmatic ECM (Ito et al., 2019; Mostaço-Guidolin et al., 2019). Imaging techniques are emerging that are capable of determining these specific pathological changes in the ECM using biochemical and structural properties of fibrillar collagen and elastin, rather than histological staining, that could be incorporated into the qHACC approach (Mostaço-Guidolin et al., 2019).

Lastly, some aspects still require time-consuming manual identification steps. Machine learning and central neural networks are well suited to image analysis and could be utilised to determine remodelling markers in an experimenter-independent manner. This will also have added benefits of reducing experimenter bias and permit higher-throughput image analysis techniques. Furthermore, alternative statistical approaches could be considered, such as regression analyses, to try and improve how airway samples represent the localisation and multidimensional effects associated with remodelling in the whole lung.

The qHIT approach should also be further developed in StrataQuest to allow the distinction of more specific remodelling markers and exclusion of unwanted inflammatory cells in the alveolar interstitium. This approach could also be adapted to incorporate measurements similar to mean linear intercept to investigate emphysematous remodelling in models of COPD in an experimenter-independent

manner. These improvements could then be used to reanalyse lung sections from the models used in these experiments using a more specified approach.

7.8.2 Further investigate the role of the CaSR in goblet cell remodelling, mucus production and mucociliary dysfunction

The evidence generated in this thesis suggests the CaSR plays a central role in goblet cell metaplasia in pre-clinical mouse models of IgE/Th2 asthma. However, there are a number of goblet cell remodelling mechanisms, such as mucus overproduction and hypersecretion that have been under investigated. There is some evidence to suggest the role of the CaSR extends to mucus production, hypersecretion and mucociliary clearance in the lung. For example, the CaSR has previously been shown to regulate hypoxia-induced mucin production in human bronchial epithelial cells (Yang et al., 2014a; Yang et al., 2014b). The CaSR also regulated secretion (via exocytosis) in lung fibroblasts exposed to TGF-ß which may extend to other cells types. This hypothesis is supported by the previously described role of the CaSR in secretion in other cell types, such as neocortical neurons, pancreatic beta cells and the parathyroid gland (Squires et al., 2000; Vyleta & Smith, 2011; Riccardi & Valenti, 2016).

Chronic bronchitis and asthma also dehydrates and thickens mucus to impair mucociliary clearance, potentially via dysregulation of anion secretion (van Heusden et al., 2021; Bennett et al., 2021; Lazrak et al., 2023). The CaSR has been shown to regulate anion secretion and fluid secretion in fetal lung development as well as colon enterocytes (Cheng et al., 2002; Brennan et al., 2016; Tang et al., 2016). Furthermore, extracellular calcium has been shown to regulate cilia beat frequency which was hypothesised to occur via the CaSR (Woodworth et al., 2010).

The role of the CaSR in goblet cell metaplasia, mucus production and mucociliary clearance could therefore be investigated in models of IgE/Th2 asthma using human cells *in vitro*. Following ovalbumin challenge or specific mediators of IgE/Th2 asthma goblet cell remodelling, human bronchial epithelial cells in air-liquid-interface could be analysed using immunofluorescence or western blotting to determine the protein expression of signalling molecules, goblet cell transdifferentiation markers, mucin

expression and vesicle exocytosis components to elucidate the role of the CaSR in these mechanisms (Ghio et al., 2013). Furthermore, in the same cells mucociliary clearance and airway mucus hydration can be assessed using a combination of the fluorescence micro-bead clearance assay and airway surface liquid diameter, respectively (Ostrowski et al., 2010; Button et al., 2013; van Heusden et al., 2021). Lastly, cilia beat frequency could be investigated using high-speed (100 frames per second) digital video analysis at an objective magnification of 63x (Woodworth et al., 2010; van Heusden et al., 2021).

7.8.3 Investigating the potential of NAM treatment to reverse CaSR-mediated ECM remodelling with comparison to current standard-of-care

The findings presented in Chapter 4, 5 and 6 and other studies demonstrate the CaSR is central to the regulation of ECM remodelling processes in mouse lungs and human lung fibroblasts (Wolffs et al., 2022). However, it is unclear how the functional composition of ECM is regulated by the CaSR and whether or not inhibition of the CaSR using NAM treatment has the potential to reverse established ECM remodelling. To do this, the shorter-term IgE/Th2 asthma model could be reanalysed using qHACC to characterise the expression of more specific ECM components, such as collagen subtypes I and III, elastin and fibronectin, the ratios of which dramatically affect ECM stiffness and subsequently ECM remodelling (Liu et al., 2021; Ramis et al., 2022). It would also be interesting to determine the effect of pharmacological or genetic ablation of the CaSR, compared to the current standards of care, pirfenidone or nintedanib, in a bleomycin-induced model of lung fibrosis, the current industry standard for investigating mechanisms of lung fibrosis. Lastly, to investigate the time-dependent factors of whether NAM treatment can reverse ECM remodelling could be investigated *in vitro* using human lung fibroblasts suspended in a hydrogel to better mimic the functional architecture of the lung (de Hilster et al., 2020).

7.8.4 Primary cells from diseased patients will permit further investigation of the role of the CaSR in pathology

Although the mechanism by which the CaSR drives goblet cell and ECM remodelling in the lung is emerging, pathological outcomes do not occur in all subjects exposed to exogenous allergens or pollutants. Genetic factors are also implicated in these

diseases, such as the CFTR, GPR183 and CaSR variants implicated asthma (El-Husseini et al., 2020; Riccardi et al., 2022; Koumpagioti et al., 2023; Dershem et al., 2023). Furthermore, the concentration of exogenous TGF-β used in these *in vitro* experiments could be argued as a more physiological, than pathological, concentration; however, the evidence for this is not clear and largely anecdotal (Kotecha et al., 1996). Due to these factors, it is important to investigate the role of the CaSR in more complete models of human pathology, such as primary cells isolated from diseased patients, to further investigate the role of the CaSR in pathology. Furthermore, although the use of NAM treatment denotes inhibition of CaSR activation in these experiments in a specific and non-competitive manner, the CaSR has not been directly activated and, due to ligand-biased signalling, may not behave the same way to different endogenous or exogenous agonists (Christopoulos & Kenakin, 2002; Ward & Riccardi, 2012). Therefore, future studies should investigate this concept using a range of known CaSR-agonists to identify the role of CaSR activation as well as any ligand-biased effects on lung remodelling.

7.9 Closing remarks

The evidence presented in this thesis supports the hypothesis that the extracellular environment in the lung is conducive for CaSR activation due to 1) ubiquitous CaSR expression; 2) increased levels of CaSR expression-regulating cytokines and growth factors; and 3) increased endogenous (inflammation and injury) and exogenous (air pollution) CaSR-activating polycations. This environment may chronically and aberrantly mimic developmental conditions where extracellular Ca^{2+} concentrations are high as well as conditions promoting lung repair, where calcium is emerging as a key messenger molecule. The findings presented in this thesis suggest that key mechanisms of remodelling rely on the same cell surface GPCR for regulation, providing a novel therapeutic target for preventing lung remodelling using existing therapeutic compounds. This is in addition to the previously described effects of NAM treatment on inflammation and airway hyperresponsiveness in the lung.

CHAPTER 8: REFERENCES

Abdulnour-Nakhoul, S., Brown, K.L., Rabon, E.C., Al-Tawil, Y., Islam, M.T., Schmieg, J.J. and Nakhoul, N.L., (2015). Cytoskeletal changes induced by allosteric modulators of calcium-sensing receptor in esophageal epithelial cells. *Physiological Reports*, 3(11), pp. 1–20.

Adriaensen, D., Brouns, I., Pintelon, I., De Proost, I. and Timmermans, J.P., (2006). Evidence for a role of neuroepithelial bodies as complex airway sensors: comparison with smooth muscle-associated airway receptors. *Journal of Applied Physiology*, *101*(3), pp.960-970.

Aggarwal, A., Prinz-Wohlgenannt, M., Gröschel, C., Tennakoon, S., Meshcheryakova, A., Chang, W., Brown, E.M., Mechtcheriakova, D. and Kállay, E., (2015). The calcium-sensing receptor suppresses epithelial-to-mesenchymal transition and stem cell-like phenotype in the colon. *Molecular cancer*, *14*(1), pp.1-15.

Aghapour, M., Raee, P., Moghaddam, S.J., Hiemstra, P.S. and Heijink, I.H., (2018). Airway epithelial barrier dysfunction in chronic obstructive pulmonary disease: role of cigarette smoke exposure. *American journal of respiratory cell and molecular biology*, *58*(2), pp.157-169.

Aikawa, T., Shimura, S., Sasaki, H., Ebina, M. and Takishima, T., (1992). Marked goblet cell hyperplasia with mucus accumulation in the airways of patients who died of severe acute asthma attack. *Chest*, *101*(4), pp.916-921.

Akhmetshina, A., Palumbo, K., Dees, C., Bergmann, C., Venalis, P., Zerr, P., Horn, A., Kireva, T., Beyer, C., Zwerina, J., Schneider, H., Sadowski, A., Riener, M.-O., Macdougald, A., Distler, O., Schett, G. and Distler, J.H.W., (2012). Activation of canonical Wnt signalling is required for TGF-β-mediated fibrosis. *Nature Communications*,

Akhmetshina, A., Palumbo, K., Dees, C., Bergmann, C., Venalis, P., Zerr, P., Horn, A., Kireva, T., Beyer, C., Zwerina, J. and Schneider, H., (2012). Activation of canonical Wnt signalling is required for TGF-ß-mediated fibrosis. *Nature communications*, *3*(1), pp.1-12.

Akizawa, T., Ikejiri, K., Kondo, Y., Endo, Y. and Fukagawa, M., (2020). Evocalcet: a new oral calcimimetic for dialysis patients with secondary hyperparathyroidism. *Therapeutic Apheresis and Dialysis*, *24*(3), pp.248-257.

Aktas, A. and Keskin, B., (2013). Statistical power analysis. *The 7th International Days of Statistics and Economics, Prague, Czech Republic*, pp.578-587.

Al-Alawi, M., Hassan, T. and Chotirmall, S.H., (2014). Transforming growth factor ß and severe asthma: a perfect storm. *Respiratory medicine*, *108*(10), pp.1409-1423.

Alber, A., Howie, S.E., Wallace, W.A. and Hirani, N., (2012). The role of macrophages in healing the wounded lung. *International journal of experimental pathology*, *93*(4), pp.243-251.

Alder, J.K., Chen, J.J.L., Lancaster, L., Danoff, S., Su, S.C., Cogan, J.D., Vulto, I., Xie, M., Qi, X., Tuder, R.M., Phillips, J.A., Lansdorp, P.M., Loyd, J.E. and Armanios, M.Y., (2008). Short telomeres are a risk factor for idiopathic pulmonary fibrosis. *Proceedings of the National Academy of Sciences of the United States of America*, 105(35), pp. 13051–13056.

Alessandrini, F., Musiol, S., Schneider, E., Blanco-Pérez, F. and Albrecht, M., (2020). Mimicking Antigen-Driven Asthma in Rodent Models—How Close Can We Get?. *Frontiers in Immunology*, *11*, p.2394.

Amano, H., Matsui, Y., Hatanaka, K., Hosono, K. and Ito, Y., (2021). VEGFR1-tyrosine kinase signaling in pulmonary fibrosis. *Inflammation and Regeneration*, *41*(1), pp.1-8.

Angeli, P., Prado, C.M., Xisto, D.G., Silva, P.L., Pássaro, C.P., Nakazato, H.D., Leick-Maldonado, E.A., Martins, M.A., Rocco, P.R. and Tibério, I.F., (2008). Effects of chronic L-NAME treatment lung tissue mechanics, eosinophilic and extracellular matrix responses induced by chronic pulmonary inflammation. *American Journal of Physiology-Lung Cellular and Molecular Physiology*, *294*(6), pp.L1197-L1205.

Annoni, R., Lanças, T., Tanigawa, R.Y., de Medeiros Matsushita, M., de Morais Fernezlian, S., Bruno, A., da Silva, L.F.F., Roughley, P.J., Battaglia, S., Dolhnikoff, M. and Hiemstra, P.S., (2012). Extracellular matrix composition in COPD. *European Respiratory Journal*, *40*(6), pp.1362-1373.

Armanios, M.Y., Chen, J.J.-L., Cogan, J.D., Alder, J.K., Ingersoll, R.G., Markin, C., Lawson, W.E., Xie, M., Vulto, I., Phillips, J.A., Lansdorp, P.M., Greider, C.W. and Loyd, J.E., (2007). Telomerase Mutations in Families with Idiopathic Pulmonary Fibrosis. *New England Journal of Medicine*, 356(13), pp. 1317–1326.

Arora, P.D. and McCulloch, C.A., (1994). Dependence of collagen remodelling on α-smooth muscle actin expression by fibroblasts. *Journal of cellular physiology*, *159*(1), pp.161-175.

Arthofer, E., Hot, B., Petersen, J., Strakova, K., Jäger, S., Grundmann, M., Kostenis, E., Gutkind, J.S. and Schulte, G., (2016). WNT stimulation dissociates a Frizzled 4 inactive-state complex with Gα12/13. *Molecular pharmacology*, *90*(4), pp.447-459.

Asgari, M., Latifi, N., Heris, H.K., Vali, H. and Mongeau, L., (2017). In vitro fibrillogenesis of tropocollagen type III in collagen type I affects its relative fibrillar topology and mechanics. *Scientific reports*, *7*(1), pp.1-10.

Ashcroft, T., Simpson, J.M. and Timbrell, V., (1988). Simple method of estimating severity of pulmonary fibrosis on a numerical scale. *Journal of clinical pathology*, *41*(4), pp.467-470.

Atabai, K., Yang, C.D. and Podolsky, M.J., (2020). You say you want a resolution (of fibrosis). American journal of respiratory cell and molecular biology, 63(4), pp.424-435.

Atkinson, J.J. and Senior, R.M., (2003). Matrix metalloproteinase-9 in lung remodeling. *American journal of respiratory cell and molecular biology*, *28*(1), pp.12-24.

Aumann, J., (1994). Differential staining of" Excretory" system mucins of Heterodera schachtii J2-juveniles. *Nematologia Mediterranea (Italy)*.

Aytenfisu, T.Y., Campbell, H.M., Chakrabarti, M., Amzel, L.M. and Gabelli, S.B., (2022). Class I PI3K Biology. In *PI3K and AKT Isoforms in Immunity* (pp. 3-49). Springer, Cham.

Baarsma, H.A. and Königshoff, M., (2017). 'WNT-er is coming': WNT signalling in chronic lung diseases. *Thorax*, *72*(8), pp.746-759.

Bachrach, U., (1970). Metabolism and function of spermine and related polyamines. *Annual Review of Microbiology*, *24*, pp.109-134.

Baines, C.P., Kaiser, R.A., Purcell, N.H., Blair, N.S., Osinska, H., Hambleton, M.A., Brunskill, E.W., Sayen, M.R., Gottlieb, R.A., Dorn, G.W. and Robbins, J., (2005). Loss of cyclophilin D reveals a critical role for mitochondrial permeability transition in cell death. *Nature*, *434*(7033), pp.658-662.

Baker, J.R., Vuppusetty, C., Colley, T., Papaioannou, A.I., Fenwick, P., Donnelly, L., Ito, K. and Barnes, P.J., (2016). Oxidative stress dependent microRNA-34a activation via PI3Kα reduces the expression of sirtuin-1 and sirtuin-6 in epithelial cells. *Scientific reports*, *6*(1), pp.1-13.

Balestrini, J.L., Chaudhry, S., Sarrazy, V., Koehler, A. and Hinz, B., (2012). The mechanical memory of lung myofibroblasts. *Integrative Biology*, *4*(4), pp.410-421.

Barnes, P.J., (1985). Clinical studies with calcium antagonists in asthma. *British journal of clinical pharmacology*, *20*(S2), pp.289S-298S.

Barnes, P.J., (2004). Mediators of chronic obstructive pulmonary disease. *Pharmacological reviews*, 56(4), pp. 515–48.

Barnes, P.J., (2011). Similarities and differences in inflammatory mechanisms of asthma and COPD. *Breathe*, *7*(3), pp.229-238.

Barnes, P.J., (2019). Small airway fibrosis in COPD. *The international journal of biochemistry & cell biology*, *116*, p.105598.

Barrett, K.E., Barman, S., Boitano, S.M. and Brooks, H.L., (2016). Introduction to pulmonary structure and mechanics. *Ganong's Review of Medical Physiology. 25th ed. New Delhi: Tata McGraw-Hill Education Publication*, pp.621-38.

Bartoli, M.L., Bacci, E., Carnevali, S., Cianchetti, S., Dente, F.L., Di Franco, A., Giannini, D., Taccola, M., Vagaggini, B. and Paggiaro, P.L., (2004). Clinical assessment of asthma severity partially corresponds to sputum eosinophilic airway inflammation. *Respiratory medicine*, *98*(2), pp.184-193.

Bartram, U. and Speer, C.P., (2004). The role of transforming growth factor ß in lung development and disease. *Chest*, *125*(2), pp.754-765.

Bates, J.H., (2017). CORP: Measurement of lung function in small animals. *Journal of Applied Physiology*, *123*(5), pp.1039-1046.

Bates, J.H., Rincon, M. and Irvin, C.G., (2009). Animal models of asthma. *American Journal of Physiology-Lung Cellular and Molecular Physiology*, *297*(3), pp.L401-L410.

Baugé, C., Cauvard, O., Leclercq, S., Galéra, P. and Boumédiene, K., (2011). Modulation of transforming growth factor beta signalling pathway genes by transforming growth factor beta in human osteoarthritic chondrocytes: involvement of Sp1 in both early and late response cells to transforming growth factor beta. *Arthritis research & therapy*, *13*(1), pp.1-13.

Bauman, K.A., Wettlaufer, S.H., Okunishi, K., Vannella, K.M., Stoolman, J.S., Huang, S.K., Courey, A.J., White, E.S., Hogaboam, C.M., Simon, R.H. and Toews, G.B., (2010). The antifibrotic effects of plasminogen activation occur via

prostaglandin E 2 synthesis in humans and mice. *The Journal of clinical investigation*, *120*(6), pp.1950-1960.

Beckett, E.L., Stevens, R.L., Jarnicki, A.G., Kim, R.Y., Hanish, I., Hansbro, N.G., Deane, A., Keely, S., Horvat, J.C., Yang, M. and Oliver, B.G., (2013). A new short-term mouse model of chronic obstructive pulmonary disease identifies a role for mast cell tryptase in pathogenesis. *Journal of Allergy and Clinical Immunology*, *131*(3), pp.752-762.

Benayoun, L., Druilhe, A., Dombret, M.C., Aubier, M. and Pretolani, M., (2003). Airway structural alterations selectively associated with severe asthma. *American journal of respiratory and critical care medicine*, *167*(10), pp.1360-1368.

Benayoun, L., Druilhe, A., Dombret, M.C., Aubier, M. and Pretolani, M., (2003). Airway structural alterations selectively associated with severe asthma. *American journal of respiratory and critical care medicine*, *167*(10), pp.1360-1368.

Benjamini, Y. and Hochberg, Y., (1995). Controlling the false discovery rate: a practical and powerful approach to multiple testing. *Journal of the Royal statistical society: series B (Methodological)*, *57*(1), pp.289-300.

Bennett, W.D., Burbank, A., Almond, M., Wu, J., Ceppe, A., Hernandez, M., Boucher, R.C. and Peden, D.B., (2021). Acute and durable effect of inhaled hypertonic saline on mucociliary clearance in adult asthma. *ERJ Open Research*, *7*(2).

Bergeron, C., Page, N., Joubert, P., Barbeau, B., Hamid, Q. and Chakir, J., (2003). Regulation of procollagen I (α1) by interleukin-4 in human bronchial fibroblasts: a possible role in airway remodelling in asthma. *Clinical & Experimental Allergy*, *33*(10), pp.1389-1397.

Bergeron, C., Tulic, M.K. and Hamid, Q., (2007). Tools used to measure airway remodelling in research. *European Respiratory Journal*, *29*(3), pp.596-604.

Bergeron, C., Tulic, M.K. and Hamid, Q., (2010). Airway remodelling in asthma: from benchside to clinical practice. *Canadian respiratory journal*, *17*(4), pp.e85-e93.

Biernacka, A., Dobaczewski, M. and Frangogiannis, N.G., (2011). TGF-ß signaling in fibrosis. *Growth factors (Chur, Switzerland)*, 29(5), p. 196.NIH Public Access,

Bikkavilli, R.K., Feigin, M.E. and Malbon, C.C., (2008). Gαo mediates WNT-JNK signaling through Dishevelled 1 and 3, RhoA family members, and MEKK 1 and 4 in mammalian cells. *Journal of cell science*, *121*(2), pp.234-245.

Black, J.L., Burgess, J.K. and Johnson, P.R., (2003). Airway smooth muscle—its relationship to the extracellular matrix. *Respiratory physiology & neurobiology*, *137*(2-3), pp.339-346.

Black, S.A., Palamakumbura, A.H., Stan, M. and Trackman, P.C., (2007). Tissue-specific mechanisms for CCN2/CTGF persistence in fibrotic gingiva: interactions between cAMP and MAPK signaling pathways, and prostaglandin E2-EP3 receptor mediated activation of the c-JUN N-terminal kinase. *Journal of Biological Chemistry*, *282*(21), pp.15416-15429.

Blacquiere, M.J., Hylkema, M.N., Postma, D.S., Geerlings, M., Timens, W. and Melgert, B.N., (2010). Airway inflammation and remodeling in two mouse models of

asthma: comparison of males and females. *International archives of allergy and immunology*, *153*(2), pp.173-181.

Blobe, G.C., Liu, X., Fang, S.J., How, T. and Lodish, H.F., (2001). A novel mechanism for regulating transforming growth factor ß (TGF-ß) signaling: functional modulation of type III TGF-ß receptor expression through interaction with the PDZ domain protein, GIPC. *Journal of Biological Chemistry*, *276*(43), pp.39608-39617.

Blundell, R., Harrison, D.J. and Wallace, W.A.H., (2004). Emphysema: the challenge of the remodelled lung. *The Journal of Pathology: A Journal of the Pathological Society of Great Britain and Ireland*, *202*(2), pp.141-144.

Bonniaud, P., Kolb, M., Galt, T., Robertson, J., Robbins, C., Stampfli, M., Lavery, C., Margetts, P.J., Roberts, A.B. and Gauldie, J., (2004). Smad3 null mice develop airspace enlargement and are resistant to TGF-ß-mediated pulmonary fibrosis. *The Journal of Immunology*, *173*(3), pp.2099-2108.

Bonniaud, P., Margetts, P.J., Kolb, M., Schroeder, J.A., Kapoun, A.M., Damm, D., Murphy, A., Chakravarty, S., Dugar, S., Higgins, L., Protter, A.A. and Gauldie, J., (2012). Progressive Transforming Growth Factor ß1–induced Lung Fibrosis Is Blocked by an Orally Active ALK5 Kinase Inhibitor. *https://doi.org/10.1164/rccm.200405-612OC*, 171(8), pp. 889–898.American Thoracic Society,

Bonser, L.R., Zlock, L., Finkbeiner, W. and Erle, D.J., (2016). Epithelial tethering of MUC5AC-rich mucus impairs mucociliary transport in asthma. *The Journal of clinical investigation*, *126*(6), pp.2367-2371.

Boonpiyathad, T., Sözener, Z.C., Satitsuksanoa, P. and Akdis, C.A., (2019). Immunologic mechanisms in asthma. In *Seminars in immunology* (Vol. 46, p. 101333). Academic Press.

Booth, A.J., Hadley, R., Cornett, A.M., Dreffs, A.A., Matthes, S.A., Tsui, J.L., Weiss, K., Horowitz, J.C., Fiore, V.F., Barker, T.H. and Moore, B.B., (2012). Acellular normal and fibrotic human lung matrices as a culture system for in vitro investigation. *American journal of respiratory and critical care medicine*, *186*(9), pp.866-876.

Boser, S.R., Mauad, T., Araújo-Paulino, B.B.D., Mitchell, I., Shrestha, G., Chiu, A., Butt, J., Kelly, M.M., Caldini, E., James, A. and Green, F.H., (2017). Myofibroblasts are increased in the lung parenchyma in asthma. *PloS one*, *12*(8), p.e0182378.

Bossé, Y., Paré, P.D. and Seow, C.Y., (2008). Airway wall remodeling in asthma: from the epithelial layer to the adventitia. *Current allergy and asthma reports*, *8*(4), pp.357-366.

Boucherat, O., Boczkowski, J., Jeannotte, L. and Delacourt, C., (2013). Cellular and molecular mechanisms of goblet cell metaplasia in the respiratory airways. *Experimental lung research*, *39*(4-5), pp.207-216.

Boutard, V., Havouis, R., Fouqueray, B., Philippe, C., Moulinoux, J.P. and Baud, L., (1995). Transforming growth factor-beta stimulates arginase activity in macrophages. Implications for the regulation of macrophage cytotoxicity. *The Journal of Immunology*, *155*(4), pp.2077-2084.

Boxall, C., Holgate, S.T. and Davies, D.E., (2006). The contribution of transforming growth factor-ß and epidermal growth factor signalling to airway remodelling in chronic asthma. *European Respiratory Journal*, *27*(1), pp.208-229.

Boyd, A.R. and Orihuela, C.J., (2011). Dysregulated inflammation as a risk factor for pneumonia in the elderly. *Aging and disease*, *2*(6), p.487.

Bradding, P., Roberts, J.A., Britten, K.M., Montefort, S., Djukanovic, R., Mueller, R., Heusser, C.H., Howarth, P.H. and Holgate, S.T., (1994). Interleukin-4, -5, and -6 and tumor necrosis factor-alpha in normal and asthmatic airways: evidence for the human mast cell as a source of these cytokines. *American journal of respiratory cell and molecular biology*, *10*(5), pp.471-480.

Braga, F.A.V., Kar, G., Berg, M., Carpaij, O.A., Polanski, K., Simon, L.M., Brouwer, S., Gomes, T., Hesse, L., Jiang, J. and Fasouli, E.S., (2019). A cellular census of human lungs identifies novel cell states in health and in asthma. *Nature medicine*, *25*(7), pp.1153-1163. Available from: https://www.proteinatlas.org/ENSG00000036828-CASR/single+cell+type [accessed 22 December 2021].

Braicu, C., Buse, M., Busuioc, C., Drula, R., Gulei, D., Raduly, L., Rusu, A., Irimie, A., Atanasov, A.G., Slaby, O. and Ionescu, C., (2019). A comprehensive review on MAPK: a promising therapeutic target in cancer. *Cancers*, *11*(10), p.1618.

Brandsma, C.A., de Vries, M., Costa, R., Woldhuis, R.R., Königshoff, M. and Timens, W., (2017). Lung ageing and COPD: is there a role for ageing in abnormal tissue repair?. *European Respiratory Review*, *26*(146).

Brandsma, C.A., Van den Berge, M., Hackett, T.L., Brusselle, G. and Timens, W., (2019). Recent advances in chronic obstructive pulmonary disease pathogenesis: from disease mechanisms to precision medicine. *Journal of Pathology*, (December 2019), pp. 624–635.

Brass, D.M., Hollingsworth, J.W., Fessler, M.B., Savov, J.D., Maxwell, A.B., Whitehead, G.S., Burch, L.H. and Schwartz, D.A., (2007a). The IL-1 type 1 receptor is required for the development of LPS-induced airways disease. *Journal of allergy and clinical immunology*, *120*(1), pp.121-127.

Brass, D.M., Hollingsworth, J.W., McElvania-Tekippe, E., Garantziotis, S., Hossain, I. and Schwartz, D.A., (2007b). CD14 is an essential mediator of LPS-induced airway disease. *American Journal of Physiology-Lung Cellular and Molecular Physiology*, *293*(1), pp.L77-L83.

Brass, D.M., Savov, J.D., Gavett, S.H., Haykal-Coates, N. and Schwartz, D.A., (2003). Subchronic endotoxin inhalation causes persistent airway disease. *American Journal of Physiology-Lung Cellular and Molecular Physiology*, *285*(3), pp.L755-L761.

Brass, D.M., Savov, J.D., Whitehead, G.S., Maxwell, A.B. and Schwartz, D.A., (2004). LPS binding protein is important in the airway response to inhaled endotoxin. *Journal of allergy and clinical immunology*, *114*(3), pp.586-592.

Breen, E., Shull, S., Burne, S., Absher, M., Kelley, J., Phan, S. and Cutroneo, K.R., (1992). Bleomycin regulation of transforming growth factor-mRNA in rat lung fibroblasts. *Am J Respir Cell Mol Biol*, *6*(2), pp.146-152.

Breitwieser, G.E., (2013). The calcium sensing receptor life cycle: trafficking, cell surface expression, and degradation. *Best practice & research Clinical endocrinology & metabolism*, *27*(3), pp.303-313.

Brennan, S.C. and Conigrave, A.D., (2009). Regulation of cellular signal transduction pathways by the extracellular calcium-sensing receptor. *Current pharmaceutical biotechnology*, *10*(3), pp.270-281.

Brennan, S.C., Thiem, U., Roth, S., Aggarwal, A., Fetahu, I.S., Tennakoon, S., Gomes, A.R., Brandi, M.L., Bruggeman, F., Mentaverri, R., Riccardi, D. and Kallay, E., (2013). Calcium sensing receptor signalling in physiology and cancer. *Biochimica et Biophysica Acta - Molecular Cell Research*, 1833(7), pp. 1732–1744.Elsevier B.V.,

Brennan, S.C., Wilkinson, W.J., Tseng, H.E., Finney, B., Monk, B., Dibble, H., Quilliam, S., Warburton, D., Galietta, L.J., Kemp, P.J. and Riccardi, D., (2016). The extracellular calcium-sensing receptor regulates human fetal lung development via CFTR. *Scientific reports*, *6*(1), pp.1-13.

Brewer, N.R. and Cruise, L.J., (1997). The respiratory system of the guinea pig: Emphasis on species differences. *Journal of the American Association for Laboratory Animal Science*, *36*(1), pp.100-108.

Brewster, C.E., Howarth, P.H., Djukanovic, R., Wilson, J., Holgate, S.T. and Roche, W.R., (1990). Myofibroblasts and subepithelial fibrosis in bronchial asthma. *Am J Respir Cell Mol Biol*, *3*(5), pp.507-511.

Bringardner, B.D., Baran, C.P., Eubank, T.D. and Marsh, B., (2008). The Role of Inflammation in the Pathogenesis of Idiopathic Pulmonary Fibrosis. *Antioxidants & redox signaling*, 10(2), pp. 287–301.

Broide, D.H., Lawrence, T., Doherty, T., Cho, J.Y., Miller, M., McElwain, K., McElwain, S. and Karin, M., (2005). Allergen-induced peribronchial fibrosis and mucus production mediated by IκB kinase ß-dependent genes in airway epithelium. *Proceedings of the National Academy of Sciences*, *102*(49), pp.17723-17728.

Brown, E.M. and MacLeod, R.J., (2001). Extracellular calcium sensing and extracellular calcium signaling. *Physiological Reviews*, 81(1), pp. 239–297.

Brown, E.M., (1983). Four-parameter model of the sigmoidal relationship between parathyroid hormone release and extracellular calcium concentration in normal and abnormal parathyroid tissue. *The Journal of clinical endocrinology and metabolism*, *56*(3), pp.572-581.

Brown, E.M., (1991). Extracellular Ca2+ sensing, regulation of parathyroid cell function, and role of Ca2+ and other ions as extracellular (first) messengers. *Physiological reviews*, *71*(2), pp.371-411.

Brown, E.M., (2013). Role of the calcium-sensing receptor in extracellular calcium homeostasis. *Best practice & research Clinical endocrinology & metabolism*, *27*(3), pp.333-343.

Brown, E.M., Chen, C.J. and Kifor, O., (1990). A comparison of the effects of divalent and trivalent cations on parathyroid hormone release, 3', 5'-cyclic-adenosine monophosphate accumulation, and the levels of inositol phosphates in bovine parathyroid cells. *Endocrinology*, *127*(3), pp.1064-1071.

Brown, E.M., Gamba, G., Riccardi, D., Lombardi, M., Butters, R., Kifor, O., Sun, A., Hediger, M.A., Lytton, J. and Hebert, S.C., (1993). Cloning and characterization of an extracellular Ca2+-sensing receptor from bovine parathyroid. *Nature*, *366*(6455), pp.575-580.

Bullone, M., Vargas, A., Elce, Y., Martin, J.G. and Lavoie, J.P., (2017). Fluticasone/salmeterol reduces remodelling and neutrophilic inflammation in severe equine asthma. *Scientific reports*, *7*(1), pp.1-13.

Burch, M.L., Ballinger, M.L., Yang, S.N., Getachew, R., Itman, C., Loveland, K., Osman, N. and Little, P.J., 2010. Thrombin stimulation of proteoglycan synthesis in vascular smooth muscle is mediated by protease-activated receptor-1 transactivation of the transforming growth factor ß type I receptor. *Journal of Biological Chemistry*, *285*(35), pp.26798-26805.

Burgess, J.K., (2009). The role of the extracellular matrix and specific growth factors in the regulation of inflammation and remodelling in asthma. *Pharmacology & therapeutics*, *122*(1), pp.19-29.

Burgess, J.K., Boustany, S., Moir, L.M., Weckmann, M., Lau, J.Y., Grafton, K., Baraket, M., Hansbro, P.M., Hansbro, N.G., Foster, P.S. and Black, J.L., (2010). Reduction of tumstatin in asthmatic airways contributes to angiogenesis, inflammation, and hyperresponsiveness. *American journal of respiratory and critical care medicine*, *181*(2), pp.106-115.

Burgess, J.K., Carlin, S., Pack, R.A., Arndt, G.M., Au, W.W., Johnson, P.R., Black, J.L. and Hunt, N.H., (2004). Detection and characterization of OX40 ligand expression in human airway smooth muscle cells: a possible role in asthma?. *Journal of Allergy and Clinical Immunology*, *113*(4), pp.683-689.

Burgess, J.K., Johnson, P.R., Ge, Q., Au, W.W., Poniris, M.H., McParland, B.E., King, G., Roth, M. and Black, J.L., (2003). Expression of connective tissue growth factor in asthmatic airway smooth muscle cells. *American Journal of Respiratory and Critical Care Medicine*, *167*(1), pp.71-77.

Burgess, J.K., Jonker, M.R., Berg, M., Ten Hacken, N.T., Meyer, K.B., van den Berge, M., Nawijn, M.C. and Heijink, I.H., (2021). Periostin: contributor to abnormal airway epithelial function in asthma?. *European Respiratory Journal*, *57*(2).

Burgess, J.K., Ketheson, A., Faiz, A., Limbert Rempel, K.A., Oliver, B.G., Ward, J.P.T. and Halayko, A.J., (2018). Phenotype and functional features of human telomerase reverse transcriptase immortalized human airway smooth muscle cells from asthmatic and non-asthmatic donors. *Scientific Reports*, *8*(1), pp.1-12.

Burgess, J.K., Lee, J.H., Ge, Q.I., Ramsay, E.E., Poniris, M.H., Parmentier, J., Roth, M., Johnson, P.R., Hunt, N.H., Black, J.L. and Ammit, A.J., (2008). Dual ERK and phosphatidylinositol 3-kinase pathways control airway smooth muscle proliferation: Differences in asthma. *Journal of cellular physiology*, *216*(3), pp.673-679.

Burgess, J.K., Mauad, T., Tjin, G., Karlsson, J.C. and Westergren-Thorsson, G., (2016). The extracellular matrix–the under-recognized element in lung disease?. *The Journal of pathology*, *240*(4), pp.397-409.

Burgess, J.K., Weckmann, M. and Karsdal, M.A., (2019). The message from the matrix—should we listen more closely?. *Journal of thoracic disease*, *11*(Suppl 3), p.S230.

Burgstaller, G., Sengupta, A., Vierkotten, S., Preissler, G., Lindner, M., Behr, J., Königshoff, M. and Eickelberg, O., (2018). Distinct niches within the extracellular matrix dictate fibroblast function in (cell free) 3D lung tissue cultures. *American Journal of Physiology-Lung Cellular and Molecular Physiology*, *314*(5), pp.L708-L723.

Busse, P.J., Birmingham, J.M., Calatroni, A., Manzi, J., Goryachokovsky, A., Fontela, G., Federman, A.D. and Wisnivesky, J.P., (2017). Effect of aging on sputum inflammation and asthma control. *Journal of Allergy and Clinical Immunology*, *139*(6), pp.1808-1818.

Busse, W.W. and Kraft, M., (2022). Current unmet needs and potential solutions to uncontrolled asthma. *European Respiratory Review*, *31*(163).

Button, B., Okada, S.F., Frederick, C.B., Thelin, W.R. and Boucher, R.C., (2013). Mechanosensitive ATP release maintains proper mucus hydration of airways. *Science signaling*, *6*(279), pp.ra46-ra46.

Cahill, E.F., Kennelly, H., Carty, F., Mahon, B.P. and English, K., (2016). Hepatocyte growth factor is required for mesenchymal stromal cell protection against bleomycin-induced pulmonary fibrosis. *Stem cells translational medicine*, *5*(10), pp.1307-1318.

Cahn, A., Hamblin, J.N., Begg, M., Wilson, R., Dunsire, L., Sriskantharajah, S., Montembault, M., Leemereise, C.N., Galinanes-Garcia, L., Watz, H. and Kirsten, A.M., (2017). Safety, pharmacokinetics and dose-response characteristics of GSK2269557, an inhaled PI3Kδ inhibitor under development for the treatment of COPD. *Pulmonary pharmacology & therapeutics*, *46*, pp.69-77.

Calhoun, C., Shivshankar, P., Saker, M., Sloane, L.B., Livi, C.B., Sharp, Z.D., Orihuela, C.J., Adnot, S., White, E.S., Richardson, A. and Jourdan Le Saux, C., (2016). Senescent cells contribute to the physiological remodeling of aged lungs. *Journals of Gerontology Series A: Biomedical Sciences and Medical Sciences*, *71*(2), pp.153-160.

Caltabiano, S., Dollery, C.T., Hossain, M., Kurtinecz, M.T., Desjardins, J.P., Favus, M.J., Kumar, R. and Fitzpatrick, L.A., (2013). Characterization of the effect of chronic administration of a calcium-sensing receptor antagonist, ronacaleret, on renal calcium excretion and serum calcium in postmenopausal women. *Bone*, *56*(1), pp.154-162.

Campa, C.C., Silva, R.L., Margaria, J.P., Pirali, T., Mattos, M.S., Kraemer, L.R., Reis, D.C., Grosa, G., Copperi, F., Dalmarco, E.M. and Lima-Júnior, R.C., (2018). Inhalation of the prodrug PI3K inhibitor CL27c improves lung function in asthma and fibrosis. *Nature communications*, *9*(1), pp.1-16.

Canaff, L. and Hendy, G.N., (2005). Calcium-sensing receptor gene transcription is up-regulated by the proinflammatory cytokine, interleukin-1ß: role of the NF-κB pathway and κB elements. *Journal of Biological Chemistry*, *280*(14), pp.14177-14188.

Canning, B.J. and Chou, Y., (2008). Using guinea pigs in studies relevant to asthma and COPD. *Pulmonary pharmacology & therapeutics*, *21*(5), pp.702-720.

Caporarello, N., Meridew, J.A., Aravamudhan, A., Jones, D.L., Austin, S.A., Pham, T.X., Haak, A.J., Moo Choi, K., Tan, Q., Haresi, A. and Huang, S.K., (2020). Vascular dysfunction in aged mice contributes to persistent lung fibrosis. *Aging cell*, *19*(8), p.e13196.

Carey, D.J., Fetterolf, S.N., Davis, F.D., Faucett, W.A., Kirchner, H.L., Mirshahi, U., Murray, M.F., Smelser, D.T., Gerhard, G.S. and Ledbetter, D.H., (2016). The Geisinger MyCode community health initiative: an electronic health record–linked biobank for precision medicine research. *Genetics in medicine*, *18*(9), pp.906-913.

Carlson, M.E., Conboy, M.J., Hsu, M., Barchas, L., Jeong, J., Agrawal, A., Mikels, A.J., Agrawal, S., Schaffer, D.V. and Conboy, I.M., (2009). Relative roles of TGF-ß1 and Wnt in the systemic regulation and aging of satellite cell responses. *Aging cell*, *8*(6), pp.676-689.

Carpenter, O.L. and Wu, S., (2014). Regulation of MSK 1-Mediated NF-κB Activation Upon UVB Irradiation. *Photochemistry and photobiology*, *90*(1), pp.155-161.

Carroll, N., Elliot, J., Morton, A. and James, A., (1993). The Structure of large and small Airways in Nonfatal and Fatal Asthma. *Am Rev Respir Dis*, *147*, pp.405-410.

Cazzola, M., Rogliani, P. and Matera, M.G., (2019). The future of bronchodilation: looking for new classes of bronchodilators. *European Respiratory Review*, *28*(154).

Celli, A., Tu, C.L., Lee, E., Bikle, D.D. and Mauro, T.M., (2021). Decreased calcium-sensing receptor expression controls calcium signaling and cell-to-cell adhesion defects in aged skin. *Journal of Investigative Dermatology*, *141*(11), pp.2577-2586.

Celli, B.R., Halbert, R.J., Isonaka, S. and Schau, B., (2003). Population impact of different definitions of airway obstruction. *European Respiratory Journal*, *22*(2), pp.268-273.

Centeno, P.P., Herberger, A., Mun, H.C., Tu, C., Nemeth, E.F., Chang, W., Conigrave, A.D. and Ward, D.T., (2019). Phosphate acts directly on the calcium-sensing receptor to stimulate parathyroid hormone secretion. *Nature communications*, *10*(1), pp.1-12.

Chakrabarty, S., Wang, H., Canaff, L., Hendy, G.N., Appelman, H. and Varani, J., (2005). Calcium sensing receptor in human colon carcinoma: interaction with Ca2+ and 1, 25-dihydroxyvitamin D3. *Cancer research*, *65*(2), pp.493-498.

Chanda, D., Otoupalova, E., Smith, S.R., Volckaert, T., De Langhe, S.P. and Thannickal, V.J., (2019). Developmental pathways in the pathogenesis of lung fibrosis. *Molecular Aspects of Medicine*, *65*, pp.56-69.

Chang, W., Pratt, S., Chen, T.H., Nemeth, E., Huang, Z. and Shoback, D., (1998). Coupling of calcium receptors to inositol phosphate and cyclic AMP generation in mammalian cells and Xenopus laevis oocytes and immunodetection of receptor protein by region-specific antipeptide antisera. *Journal of Bone and Mineral Research*, *13*(4), pp.570-580.

Chang, W., Tu, C., Chen, T.H., Bikle, D. and Shoback, D., (2008). The extracellular calcium-sensing receptor (CaSR) is a critical modulator of skeletal development. *Science signaling*, *1*(35), pp.ra1-ra1.

Chang, W., Wei, K., Ho, L., Berry, G.J., Jacobs, S.S., Chang, C.H. and Rosen, G.D., (2014). A critical role for the mTORC2 pathway in lung fibrosis. *PloS one*, *9*(8), p.e106155.

Chaouat, A., Bugnet, A.S., Kadaoui, N., Schott, R., Enache, I., Ducoloné, A., Ehrhart, M., Kessler, R. and Weitzenblum, E., (2005). Severe pulmonary hypertension and chronic obstructive pulmonary disease. *American journal of respiratory and critical care medicine*, *172*(2), pp.189-194.

Chapman, D.G. and Irvin, C.G., (2015). Mechanisms of airway hyper-responsiveness in asthma: the past, present and yet to come. *Clinical & Experimental Allergy*, *45*(4), pp.706-719.

Chapman, R.W., (2008). Canine models of asthma and COPD. *Pulmonary pharmacology & therapeutics*, *21*(5), pp.731-742.

Chardin, P., Camonis, J.H., Gale, N.W., Van Aelst, L., Schlessinger, J., Wigler, M.H. and Bar-Sagi, D., (1993). Human Sos1: a guanine nucleotide exchange factor for Ras that binds to GRB2. *Science*, *260*(5112), pp.1338-1343.

Chattopadhyay, N., Yano, S., Tfelt-Hansen, J., Rooney, P., Kanuparthi, D., Bandyopadhyay, S., Ren, X., Terwilliger, E. and Brown, E.M., (2004). Mitogenic action of calcium-sensing receptor on rat calvarial osteoblasts. *Endocrinology*, *145*(7), pp.3451-3462.

Chauvin, C., Koka, V., Nouschi, A., Mieulet, V., Hoareau-Aveilla, C., Dreazen, A., Cagnard, N., Carpentier, W., Kiss, T., Meyuhas, O. and Pende, M., (2014). Ribosomal protein S6 kinase activity controls the ribosome biogenesis transcriptional program. *Oncogene*, *33*(4), pp.474-483.

Chen, I., Hsu, P.H., Hsu, W.C., Chen, N.J. and Tseng, P.H., (2015). Polyubiquitination of transforming growth factor β-activated kinase 1 (TAK1) at lysine 562 residue regulates TLR4-mediated JNK and p38 MAPK activation. *Scientific reports*, *5*(1), pp.1-15.

Chen, J., Miller, M., Unno, H., Rosenthal, P., Sanderson, M.J. and Broide, D.H., (2018). Orosomucoid-like 3 (ORMDL3) upregulates airway smooth muscle proliferation, contraction, and Ca2+ oscillations in asthma. *Journal of Allergy and Clinical Immunology*, *142*(1), pp.207-218.

Chen, S.J., Yuan, W., Mori, Y., Levenson, A., Varga, J. and Trojanowska, M., (1999). Stimulation of type I collagen transcription in human skin fibroblasts by TGF-β: involvement of Smad 3. *Journal of Investigative Dermatology*, *112*(1), pp.49-57.

Chen, Y., Chen, P., Hanaoka, M., Droma, Y. and Kubo, K., (2008). Enhanced levels of prostaglandin E2 and matrix metalloproteinase-2 correlate with the severity of airflow limitation in stable COPD. *Respirology*, *13*(7), pp.1014-1021.

Chen, Y., Thai, P., Zhao, Y.H., Ho, Y.S., DeSouza, M.M. and Wu, R., (2003). Stimulation of airway mucin gene expression by interleukin (IL)-17 through IL-6 paracrine/autocrine loop. *Journal of Biological Chemistry*, *278*(19), pp.17036-17043.

Cheng, S.X., Okuda, M., Hall, A.E., Geibel, J.P. and Hebert, S.C., (2002). Expression of calcium-sensing receptor in rat colonic epithelium: evidence for modulation of

fluid secretion. *American Journal of Physiology-Gastrointestinal and Liver Physiology*, *283*(1), pp.G240-G250.

Chernyavsky, I.L., Croisier, H., Chapman, L.A., Kimpton, L.S., Hiorns, J.E., Brook, B.S., Jensen, O.E., Billington, C.K., Hall, I.P. and Johnson, S.R., (2014). The role of inflammation resolution speed in airway smooth muscle mass accumulation in asthma: insight from a theoretical model. *PloS one*, *9*(3), p.e90162.

Chilosi, M., Zamò, A., Doglioni, C., Reghellin, D., Lestani, M., Montagna, L., Pedron, S., Ennas, M.G., Cancellieri, A., Murer, B. and Poletti, V., (2006). Migratory marker expression in fibroblast foci of idiopathic pulmonary fibrosis. *Respiratory research*, *7*(1), pp.1-10.

Cho, S.J. and Stout-Delgado, H.W., (2020). Aging and lung disease. *Annual review of physiology*, *82*, p.433.

Chodon, T., Sugihara, T., Igawa, H.H., Funayama, E. and Furukawa, H., (2000). Keloid-derived fibroblasts are refractory to Fas-mediated apoptosis and neutralization of autocrine transforming growth factor-ß1 can abrogate this resistance. *The American journal of pathology*, *157*(5), pp.1661-1669.

Chong, D.L.W., Rebeyrol, C., Khawaja, A., Forty, E.J., Kanda, N., Scotton, C.J. and Porter, J.C., (2016). S49 The role of platelet-derived TGF [beta] in pulmonary fibrosis. *Thorax*, *71*, p.A30.

Christopoulos, A. and Kenakin, T., (2002). G protein-coupled receptor allosterism and complexing. *Pharmacological reviews*, *54*(2), pp.323-374.

Chu, H.W., Balzar, S., Seedorf, G.J., Westcott, J.Y., Trudeau, J.B., Silkoff, P. and Wenzel, S.E., (2004). Transforming growth factor-ß2 induces bronchial epithelial mucin expression in asthma. *The American journal of pathology*, *165*(4), pp.1097-1106.

Chung, K.F. and Adcock, I.M., (2008). Multifaceted mechanisms in COPD: inflammation, immunity, and tissue repair and destruction. *European Respiratory Journal*, *31*(6), pp.1334-1356.

Chung, K.F., Wenzel, S.E., Brozek, J.L., Bush, A., Castro, M., Sterk, P.J., Adcock, I.M., Bateman, E.D., Bel, E.H., Bleecker, E.R. and Boulet, L.P., (2014). International ERS/ATS guidelines on definition, evaluation and treatment of severe asthma. *European respiratory journal*, *43*(2), pp.343-373.

Churg, A., Zhou, S. and Wright, J.L., (2012). Matrix metalloproteinases in COPD. *European Respiratory Journal*, *39*(1), pp.197-209.

Ciardiello, D., Elez, E., Tabernero, J. and Seoane, J., (2020). Clinical development of therapies targeting TGF-ß: current knowledge and future perspectives. *Annals of Oncology*, 31(10), pp. 1336–1349.Elsevier,

Cisneros, J., Hagood, J., Checa, M., Ortiz-Quintero, B., Negreros, M., Herrera, I., Ramos, C., Pardo, A. and Selman, M., (2012). Hypermethylation-mediated silencing of p14ARF in fibroblasts from idiopathic pulmonary fibrosis. *American Journal of Physiology-Lung Cellular and Molecular Physiology*, *303*(4), pp.L295-L303.

Clancy, R.M., Zheng, P., O'Mahony, M., Izmirly, P., Zavadil, J., Gardner, L. and Buyon, J.P., (2007). Role of hypoxia and cAMP in the transdifferentiation of human fetal cardiac fibroblasts: implications for progression to scarring in autoimmune-

associated congenital heart block. *Arthritis & Rheumatism: Official Journal of the American College of Rheumatology*, *56*(12), pp.4120-4131.

Cohen, L., E, X., Tarsi, J., Ramkumar, T., Horiuchi, T.K., Cochran, R., DeMartino, S., Schechtman, K.B., Hussain, I., Holtzman, M.J. and Castro, M., (2007). Epithelial cell proliferation contributes to airway remodeling in severe asthma. *American journal of respiratory and critical care medicine*, *176*(2), pp.138-145.

Coker, R.K., Laurent, G.J., Shahzeidi, S., Lympany, P.A., Du Bois, R.M., Jeffery, P.K. and McAnulty, R.J., (1997). Transforming growth factors-beta 1,-beta 2, and-beta 3 stimulate fibroblast procollagen production in vitro but are differentially expressed during bleomycin-induced lung fibrosis. The American journal of pathology, 150(3), p.981.

Conigrave, A.D. and Ward, D.T., (2013). Calcium-sensing receptor (CaSR): pharmacological properties and signaling pathways. *Best practice & research Clinical endocrinology & metabolism*, *27*(3), pp.315-331.

Conigrave, A.D. and Ward, D.T., (2013). Calcium-sensing receptor (CaSR): pharmacological properties and signaling pathways. *Best practice & research Clinical endocrinology & metabolism*, *27*(3), pp.315-331.

Conlon, I. and Raff, M., (1999). Size control in animal development. *Cell*, *96*(2), pp.235-244.

Conte, E., Fruciano, M., Fagone, E., Gili, E., Caraci, F., Iemmolo, M., Crimi, N. and Vancheri, C., (2011). Inhibition of PI3K prevents the proliferation and differentiation of human lung fibroblasts into myofibroblasts: the role of class I P110 isoforms. *PloS one*, *6*(10), p.e24663.

Conte, E., Fruciano, M., Fagone, E., Gili, E., Caraci, F., Iemmolo, M., Crimi, N. and Vancheri, C., (2011). Inhibition of PI3K prevents the proliferation and differentiation of human lung fibroblasts into myofibroblasts: the role of class I P110 isoforms. *PloS one*, *6*(10), p.e24663.

Conte, E., Gili, E., Fagone, E., Fruciano, M., Iemmolo, M. and Vancheri, C., (2014). Effect of pirfenidone on proliferation, TGF-ß-induced myofibroblast differentiation and fibrogenic activity of primary human lung fibroblasts. *European Journal of Pharmaceutical Sciences*, *58*, pp.13-19.

Cooper, G. and Schiller, A.L., (1975). *Anatomy of the guinea pig*. Harvard University Press.

Costanza, B., Umelo, I.A., Bellier, J., Castronovo, V. and Turtoi, A., (2017). Stromal modulators of TGF-ß in cancer. *Journal of clinical medicine*, *6*(1), p.7.

Courtney, J.-M. and Spafford, P.L., (2017). The Role of Epithelial-Mesenchymal Transition in Chronic Obstructive Pulmonary Disease. *Cells Tissues Organs*, 203(2), pp. 99–104.

Crapo, J.D., Young, S.L., Fram, E.K., Pinkerton, K.E., Barry, B.E. and Crapo, R.O., (1983). Morphometric characteristics of cells in the alveolar region of mammalian lungs. *American Review of Respiratory Disease*, *128*(2P2), pp.S42-S46.

Crosby, L.M. and Waters, C.M., (2010). Epithelial repair mechanisms in the lung. *American Journal of Physiology-Lung Cellular and Molecular Physiology*, *298*(6), pp.L715-L731.

Cutz, E. and Jackson, A., (1999). Neuroepithelial bodies as airway oxygen sensors. *Respiration physiology*, *115*(2), pp.201-214.

Danopoulos, S., Alonso, I., Thornton, M.E., Grubbs, B.H., Bellusci, S., Warburton, D. and Al Alam, D., (2018). Human lung branching morphogenesis is orchestrated by the spatiotemporal distribution of ACTA2, SOX2, and SOX9. *American Journal of Physiology-Lung Cellular and Molecular Physiology*, *314*(1), pp.L144-L149.

Danopoulos, S., Shiosaki, J. and Al Alam, D., (2019). FGF signaling in lung development and disease: human versus mouse. *Frontiers in genetics*, *10*, p.170.

Davies, M., Robinson, M., Smith, E., Huntley, S., Prime, S. and Paterson, I., (2005). Induction of an epithelial to mesenchymal transition in human immortal and malignant keratinocytes by TGF-β1 involves MAPK, Smad and AP-1 signalling pathways. *Journal of cellular biochemistry*, *95*(5), pp.918-931.

Dayati, P., Rezaei, H.B., Sharifat, N., Kamato, D. and Little, P.J., (2018). G protein coupled receptors can transduce signals through carboxy terminal and linker region phosphorylation of Smad transcription factors. *Life sciences*, *199*, pp.10-15.

de Hilster, R.H.J., Sharma, P.K., Jonker, M.R., White, E.S., Gercama, E.A., Roobeek, M., Timens, W., Harmsen, M.C., Hylkema, M.N. and Burgess, J.K., (2020). Human lung extracellular matrix hydrogels resemble the stiffness and viscoelasticity of native lung tissue. *American Journal of Physiology-Lung Cellular and Molecular Physiology*, *318*(4), pp.L698-L704.

de Jesus Ferreira, M.C., Héliès-Toussaint, C., Imbert-Teboul, M., Bailly, C., Verbavatz, J.M., Bellanger, A.C. and Chabardès, D., (1998). Co-expression of a Ca2+-inhibitable Adenylyl Cyclase and of a Ca2+-sensing Receptor in the Cortical Thick Ascending Limb Cell of the Rat Kidney: Inhibition of hormone-dependent cAMP accumulation by extracellular Ca2+. *Journal of Biological Chemistry*, *273*(24), pp.15192-15202.

De Marco, R., Accordini, S., Cerveri, I., Corsico, A., Sunyer, J., Neukirch, F., Künzli, N., Leynaert, B., Janson, C., Gislason, T. and Vermeire, P., (2004). An international survey of chronic obstructive pulmonary disease in young adults according to GOLD stages. *Thorax*, *59*(2), pp.120-125.

Deak, M., Clifton, A.D., Lucocq, J.M. and Alessi, D.R., (1998). Mitogen-and stress-activated protein kinase-1 (MSK1) is directly activated by MAPK and SAPK2/p38, and may mediate activation of CREB. *The EMBO journal*, *17*(15), pp.4426-4441.

Debacq-Chainiaux, F., Borlon, C., Pascal, T., Royer, V., Eliaers, F., Ninane, N., Carrard, G., Friguet, B., de Longueville, F., Boffe, S. and Remacle, J., (2005). Repeated exposure of human skin fibroblasts to UVB at subcytotoxic level triggers premature senescence through the TGF-β1 signaling pathway. *Journal of cell science*, *118*(4), pp.743-758.

Defnet, A.E., Hasday, J.D. and Shapiro, P., (2020). Kinase inhibitors in the treatment of obstructive pulmonary diseases. *Current opinion in pharmacology*, *51*, pp.11-18.

Degryse, A.L. and Lawson, W.E., (2011). Progress toward improving animal models for idiopathic pulmonary fibrosis. *The American journal of the medical sciences*, *341*(6), pp.444-449.

Denecker, N.E.J., Kullberg, B.J., Drenth, J.P.H., Raemaekers, J.M.M. and Van Der Meer, J.W.M., (1997). Regulation of the production of pro-inflammatory cytokines and antagonists during chemotherapy-induced neutropenia in patients with haematological malignancies. *Cytokine*, 9(9), pp. 702–710.

D'Errico, A., Scarani, P., Colosimo, E., Spina, M., Grigioni, W.F. and Mancini, A.M., (1989). Changes in the alveolar connective tissue of the ageing lung: an immunohistochemical study. *Virchows Archiv A*, *415*, pp.137-144.

D'Errico, A., Scarani, P., Colosimo, E., Spina, M., Grigioni, W.F. and Mancini, A.M., (1989). Changes in the alveolar connective tissue of the ageing lung. *Virchows Archiv A*, *415*(2), pp.137-144.

Dershem, R., Gorvin, C.M., Metpally, R.P., Krishnamurthy, S., Smelser, D.T., Hannan, F.M., Carey, D.J., Thakker, R.V. and Breitwieser, G.E., (2020). Familial hypocalciuric hypercalcemia type 1 and autosomal-dominant hypocalcemia type 1: prevalence in a large healthcare population. *The American Journal of Human Genetics*, *106*(6), pp.734-747.

Derynck, R. and Zhang, Y.E., (2003). Smad-dependent and Smad-independent pathways in TGF-β family signalling. *Nature*, *425*(6958), pp.577-584.

Deshpande, D.A. and Penn, R.B., (2006). Targeting G protein-coupled receptor signaling in asthma. *Cellular signalling*, *18*(12), pp.2105-2120.

Dimopoulos, G., Lerikou, M., Tsiodras, S., Chranioti, A., Perros, E., Anagnostopoulou, U., Armaganidis, A. and Karakitsos, P., (2012). Viral epidemiology of acute exacerbations of chronic obstructive pulmonary disease. *Pulmonary pharmacology & therapeutics*, *25*(1), pp.12-18.

Dituri, F., Cossu, C., Mancarella, S. and Giannelli, G., (2019). The Interactivity between TGF-β and BMP Signaling in Organogenesis, Fibrosis, and Cancer. *Cells*, 8(10)Multidisciplinary Digital Publishing Institute (MDPI),

Doherty, T. and Broide, D., (2007). Cytokines and growth factors in airway remodeling in asthma. *Current opinion in immunology*, *19*(6), pp.676-680.

Dolhnikoff, M., Morin, J. and Ludwig, M.S., (1998). Human lung parenchyma responds to contractile stimulation. *American journal of respiratory and critical care medicine*, *158*(5), pp.1607-1612.

Dos Santos, C.C., (2008). Advances in mechanisms of repair and remodelling in acute lung injury. *Intensive care medicine*, *34*, pp.619-630.

Dulek, D.E., Newcomb, D.C., Goleniewska, K., Cephus, J., Zhou, W., Reiss, S., Toki, S., Ye, F., Zaynagetdinov, R., Sherrill, T.P. and Blackwell, T.S., (2014). Allergic airway inflammation decreases lung bacterial burden following acute Klebsiella pneumoniae infection in a neutrophil-and CCL8-dependent manner. *Infection and Immunity*, *82*(9), pp.3723-3739.

Dunkern, T.R., Feurstein, D., Rossi, G.A., Sabatini, F. and Hatzelmann, A., (2007). Inhibition of TGF-β induced lung fibroblast to myofibroblast conversion by phosphodiesterase inhibiting drugs and activators of soluble guanylyl cyclase. *European journal of pharmacology*, *572*(1), pp.12-22.

Durham, A.L., Caramori, G., Chung, K.F. and Adcock, I.M., (2016). Targeted anti-inflammatory therapeutics in asthma and chronic obstructive lung disease. *Translational Research*, 167(1), pp. 192–203.Elsevier Inc.,

Działo, E., Tkacz, K. and Błyszczuk, P., (2018). Crosstalk between the TGF-β and WNT signalling pathways during cardiac fibrogenesis. *Acta Biochimica Polonica*, *65*(3).

Edlund, S., Bu, S., Schuster, N., Aspenstrom, P., Heuchel, R., Heldin, N.E., ten Dijke, P., Heldin, C.H. and Landstrom, M., (2003). Transforming growth factor-β1 (TGF-β)–induced apoptosis of prostate cancer cells involves Smad7-dependent activation of p38 by TGF-β-activated kinase 1 and mitogen-activated protein kinase kinase 3. *Molecular biology of the cell*, *14*(2), pp.529-544.

Ehre, C., Rossi, A.H., Abdullah, L.H., De Pestel, K., Hill, S., Olsen, J.C. and Davis, C.W., (2005). Barrier role of actin filaments in regulated mucin secretion from airway goblet cells. *American Journal of Physiology-Cell Physiology*.

Elderbroom, J.L., Huang, J.J., Gatza, C.E., Chen, J., How, T., Starr, M., Nixon, A.B. and Blobe, G.C., (2014). Ectodomain shedding of TβRIII is required for TβRIII-mediated suppression of TGF-β signaling and breast cancer migration and invasion. *Molecular biology of the cell*, *25*(16), pp.2320-2332.

El-Husseini, Z.W., Gosens, R., Dekker, F. and Koppelman, G.H., (2020). The genetics of asthma and the promise of genomics-guided drug target discovery. *The Lancet Respiratory Medicine*, *8*(10), pp.1045-1056.

Ellis, L.R., Warner, D.R., Greene, R.M. and Pisano, M.M., (2003b). Interaction of Smads with collagen types I, III, and V. *Biochemical and biophysical research communications*, *310*(4), pp.1117-1123.

Ellis, R., Leigh, R., Southam, D., O'Byrne, P.M. and Inman, M.D., (2003). Morphometric analysis of mouse airways after chronic allergen challenge. *Laboratory investigation*, *83*(9), pp.1285-1291.

Epa, A.P., Thatcher, T.H., Pollock, S.J., Wahl, L.A., Lyda, E., Kottmann, R.M., Phipps, R.P. and Sime, P.J., (2015). Normal human lung epithelial cells inhibit transforming growth factor-β induced myofibroblast differentiation via prostaglandin E2. *PloS one*, *10*(8), p.e0135266.

Ershler, W.B. and Keller, E.T., (2000). Age-associated increased interleukin-6 gene expression, late-life diseases, and frailty. *Annual review of medicine*, *51*(1), pp.245-270.

Eunhee, S.Y., Bedoya, A., Lee, H., Chin, E., Saunders, W., Kim, S.J., Danielpour, D., Remick, D.G., Yin, S. and Ulich, T.R., (1996). Radiation-induced lung injury in vivo: Expression of transforming growth factor—Beta precedes fibrosis. *Inflammation*, *20*(4), pp.339-352.

Evans, R.L., Nials, A.T., Knowles, R.G., Kidd, E.J., Ford, W.R. and Broadley, K.J., (2012). A comparison of antiasthma drugs between acute and chronic ovalbumin-challenged guinea-pig models of asthma. *Pulmonary pharmacology & therapeutics*, *25*(6), pp.453-464.

Fagone, E., Conte, E., Gili, E., Fruciano, M., Pistorio, M.P., Lo Furno, D., Giuffrida, R., Crimi, N. and Vancheri, C., (2011). Resveratrol inhibits transforming growth

factor-β–induced proliferation and differentiation of ex vivo human lung fibroblasts into myofibroblasts through ERK/Akt inhibition and PTEN restoration. *Experimental lung research*, *37*(3), pp.162-174.

Fahy, W.A., Homayoun-Valiani, F., Cahn, A., Robertson, J., Templeton, A., Meeraus, W.H., Wilson, R., Lowings, M., Marotti, M., West, S.L. and Tabberer, M., (2021). Nemiralisib in patients with an acute exacerbation of COPD: placebo-controlled, dose-ranging study. *International journal of chronic obstructive pulmonary disease*, pp.1637-1646.

Fahya, J.V., Kimb, K.W., Liub, J. and Bousheya, H.A., (1995). Prominent neutrophilic inflammation in sputum from subjects with asthma exacerbation. *Journal of Allergy and Clinical Immunology*, *95*(4), pp.843-852.

Farkas, L., Gauldie, J., Voelkel, N.F. and Kolb, M., (2011). Pulmonary hypertension and idiopathic pulmonary fibrosis: A tale of angiogenesis, apoptosis, and growth factors. *American Journal of Respiratory Cell and Molecular Biology*, 45(1), pp. 1–15.

Fedorov, I.A., Wilson, S.J., Davies, D.E. and Holgate, S.T., (2005). Epithelial stress and structural remodelling in childhood asthma. *Thorax*, *60*(5), pp.389-394.

Fehrenbach, H., Wagner, C. and Wegmann, M., (2017). Airway remodeling in asthma: what really matters. *Cell and tissue research*, *367*(3), pp.551-569.

Feng, X.H. and Derynck, R., (1997). A kinase subdomain of transforming growth factor-β (TGF-β) type I receptor determines the TGF-β intracellular signaling specificity. *The EMBO journal*, *16*(13), pp.3912-3923.

Fernandez, I.E. and Eickelberg, O., (2012). The impact of TGF-β on lung fibrosis: from targeting to biomarkers. *Proceedings of the American Thoracic Society*, *9*(3), pp.111-116.

Fernandez, I.E. and Eickelberg, O., 2012. The impact of TGF-β on lung fibrosis: from targeting to biomarkers. *Proceedings of the American Thoracic Society*, *9*(3), pp.111-116.

Fetahu, I.S., Hummel, D.M., Manhardt, T., Aggarwal, A., Baumgartner-Parzer, S. and Kállay, E., (2014). Regulation of the calcium-sensing receptor expression by 1, 25-dihydroxyvitamin D3, interleukin-6, and tumor necrosis factor alpha in colon cancer cells. *The Journal of steroid biochemistry and molecular biology*, *144*, pp.228-231.

Finney, B.A., Del Moral, P.M., Wilkinson, W.J., Cayzac, S., Cole, M., Warburton, D., Kemp, P.J. and Riccardi, D., (2008). Regulation of mouse lung development by the extracellular calcium-sensing receptor, CaR. *The Journal of physiology*, *586*(24), pp.6007-6019.

Finnson, K.W., Almadani, Y. and Philip, A., (2020). Non-canonical (non-SMAD2/3) TGF-β signaling in fibrosis: Mechanisms and targets. In *Seminars in cell & developmental biology* (Vol. 101, pp. 115-122). Academic Press.

Finnson, K.W., Almadani, Y. and Philip, A., (2020). Non-canonical (non-SMAD2/3) TGF-β signaling in fibrosis: Mechanisms and targets. *Seminars in cell & developmental biology*, 101, pp.115-122.

FitzGerald, J.M., Tavakoli, H., Lynd, L.D., Al Efraij, K. and Sadatsafavi, M., (2017). The impact of inappropriate use of short acting beta agonists in asthma. *Respiratory medicine*, *131*, pp.135-140.

Forsey, R.J., Thompson, J.M., Ernerudh, J., Hurst, T.L., Strindhall, J., Johansson, B., Nilsson, B.O. and Wikby, A., (2003). Plasma cytokine profiles in elderly humans. *Mechanisms of ageing and development*, *124*(4), pp.487-493.

Franceschi, C., Bonafe, M. and Valensin, S., (2000). Human immunosenescence: the prevailing of innate immunity, the failing of clonotypic immunity, and the filling of immunological space. *Vaccine*, *18*(16), pp.1717-1720.

Franceschi, C., Bonafe, M., Valensin, S., Olivieri, F., De Luca, M., Ottaviani, E. and De Benedictis, G., (2000). Inflamm-aging: an evolutionary perspective on immunosenescence. *Annals of the new York Academy of Sciences*, *908*(1), pp.244-254.

Franks, T.J., Colby, T.V., Travis, W.D., Tuder, R.M., Reynolds, H.Y., Brody, A.R., Cardoso, W.V., Crystal, R.G., Drake, C.J., Engelhardt, J. and Frid, M., (2008). Resident cellular components of the human lung: current knowledge and goals for research on cell phenotyping and function. *Proceedings of the American Thoracic Society*, *5*(7), pp.763-766.

Fujisawa, Y., Matsuda, K. and Uehara, T., (2020). Osteopontin enhances the migration of lung fibroblasts via upregulation of interleukin-6 through the extracellular signal-regulated kinase (ERK) pathway. *Biological Chemistry*, *401*(9), pp.1071-1080.

Fulöp Jr, T., Douziech, N., Jacob, M.P., Hauck, M., Wallach, J. and Robert, L., (2001). Age-related alterations in the signal transduction pathways of the elastin-laminin receptor. *Pathologie Biologie*, *49*(4), pp.339-348.

Gagliardo, R., Chanez, P., Mathieu, M., Bruno, A., Costanzo, G., Gougat, C., Vachier, I., Bousquet, J., Bonsignore, G. and Vignola, A.M., (2003). Persistent activation of nuclear factor–κB signaling pathway in severe uncontrolled asthma. *American journal of respiratory and critical care medicine*, *168*(10), pp.1190-1198.

Gaikwad, A.V., Eapen, M.S., McAlinden, K.D., Chia, C., Larby, J., Myers, S., Dey, S., Haug, G., Markos, J., Glanville, A.R. and Sohal, S.S., (2020). Endothelial to mesenchymal transition (EndMT) and vascular remodeling in pulmonary hypertension and idiopathic pulmonary fibrosis. *Expert Review of Respiratory Medicine*, *14*(10), pp.1027-1043.

Galli, J.A., Pandya, A., Vega-Olivo, M., Dass, C., Zhao, H. and Criner, G.J., (2017). Pirfenidone and nintedanib for pulmonary fibrosis in clinical practice: tolerability and adverse drug reactions. *Respirology*, *22*(6), pp.1171-1178.

Ge, Q., Chen, L., Jaffar, J., Argraves, W.S., Twal, W.O., Hansbro, P., Black, J.L., Burgess, J.K. and Oliver, B., (2015). Fibulin1C peptide induces cell attachment and extracellular matrix deposition in lung fibroblasts. *Scientific reports*, *5*(1), pp.1-6.

Ge, Q., Wang, J., Simcock, D., Kanabar-Raivadera, V., Hirst, S., Ward, J., Sawant, S., Van De Velde, R., Oliver, B.G., Ashton, A. and Burgess, J.K., (2017). Connective Tissue Growth Factor (ctgf)-A Key Factor In Asthmatic Airway Angiogenesis. In *C108*.

GETTING INFLAMED: MARKERS OF LUNG INJURY AND REMODELLING (pp. A6942-A6942). American Thoracic Society.

Geibel, J.P. and Hebert, S.C., (2009). The functions and roles of the extracellular Ca2+–sensing receptor along the gastrointestinal tract. *Annual Review of Physiology*, *71*, pp.205-217.

Geng, Y., Mosyak, L., Kurinov, I., Zuo, H., Sturchler, E., Cheng, T.C., Subramanyam, P., Brown, A.P., Brennan, S.C., Mun, H.C. and Bush, M., (2016). Structural mechanism of ligand activation in human calcium-sensing receptor. *Elife*, *5*, p.e13662.

George, P.M., Spagnolo, P., Kreuter, M., Altinisik, G., Bonifazi, M., Martinez, F.J., Molyneaux, P.L., Renzoni, E.A., Richeldi, L., Tomassetti, S. and Valenzuela, C., (2020). Progressive fibrosing interstitial lung disease: clinical uncertainties, consensus recommendations, and research priorities. *The lancet Respiratory medicine*, *8*(9), pp.925-934.

Gerthoffer, W.T., (2007). Migration of Airway Smooth Muscle Cells. *Proceedings of the American Thoracic Society*, 5(1), pp. 97–105.

Gharaee-Kermani, M., Hu, B., Phan, S.H. and Gyetko, M.R., (2009). Recent advances in molecular targets and treatment of idiopathic pulmonary fibrosis: focus on TGF-ß signaling and the myofibroblast. *Current medicinal chemistry*, *16*(11), pp.1400-1417.

Gheyas, R., Brennan, L.A., Kantorow, M. and Menko, A.S., (2017). A role for the PI3K regulator PIK3IP1 in signaling the autophagy-dependent removal of organelles during lens development. *Investigative Ophthalmology & Visual Science*, *58*(8), pp.1712-1712.

Ghio, A.J., Dailey, L.A., Soukup, J.M., Stonehuerner, J., Richards, J.H. and Devlin, R.B., (2013). Growth of human bronchial epithelial cells at an air-liquid interface alters the response to particle exposure. *Particle and fibre toxicology*, *10*(1), pp.1-8.

Ghorani, V., Boskabady, M.H., Khazdair, M.R. and Kianmeher, M., (2017). Experimental animal models for COPD: a methodological review. *Tobacco induced diseases*, *15*(1), pp.1-13.

Ghorani, V., Boskabady, M.H., Khazdair, M.R. and Kianmeher, M., (2017). Experimental animal models for COPD: a methodological review. *Tobacco induced diseases*, *15*(1), pp.1-13.

Ghosh, A.K., Yuan, W., Mori, Y. and Varga, J., (2000). Smad-dependent stimulation of type I collagen gene expression in human skin fibroblasts by TGF-ß involves functional cooperation with p300/CBP transcriptional coactivators. *Oncogene*, *19*(31), pp.3546-3555.

Gibson, P.G., Woolley, K.L., Carty, K., Murree-Allen, K. and Saltos, N., (1998). Induced sputum eosinophil cationic protein (ECP) measurement in asthma and chronic obstructive airway disease (COAD). *Clinical and experimental allergy: Journal of the British Society for Allergy and Clinical Immunology*, *28*(9), pp.1081-1088.

GINA Guidelines, (2018). Global Strategy for Asthma Management and Prevention.

Glasser, S.W., Hagood, J.S., Wong, S., Taype, C.A., Madala, S.K. and Hardie, W.D., (2016). Mechanisms of lung fibrosis resolution. *The American journal of pathology*, *186*(5), pp.1066-1077.

Godin, L.M., Sandri, B.J., Wagner, D.E., Meyer, C.M., Price, A.P., Akinnola, I., Weiss, D.J. and Panoskaltsis-Mortari, A., (2016). Decreased laminin expression by human lung epithelial cells and fibroblasts cultured in acellular lung scaffolds from aged mice. *PloS one*, *11*(3), p.e0150966.

Goffin, J.M., Pittet, P., Csucs, G., Lussi, J.W., Meister, J.J. and Hinz, B., (2006). Focal adhesion size controls tension-dependent recruitment of α-smooth muscle actin to stress fibers. *Journal of Cell Biology*, 172(2), pp. 259–268.

Gohy, S.T., Hupin, C., Fregimilicka, C., Detry, B.R., Bouzin, C., Chevronay, H.G., Lecocq, M., Weynand, B., Ladjemi, M.Z., Pierreux, C.E. and Birembaut, P., (2015). Imprinting of the COPD airway epithelium for dedifferentiation and mesenchymal transition. *European Respiratory Journal*, *45*(5), pp.1258-1272.

Gómez, C.R., Acuna-Castillo, C., Nishimura, S., Pérez, V., Escobar, A., Salazar-Onfray, F., Sabaj, V., Torres, C., Walter, R. and Sierra, F., (2006). Serum from aged F344 rats conditions the activation of young macrophages. *Mechanisms of ageing and development*, *127*(3), pp.257-263.

Gomez, C.R., Nomellini, V., Baila, H., Oshima, K. and Kovacs, E.J., (2009). Comparison of the effects of aging and IL-6 on the hepatic inflammatory response in two models of systemic injury: scald injury versus ip LPS administration. *Shock (Augusta, Ga.)*, *31*(2), p.178.

Gon, Y., Hashimoto, S., Nakayama, T., Matsumoto, K., Koura, T., Takeshita, I. and Horie, T., (2000). N-acetyl-L-cysteine inhibits bleomycin-induced interleukin-8 secretion by bronchial epithelial cells. *Respirology*, *5*(4), pp.309-313.

Graca, J.A.Z., Schepelmann, M., Brennan, S.C., Reens, J., Chang, W., Yan, P., Toka, H., Riccardi, D. and Price, S.A., (2016). Comparative expression of the extracellular calcium-sensing receptor in the mouse, rat, and human kidney. *American Journal of Physiology-Renal Physiology*, *310*(6), pp.F518-F533.

Grewal, S.S. and Edgar, B.A., (2003). Controlling cell division in yeast and animals: does size matter?. *Journal of biology*, *2*(1), pp.1-4.

Grigoras, A., Caruntu, I.D., Grigoras, C.C., Mihaescu, T. and Amalinei, C., (2012). Relationship between immunohistochemical assessment of bronchial mucosa microvascularization and clinical stage in asthma. *Rom J Morphol Embryol*, *53*(3), pp.485-90.

Grubek-Jaworska, H., Paplińska, M., Hermanowicz-Salamon, J., Białek-Gosk, K., Dąbrowska, M., Grabczak, E., Domagała-Kulawik, J., Stępień, J. and Chazan, R., (2012). IL-6 and IL-13 in induced sputum of COPD and asthma patients: correlation with respiratory tests. *Respiration*, *84*(2), pp.101-107.

Guan, P., Cai, W., Yu, H., Wu, Z., Li, W., Wu, J., Chen, J. and Feng, G., (2017). Cigarette smoke extract promotes proliferation of airway smooth muscle cells through suppressing C/EBP-α expression. *Experimental and Therapeutic Medicine*, *13*(4), pp.1408-1414.

Gulati, S. and Thannickal, V.J., (2019). The aging lung and idiopathic pulmonary fibrosis. *The American journal of the medical sciences*, *357*(5), pp.384-389.

Gulati, S., Wells, J.M., Urdaneta, G.P., Balestrini, K., Vital, I., Tovar, K., Barnes, J.W., Bhatt, S.P., Campos, M. and Krick, S., (2019). Fibroblast growth factor 23 is associated with a frequent Exacerbator phenotype in COPD: a cross-sectional pilot study. *International journal of molecular sciences*, *20*(9), p.2292.

Haidar, M., Whitworth, J., Noé, G., Liu, W.Q., Vidal, M. and Langsley, G., (2015). TGF-β2 induces Grb2 to recruit PI3-K to TGF-RII that activates JNK/AP-1-signaling and augments invasiveness of Theileria-transformed macrophages. *Scientific reports*, *5*(1), pp.1-11.

Hallgren, O., Rolandsson, S., Andersson-Sjöland, A., Nihlberg, K., Wieslander, E., Kvist-Reimer, M., Dahlbäck, M., Eriksson, L., Bjermer, L., Erjefält, J.S., Löfdahl, C.G. and Westergren-Thorsson, G., (2012). Enhanced ROCK1 dependent contractility in fibroblast from chronic obstructive pulmonary disease patients. *Journal of Translational Medicine*, 10(1), pp. 1–11.

Halpin, D.M., Criner, G.J., Papi, A., Singh, D., Anzueto, A., Martinez, F.J., Agusti, A. and Vogelmeier, C.F., (2020). Committee GS. Global initiative for the diagnosis, management, and prevention of chronic obstructive lung disease: the 2020 GOLD science committee report on COVID-19 & COPD. *Am J Respir Crit Care Med*.

Halse, J., Greenspan, S., Cosman, F., Ellis, G., Santora, A., Leung, A., Heyden, N., Samanta, S., Doleckyj, S., Rosenberg, E. and Denker, A.E., (2014). A phase 2, randomized, placebo-controlled, dose-ranging study of the calcium-sensing receptor antagonist MK-5442 in the treatment of postmenopausal women with osteoporosis. *The Journal of Clinical Endocrinology & Metabolism*, *99*(11), pp.E2207-E2215.

Halwani, R., Al-Muhsen, S., Al-Jahdali, H. and Hamid, Q., (2011). Role of transforming growth factor–β in airway remodeling in asthma. *American journal of respiratory cell and molecular biology*, *44*(2), pp.127-133.

Hamanaka, R.B., O'Leary, E.M., Witt, L.J., Tian, Y., Gökalp, G.A., Meliton, A.Y., Dulin, N.O. and Mutlu, G.M., (2019). Glutamine metabolism is required for collagen protein synthesis in lung fibroblasts. *American journal of respiratory cell and molecular biology*, *61*(5), pp.597-606.

Hamilton Jr, R.F., Li, L., Felder, T.B. and Holian, A., (1995). Bleomycin induces apoptosis in human alveolar macrophages. *American Journal of Physiology-Lung Cellular and Molecular Physiology*, *269*(3), pp.L318-L325.

Hammer III, J.A. and Wu, X.S., (2002). Rabs grab motors: defining the connections between Rab GTPases and motor proteins. *Current opinion in cell biology*, *14*(1), pp.69-75.

Hamzaoui, A., Berraies, A., Kaabachi, W., Haifa, M., Ammar, J. and Kamel, H., (2013). Induced sputum levels of IL-33 and soluble ST2 in young asthmatic children. *Journal of Asthma*, *50*(8), pp.803-809.

Hansbro, P.M., Liu, G., Cooley, M.A., Jarnicki, A.G., Hsu, A.C., Nair, P.M., Haw, T.J., Fricker, M., Gellatly, S.L., Kim, R.Y. and Inman, M.D., (2016). Fibulin-1 Plays

Critical Roles In The Pathogenesis Of Pulmonary Diseases. In *C98. AIRWAY REMODELING IN COPD AND ASTHMA* (pp. A6175-A6175). American Thoracic Society.

Hansell, D.M., Bankier, A.A., MacMahon, H., McLoud, T.C., Muller, N.L. and Remy, J., (2008). Fleischner Society: glossary of terms for thoracic imaging. *Radiology*, *246*(3), pp.697-722.

Hargaden, M. and Singer, L., (2012). Anatomy, physiology, and behavior. In *The laboratory rabbit, guinea pig, hamster, and other rodents* (pp. 575-602). Academic Press.

Hargreave, F.E. and Parameswaran, K., (2006). Asthma, COPD and bronchitis are just components of airway disease. *European Respiratory Journal*, 28(2), pp. 264–267.European Respiratory Society,

Hasday, J.D., Bascom, R., Costa, J.J., Fitzgerald, T. and Dubin, W., (1999). Bacterial endotoxin is an active component of cigarette smoke. *Chest*, *115*(3), pp.829-835.

Hayakawa, H., Hayakawa, M., Kume, A. and Tominaga, S.I., (2007). Soluble ST2 blocks interleukin-33 signaling in allergic airway inflammation. *Journal of Biological Chemistry*, *282*(36), pp.26369-26380.

Hecker, L., Logsdon, N.J., Kurundkar, D., Kurundkar, A., Bernard, K., Hock, T., Meldrum, E., Sanders, Y.Y. and Thannickal, V.J., (2014). Reversal of persistent fibrosis in aging by targeting Nox4-Nrf2 redox imbalance. *Science translational medicine*, *6*(231), pp.231ra47-231ra47.

Heijink, I.H., de Bruin, H.G., Dennebos, R., Jonker, M.R., Noordhoek, J.A., Brandsma, C.A., van den Berge, M. and Postma, D.S., (2016). Cigarette smoke-induced epithelial expression of WNT-5B: implications for COPD. *European Respiratory Journal*, *48*(2), pp.504-515.

Hekking, P.P.W., Wener, R.R., Amelink, M., Zwinderman, A.H., Bouvy, M.L. and Bel, E.H., (2015). The prevalence of severe refractory asthma. *Journal of Allergy and Clinical Immunology*, *135*(4), pp.896-902.

Heldin, C.H., Landström, M. and Moustakas, A., (2009). Mechanism of TGF-β signaling to growth arrest, apoptosis, and epithelial–mesenchymal transition. *Current opinion in cell biology*, *21*(2), pp.166-176.

Hendy, G.N. and Canaff, L., (2016), January. Calcium-sensing receptor, proinflammatory cytokines and calcium homeostasis. In *Seminars in cell & developmental biology* (Vol. 49, pp. 37-43). Academic Press.

Hesse, M., Modolell, M., La Flamme, A.C., Schito, M., Fuentes, J.M., Cheever, A.W., Pearce, E.J. and Wynn, T.A., (2001). Differential regulation of nitric oxide synthase-2 and arginase-1 by type 1/type 2 cytokines in vivo: granulomatous pathology is shaped by the pattern of L-arginine metabolism. *The Journal of Immunology*, *167*(11), pp.6533-6544.

Hikichi, M., Mizumura, K., Maruoka, S. and Gon, Y., (2019). Pathogenesis of chronic obstructive pulmonary disease (COPD) induced by cigarette smoke. *Journal of thoracic disease*, *11*(Suppl 17), p.S2129.

Hills, C.E., Younis, M.Y., Bennett, J., Siamantouras, E., Liu, K.K. and Squires, P.E., (2012). Calcium-sensing receptor activation increases cell-cell adhesion and β-cell function. *Cellular Physiology and Biochemistry*, *30*(3), pp.575-586.

Hinz, B., (2016). Myofibroblasts. *Experimental eye research*, *142*, pp.56-70.

Hinz, B., Phan, S.H., Thannickal, V.J., Galli, A., Bochaton-Piallat, M.L. and Gabbiani, G., (2007). The myofibroblast: one function, multiple origins. *The American journal of pathology*, *170*(6), pp.1807-1816.

Hirota, J.A., Ellis, R. and Inman, M.D., (2006). Regional differences in the pattern of airway remodeling following chronic allergen exposure in mice. *Respiratory research*, *7*(1), pp.1-9.

Hirota, N. and Martin, J.G., (2013). Mechanisms of airway remodeling. *Chest*, *144*(3), pp.1026-1032.

Hobson, S.A., McNeil, S.E., Lee, F. and Rodland, K.D., (2000). Signal transduction mechanisms linking increased extracellular calcium to proliferation in ovarian surface epithelial cells. *Experimental cell research*, *258*(1), pp.1-11.

Hofer, A.M. and Brown, E.M., (2003). Extracellular calcium sensing and signalling. *Nature reviews Molecular cell biology*, *4*(7), pp.530-538.

Hoff, C.R., Perkins, D.R. and Davidson, J.M., (1999). Elastin gene expression is upregulated during pulmonary fibrosis. *Connective tissue research*, *40*(2), pp.145-153.

Hogg, J.C. and Timens, W., (2009). The pathology of chronic obstructive pulmonary disease. *Annual Review of Pathology: Mechanisms of Disease*, *4*, pp.435-459.

Hogg, J.C., Chu, F., Utokaparch, S., Woods, R., Elliott, W.M., Buzatu, L., Cherniack, R.M., Rogers, R.M., Sciurba, F.C., Coxson, H.O. and Paré, P.D., (2004). The nature of small-airway obstruction in chronic obstructive pulmonary disease. *New England Journal of Medicine*, *350*(26), pp.2645-2653.

Hogg, J.C., Macklem, P.T. and Thurlbeck, W.M., (1968). Site and nature of airway obstruction in chronic obstructive lung disease. *New England Journal of Medicine*, *278*(25), pp.1355-1360.

Hogg, J.C., McDonough, J.E., Gosselink, J. V. and Hayashi, S., (2009). What drives the peripheral lung-remodeling process in chronic obstructive pulmonary disease? *Proceedings of the American Thoracic Society*, 6(8), pp. 668–672.

Hohmann, M.S., Habiel, D.M., Coelho, A.L., Verri Jr, W.A. and Hogaboam, C.M., (2019). Quercetin enhances ligand-induced apoptosis in senescent idiopathic pulmonary fibrosis fibroblasts and reduces lung fibrosis in vivo. *American journal of respiratory cell and molecular biology*, *60*(1), pp.28-40.

Holtwick, R., Gotthardt, M., Skryabin, B., Steinmetz, M., Potthast, R., Zetsche, B., Hammer, R.E., Herz, J. and Kuhn, M., (2002). Smooth muscle-selective deletion of guanylyl cyclase-A prevents the acute but not chronic effects of ANP on blood pressure. *Proceedings of the National Academy of Sciences*, *99*(10), pp.7142-7147.

Hong, K.M., Belperio, J.A., Keane, M.P., Burdick, M.D. and Strieter, R.M., (2007). Differentiation of human circulating fibrocytes as mediated by transforming growth factor-β and peroxisome proliferator-activated receptor γ. *Journal of Biological Chemistry*, *282*(31), pp.22910-22920.

Hong, W., (2005). SNAREs and traffic. *Biochimica et Biophysica Acta (BBA)-Molecular Cell Research*, *1744*(2), pp.120-144.

Horowitz, J.C., Ajayi, I.O., Kulasekaran, P., Rogers, D.S., White, J.B., Townsend, S.K., White, E.S., Nho, R.S., Higgins, P.D., Huang, S.K. and Sisson, T.H., (2012). Survivin expression induced by endothelin-1 promotes myofibroblast resistance to apoptosis. *The international journal of biochemistry & cell biology*, *44*(1), pp.158-169.

Hoshino, M., Takahashi, M. and Aoike, N., (2001). Expression of vascular endothelial growth factor, basic fibroblast growth factor, and angiogenin immunoreactivity in asthmatic airways and its relationship to angiogenesis. *Journal of Allergy and Clinical Immunology*, *107*(2), pp.295-301.

Hough, K.P., Curtiss, M.L., Blain, T.J., Liu, R.M., Trevor, J., Deshane, J.S. and Thannickal, V.J., (2020). Airway remodeling in asthma. *Frontiers in Medicine*, *7*, p.191.

Hoyles, R.K., Derrett-Smith, E.C., Khan, K., Shiwen, X., Howat, S.L., Wells, A.U., Abraham, D.J. and Denton, C.P., (2011). An essential role for resident fibroblasts in experimental lung fibrosis is defined by lineage-specific deletion of high-affinity type II transforming growth factor ß receptor. *American journal of respiratory and critical care medicine*, *183*(2), pp.249-261.

Hoyt, D.G. and Lazo, J.S., (1988). Alterations in pulmonary mRNA encoding procollagens, fibronectin and transforming growth factor-beta precede bleomycin-induced pulmonary fibrosis in mice. *Journal of Pharmacology and Experimental Therapeutics*, *246*(2), pp.765-771.

Hsu, H.S., Liu, C.C., Lin, J.H., Hsu, T.W., Hsu, J.W., Su, K. and Hung, S.C., (2017). Involvement of ER stress, PI3K/AKT activation, and lung fibroblast proliferation in bleomycin-induced pulmonary fibrosis. *Scientific reports*, *7*(1), pp.1-11.

Hu, B., Wu, Z. and Phan, S.H., (2003). Smad3 mediates transforming growth factor-ß–induced α-smooth muscle actin expression. *American journal of respiratory cell and molecular biology*, *29*(3), pp.397-404.

Hu, B., Wu, Z. and Phan, S.H., (2003). Smad3 mediates transforming growth factor-ß–induced α-smooth muscle actin expression. *American journal of respiratory cell and molecular biology*, *29*(3), pp.397-404.

Hu, H.H., Cao, G., Wu, X.Q., Vaziri, N.D. and Zhao, Y.Y., (2020a). Wnt signaling pathway in aging-related tissue fibrosis and therapies. *Ageing research reviews*, *60*, p.101063.

Hu, H.H., Chen, D.Q., Wang, Y.N., Feng, Y.L., Cao, G., Vaziri, N.D. and Zhao, Y.Y., (2018). New insights into TGF-ß/Smad signaling in tissue fibrosis. *Chemico-biological interactions*, *292*, pp.76-83.

Hu, X., Xu, Q., Wan, H., Hu, Y., Xing, S., Yang, H., Gao, Y. and He, Z., (2020b). PI3K-Akt-mTOR/PFKFB3 pathway mediated lung fibroblast aerobic glycolysis and collagen synthesis in lipopolysaccharide-induced pulmonary fibrosis. *Laboratory Investigation*, *100*(6), pp.801-811.

Hu, Y., Peng, J., Feng, D., Chu, L., Li, X., Jin, Z., Lin, Z. and Zeng, Q., (2006). Role of extracellular signal-regulated kinase, p38 kinase, and activator protein-1 in transforming growth factor-ß1–induced alpha smooth muscle actin expression in human fetal lung fibroblasts in vitro. *Lung*, *184*(1), pp.33-42.

Huang, C. and Miller, R.T., (2007). The calcium-sensing receptor and its interacting proteins. *Journal of cellular and molecular medicine*, *11*(5), pp.923-934.

Huang, C. Da, Ammit, A.J., Tliba, O., Kuo, H.P., Penn, R.B., Panettieri, R.A. and Amrani, Y., (2005). G-Protein-coupled receptor agonists differentially regulate basal or tumor necrosis factor-α-stimulated activation of interleukin-6 and RANTES in human airway smooth muscle cells. *Journal of Biomedical Science*, 12(5), pp. 763–776.

Huang, C., Hujer, K.M., Wu, Z. and Miller, R.T., (2004). The Ca2+-sensing receptor couples to Gα12/13 to activate phospholipase D in Madin-Darby canine kidney cells. *American Journal of Physiology-Cell Physiology*, *286*(1), pp.C22-C30.

Huang, K., Rabold, R., Schofield, B., Mitzner, W. and Tankersley, C.G., (2007). Age-dependent changes of airway and lung parenchyma in C57BL/6J mice. *Journal of Applied Physiology*, *102*(1), pp.200-206.

Huang, S.K., Wettlaufer, S.H., Chung, J. and Peters-Golden, M., (2008). Prostaglandin E2 inhibits specific lung fibroblast functions via selective actions of PKA and Epac-1. *American journal of respiratory cell and molecular biology*, *39*(4), pp.482-489.

Huang, S.K., White, E.S., Wettlaufer, S.H., Grifka, H., Hogaboam, C.M., Thannickal, V.J., Horowitz, J.C. and Peters-Golden, M., (2009). Prostaglandin E2 induces fibroblast apoptosis by modulating multiple survival pathways. *The FASEB Journal*, *23*(12), pp.4317-4326.

Hübner, R.H., Gitter, W., Eddine El Mokhtari, N., Mathiak, M., Both, M., Bolte, H., Freitag-Wolf, S. and Bewig, B., (2008). Standardized quantification of pulmonary fibrosis in histological samples. *Biotechniques*, *44*(4), pp.507-517.

Hudgins, A.D., Tazearslan, C., Tare, A., Zhu, Y., Huffman, D. and Suh, Y., (2018). Age-and tissue-specific expression of senescence biomarkers in mice. *Frontiers in genetics*, *9*, p.59.

Hung, W.Y., Lee, W.J., Cheng, G.Z., Tsai, C.H., Yang, Y.C., Lai, T.C., Chen, J.Q., Chung, C.L., Chang, J.H. and Chien, M.H., (2021). Blocking MMP-12-modulated epithelial-mesenchymal transition by repurposing penfluridol restrains lung adenocarcinoma metastasis via uPA/uPAR/TGF-β/Akt pathway. *Cellular Oncology*, *44*(5), pp.1087-1103.

Hussain, M., Xu, C., Lu, M., Wu, X., Tang, L. and Wu, X., (2017). Wnt/β-catenin signaling links embryonic lung development and asthmatic airway remodeling. *Biochimica et Biophysica Acta (BBA)-Molecular Basis of Disease*, *1863*(12), pp.3226-3242.

Hynes, R.O. and Naba, A., (2012). Overview of the matrisome—an inventory of extracellular matrix constituents and functions. *Cold Spring Harbor perspectives in biology*, *4*(1), p.a004903.

Iadevaia, V., Liu, R. and Proud, C.G., (2014). mTORC1 signaling controls multiple steps in ribosome biogenesis. In *Seminars in cell & developmental biology* (Vol. 36, pp. 113-120). Academic Press.

Ingram, J.L., Huggins, M.J., Church, T.D., Li, Y., Francisco, D.C., Degan, S., Firszt, R., Beaver, D.M., Lugogo, N.L., Wang, Y. and Sunday, M.E., (2011). Airway

fibroblasts in asthma manifest an invasive phenotype. *American journal of respiratory and critical care medicine*, *183*(12), pp.1625-1632.

Innes, A.L., Woodruff, P.G., Ferrando, R.E., Donnelly, S., Dolganov, G.M., Lazarus, S.C. and Fahy, J.V., (2006). Epithelial mucin stores are increased in the large airways of smokers with airflow obstruction. *Chest*, *130*(4), pp.1102-1108.

Inomata, M., Kamio, K., Azuma, A., Matsuda, K., Usuki, J., Morinaga, A., Tanaka, T., Kashiwada, T., Atsumi, K., Hayashi, H. and Fujita, K., (2021). Rictor-targeting exosomal microRNA-16 ameliorates lung fibrosis by inhibiting the mTORC2-SPARC axis. *Experimental Cell Research*, *398*(2), p.112416.

Insel, P.A., Murray, F., Yokoyama, U., Romano, S., Yun, H., Brown, L., Snead, A., Lu, D. and Aroonsakool, N., (2012). cAMP and Epac in the regulation of tissue fibrosis. *British journal of pharmacology*, *166*(2), pp.447-456.

Israel, E. and Reddel, H.K., (2017). Severe and difficult-to-treat asthma in adults. *New England Journal of Medicine*, *377*(10), pp.965-976.

Ito, J.T., Lourenço, J.D., Righetti, R.F., Tibério, I.F., Prado, C.M. and Lopes, F.D., (2019). Extracellular matrix component remodeling in respiratory diseases: what has been found in clinical and experimental studies?. *Cells*, *8*(4), p.342.

Janknecht, R., Ernst, W.H., Pingoud, V. and Nordheim, A., (1993). Activation of ternary complex factor Elk-1 by MAP kinases. *The EMBO journal*, *12*(13), pp.5097-5104.

Janssens, W., Lehouck, A., Carremans, C., Bouillon, R., Mathieu, C. and Decramer, M., (2009). Vitamin D beyond bones in chronic obstructive pulmonary disease: time to act. *American journal of respiratory and critical care medicine*, *179*(8), pp.630-636.

Jayakrishnan, B., Al-Mubaihsi, S.M., Kashoub, M.S. and George, J., (2018). Hypercalcaemia: A portent of sarcoidosis in cystic fibrosis. *Sultan Qaboos University Medical Journal*, *18*(4), p.e533.

Jeffery, P.K., 1983. Morphologic features of airway surface epithelial cells and glands. *American Review of Respiratory Disease*, *128*(2P2), pp.S14-S20.

Jeffery, P.K., Wardlaw, A.J., Nelson, F.C., Collins, J.V. and Kay, A.B., (1989). Bronchial biopsies in asthma: an ultrastructural quantitative study and correlation with hyperactivity. *Am Rev Respir Dis*, *140*, pp.1745-1753.

Jenkins, H.A., Cool, C., Szefler, S.J., Covar, R., Brugman, S., Gelfand, E.W. and Spahn, J.D., (2003). Histopathology of severe childhood asthma: a case series. *Chest*, *124*(1), pp.32-41.

Jhanwar-Uniyal, M., Wainwright, J.V., Mohan, A.L., Tobias, M.E., Murali, R., Gandhi, C.D. and Schmidt, M.H., (2019). Diverse signaling mechanisms of mTOR complexes: mTORC1 and mTORC2 in forming a formidable relationship. *Advances in biological regulation*, *72*, pp.51-62.

John, M.R., Harfst, E., Loeffler, J., Belleli, R., Mason, J., Bruin, G.J., Seuwen, K., Klickstein, L.B., Mindeholm, L., Widler, L. and Kneissel, M., (2014). AXT914 a novel, orally-active parathyroid hormone-releasing drug in two early studies of healthy volunteers and postmenopausal women. *Bone*, *64*, pp.204-210.

Johnson, P.R., Burgess, J.K., Underwood, P.A., Au, W., Poniris, M.H., Tamm, M., Ge, Q., Roth, M. and Black, J.L., (2004). Extracellular matrix proteins modulate asthmatic airway smooth muscle cell proliferation via an autocrine mechanism. *Journal of Allergy and Clinical Immunology*, *113*(4), pp.690-696.

Johnson, P.R., Roth, M., Tamm, M., Hughes, M., Ge, Q., King, G., Burgess, J.K. and Black, J.L., (2001). Airway smooth muscle cell proliferation is increased in asthma. *American journal of respiratory and critical care medicine*, *164*(3), pp.474-477.

Jones, R.L., Noble, P.B., Elliot, J.G. and James, A.L., (2016). Airway remodelling in COPD: It's not asthma!. *Respirology*, *21*(8), pp.1347-1356.

Jones, R.L., Noble, P.B., Elliot, J.G. and James, A.L., (2016). Airway remodelling in COPD: It's not asthma!. *Respirology*, *21*(8), pp.1347-1356.

Jun, J.I. and Lau, L.F., (2010). The matricellular protein CCN1 induces fibroblast senescence and restricts fibrosis in cutaneous wound healing. *Nature cell biology*, *12*(7), pp.676-685.

Justice, J.P., Crosby, J., Borchers, M.T., Tomkinson, A., Lee, J.J. and Lee, N.A., (2002). CD4+ T cell-dependent airway mucus production occurs in response to IL-5 expression in lung. *American Journal of Physiology-Lung Cellular and Molecular Physiology*, *282*(5), pp.L1066-L1074.

Kadler, K.E., Holmes, D.F., Trotter, J.A. and Chapman, J.A., (1996). Collagen fibril formation. *Biochemical Journal*, *316*(1), pp.1-11.

Kagan, H.M., (2000). Intra-and extracellular enzymes of collagen biosynthesis as biological and chemical targets in the control of fibrosis. *Acta tropica*, *77*(1), pp.147-152.

Kaneko, Y., Takashima, K., Suzuki, N. and Yamana, K., (2007). Effects of theophylline on chronic inflammatory lung injury induced by LPS exposure in guinea pigs. *Allergology International*, *56*(4), pp.445-456.

Karakioulaki, M., Papakonstantinou, E. and Stolz, D., (2020). Extracellular matrix remodelling in COPD. *European Respiratory Review*, *29*(158).

Karlsson, M., Zhang, C., Méar, L., Zhong, W., Digre, A., Katona, B., Sjöstedt, E., Butler, L., Odeberg, J., Dusart, P. and Edfors, F., (2021). A single–cell type transcriptomics map of human tissues. *Science Advances*, *7*(31), p.eabh2169.

Karsdal, M.A., Genovese, F., Madsen, E.A., Manon-Jensen, T. and Schuppan, D., (2016). Collagen and tissue turnover as a function of age: Implications for fibrosis. *Journal of hepatology*, *64*(1), pp.103-109.

Karsdal, M.A., Nielsen, S.H., Leeming, D.J., Langholm, L.L., Nielsen, M.J., Manon-Jensen, T., Siebuhr, A., Gudmann, N.S., Rønnow, S., Sand, J.M. and Daniels, S.J., (2017). The good and the bad collagens of fibrosis–their role in signaling and organ function. *Advanced drug delivery reviews*, *121*, pp.43-56.

Kato, K., Logsdon, N.J., Shin, Y.J., Palumbo, S., Knox, A., Irish, J.D., Rounseville, S.P., Rummel, S.R., Mohamed, M., Ahmad, K. and Trinh, J.M., (2020). Impaired myofibroblast dedifferentiation contributes to nonresolving fibrosis in aging. *American journal of respiratory cell and molecular biology*, *62*(5), pp.633-644.

Katzenstein, A.L.A., Mukhopadhyay, S. and Myers, J.L., (2008). Diagnosis of usual interstitial pneumonia and distinction from other fibrosing interstitial lung diseases. *Human pathology*, *39*(9), pp.1275-1294.

Kay, E.P., Lee, H.K., Park, K.S. and Lee, S.C., (1998). Indirect mitogenic effect of transforming growth factor-beta on cell proliferation of subconjunctival fibroblasts. *Investigative ophthalmology & visual science*, *39*(3), pp.481-486.

Ke, X., Do, D.C., Li, C., Zhao, Y., Kollarik, M., Fu, Q., Wan, M. and Gao, P., (2019). Ras homolog family member A/Rho-associated protein kinase 1 signaling modulates lineage commitment of mesenchymal stem cells in asthmatic patients through lymphoid enhancer–binding factor 1. *Journal of Allergy and Clinical Immunology*, *143*(4), pp.1560-1574.

Kenyon, N.J., Ward, R.W., McGrew, G. and Last, J.A., (2003). TGF-ß1 causes airway fibrosis and increased collagen I and III mRNA in mice. *Thorax*, *58*(9), pp.772-777.

Khalil, M.I., Madere, C., Ghosh, I., Adam, R.M. and De Benedetti, A., (2021). Interaction of TLK1 and AKTIP as a potential regulator of AKT activation in castration-resistant prostate cancer progression. *Pathophysiology*, *28*(3), pp.339-354.

Khalil, N., Corne, S., Whitman, C. and Yacyshyn, H., (1996). Plasmin regulates the activation of cell-associated latent TGF-beta 1 secreted by rat alveolar macrophages after in vivo bleomycin injury. *American journal of respiratory cell and molecular biology*, *15*(2), pp.252-259.

Khalil, N., Xu, Y.D., O'Connor, R. and Duronio, V., (2005). Proliferation of pulmonary interstitial fibroblasts is mediated by transforming growth factor-ß1-induced release of extracellular fibroblast growth factor-2 and phosphorylation of p38 MAPK and JNK. *Journal of Biological Chemistry*, *280*(52), pp.43000-43009.

Kifor, O., MacLeod, R.J., Diaz, R., Bai, M., Yamaguchi, T., Yao, T., Kifor, I. and Brown, E.M., (2001). Regulation of MAP kinase by calcium-sensing receptor in bovine parathyroid and CaR-transfected HEK293 cells. *American Journal of Physiology-Renal Physiology*, *280*(2), pp.F291-F302.

Kifor, O., MacLeod, R.J., Diaz, R., Bai, M., Yamaguchi, T., Yao, T., Kifor, I. and Brown, E.M., (2001). Regulation of MAP kinase by calcium-sensing receptor in bovine parathyroid and CaR-transfected HEK293 cells. *American Journal of Physiology-Renal Physiology*, *280*(2), pp.F291-F302.

Kim, C.S., Kim, J.M., Nam, S.Y., Yang, K.H., Jeong, M., Kim, H.S., Lim, Y.K., Kim, C.S., Jin, Y.W. and Kim, J., (2007a). Low-dose of ionizing radiation enhances cell proliferation via transient ERK1/2 and p38 activation in normal human lung fibroblasts. *Journal of radiation research*, *48*(5), pp.407-415.

Kim, K.K., Sheppard, D. and Chapman, H.A., (2018). TGF-ß1 signaling and tissue fibrosis. *Cold Spring Harbor perspectives in biology*, *10*(4), p.a022293.

Kim, S.I., Kwak, J.H., Zachariah, M., He, Y., Wang, L. and Choi, M.E., (2007b). TGF-ß-activated kinase 1 and TAK1-binding protein 1 cooperate to mediate TGF-ß1-induced MKK3-p38 MAPK activation and stimulation of type I collagen. *American Journal of Physiology-Renal Physiology*, *292*(5), pp.F1471-F1478.

King Jr, T.E., Bradford, W.Z., Castro-Bernardini, S., Fagan, E.A., Glaspole, I., Glassberg, M.K., Gorina, E., Hopkins, P.M., Kardatzke, D., Lancaster, L. and Lederer, D.J., (2014). A phase 3 trial of pirfenidone in patients with idiopathic pulmonary fibrosis. *New England Journal of Medicine*, *370*(22), pp.2083-2092.

King, T.E., Pardo, A. and Selman, M., (2011). Idiopathic pulmonary fibrosis. *The Lancet*, 378(9807), pp. 1949–1961.

Kjøller, L. and Hall, A., (1999). Signaling to rho GTPases. *Experimental cell research*, *253*(1), pp.166-179.

Kling, M.A., (2011). A review of respiratory system anatomy, physiology, and disease in the mouse, rat, hamster, and gerbil. *Veterinary Clinics: Exotic Animal Practice*, *14*(2), pp.287-337.

Knipe, R.S., Probst, C.K., Lagares, D., Franklin, A., Spinney, J.J., Brazee, P.L., Grasberger, P., Zhang, L., Black, K.E., Sakai, N., Shea, B.S., Liao, J.K., Medoff, B.D. and Tager, A.M., (2018). The rho kinase isoforms ROCK1 and ROCK2 each contribute to the development of experimental pulmonary fibrosis. *American Journal of Respiratory Cell and Molecular Biology*, 58(4), pp. 471–481.

Knudsen, L., Ruppert, C. and Ochs, M., (2017). Tissue remodelling in pulmonary fibrosis. *Cell and tissue research*, *367*(3), pp.607-626.

Kohyama, T., Yamauchi, Y., Takizawa, H., Itakura, S., Kamitani, S., Desaki, M., Kawasaki, S. and Nagase, T., (2009). Procaterol inhibits lung fibroblast migration. *Inflammation*, *32*(6), pp.387-392.

Koller, D.Y., Halmerbauer, G., Frischer, T. and Roithner, B., (1999). Assessment of eosinophil granule proteins in various body fluids: is there a relation to clinical variables in childhood asthma?. *Clinical and experimental allergy: journal of the British Society for Allergy and Clinical Immunology*, *29*(6), pp.786-793.

Kortlever, R.M., Higgins, P.J. and Bernards, R., (2006). Plasminogen activator inhibitor-1 is a critical downstream target of p53 in the induction of replicative senescence. *Nature cell biology*, *8*(8), pp.877-884.

Kotecha, S., Wangoo, A., Silverman, M. and Shaw, R.J., (1996). Increase in the concentration of transforming growth factor beta-1 in bronchoalveolar lavage fluid before development of chronic lung disease of prematurity. *The Journal of pediatrics*, *128*(4), pp.464-469.

Koumpagioti, D., Moriki, D., Boutopoulou, B., Matziou, V., Loukou, I., Priftis, K.N. and Douros, K., (2023). The Association between CFTR Gene Mutation Heterozygosity and Asthma Development: A Systematic Review. *Journal of Clinical Medicine*, *12*(6), p.2403.

Koussounadis, A., Langdon, S.P., Um, I.H., Harrison, D.J. and Smith, V.A., (2015). Relationship between differentially expressed mRNA and mRNA-protein correlations in a xenograft model system. *Scientific reports*, *5*(1), pp.1-9.

Kovacs, C.S., Ho-Pao, C.L., Hunzelman, J.L., Lanske, B., Fox, J., Seidman, J.G., Seidman, C.E. and Kronenberg, H.M., (1998). Regulation of murine fetal-placental calcium metabolism by the calcium-sensing receptor. *The Journal of clinical investigation*, *101*(12), pp.2812-2820.

Kovacs, E.J., Boe, D.M., Boule, L.A. and Curtis, B.J., 2017. Inflammaging and the lung. *Clinics in geriatric medicine*, *33*(4), pp.459-471.

Kovacs, E.J., Grabowski, K.A., Duffner, L.A., Plackett, T.P. and Gregory, M.S., (2002). Survival and cell mediated immunity after burn injury in aged mice. *Journal of the American Aging Association*, *25*(1), pp.3-9.

Kranenburg, A.R., Willems-Widyastuti, A., Mooi, W.J., Sterk, P.J., Alagappan, V.K., de Boer, W.I. and Sharma, H.S., (2006). Enhanced bronchial expression of extracellular matrix proteins in chronic obstructive pulmonary disease. *American journal of clinical pathology*, *126*(5), pp.725-735.

Kranenburg, O., Verlaan, I., Hordijk, P.L. and Moolenaar, W.H., (1997). Gi-mediated activation of the Ras/MAP kinase pathway involves a 100 kDa tyrosine-phosphorylated Grb2 SH3 binding protein, but not Src nor Shc. *The EMBO Journal*, *16*(11), pp.3097-3105.

Krizhanovsky, V., Yon, M., Dickins, R.A., Hearn, S., Simon, J., Miething, C., Yee, H., Zender, L. and Lowe, S.W., (2008). Senescence of activated stellate cells limits liver fibrosis. *Cell*, *134*(4), pp.657-667.

Kuang, P.P., Zhang, X.H., Rich, C.B., Foster, J.A., Subramanian, M. and Goldstein, R.H., (2007). Activation of elastin transcription by transforming growth factor-β in human lung fibroblasts. *American Journal of Physiology-Lung Cellular and Molecular Physiology*, *292*(4), pp.L944-L952.

Kühl, M., Sheldahl, L.C., Park, M., Miller, J.R. and Moon, R.T., (2000). The Wnt/Ca2+ pathway: a new vertebrate Wnt signaling pathway takes shape. *Trends in genetics*, *16*(7), pp.279-283.

Kular, J.K., Basu, S. and Sharma, R.I., (2014). The extracellular matrix: structure, composition, age-related differences, tools for analysis and applications for tissue engineering. *Journal of tissue engineering*, *5*, p.2041731414557112.

Kumar, A., Singh, U.K., Kini, S.G., Garg, V., Agrawal, S., Tomar, P.K., Pathak, P., Chaudhary, A., Gupta, P. and Malik, A., (2015). JNK pathway signaling: a novel and smarter therapeutic targets for various biological diseases. *Future medicinal chemistry*, *7*(15), pp.2065-2086.

Kumar, R.K. and Herbert, C., (2017). Airway epithelial cytokines in asthma and chronic obstructive pulmonary disease. In *Cytokine Effector Functions in Tissues* (pp. 163-172). Academic Press.

Kumar, R.K., Herbert, C. and Foster, P.S., (2008). The "classical" ovalbumin challenge model of asthma in mice. *Current drug targets*, *9*(6), pp.485-494.

Kumar, S., Matheny, C.J., Hoffman, S.J., Marquis, R.W., Schultz, M., Liang, X., Vasko, J.A., Stroup, G.B., Vaden, V.R., Haley, H. and Fox, J., (2010). An orally active calcium-sensing receptor antagonist that transiently increases plasma concentrations of PTH and stimulates bone formation. *Bone*, *46*(2), pp.534-542.

Kuperman, D.A., Huang, X., Koth, L.L., Chang, G.H., Dolganov, G.M., Zhu, Z., Elias, J.A., Sheppard, D. and Erle, D.J., (2002). Direct effects of interleukin-13 on epithelial cells cause airway hyperreactivity and mucus overproduction in asthma. *Nature medicine*, *8*(8), pp.885-889.

Kurosawa, M., Shimizu, Y., Tsukagoshi, H. and Ueki, M., (1992). Elevated levels of peripheral-blood, naturally occurring aliphatic polyamines in bronchial asthmatic patients with active symptoms. *Allergy*, *47*(6), pp.638-643.

Kurowska-Stolarska, M., Kewin, P., Murphy, G., Russo, R.C., Stolarski, B., Garcia, C.C., Komai-Koma, M., Pitman, N., Li, Y., McKenzie, A.N. and Teixeira, M.M., (2008). IL-33 induces antigen-specific IL-5+ T cells and promotes allergic-induced airway inflammation independent of IL-4. *The Journal of Immunology*, *181*(7), pp.4780-4790.

Laddha, A.P. and Kulkarni, Y.A., (2019). VEGF and FGF-2: promising targets for the treatment of respiratory disorders. *Respiratory medicine*, *156*, pp.33-46.

Lähteenvuo, J. and Rosenzweig, A., (2012). Effects of aging on angiogenesis. *Circulation research*, *110*(9), pp.1252-1264.

Laitinen, L.A., Heino, M., Laitinen, A., Kava, T. and Haahtela, T., (1985). Damage of the airway epithelium and bronchial reactivity in patients with asthma. *American Review of Respiratory Disease*, *131*(4), pp.599-606.

Lambrecht, B., and Hammad, H., (2015). The immunology of asthma. *Nature Immunology*, 16(1), pp.45-56.

Lammert, E., Lammert, E., Zeeb, M. and Zeeb, M., (2014). *Metabolism of human diseases: Organ physiology and pathophysiology*. springer.

Landström, M., (2010). The TAK1–TRAF6 signalling pathway. *The international journal of biochemistry & cell biology*, *42*(5), pp.585-589.

Laplante, M. and Sabatini, D.M., (2012). mTOR signaling in growth control and disease. *cell*, *149*(2), pp.274-293.

Laucho-Contreras, M.E., Polverino, F., Rojas-Quintero, J., Wang, X. and Owen, C.A., (2018). Club cell protein 16 (Cc16) deficiency increases inflamm-aging in the lungs of mice. *Physiological Reports*, *6*(15), p.e13797.

Lawson, D., Harrison, M. and Shapland, C., (1997). Fibroblast transgelin and smooth muscle SM22α are the same protein, the expression of which is down-regulated in many cell lines. *Cell motility and the cytoskeleton*, *38*(3), pp.250-257.

Lazrak, A., Song, W., Yu, Z., Zhang, S., Nellore, A., Hoopes, C.W., Woodworth, B.A. and Matalon, S., (2023). Low molecular weight hyaluronan inhibits lung epithelial ion channels by activating the calcium-sensing receptor. *Matrix Biology*, *116*, pp.67-84.

Le Cras, T.D., Korfhagen, T.R., Davidson, C., Schmidt, S., Fenchel, M., Ikegami, M., Whitsett, J.A. and Hardie, W.D., (2010). Inhibition of PI3K by PX-866 Prevents Transforming Growth Factor-α–Induced Pulmonary Fibrosis. *The American journal of pathology*, *176*(2), pp.679-686.

Le Saux, C.J., Davy, P., Brampton, C., Ahuja, S.S., Fauce, S., Shivshankar, P., Nguyen, H., Ramaseshan, M., Tressler, R., Pirot, Z. and Harley, C.B., (2013). A novel telomerase activator suppresses lung damage in a murine model of idiopathic pulmonary fibrosis. *PloS one*, *8*(3), p.e58423.

Leach, K., Hannan, F.M., Josephs, T.M., Keller, A.N., Møller, T.C., Ward, D.T., Kallay, E., Mason, R.S., Thakker, R.V., Riccardi, D. and Conigrave, A.D., (2020).

International Union of Basic and Clinical Pharmacology. CVIII. Calcium-sensing receptor nomenclature, pharmacology, and function. *Pharmacological Reviews*, *72*(3), pp.558-604.

Leask, A. and Abraham, D.J., (2004). TGF-ß signaling and the fibrotic response. *The FASEB Journal*, *18*(7), pp.816-827.

Leask, A. and Abraham, D.J., (2004). TGF-ß signaling and the fibrotic response. *The FASEB Journal*, *18*(7), pp.816-827.

Leask, A., (2009). Signaling in fibrosis: Targeting the TGFbeta, endothelin-1 and CCN2 axis in scleroderma. *Frontiers in Bioscience-Elite*, *1*(1), pp.115-122.

Leclere, M., Lavoie-Lamoureux, A., Joubert, P., Relave, F., Setlakwe, E.L., Beauchamp, G., Couture, C., Martin, J.G. and Lavoie, J.P., (2012). Corticosteroids and antigen avoidance decrease airway smooth muscle mass in an equine asthma model. *American Journal of Respiratory Cell and Molecular Biology*, *47*(5), pp.589-596.

Lee, C.G., Cho, S.J., Kang, M.J., Chapoval, S.P., Lee, P.J., Noble, P.W., Yehualaeshet, T., Lu, B., Flavell, R.A., Milbrandt, J. and Homer, R.J., (2004). Early growth response gene 1–mediated apoptosis is essential for transforming growth factor ß1–induced pulmonary fibrosis. *Journal of Experimental Medicine*, *200*(3), pp.377-389.

Lee, G.S., Subramanian, N., Kim, A.I., Aksentijevich, I., Goldbach-Mansky, R., Sacks, D.B., Germain, R.N., Kastner, D.L. and Chae, J.J., (2012a). The calcium-sensing receptor regulates the NLRP3 inflammasome through Ca 2+ and cAMP. *Nature*, *492*(7427), pp.123-127.

Lee, H.J., Yang, Y.M., Kim, K., Shin, D.M., Yoon, J.H., Cho, H.J. and Choi, J.Y., (2012b). Protease-activated receptor 2 mediates mucus secretion in the airway submucosal gland.

Lee, J.W., Park, J.W., Kwon, O.K., Lee, H.J., Jeong, H.G., Kim, J.H., Oh, S.R. and Ahn, K.S., (2017). NPS2143 inhibits MUC5AC and proinflammatory mediators in cigarette smoke extract (CSE)-stimulated human airway epithelial cells. *Inflammation*, *40*(1), pp.184-194.

Lehmann, M., Hu, Q., Hu, Y., Hafner, K., Costa, R., van den Berg, A. and Königshoff, M., (2020). Chronic WNT/ß-catenin signaling induces cellular senescence in lung epithelial cells. *Cellular signalling*, *70*, p.109588.

Leivonen, S.K., Häkkinen, L., Liu, D. and Kähäri, V.M., (2005). Smad3 and extracellular signal-regulated kinase 1/2 coordinately mediate transforming growth factor-ß-induced expression of connective tissue growth factor in human fibroblasts. *Journal of investigative dermatology*, *124*(6), pp.1162-1169.

Lemjabbar, H., Gosset, P., Lamblin, C., Tillie, I., Hartmann, D., Wallaert, B., Tonnel, A.B. and Lafuma, C., (1999). Contribution of 92 kDa gelatinase/type IV collagenase in bronchial inflammation during status asthmaticus. *American Journal of Respiratory and Critical Care Medicine*, *159*(4), pp.1298-1307.

Lepore, J.J., Cheng, L., Min Lu, M., Mericko, P.A., Morrisey, E.E. and Parmacek, M.S., (2005). High-efficiency somatic mutagenesis in smooth muscle cells and cardiac myocytes in SM22α-Cre transgenic mice. *Genesis*, *41*(4), pp.179-184.

Lettieri, C.J., Nathan, S.D., Barnett, S.D., Ahmad, S. and Shorr, A.F., (2006). Prevalence and outcomes of pulmonary arterial hypertension in advanced idiopathic pulmonary fibrosis. *Chest*, *129*(3), pp.746-752.

Ley, B., Swigris, J., Day, B.M., Stauffer, J.L., Raimundo, K., Chou, W. and Collard, H.R., (2017). Pirfenidone reduces respiratory-related hospitalizations in idiopathic pulmonary fibrosis. *American journal of respiratory and critical care medicine*, *196*(6), pp.756-761.

Li, G.W., Xing, W.J., Bai, S.Z., Hao, J.H., Guo, J., Li, H.Z., Li, H.X., Zhang, W.H., Yang, B.F., Wu, L.Y. and Wang, R., (2011). The calcium-sensing receptor mediates hypoxia-induced proliferation of rat pulmonary artery smooth muscle cells through MEK1/ERK1, 2 and PI3K pathways. *Basic & clinical pharmacology & toxicology*, *108*(3), pp.185-193.

Li, T., Gao, L., Ma, H.X., Wei, Y.Y., Liu, Y.H., Qin, K.R., Wang, W.T., Wang, H.L. and Pang, M., (2020). Clinical value of IL-13 and ECP in the serum and sputum of eosinophilic AECOPD patients. *Experimental Biology and Medicine*, *245*(14), pp.1290-1298.

Li, X.U.N. and Wilson, J.W., (1997). Increased vascularity of the bronchial mucosa in mild asthma. *American journal of respiratory and critical care medicine*, *156*(1), pp.229-233.

Li, Y., Martin, L.D., Spizz, G. and Adler, K.B., (2001). MARCKS protein is a key molecule regulating mucin secretion by human airway epithelial cells in vitro. *Journal of Biological Chemistry*, *276*(44), pp.40982-40990.

Li, Y., Wang, W., Huang, P., Zhang, Q., Yao, X., Wang, J., Lv, Z., An, Y., Corrigan, C.J., Huang, K. and Ying, S., (2015). Distinct sustained structural and functional effects of interleukin-33 and interleukin-25 on the airways in a murine asthma surrogate. *Immunology*, *145*(4), pp.508-518.

Li, Z., Li, J., Bu, X., Liu, X., Tankersley, C.G., Wang, C. and Huang, K., (2011). Age-induced augmentation of p38 MAPK phosphorylation in mouse lung. *Experimental gerontology*, *46*(8), pp.694-702.

Liapikou, A., Toumbis, M. and Torres, A., (2015). Managing the safety of inhaled corticosteroids in COPD and the risk of pneumonia. *Expert Opinion on Drug Safety*, *14*(8), pp.1237-1247.

Liesker, J.J., Hacken, N.H.T., Zeinstra-Smith, M., Rutgers, S.R., Postma, D.S. and Timens, W., (2009). Reticular basement membrane in asthma and COPD: similar thickness, yet different composition. *International journal of chronic obstructive pulmonary disease*, pp.127-135.

Lighthouse, J.K. and Small, E.M., 2016. Transcriptional control of cardiac fibroblast plasticity. *Journal of molecular and cellular cardiology*, *91*, pp.52-60.

Lin, C.H., Shih, C.H., Lin, Y.C., Yang, Y.L. and Chen, B.C., (2018). MEKK1, JNK, and SMAD3 mediate CXCL12-stimulated connective tissue growth factor expression in human lung fibroblasts. *Journal of biomedical science*, *25*(1), pp.1-11.

Liotta, L.A., Falanga, V., Kehrl, J.H. and Fauci, A.S., (1986). Transforming growth factor: rapid induction of fibrosis and angiogenesis in vivo and stimulation of collagen formation in vitro. *Proc Natl Acad Sci USA*, *83*, pp.4167-71.

Little, P.J., Burch, M.L., Al-aryahi, S. and Zheng, W., (2011). The paradigm of G protein receptor transactivation: a mechanistic definition and novel example. *TheScientificWorldJOURNAL*, *11*, pp.709-714.

Little, P.J., Burch, M.L., Getachew, R., Al-Aryahi, S. and Osman, N., (2010). Endothelin-1 stimulation of proteoglycan synthesis in vascular smooth muscle is mediated by endothelin receptor transactivation of the transforming growth factor-ß type I receptor. *Journal of cardiovascular pharmacology*, *56*(4), pp.360-368.

Liu, D. and Hornsby, P.J., (2007). Senescent human fibroblasts increase the early growth of xenograft tumors via matrix metalloproteinase secretion. *Cancer research*, *67*(7), pp.3117-3126.

Liu, D.S., Wang, T., Han, S.X., Dong, J.J., Liao, Z.L., He, G.M., Chen, L., Chen, Y.J., Xu, D., Hou, Y. and Li, Y.P., (2009a). p38 MAPK and MMP-9 cooperatively regulate mucus overproduction in mice exposed to acrolein fog. *International immunopharmacology*, *9*(10), pp.1228-1235.

Liu, F., Mih, J.D., Shea, B.S., Kho, A.T., Sharif, A.S., Tager, A.M. and Tschumperlin, D.J., (2010a). Feedback amplification of fibrosis through matrix stiffening and COX-2 suppression. *Journal of Cell Biology*, 190(4), pp. 693–706.

Liu, G., Cooley, M.A., Jarnicki, A.G., Hsu, A.C., Nair, P.M., Haw, T.J., Fricker, M., Gellatly, S.L., Kim, R.Y., Inman, M.D. and Tjin, G., (2016a). Fibulin-1 regulates the pathogenesis of tissue remodeling in respiratory diseases. *JCI insight*, *1*(9).

Liu, G., Philp, A.M., Corte, T., Travis, M.A., Schilter, H., Hansbro, N.G., Burns, C.J., Eapen, M.S., Sohal, S.S., Burgess, J.K. and Hansbro, P.M., (2021). Therapeutic targets in lung tissue remodelling and fibrosis. *Pharmacology & therapeutics*, *225*, p.107839.

Liu, G., Philp, A.M., Corte, T., Travis, M.A., Schilter, H., Hansbro, N.G., Burns, C.J., Eapen, M.S., Sohal, S.S., Burgess, J.K. and Hansbro, P.M., (2021). Therapeutic targets in lung tissue remodelling and fibrosis. *Pharmacology & therapeutics*, *225*, p.107839.

Liu, L., Wang, C., Lin, Y., Xi, Y., Li, H., Shi, S., Li, H., Zhang, W., Zhao, Y., Tian, Y. and Xu, C., (2016b). Suppression of calcium-sensing receptor ameliorates cardiac hypertrophy through inhibition of autophagy. *Molecular Medicine Reports*, *14*(1), pp.111-120.

Liu, L., Wang, C., Sun, D., Jiang, S., Li, H., Zhang, W., Zhao, Y., Xi, Y., Shi, S., Lu, F. and Tian, Y., (2015a). Calhex231 ameliorates cardiac hypertrophy by inhibiting cellular autophagy in vivo and in vitro. *Cellular Physiology and Biochemistry*, *36*(4), pp.1597-1612.

Liu, T., Liu, X., Wang, H.Y., Moon, R.T. and Malbon, C.C., (1999). Activation of rat frizzled-1 promotes Wnt signaling and differentiation of mouse F9 teratocarcinoma cells via pathways that require Gαq and Gαo function. *Journal of Biological Chemistry*, *274*(47), pp.33539-33544.

Liu, X., Li, F., Sun, S.Q., Thangavel, M., Kaminsky, J., Balazs, L. and Ostrom, R.S., (2010b). Fibroblast-specific expression of AC6 enhances ß-adrenergic and prostacyclin signaling and blunts bleomycin-induced pulmonary fibrosis. *American*

Journal of Physiology-Lung Cellular and Molecular Physiology, *298*(6), pp.L819-L829.

Liu, X., Ostrom, R.S. and Insel, P.A., (2004). cAMP-elevating agents and adenylyl cyclase overexpression promote an antifibrotic phenotype in pulmonary fibroblasts. *American Journal of Physiology-Cell Physiology*, *286*(5), pp.C1089-C1099.

Liu, X., Sun, S.Q. and Ostrom, R.S., (2005). Fibrotic lung fibroblasts show blunted inhibition by cAMP due to deficient cAMP response element-binding protein phosphorylation. *Journal of Pharmacology and Experimental Therapeutics*, *315*(2), pp.678-687.

Liu, Y., Yang, Y., Ward, R., An, S., Guo, X.-X., Li, W. and Xu, T.-R., (2015b). Biased signalling: the instinctive skill of the cell in the selection of appropriate signalling pathways. *Biochemical Journal*, 470(2), pp. 155–167.

Liu, Y.H. and Tao, Z.Z., (2009b). Effect of intranasal glucocorticoid on the pathological change of nasal mucosa in rats with allergic rhinitis. *Chinese journal of otorhinolaryngology head and neck surgery*, *44*(11), pp.935-940.

Loirand, G., (2015). Rho kinases in health and disease: from basic science to translational research. *Pharmacological reviews*, *67*(4), pp.1074-1095.

Lönnkvist, K., Hellman, C., Lundahl, J., Halldén, G. and Hedlin, G., (2001). Eosinophil markers in blood, serum, and urine for monitoring the clinical course in childhood asthma: impact of budesonide treatment and withdrawal. *Journal of allergy and clinical immunology*, *107*(5), pp.812-817.

Lora, J.M., Zhang, D.M., Liao, S.M., Burwell, T., King, A.M., Barker, P.A., Singh, L., Keaveney, M., Morgenstern, J., Gutiérrez-Ramos, J.C. and Coyle, A.J., (2005). Tumor necrosis factor-α triggers mucus production in airway epithelium through an IκB kinase ß-dependent mechanism. *Journal of Biological Chemistry*, *280*(43), pp.36510-36517.

Love, M.I., Huber, W. and Anders, S., (2014). Moderated estimation of fold change and dispersion for RNA-seq data with DESeq2. *Genome biology*, *15*(12), pp.1-21.

Lowery, E.M., Brubaker, A.L., Kuhlmann, E. and Kovacs, E.J., (2013). The aging lung. *Clinical interventions in aging*, *8*, p.1489.

Lu, Y.Y., Zhao, X.K., Yu, L., Qi, F., Zhai, B., Gao, C.Q. and Ding, Q., (2017). Interaction of Src and Alpha-V integrin regulates fibroblast migration and modulates lung fibrosis in a preclinical model of lung fibrosis. *Scientific reports*, *7*(1), pp.1-11.

Lugade, A.A., Bogner, P.N., Thatcher, T.H., Sime, P.J., Phipps, R.P. and Thanavala, Y., (2014). Cigarette smoke exposure exacerbates lung inflammation and compromises immunity to bacterial infection. *The Journal of Immunology*, *192*(11), pp.5226-5235.

Lukey, P.T., Harrison, S.A., Yang, S., Man, Y., Holman, B.F., Rashidnasab, A., Azzopardi, G., Grayer, M., Simpson, J.K., Bareille, P. and Paul, L., (2019). A randomised, placebo-controlled study of omipalisib (PI3K/mTOR) in idiopathic pulmonary fibrosis. *European Respiratory Journal*, *53*(3).

Luttrell, L.M., Della Rocca, G.J., van Biesen, T., Luttrell, D.K. and Lefkowitz, R.J., (1997). Gβγ subunits mediate Src-dependent phosphorylation of the epidermal

growth factor receptor: a scaffold for G protein-coupled receptor-mediated Ras activation. *Journal of Biological Chemistry*, *272*(7), pp.4637-4644.

Luttrell, L.M., Hawes, B.E., van Biesen, T., Luttrell, D.K., Lansing, T.J. and Lefkowitz, R.J., (1996). Role of c-Src tyrosine kinase in G protein-coupled receptorand Gβγ subunit-mediated activation of mitogen-activated protein kinases. *Journal of Biological Chemistry*, *271*(32), pp.19443-19450.

Ma, B., Athari, S.S., Mehrabi Nasab, E. and Zhao, L., (2021). PI3K/AKT/mTOR and TLR4/MyD88/NF-κB signaling inhibitors attenuate pathological mechanisms of allergic asthma. *Inflammation*, *44*, pp.1895-1907.

Ma, B., Athari, S.S., Nasab, E.M. and Zhao, L., (2021). PI3K/AKT/mTOR and TLR4/MyD88/NF-κB Signaling Inhibitors Attenuate Pathological Mechanisms of Allergic Asthma. *Inflammation*, pp.1-13.

Mabalirajan, U., Dinda, A.K., Kumar, S., Roshan, R., Gupta, P., Sharma, S.K. and Ghosh, B., (2008). Mitochondrial structural changes and dysfunction are associated with experimental allergic asthma. *The Journal of Immunology*, *181*(5), pp.3540-3548.

MacLeod, R.J., (2013). Extracellular calcium-sensing receptor/PTH knockout mice colons have increased Wnt/β-catenin signaling, reduced non-canonical Wnt signaling, and increased susceptibility to azoxymethane-induced aberrant crypt foci. *Laboratory Investigation*, *93*(5), pp.520-527.

MacLeod, R.J., Chattopadhyay, N. and Brown, E.M., (2003). PTHrP stimulated by the calcium-sensing receptor requires MAP kinase activation. *American Journal of Physiology-Endocrinology and Metabolism*, *284*(2), pp.E435-E442.

MacParland, S.A., Liu, J.C., Ma, X.Z., Innes, B.T., Bartczak, A.M., Gage, B.K., Manuel, J., Khuu, N., Echeverri, J., Linares, I. and Gupta, R., (2018). Single cell RNA sequencing of human liver reveals distinct intrahepatic macrophage populations. *Nature communications*, *9*(1), pp.1-21. Available from: https://www.proteinatlas.org/ENSG00000036828-CASR/single+cell+type [accessed 22 December 2021].

Madala, S.K., Schmidt, S., Davidson, C., Ikegami, M., Wert, S. and Hardie, W.D., (2012). MEK-ERK pathway modulation ameliorates pulmonary fibrosis associated with epidermal growth factor receptor activation. *American journal of respiratory cell and molecular biology*, *46*(3), pp.380-388.

Maffulli, N., Moller, H.D. and Evans, C.H., (2002). Tendon healing: can it be optimised?. *British journal of sports medicine*, *36*(5), pp.315-316.

Mahler, D.A., Rosiello, R.A. and Loke, J., (1986). The aging lung. *Clinics in geriatric medicine*, *2*(2), pp.215-225.

Mahn, K., Hirst, S.J., Ying, S., Holt, M.R., Lavender, P., Ojo, O.O., Siew, L., Simcock, D.E., McVicker, C.G., Kanabar, V., Snetkov, V.A., O'Connor, B.J., Karner, C., Cousins, D.J., Macedo, P., Chung, K.F., Corrigan, C.J., Ward, J.P.T. and Lee, T.H., (2009). Diminished sarco/endoplasmic reticulum Ca2+ ATPase (SERCA) expression contributes to airway remodelling in bronchial asthma. *Proceedings of the National Academy of Sciences*, 106(26), pp. 10775–10780.

Mahn, K., Ojo, O.O., Chadwick, G., Aaronson, P.I., Ward, J.P. and Lee, T.H., (2010). Ca2+ homeostasis and structural and functional remodelling of airway smooth muscle in asthma. *Thorax*, *65*(6), pp.547-552.

Makinde, T., Murphy, R.F. and Agrawal, D.K., (2007). The regulatory role of TGF-ß in airway remodeling in asthma. *Immunology and cell biology*, *85*(5), pp.348-356.

Malmströ̈m, J., Lindberg, H., Lindberg, C., Bratt, C., Wieslander, E., Delander, E.L., Särnstrand, B., Burns, J.S., Mose-Larsen, P., Fey, S. and Marko-Varga, G., (2004). Transforming growth factor-ß1 specifically induce proteins involved in the myofibroblast contractile apparatus. *Molecular & Cellular Proteomics*, *3*(5), pp.466-477.

Mamillapalli, R. and Wysolmerski, J., (2010). The calcium-sensing receptor couples to Gαs and regulates PTHrP and ACTH secretion in pituitary cells. *The Journal of endocrinology*, *204*(3), p.287.

Mamillapalli, R. and Wysolmerski, J., (2010). The calcium-sensing receptor couples to Gαs and regulates PTHrP and ACTH secretion in pituitary cells. *The Journal of endocrinology*, *204*(3), p.287.

Mamillapalli, R., VanHouten, J., Zawalich, W. and Wysolmerski, J., (2008). Switching of G-protein usage by the calcium-sensing receptor reverses its effect on parathyroid hormone-related protein secretion in normal versus malignant breast cells. *Journal of Biological Chemistry*, *283*(36), pp.24435-24447.

Mamillapalli, R., VanHouten, J., Zawalich, W. and Wysolmerski, J., (2008). Switching of G-protein usage by the calcium-sensing receptor reverses its effect on parathyroid hormone-related protein secretion in normal versus malignant breast cells. *Journal of Biological Chemistry*, *283*(36), pp.24435-24447.

Mansfield, B., (2022). *The Calcium-Sensing Receptor (CaSR) as a potential mediator of pollution-induced airway cell responses*. PhD thesis. Cardiff University.

Mariani, L.E., Bijlsma, M.F., Ivanova, A.A., Suciu, S.K., Kahn, R.A. and Caspary, T., (2016). Arl13b regulates Shh signaling from both inside and outside the cilium. *Molecular biology of the cell*, *27*(23), pp.3780-3790.

Martínez-Zamudio, R.I., Robinson, L., Roux, P.F. and Bischof, O., (2017). SnapShot: cellular senescence pathways. *Cell*, *170*(4), pp.816-816.

Maselli, D.J. and Hanania, N.A., (2018). Asthma COPD overlap: impact of associated comorbidities. *Pulmonary pharmacology & therapeutics*, *52*, pp.27-31.

Maslan, J. and Mims, J.W., (2014). What is asthma? Pathophysiology, demographics, and health care costs. *Otolaryngologic Clinics of North America*, *47*(1), pp. 13–22.Elsevier Inc,

Mason, R.J. and Williams, M.C., (1977). Type II alveolar cell: defender of the alveolus. *American review of respiratory disease*, *115*(S), pp.81-91.

Massagué, J., (2000). How cells read TGF-ß signals. *Nature reviews Molecular cell biology*, *1*(3), pp.169-178.

Massagué, J., Seoane, J. and Wotton, D., (2005). Smad transcription factors. *Genes & development*, *19*(23), pp.2783-2810.

Masszi, A., Di Ciano, C., Sirokmány, G., Arthur, W.T., Rotstein, O.D., Wang, J., McCulloch, C.A., Rosivall, L., Mucsi, I. and Kapus, A., (2003). Central role for Rho in TGF-β1-induced α-smooth muscle actin expression during epithelial-mesenchymal transition. *American Journal of Physiology-Renal Physiology*, *284*(5), pp.F911-F924.

Matera, D.L., DiLillo, K.M., Smith, M.R., Davidson, C.D., Parikh, R., Said, M., Wilke, C.A., Lombaert, I.M., Arnold, K.B., Moore, B.B. and Baker, B.M., (2020). Microengineered 3D pulmonary interstitial mimetics highlight a critical role for matrix degradation in myofibroblast differentiation. *Science Advances*, *6*(37), p.eabb5069.

Mattos, W., Lim, S., Russell, R., Jatakanon, A., Chung, K.F. and Barnes, P.J., (2002). Matrix metalloproteinase-9 expression in asthma: effect of asthma severity, allergen challenge, and inhaled corticosteroids. *Chest*, *122*(5), pp.1543-1552.

Mauad, T., Bel, E.H. and Sterk, P.J., (2007). Asthma therapy and airway remodeling. *Journal of allergy and clinical immunology*, *120*(5), pp.997-1009.

McCann, P., (1987). *Inhibition of Polyamine Metabolism: Biological Significance and Basis for New Therapies* (Academic Press, Orlando, FL).

McCartney-Francis, N.L., Frazier-Jessen, M. and Wahl, S.M., (1998). TGF-β: a balancing act. *International reviews of immunology*, *16*(5-6), pp.553-580.

McLarnon, S.J., Holden, D., Ward, D.T., Jones, M.N., Elliott, A.C. and Riccardi, D., (2002). Aminoglycoside antibiotics induce pH-sensitive activation of the calcium-sensing receptor. *Biochemical and biophysical research communications*, *297*(1), pp.71-77.

McMillan, S.J., Xanthou, G. and Lloyd, C.M., (2005). Manipulation of allergen-induced airway remodeling by treatment with anti-TGF-β antibody: effect on the Smad signaling pathway. *The Journal of Immunology*, *174*(9), pp.5774-5780.

Melgert, B.N., Postma, D.S., Kuipers, I., Geerlings, M., Luinge, M.A., Van Der Strate, B.W.A., Kerstjens, H.A.M., Timens, W. and Hylkema, M.N., (2005). Female mice are more susceptible to the development of allergic airway inflammation than male mice. *Clinical & Experimental Allergy*, *35*(11), pp.1496-1503.

Mercer, P.F., Woodcock, H.V., Eley, J.D., Platé, M., Sulikowski, M.G., Durrenberger, P.F., Franklin, L., Nanthakumar, C.B., Man, Y., Genovese, F. and McAnulty, R.J., (2016). Exploration of a potent PI3 kinase/mTOR inhibitor as a novel anti-fibrotic agent in IPF. *Thorax*, *71*(8), pp.701-711.

Meurs, H., Schuurman, F.E., Duyvendak, M. and Zaagsma, J., (1999). Deficiency of nitric oxide in polycation-induced airway hyperreactivity. *British Journal of Pharmacology*, 126(3), pp. 559–562.

Meyer, K., Hodwin, B., Ramanujam, D., Engelhardt, S. and Sarikas, A., (2016). Essential role for premature senescence of myofibroblasts in myocardial fibrosis. *Journal of the American college of cardiology*, *67*(17), pp.2018-2028.

Meyer, K.C., (2018). Age-Associated Changes in Structure and Function of the Aging Human Lung. In *Conn's Handbook of Models for Human Aging* (pp. 873-888). Academic Press.

Meyer, K.C., Ershler, W., Rosenthal, N.S., Lu, X.G. and Peterson, K., (1996). Immune dysregulation in the aging human lung. *American journal of respiratory and critical care medicine*, *153*(3), pp.1072-1079.

Michalik, M., Pierzchalska, M., Legutko, A., Ura, M., Ostaszewska, A., Soja, J. and Sanak, M., (2009). Asthmatic bronchial fibroblasts demonstrate enhanced potential to differentiate into myofibroblasts in culture. *Medical Science Monitor*, *15*(7), pp.BR194-BR201.

Milara, J., Mata, M., Serrano, A., Peiró, T., Morcillo, E.J. and Cortijo, J., (2010). Extracellular calcium-sensing receptor mediates human bronchial epithelial wound repair. *Biochemical pharmacology*, *80*(2), pp.236-246.

Minagawa, S., Araya, J., Numata, T., Nojiri, S., Hara, H., Yumino, Y., Kawaishi, M., Odaka, M., Morikawa, T., Nishimura, S.L. and Nakayama, K., (2011). Accelerated epithelial cell senescence in IPF and the inhibitory role of SIRT6 in TGF-β-induced senescence of human bronchial epithelial cells. *American Journal of Physiology-Lung Cellular and Molecular Physiology*, *300*(3), pp.L391-L401.

Minois, N., Carmona-Gutierrez, D. and Madeo, F., (2011). Polyamines in aging and disease. *Aging (Albany NY)*, *3*(8), p.716.

Mio, T., Liu, X.D., Adachi, Y., Striz, I., Sköld, C.M., Romberger, D.J., Spurzem, J.R., Illig, M.G., Ertl, R. and Rennard, S.I., (1998). Human bronchial epithelial cells modulate collagen gel contraction by fibroblasts. *American Journal of Physiology-Lung Cellular and Molecular Physiology*, *274*(1), pp.L119-L126.

Miravitlles, M., Ferrer, J., Baró, E., Lleonart, M. and Galera, J., (2013). Differences between physician and patient in the perception of symptoms and their severity in COPD. *Respiratory medicine*, *107*(12), pp.1977-1985.

Misharin, A.V. and Budinger, G.S., (2018). Targeting the myofibroblast in pulmonary fibrosis. *Am J Respir Crit Care Med* 198(7), pp.834–835.

Mittermayer, C.H., Hassenstein, J. and Riede, U.N., (1978). Is Shock-Induced Lung Fibrosis Reversible? A Report on Recovery from „Shock-Lung". *Pathology-Research and Practice*, *162*(1), pp.73-87.

Mondrinos, M.J. and Huh, D., (2015). A Tissue-engineered Microphysiological Platform for the Study of Human Organ Fibrosis. *TISSUE ENGINEERING PART A*, 21(1), pp.S267-S267.

Montoro, D.T., Haber, A.L., Biton, M., Vinarsky, V., Lin, B., Birket, S.E., Yuan, F., Chen, S., Leung, H.M., Villoria, J. and Rogel, N., (2018). A revised airway epithelial hierarchy includes CFTR-expressing ionocytes. *Nature*, *560*(7718), pp.319-324.

Morty, R.E., Königshoff, M. and Eickelberg, O., (2009). Transforming growth factor-β signaling across ages: from distorted lung development to chronic obstructive pulmonary disease. *Proceedings of the American Thoracic Society*, *6*(7), pp.607-613.

Mostaço-Guidolin, L.B., Osei, E.T., Ullah, J., Hajimohammadi, S., Fouadi, M., Li, X., Li, V., Shaheen, F., Yang, C.X., Chu, F. and Cole, D.J., (2019). Defective fibrillar collagen organization by fibroblasts contributes to airway remodeling in asthma. *American journal of respiratory and critical care medicine*, *200*(4), pp.431-443.

Moustakas, A., Souchelnytskyi, S. and Heldin, C.H., (2001). Smad regulation in TGF-ß signal transduction. *Journal of cell science*, *114*(24), pp.4359-4369.

Mukherjee, S., Ayaub, E.A., Murphy, J., Lu, C., Kolb, M., Ask, K. and Janssen, L.J. (2015). Disruption of calcium signaling in fibroblasts and attenuation of bleomycin-induced fibrosis by nifedipine. *American Journal of Respiratory Cell and Molecular Biology* **53**:450–458.

Muñoz-Espín, D. and Serrano, M., (2014). Cellular senescence: from physiology to pathology. *Nature reviews Molecular cell biology*, *15*(7), pp.482-496.

Murray, M.A. and Chotirmall, S.H., (2015). The impact of immunosenescence on pulmonary disease. *Mediators of inflammation*, *2015*.

Mushaben, E.M., Kramer, E.L., Brandt, E.B., Khurana Hershey, G.K. and Le Cras, T.D., 2011. Rapamycin attenuates airway hyperreactivity, goblet cells, and IgE in experimental allergic asthma. *The Journal of Immunology*, *187*(11), pp.5756-5763.

Naba, A., Hoersch, S. and Hynes, R.O., (2012). Towards definition of an ECM parts list: an advance on GO categories. *Matrix biology: journal of the International Society for Matrix Biology*, *31*, p.371.

Nadrous, H.F., Pellikka, P.A., Krowka, M.J., Swanson, K.L., Chaowalit, N., Decker, P.A. and Ryu, J.H., (2005). Pulmonary hypertension in patients with idiopathic pulmonary fibrosis. *Chest*, *128*(4), pp.2393-2399.

Naidoo, N., (2009). ER and aging-Protein folding and the ER stress response. *Ageing Research Reviews*, 8(3), pp. 150–159.

Nair, P., Martin, J.G., Cockcroft, D.C., Dolovich, M., Lemiere, C., Boulet, L.P. and O'Byrne, P.M., (2017). Airway Hyperresponsiveness in Asthma: Measurement and Clinical Relevance. *Journal of Allergy and Clinical Immunology: In Practice*, 5(3), pp. 649-659.e2.American Academy of Allergy, Asthma and Immunology,

Narciso, M., Ulldemolins, A., Navajas, D., Farre, R., Gavara, N. and Lopez, I.A., (2022). Aging Induces Stiffening of the Lung Extracellular Matrix.

Neveu, W.A., Allard, J.B., Dienz, O., Wargo, M.J., Ciliberto, G., Whittaker, L.A. and Rincon, M., (2009). IL-6 is required for airway mucus production induced by inhaled fungal allergens. *The Journal of Immunology*, *183*(3), pp.1732-1738.

Newman, D.R., Sills, W.S., Hanrahan, K., Ziegler, A., Tidd, K.M., Cook, E. and Sannes, P.L., (2016). Expression of WNT5A in idiopathic pulmonary fibrosis and its control by TGF-ß and WNT7B in human lung fibroblasts. *Journal of Histochemistry & Cytochemistry*, *64*(2), pp.99-111.

Nigdelioglu, R., Hamanaka, R.B., Meliton, A.Y., O'Leary, E., Witt, L.J., Cho, T., Sun, K., Bonham, C., Wu, D., Woods, P.S. and Husain, A.N., (2016). Transforming growth factor (TGF)-ß promotes de novo serine synthesis for collagen production. *Journal of Biological Chemistry*, *291*(53), pp.27239-27251.

Nikolić, M.Z., Caritg, O., Jeng, Q., Johnson, J.A., Sun, D., Howell, K.J., Brady, J.L., Laresgoiti, U., Allen, G., Butler, R. and Zilbauer, M., (2017). Human embryonic lung epithelial tips are multipotent progenitors that can be expanded in vitro as long-term self-renewing organoids. *Elife*, *6*, p.e26575.

North, M.L., Grasemann, H., Khanna, N., Inman, M.D., Gauvreau, G.M. and Scott, J.A., (2013). Increased ornithine-derived polyamines cause airway hyperresponsiveness in a mouse model of asthma. *American journal of respiratory cell and molecular biology*, *48*(6), pp.694-702.

Nusse, R., (2012). Wnt signaling. *Cold Spring Harbor perspectives in biology*, *4*(5), p.a011163.

Oda, Y., Hu, L., Nguyen, T., Fong, C., Tu, C.L. and Bikle, D.D., (2017). Combined deletion of the vitamin D receptor and calcium-sensing receptor delays wound re-epithelialization. *Endocrinology*, *158*(6), pp.1929-1938.

Ogawa, K., Suzuki, K., Okutsu, M., Yamazaki, K. and Shinkai, S., (2008). The association of elevated reactive oxygen species levels from neutrophils with low-grade inflammation in the elderly. *Immunity & Ageing*, *5*(1), pp.1-8.

Oh, Y.S., Seo, E.H., Lee, Y.S., Cho, S.C., Jung, H.S., Park, S.C. and Jun, H.S., (2016). Increase of calcium sensing receptor expression is related to compensatory insulin secretion during aging in mice. *PloS one*, *11*(7), p.e0159689.

Ohbayashi, H. and Shimokata, K., (2005). Matrix metalloproteinase-9 and airway remodeling in asthma. *Current Drug Targets-Inflammation & Allergy*, *4*(2), pp.177-181.

Ohnishi, M. and Razzaque, M.S., (2010). Dietary and genetic evidence for phosphate toxicity accelerating mammalian aging. *The FASEB Journal*, *24*(9), pp.3562-3571.

Olczyk, P., Mencner, Ł. and Komosinska-Vassev, K., (2014). The role of the extracellular matrix components in cutaneous wound healing. *BioMed research international*, *2014*.

Olszak, I.T., Poznansky, M.C., Evans, R.H., Olson, D., Kos, C., Pollak, M.R., Brown, E.M. and Scadden, D.T., (2000). Extracellular calcium elicits a chemokinetic response from monocytes in vitro and in vivo. *The Journal of clinical investigation*, *105*(9), pp.1299-1305.

Onursal, C., Dick, E., Angelidis, I., Schiller, H.B. and Staab-Weijnitz, C.A., (2021). Collagen biosynthesis, processing, and maturation in lung ageing. *Frontiers in Medicine*, *8*, p.593874.

Opal, S.M., Girard, T.D. and Ely, E.W., (2005). The immunopathogenesis of sepsis in elderly patients. *Clinical infectious diseases*, *41*(Supplement_7), pp.S504-S512.

Oppenheimer, J. and Kelly, H.W., (2017). Could calcium channel blockers treat 2 illnesses with 1 pill?. *Annals of Allergy, Asthma & Immunology*, *119*(6), pp.473-474.

Ordoñez, C.L., Khashayar, R., Wong, H.H., Ferrando, R.O.N., Wu, R., Hyde, D.M., Hotchkiss, J.A., Zhang, Y., Novikov, A., Dolganov, G. and Fahy, J.V., (2001). Mild and moderate asthma is associated with airway goblet cell hyperplasia and abnormalities in mucin gene expression. *American journal of respiratory and critical care medicine*, *163*(2), pp.517-523.

Ostrowski, L.E., Yin, W., Rogers, T.D., Busalacchi, K.B., Chua, M., O'Neal, W.K. and Grubb, B.R., (2010). Conditional deletion of dnaic1 in a murine model of primary ciliary dyskinesia causes chronic rhinosinusitis. *American journal of respiratory cell and molecular biology*, *43*(1), pp.55-63.

Page, C. and Cazzola, M., (2014). Bifunctional drugs for the treatment of asthma and chronic obstructive pulmonary disease. *European Respiratory Journal*, *44*(2), pp.475-482.

Page, C. and Cazzola, M., (2016). Bifunctional drugs for the treatment of respiratory diseases. *Pharmacology and Therapeutics of Asthma and COPD*, pp.197-212.

Panda, A., Arjona, A., Sapey, E., Bai, F., Fikrig, E., Montgomery, R.R., Lord, J.M. and Shaw, A.C., (2009). Human innate immunosenescence: causes and consequences for immunity in old age. *Trends in immunology*, *30*(7), pp.325-333.

Pandur, P., Maurus, D. and Kühl, M., (2002). Increasingly complex: new players enter the Wnt signaling network. *Bioessays*, *24*(10), pp.881-884.

Papageorgis, P., (2017). Complex interplay between aging and cancer: role of TGF-ß signaling. *Critical Reviews™ in Oncogenesis*, *22*(3-4).

Pardo, A., Cabrera, S., Maldonado, M. and Selman, M., (2016). Role of matrix metalloproteinases in the pathogenesis of idiopathic pulmonary fibrosis. *Respiratory research*, *17*(1), pp.1-10.

Parikh, P., Wicher, S., Khandalavala, K., Pabelick, C.M., Britt Jr, R.D. and Prakash, Y.S., (2019). Cellular senescence in the lung across the age spectrum. *American Journal of Physiology-Lung Cellular and Molecular Physiology*, *316*(5), pp.L826-L842.

Parimon, T., Hohmann, M.S. and Yao, C., (2021). Cellular senescence: pathogenic mechanisms in lung fibrosis. *International Journal of Molecular Sciences*, *22*(12), p.6214.

Park, J.H., Park, H.K., Jung, H., Lee, S.S. and Koo, H.K., (2015). Parathyroid hormone as a novel biomarker for chronic obstructive pulmonary disease: Korean National Health and Nutrition Examination Survey. *Plos one*, *10*(9), p.e0138482.

Patel, A.S., Lin, L., Geyer, A., Haspel, J.A., An, C.H., Cao, J., Rosas, I.O. and Morse, D., (2012). Autophagy in idiopathic pulmonary fibrosis. *PloS one*, *7*(7), p.e41394.

Patel, I., Seemungal, T.A.R., Wilks, M., Lloyd-Owen, S.J., Donaldson, G.C. and Wedzicha, J.A., (2002). Relationship between bacterial colonisation and the frequency, character, and severity of COPD exacerbations. *Thorax*, *57*(9), pp.759-764.

Patel, N.M., Lederer, D.J., Borczuk, A.C. and Kawut, S.M., (2007). Pulmonary hypertension in idiopathic pulmonary fibrosis. *Chest*, *132*(3), pp.998-1006.

Payne, D.N., Rogers, A.V., Ädelroth, E., Bandi, V., Guntupalli, K.K., Bush, A. and Jeffery, P.K., (2003). Early thickening of the reticular basement membrane in children with difficult asthma. *American journal of respiratory and critical care medicine*, *167*(1), pp.78-82.

Pégorier, S., Wagner, L.A., Gleich, G.J. and Pretolani, M., (2006). Eosinophil-derived cationic proteins activate the synthesis of remodeling factors by airway epithelial cells. *The Journal of Immunology*, *177*(7), pp.4861-4869.

Peng, R., Sridhar, S., Tyagi, G., Phillips, J.E., Garrido, R., Harris, P., Burns, L., Renteria, L., Woods, J., Chen, L. and Allard, J., (2013). Bleomycin induces molecular

changes directly relevant to idiopathic pulmonary fibrosis: a model for “active” disease. *PloS one*, *8*(4), p.e59348.

Pera, T., (2011). Inflammation and remodelling in experimental models of COPD. PhD thesis. University of Groningen.

Pera, T., Zuidhof, A., Valadas, J., Smit, M., Schoemaker, R.G., Gosens, R., Maarsingh, H., Zaagsma, J. and Meurs, H., (2011). Tiotropium inhibits pulmonary inflammation and remodelling in a guinea pig model of COPD. *European Respiratory Journal*, *38*(4), pp.789-796.

Phan, S.H. and Kunkel, S.L., (1992). Lung cytokine production in bleomycin-induced pulmonary fibrosis. *Experimental lung research*, *18*(1), pp.29-43.

Phan, S.H., (2002). The myofibroblast in pulmonary fibrosis. *Chest*, *122*(6), pp.286S-289S.

Phang, J.M., Liu, W., Hancock, C.N. and Fischer, J.W., (2015). Proline metabolism and cancer: emerging links to glutamine and collagen. *Current opinion in clinical nutrition and metabolic care*, *18*(1), p.71.

Pi, M., Spurney, R.F., Tu, Q., Hinson, T. and Quarles, L.D., (2002). Calcium-sensing receptor activation of rho involves filamin and rho-guanine nucleotide exchange factor. *Endocrinology*, *143*(10), pp.3830-3838.

Pigati, P.A., Righetti, R.F., Possa, S.S., Romanholo, B.S., Rodrigues, A.P.D., dos Santos, A.S.A., Xisto, D.G., Antunes, M.A., Prado, C.M., Leick, E.A. and de Arruda Martins, M., (2015). Y-27632 is associated with corticosteroid-potentiated control of pulmonary remodeling and inflammation in guinea pigs with chronic allergic inflammation. *BMC pulmonary medicine*, *15*(1), pp.1-16.

Pillai, P., Corrigan, C.J. and Ying, S., (2011). Airway epithelium in atopic and nonatopic asthma: similarities and differences. *International Scholarly Research Notices*, *2011*.

Pini, A., Shemesh, R., Samuel, C.S., Bathgate, R.A., Zauberman, A., Hermesh, C., Wool, A., Bani, D. and Rotman, G., (2010). Prevention of bleomycin-induced pulmonary fibrosis by a novel antifibrotic peptide with relaxin-like activity. *Journal of Pharmacology and Experimental Therapeutics*, *335*(3), pp.589-599.

Placido, L., Romero, Y., Maldonado, M., Toscano-Marquez, F., Ramírez, R., Calyeca, J., Mora, A.L., Selman, M. and Pardo, A., (2021). Loss of mt1-mmp in alveolar epithelial cells exacerbates pulmonary fibrosis. *International Journal of Molecular Sciences*, *22*(6), p.2923.

Plasschaert, L.W., Žilionis, R., Choo-Wing, R., Savova, V., Knehr, J., Roma, G., Klein, A.M. and Jaffe, A.B., (2018). A single-cell atlas of the airway epithelium reveals the CFTR-rich pulmonary ionocyte. *Nature*, *560*(7718), pp.377-381.

Platé, M., Guillotin, D. and Chambers, R.C., (2020). The promise of mTOR as a therapeutic target pathway in idiopathic pulmonary fibrosis. *European Respiratory Review*, *29*(157).

Polosa, R. and Thomson, N.C., (2013). Smoking and asthma: dangerous liaisons. *European respiratory journal*, *41*(3), pp.716-726.

Pomaznoy, M., Ha, B. and Peters, B., (2018). GOnet: a tool for interactive Gene Ontology analysis. *Bmc Bioinformatics*, *19*(1), pp.1-8.

Poncelet, A.C. and Schnaper, H.W., (2001). Sp1 and Smad proteins cooperate to mediate transforming growth factor-β1-induced α2 (I) collagen expression in human glomerular mesangial cells. *Journal of Biological Chemistry*, *276*(10), pp.6983-6992.

Possa, S.S., Charafeddine, H.T., Righetti, R.F., da Silva, P.A., Almeida-Reis, R., Saraiva-Romanholo, B.M., Perini, A., Prado, C.M., Leick-Maldonado, E.A., Martins, M.A. and Tibério, I.D.F.L.C., (2012). Rho-kinase inhibition attenuates airway responsiveness, inflammation, matrix remodeling, and oxidative stress activation induced by chronic inflammation. *American Journal of Physiology-Lung Cellular and Molecular Physiology*, *303*(11), pp.L939-L952.

Postma, D.S. and Timens, W., (2006). Remodeling in asthma and chronic obstructive pulmonary disease. *Proceedings of the American Thoracic Society*, *3*(5), pp.434-439.

Prasad, S., Hogaboam, C.M. and Jarai, G., (2014). Deficient repair response of IPF fibroblasts in a co-culture model of epithelial injury and repair. *Fibrogenesis & tissue repair*, *7*(1), pp.1-14.

Prikk, K., Maisi, P., Pirilä, E., Reintam, M.A., Salo, T., Sorsa, T. and Sepper, R., (2002). Airway obstruction correlates with collagenase-2 (MMP-8) expression and activation in bronchial asthma. *Laboratory investigation*, *82*(11), pp.1535-1545.

Pritchard, K., Smith, A.K. and Rogers, D.F., (2001). Measurement of Airway Mucin Gene Expression. In *Human Airway Inflammation* (pp. 285-294). Humana Press.

Promchainant, C., (1975). Cytogenetic effect of bleomycin on human leukocytes in vitro. *Mutation Research/Fundamental and Molecular Mechanisms of Mutagenesis*, *28*(1), pp.107-112.

Puchelle, E., Zahm, J.M., Tournier, J.M. and Coraux, C., (2006). Airway epithelial repair, regeneration, and remodeling after injury in chronic obstructive pulmonary disease. *Proceedings of the American Thoracic Society*, *3*(8), pp.726-733.

Puljic, R., Benediktus, E., Plater-Zyberk, C., Baeuerle, P.A., Szelenyi, S., Brune, K. and Pahl, A., (2007). Lipopolysaccharide-induced lung inflammation is inhibited by neutralization of GM-CSF. *European journal of pharmacology*, *557*(2-3), pp.230-235.

Qin, A., Reddy, H.G., Weinberg, F.D. and Kalemkerian, G.P., (2020). Cyclin-dependent kinase inhibitors for the treatment of lung cancer. *Expert opinion on pharmacotherapy*, *21*(8), pp.941-952.

Qin, G., Luo, M., Chen, J., Dang, Y., Chen, G., Li, L., Zeng, J., Lu, Y. and Yang, J., (2016). Reciprocal activation between MMP-8 and TGF-β1 stimulates EMT and malignant progression of hepatocellular carcinoma. *Cancer letters*, *374*(1), pp.85-95.

Qiu, P., Ritchie, R.P., Fu, Z., Cao, D., Cumming, J., Miano, J.M., Wang, D.Z., Li, H.J. and Li, L., (2005). Myocardin Enhances Smad3-Mediated Transforming Growth Factor-β1 Signaling in a CArG Box-Independent Manner: Smad-Binding Element Is an Important cis Element for SM22 α Transcription In Vivo. *Circulation research*, *97*(10), pp.983-991.

Quinn, S.J., Ye, C.P., Diaz, R., Kifor, O., Bai, M., Vassilev, P. and Brown, E., (1997). The Ca2+-sensing receptor: a target for polyamines. *American Journal of Physiology-Cell Physiology*, *273*(4), pp.C1315-C1323.

Quirk, J.D., Sukstanskii, A.L., Woods, J.C., Lutey, B.A., Conradi, M.S., Gierada, D.S., Yusen, R.D., Castro, M. and Yablonskiy, D.A., (2016). Experimental evidence of age-related adaptive changes in human acinar airways. *Journal of Applied Physiology*, *120*(2), pp.159-165.

Raghu, G., Chen, S.Y., Yeh, W.S., Maroni, B., Li, Q., Lee, Y.C. and Collard, H.R., (2014). Idiopathic pulmonary fibrosis in US Medicare beneficiaries aged 65 years and older: incidence, prevalence, and survival, 2001–11. *The lancet Respiratory medicine*, *2*(7), pp.566-572.

Rajanandh, M.G., (2015). An overview and update on asthma and its management. *Journal of Medical Sciences*, *15*(3), p.122.

Ramirez, A.M., Wongtrakool, C., Welch, T., Steinmeyer, A., Zügel, U. and Roman, J., (2010). Vitamin D inhibition of pro-fibrotic effects of transforming growth factor β1 in lung fibroblasts and epithelial cells. *The Journal of steroid biochemistry and molecular biology*, *118*(3), pp.142-150.

Ramirez, J.A., Goodman, W.G., Gornbein, J., Menezes, C., Moulton, L., Segre, G.V. and Salusky, I.B., (1993). Direct in vivo comparison of calcium-regulated parathyroid hormone secretion in normal volunteers and patients with secondary hyperparathyroidism. *The Journal of clinical endocrinology and metabolism*, *76*(6), pp.1489-1494.

Ramis, J., Middlewick, R., Pappalardo, F., Cairns, J.T., Stewart, I.D., John, A.E., Krishnan, R., Miller, S., Shaw, D.E., Brightling, C.E. and Buttery, L., (2022). Lysyl oxidase like 2 is increased in asthma and contributes to asthmatic airway remodelling. *European Respiratory Journal*, *60*(1).

Rashid, K., Sundar, I.K., Gerloff, J., Li, D. and Rahman, I., (2018). Lung cellular senescence is independent of aging in a mouse model of COPD/emphysema. *Scientific reports*, *8*(1), pp.1-14.

Ray, A., Jaiswal, A., Dutta, J., Singh, S. and Mabalirajan, U., (2020). A looming role of mitochondrial calcium in dictating the lung epithelial integrity and pathophysiology of lung diseases. *Mitochondrion*, *55*, pp.111-121.

Ray, K., (2015). Calcium-sensing receptor: trafficking, endocytosis, recycling, and importance of interacting proteins. *Progress in molecular biology and translational science*, *132*, pp.127-150.

Reddel, H.K., Bacharier, L.B., Bateman, E.D., Brightling, C.E., Brusselle, G.G., Buhl, R., Cruz, A.A., Duijts, L., Drazen, J.M., FitzGerald, J.M. and Fleming, L.J., (2021). Global Initiative for Asthma (GINA) Strategy 2021–Executive summary and rationale for key changes. *The Journal of Allergy and Clinical Immunology: In Practice*.

Reddy, P.H., (2011). Mitochondrial dysfunction and oxidative stress in asthma: implications for mitochondria-targeted antioxidant therapeutics. *Pharmaceuticals*, *4*(3), pp.429-456.

Redington, A.E., Roche, W.R., Holgate, S.T. and Howarth, P.H., (1998). Co-localization of immunoreactive transforming growth factor-beta1 and decorin in

bronchial biopsies from asthmatic and normal subjects. *The Journal of Pathology: A Journal of the Pathological Society of Great Britain and Ireland*, *186*(4), pp.410-415.

Reif, S., Lang, A., Lindquist, J.N., Yata, Y., Gäbele, E., Scanga, A., Brenner, D.A. and Rippe, R.A., (2003). The role of focal adhesion kinase-phosphatidylinositol 3-kinase-akt signaling in hepatic stellate cell proliferation and type I collagen expression. *Journal of Biological Chemistry*, *278*(10), pp.8083-8090.

Renzoni, E.A., Abraham, D.J., Howat, S., Shi-Wen, X., Sestini, P., Bou-Gharios, G., Wells, A.U., Veeraraghavan, S., Nicholson, A.G., Denton, C.P. and Leask, A., (2004). Gene expression profiling reveals novel TGF-ß targets in adult lung fibroblasts. *Respiratory research*, *5*(1), pp.1-12.

Rey, O., Chang, W., Bikle, D., Rozengurt, N., Young, S.H. and Rozengurt, E., (2012). Negative cross-talk between calcium-sensing receptor and ß-catenin signaling systems in colonic epithelium. *Journal of Biological Chemistry*, *287*(2), pp.1158-1167.

Ricard-Blum, S., Baffet, G. and Théret, N., (2018). Molecular and tissue alterations of collagens in fibrosis. *Matrix Biology*, *68*, pp.122-149.

Riccardi, D. and Kemp, P.J., (2012). The calcium-sensing receptor beyond extracellular calcium homeostasis: conception, development, adult physiology, and disease. *Annual review of physiology*, *74*, pp.271-297.

Riccardi, D. and Valenti, G., (2016). Localization and function of the renal calcium-sensing receptor. *Nature Reviews Nephrology*, *12*(7), pp.414-425.

Riccardi, D., Brennan, S.C. and Chang, W., (2013). The extracellular calcium-sensing receptor, CaSR, in fetal development. *Best Practice & Research Clinical Endocrinology & Metabolism*, 27(3), pp. 443–453.Baillière Tindall,

Riccardi, D., Ward, J.P., Yarova, P.L., Janssen, L.J., Lee, T.H., Ying, S. and Corrigan, C.J., (2022). Topical therapy with negative allosteric modulators of the calcium-sensing receptor (calcilytics) for the management of asthma: the beginning of a new era?. *European Respiratory Journal*, *60*(2).

Richeldi, L., Collard, H.R. and Jones, M.G., (2017). Idiopathic pulmonary fibrosis. *The Lancet*, *389*(10082), pp.1941-1952.

Richeldi, L., Du Bois, R.M., Raghu, G., Azuma, A., Brown, K.K., Costabel, U., Cottin, V., Flaherty, K.R., Hansell, D.M., Inoue, Y. and Kim, D.S., (2014). Efficacy and safety of nintedanib in idiopathic pulmonary fibrosis. *New England Journal of Medicine*, *370*(22), pp.2071-2082.

Riesenfeld, E.P., Sullivan, M.J., Thompson-Figueroa, J.A., Haverkamp, H.C., Lundblad, L.K., Bates, J.H. and Irvin, C.G., (2010). Inhaled salmeterol and/or fluticasone alters structure/function in a murine model of allergic airways disease. *Respiratory research*, *11*(1), pp.1-11.

Rivard, A., Fabre, J.E., Silver, M., Chen, D., Murohara, T., Kearney, M., Magner, M., Asahara, T. and Isner, J.M., (1999). Age-dependent impairment of angiogenesis. *Circulation*, *99*(1), pp.111-120.

Roberts, M.S., Gafni, R.I., Brillante, B., Guthrie, L.C., Streit, J., Gash, D., Gelb, J., Krusinska, E., Brennan, S.C., Schepelmann, M. and Riccardi, D., (2019). Treatment

of autosomal dominant hypocalcemia type 1 with the calcilytic NPSP795 (SHP635). *Journal of Bone and Mineral Research*, *34*(9), pp.1609-1618.

Roche, W., Williams, J., Beasley, R. and Holgate, S., (1989). Subepithelial fibrosis in the bronchi of asthmatics. *The Lancet*, *333*(8637), pp.520-524.

Roesler, A.M., Wicher, S.A., Ravix, J., Britt, R.D., Manlove, L., Teske, J.J., Cummings, K., Thompson, M.A., Farver, C., MacFarlane, P., Pabelick, C.M. and Prakash, Y.S., (2019). Calcium sensing receptor in developing human airway smooth muscle. *Journal of Cellular Physiology*, (July 2018), pp. 1–11.

Rogers, N.K., Clements, D., Dongre, A., Harrison, T.W., Shaw, D. and Johnson, S.R., (2014). Extra-cellular matrix proteins induce matrix metalloproteinase-1 (MMP-1) activity and increase airway smooth muscle contraction in asthma. *PloS one*, *9*(2), p.e90565.

Rolewska, P., Al-Robaiy, S., Santos, A.N., Simm, A., Silber, R.E. and Bartling, B., (2013). Age-related expression, enzymatic solubility and modification with advanced glycation end-products of fibrillar collagens in mouse lung. *Experimental Gerontology*, *48*(1), pp.29-37.

Roman, J., (2014). Remodeling of the extracellular matrix in the aging lung. *Molecular Aspects of Aging: Understanding Lung Aging*, pp.145-157.

Rossert, J., Terraz, C. and Dupont, S., (2000). Regulation of type I collagen genes expression. *Nephrology Dialysis Transplantation*, *15*(suppl_6), pp.66-68.

Rossios, C., Pavlidis, S., Hoda, U., Kuo, C.H., Wiegman, C., Russell, K., Sun, K., Loza, M.J., Baribaud, F., Durham, A.L. and Ojo, O., (2018). Sputum transcriptomics reveal upregulation of IL-1 receptor family members in patients with severe asthma. *Journal of Allergy and Clinical Immunology*, *141*(2), pp.560-570.

Rossol, M., Pierer, M., Raulien, N., Quandt, D., Meusch, U., Rothe, K., Schubert, K., Schöneberg, T., Schaefer, M., Krügel, U., Smajilovic, S., Bräuner-Osborne, H., Baerwald, C. and Wagner, U., (2012). Extracellular Ca2+ is a danger signal activating the NLRP3 inflammasome through G protein-coupled calcium sensing receptors. *Nature communications*, *3*(1), pp.1-9.

Roth, M., Johnson, P.R., Rüdiger, J.J., King, G.G., Ge, Q., Burgess, J.K., Anderson, G., Tamm, M. and Black, J.L., (2002). Interaction between glucocorticoids and β2 agonists on bronchial airway smooth muscle cells through synchronised cellular signalling. *The Lancet*, *360*(9342), pp.1293-1299.

Roux, P.P. and Topisirovic, I., (2012). Regulation of mRNA translation by signaling pathways. *Cold Spring Harbor perspectives in biology*, *4*(11), p.a012252.

Royce, S.G., Cheng, V., Samuel, C.S. and Tang, M.L., (2012). The regulation of fibrosis in airway remodeling in asthma. *Molecular and cellular endocrinology*, *351*(2), pp.167-175.

Royce, S.G., Miao, Y.R., Lee, M., Samuel, C.S., Tregear, G.W. and Tang, M.L., (2009). Relaxin reverses airway remodeling and airway dysfunction in allergic airways disease. *Endocrinology*, *150*(6), pp.2692-2699.

Royce, S.G., Moodley, Y. and Samuel, C.S., (2014). Novel therapeutic strategies for lung disorders associated with airway remodelling and fibrosis. *Pharmacology and Therapeutics*, 141(3), pp. 250–260.Elsevier Inc.,

Rozen-Zvi, B., Hayashida, T., Hubchak, S.C., Hanna, C., Platanias, L.C. and William Schnaper, H., (2013). TGF-ß/Smad3 activates mammalian target of rapamycin complex-1 to promote collagen production by increasing HIF-1α expression. *American Journal of Physiology-Renal Physiology*, *305*(4), pp.F485-F494.

Rudolphus, A., Stolk, J., Dijkman, J.H. and Kramps, J.A., (1993). Inhibition of lipopolysaccharide-induced pulmonary emphysema by intratracheally instilled recombinant secretory leukocyte proteinase inhibitor. *American Review of Respiratory Disease*, *147*, pp.442-442.

Runyan, C.E., Schnaper, H.W. and Poncelet, A.C., (2004). The phosphatidylinositol 3-kinase/Akt pathway enhances Smad3-stimulated mesangial cell collagen I expression in response to transforming growth factor-ß1. *Journal of Biological Chemistry*, *279*(4), pp.2632-2639.

Rutten, M.J., Bacon, K.D., Marlink, K.L., Stoney, M., Meichsner, C.L., Lee, F.P., Hobson, S.A., Rodland, K.D., Sheppard, B.C., Trunkey, D.D. and Deveney, K.E., (1999). Identification of a functional Ca2+-sensing receptor in normal human gastric mucous epithelial cells. *American Journal of Physiology-Gastrointestinal and Liver Physiology*, *277*(3), pp.G662-G670.

Rybchyn, M.S., Islam, K.S., Brennan-Speranza, T.C., Cheng, Z., Brennan, S.C., Chang, W., Mason, R.S. and Conigrave, A.D., (2019). Homer1 mediates CaSR-dependent activation of mTOR complex 2 and initiates a novel pathway for AKT-dependent ß-catenin stabilization in osteoblasts. *Journal of Biological Chemistry*, *294*(44), pp.16337-16350.

Rybchyn, M.S., Islam, K.S., Brennan-Speranza, T.C., Cheng, Z., Brennan, S.C., Chang, W., Mason, R.S. and Conigrave, A.D., (2019). Homer1 mediates CaSR-dependent activation of mTOR complex 2 and initiates a novel pathway for AKT-dependent ß-catenin stabilization in osteoblasts. *Journal of Biological Chemistry*, *294*(44), pp.16337-16350.

Rydell-Törmänen, K. and Johnson, J.R., (2019). The applicability of mouse models to the study of human disease. *Mouse Cell Culture*, *1940*, p.3.

Rydell-Törmänen, K., Risse, P.A., Kanabar, V., Bagchi, R., Czubryt, M.P. and Johnson, J.R., (2013). Smooth muscle in tissue remodeling and hyper-reactivity: airways and arteries. *Pulmonary pharmacology & therapeutics*, *26*(1), pp.13-23.

Rylander, R., (2006). Endotoxin and occupational airway disease. *Current opinion in allergy and clinical immunology*, *6*(1), pp.62-66.

Sachs, B.D., Baillie, G.S., McCall, J.R., Passino, M.A., Schachtrup, C., Wallace, D.A., Dunlop, A.J., MacKenzie, K.F., Klussmann, E., Lynch, M.J. and Sikorski, S.L., (2007). p75 neurotrophin receptor regulates tissue fibrosis through inhibition of plasminogen activation via a PDE4/cAMP/PKA pathway. *Journal of Cell Biology*, *177*(6), pp.1119-1132.

Saetta, M., Turato, G., Timens, W. and Jeffery, P.K., (2006). Pathology of chronic obstructive pulmonary. *Management of Chronic Obstructive Pulmonary Disease: European Respiratory Monograph*, *38*, p.159.

Saito, S., Zhuang, Y., Shan, B., Danchuk, S., Luo, F., Korfei, M., Guenther, A. and Lasky, J.A., (2017). Tubastatin ameliorates pulmonary fibrosis by targeting the TGF-β-PI3K-Akt pathway. *PLoS One*, *12*(10), p.e0186615.

Salama, R., Sadaie, M., Hoare, M. and Narita, M., (2014). Cellular senescence and its effector programs. *Genes & development*, *28*(2), pp.99-114.

Salathe, M., Ivonnet, P.I., Lieb, T. and Bookman, R.J., (2001). Agonist-stimulated calcium decreases in ovine ciliated airway epithelial cells: role of mitochondria. *The Journal of physiology*, *531*(1), pp.13-26.

Salminen, A., Kauppinen, A. and Kaarniranta, K., (2012). Emerging role of NF-κB signaling in the induction of senescence-associated secretory phenotype (SASP). *Cellular signalling*, *24*(4), pp.835-845.

Salter, J., (2016). blindanalysis: v1.0 [Data set]. Zenodo.

Salvato, G., (2001). Quantitative and morphological analysis of the vascular bed in bronchial biopsy specimens from asthmatic and non-asthmatic subjects. *Thorax*, *56*(12), pp.902-906.

Sandbo, N., Kregel, S., Taurin, S., Bhorade, S. and Dulin, N.O., (2009). Critical role of serum response factor in pulmonary myofibroblast differentiation induced by TGF-β. *American journal of respiratory cell and molecular biology*, *41*(3), pp.332-338.

Santamaria, F., Borrelli, M. and Baraldi, E., (2021). GINA 2021: the missing pieces in the childhood asthma puzzle. *The Lancet Respiratory Medicine*, *9*(10), p.e98.

Savov, J.D., Brass, D.M., Berman, K.G., McElvania, E. and Schwartz, D.A., (2003). Fibrinolysis in LPS-induced chronic airway disease. *American Journal of Physiology-Lung Cellular and Molecular Physiology*, *285*(4), pp.L940-L948.

Savov, J.D., Brass, D.M., Lawson, B.L., McElvania-Tekippe, E., Walker, J.K. and Schwartz, D.A., (2005). Toll-like receptor 4 antagonist (E5564) prevents the chronic airway response to inhaled lipopolysaccharide. *American Journal of Physiology-Lung Cellular and Molecular Physiology*, *289*(2), pp.L329-L337.

Savov, J.D., Gavett, S.H., Brass, D.M., Costa, D.L. and Schwartz, D.A., (2002). Neutrophils play a critical role in development of LPS-induced airway disease. *American Journal of Physiology-Lung Cellular and Molecular Physiology*, *283*(5), pp.L952-L962.

Schaafsma, D., Gosens, R., Zaagsma, J., Halayko, A.J. and Meurs, H., (2008). Rho kinase inhibitors: a novel therapeutical intervention in asthma?. *European journal of pharmacology*, *585*(2-3), pp.398-406.

Schafer, M.J., White, T.A., Iijima, K., Haak, A.J., Ligresti, G., Atkinson, E.J., Oberg, A.L., Birch, J., Salmonowicz, H., Zhu, Y.I. and Mazula, D.L., (2017). Cellular senescence mediates fibrotic pulmonary disease. *Nature communications*, *8*(1), pp.1-11.

Schepelmann, M., Yarova, P.L., Davies, T., Brennan, S.C., Graca, J., Chang, W., Bikle, D., Ward, D.T., Canfield, A.E., Richards, W.G. and Edwards, D.H., (2013). The vascular smooth muscle cell calcium-sensing receptor is involved in blood pressure regulation, calcium-homeostasis and protection from calcification.[Abstract.]. *J Am Soc Nephrol*, *24*, p.874A.

Schepelmann, M., Yarova, P.L., Lopez-Fernandez, I., Davies, T.S., Brennan, S.C., Edwards, P.J., Aggarwal, A., Graca, J., Rietdorf, K., Matchkov, V., Fenton, R.A., Chang, W., Krssak, M., Stewart, A., Broadley, K.J., Ward, D.T., Price, S.A., Edwards, D.H., Kemp, P.J. and Riccardi, D., (2016). The vascular Ca2+-sensing receptor regulates blood vessel tone and blood pressure. *American Journal of Physiology-Cell Physiology*, *310*(3), pp.C193-C204.

Schiller, H.B., Montoro, D.T., Simon, L.M., Rawlins, E.L., Meyer, K.B., Strunz, M., Vieira Braga, F.A., Timens, W., Koppelman, G.H., Budinger, G.S. and Burgess, J.K., (2019). The human lung cell atlas: a high-resolution reference map of the human lung in health and disease. *American journal of respiratory cell and molecular biology*, *61*(1), pp.31-41.

Schmelzle, T. and Hall, M.N., (2000). TOR, a central controller of cell growth. *Cell*, *103*(2), pp.253-262.

Schmid, A. and Salathe, M., (2011). Ciliary beat co-ordination by calcium. *Biology of the Cell*, *103*(4), pp.159-169.

Schneider, C.A., Rasband, W.S. and Eliceiri, K.W., (2018). NIH image to imagej. *25 years of image analysis*, *2012*, p.9.

Schuliga, M., Javeed, A., Harris, T., Xia, Y., Qin, C., Wang, Z., Zhang, X., Lee, P.V., Camoretti-Mercado, B. and Stewart, A.G., (2013). Transforming growth factor–β–induced differentiation of airway smooth muscle cells Is inhibited by fibroblast growth Factor–2. *American journal of respiratory cell and molecular biology*, *48*(3), pp.346-353.

Schuliga, M., Kanwal, A., Read, J., Blokland, K.E., Burgess, J.K., Prêle, C.M., Mutsaers, S.E., Grainge, C., Thomson, C., James, A. and Bartlett, N.W., (2021). A cGAS-dependent response links DNA damage and senescence in alveolar epithelial cells: A potential drug target in IPF. *American Journal of Physiology-Lung Cellular and Molecular Physiology*, *321*(5), pp.L859-L871.

Schulte, G. and Wright, S.C., (2018). Frizzleds as GPCRs–more conventional than we thought!. *Trends in pharmacological sciences*, *39*(9), pp.828-842.

Sebag, S.C., Koval, O.M., Paschke, J.D., Winters, C.J., Comellas, A.P. and Grumbach, I.M., (2018). Inhibition of the mitochondrial calcium uniporter prevents IL-13 and allergen-mediated airway epithelial apoptosis and loss of barrier function. *Experimental cell research*, *362*(2), pp.400-411.

Selige, J., Tenor, H., Hatzelmann, A. and Dunkern, T., (2010). Cytokine-dependent balance of mitogenic effects in primary human lung fibroblasts related to cyclic AMP signaling and phosphodiesterase 4 inhibition. *Journal of cellular physiology*, *223*(2), pp.317-326.

Selvarajah, B., Azuelos, I., Platé, M., Guillotin, D., Forty, E.J., Contento, G., Woodcock, H.V., Redding, M., Taylor, A., Brunori, G. and Durrenberger, P.F., (2019). mTORC1 amplifies the ATF4-dependent de novo serine-glycine pathway to supply glycine during TGF-β1–induced collagen biosynthesis. *Science signaling*, *12*(582).

Senturk, S., Mumcuoglu, M., Gursoy-Yuzugullu, O., Cingoz, B., Akcali, K.C. and Ozturk, M., (2010). Transforming growth factor-beta induces senescence in

hepatocellular carcinoma cells and inhibits tumor growth. *Hepatology*, *52*(3), pp.966-974.

Settipane, R.J., Hagy, G.W. and Settipane, G.A., (1994). Long-term risk factors for developing asthma and allergic rhinitis: a 23-year follow-up study of college students. In *Allergy and Asthma Proceedings* (Vol. 15, No. 1, p. 21). OceanSide Publications.

Shale, D.J. and Ionescu, A.A., (2004). Mucus hypersecretion: a common symptom, a common mechanism?. *European Respiratory Journal*, *23*(6), pp.797-798.

Sharif, R., (2017). Overview of idiopathic pulmonary fibrosis (IPF) and evidence-based guidelines. *Am J Manag Care*, *23*(11 Suppl), pp.S176-82.

Shi, J., Li, F., Luo, M., Wei, J. and Liu, X., (2017). Distinct roles of Wnt/β-catenin signaling in the pathogenesis of chronic obstructive pulmonary disease and idiopathic pulmonary fibrosis. *Mediators of inflammation*, *2017*.

Shi, L., Chang, Y., Yang, Y., Zhang, Y., Yu, F.S.X. and Wu, X., (2012). Activation of JNK signaling mediates connective tissue growth factor expression and scar formation in corneal wound healing. *PloS one*, *7*(2), p.e32128.

Shi, M., Zhu, J., Wang, R., Chen, X., Mi, L., Walz, T. and Springer, T.A., (2011). Latent TGF-β structure and activation. *Nature*, *474*(7351), pp.343-349.

Shivshankar, P., Brampton, C., Miyasato, S., Kasper, M., Thannickal, V.J. and Le Saux, C.J., (2012). Caveolin-1 deficiency protects from pulmonary fibrosis by modulating epithelial cell senescence in mice. *American journal of respiratory cell and molecular biology*, *47*(1), pp.28-36.

Shi-Wen, X., Chen, Y., Denton, C.P., Eastwood, M., Renzoni, E.A., Bou-Gharios, G., Pearson, J.D., Dashwood, M., du Bois, R.M., Black, C.M. and Leask, A., (2004). Endothelin-1 promotes myofibroblast induction through the ETA receptor via a rac/phosphoinositide 3-kinase/Akt-dependent pathway and is essential for the enhanced contractile phenotype of fibrotic fibroblasts. *Molecular biology of the cell*, *15*(6), pp.2707-2719.

Shi-wen, X., Kennedy, L., Renzoni, E.A., Bou-Gharios, G., du Bois, R.M., Black, C.M., Denton, C.P., Abraham, D.J. and Leask, A., (2007). Endothelin is a downstream mediator of profibrotic responses to transforming growth factor β in human lung fibroblasts. *Arthritis & Rheumatism: Official Journal of the American College of Rheumatology*, *56*(12), pp.4189-4194.

Shi-Wen, X., Rodríguez-Pascual, F., Lamas, S., Holmes, A., Howat, S., Pearson, J.D., Dashwood, M.R., du Bois, R.M., Denton, C.P., Black, C.M. and Abraham, D.J., (2006). Constitutive ALK5-independent c-Jun N-terminal kinase activation contributes to endothelin-1 overexpression in pulmonary fibrosis: evidence of an autocrine endothelin loop operating through the endothelin A and B receptors. *Molecular and cellular biology*, *26*(14), pp.5518-5527.

Shrestha, J., Razavi Bazaz, S., Aboulkheyr Es, H., Yaghobian Azari, D., Thierry, B., Ebrahimi Warkiani, M. and Ghadiri, M., (2020). Lung-on-a-chip: the future of respiratory disease models and pharmacological studies. *Critical reviews in biotechnology*, *40*(2), pp.213-230.

Sibila, O., Soto-Gomez, N. and Restrepo, M.I., (2015). The risk and outcomes of pneumonia in patients on inhaled corticosteroids. *Pulmonary pharmacology & therapeutics*, *32*, pp.130-136.

Šileikytė, J., Petronilli, V., Zulian, A., Dabbeni-Sala, F., Tognon, G., Nikolov, P., Bernardi, P. and Ricchelli, F., (2011). Regulation of the inner membrane mitochondrial permeability transition by the outer membrane translocator protein (peripheral benzodiazepine receptor). *Journal of Biological Chemistry*, *286*(2), pp.1046-1053.

Sime, P.J., Xing, Z., Graham, F.L., Csaky, K.G. and Gauldie, J., (1997). Adenovector-mediated gene transfer of active transforming growth factor-beta1 induces prolonged severe fibrosis in rat lung. *The Journal of clinical investigation*, *100*(4), pp.768-776.

Simpson, J.L., Phipps, S., Baines, K.J., Oreo, K.M., Gunawardhana, L. and Gibson, P.G., (2014). Elevated expression of the NLRP3 inflammasome in neutrophilic asthma. *European Respiratory Journal*, *43*(4), pp.1067-1076.

Singer, M., Martin, L.D., Vargaftig, B.B., Park, J., Gruber, A.D., Li, Y. and Adler, K.B., (2004). A MARCKS-related peptide blocks mucus hypersecretion in a mouse model of asthma. *Nature medicine*, *10*(2), pp.193-196.

Singh, N. and Singh, S., (2021). Interstitial lung diseases and air pollution: narrative review of literature. *Pulmonary Therapy*, *7*(1), pp.89-100.

Singh, N., Promkan, M., Liu, G., Varani, J. and Chakrabarty, S., (2013). Role of calcium sensing receptor (CaSR) in tumorigenesis. *Best practice & research Clinical endocrinology & metabolism*, *27*(3), pp.455-463.

Singh, R.K. and Najmi, A.K., (2019). Novel therapeutic potential of mitogen-activated protein kinase activated protein kinase 2 (MK2) in chronic airway inflammatory disorders. *Current drug targets*, *20*(4), pp.367-379.

Sisson, T.H., Maher, T.M., Ajayi, I.O., King, J.E., Higgins, P.D., Booth, A.J., Sagana, R.L., Huang, S.K., White, E.S., Moore, B.B. and Horowitz, J.C., (2012). Increased survivin expression contributes to apoptosis-resistance in IPF fibroblasts. *Advances in bioscience and biotechnology (Print)*, *3*(6A), p.657.

Skeoch, S., Weatherley, N., Swift, A.J., Oldroyd, A., Johns, C., Hayton, C., Giollo, A., Wild, J.M., Waterton, J.C., Buch, M. and Linton, K., (2018). Drug-induced interstitial lung disease: a systematic review. *Journal of clinical medicine*, *7*(10), p.356.

Slobodnyuk, K., Radic, N., Ivanova, S., Llado, A., Trempolec, N., Zorzano, A. and Nebreda, A.R., (2019). Autophagy-induced senescence is regulated by p38α signaling. *Cell death & disease*, *10*(6), pp.1-18.

Šmerdová, L., Svobodová, J., Kabátková, M., Kohoutek, J., Blažek, D., Machala, M. and Vondráček, J., (2014). Upregulation of CYP1B1 expression by inflammatory cytokines is mediated by the p38 MAP kinase signal transduction pathway. *Carcinogenesis*, *35*(11), pp.2534-2543.

Snider, G.L., Kleinerman, J., Thurlbeck, W.M. and Bengali, Z.H., (1985). The definition of emphysema: report of a National Heart, Lung, and Blood Institute, Division of Lung Diseases workshop.

So, S.Y., Ip, M. and Lam, W.K., (1986). Calcium channel blockers and asthma. *Lung*, *164*(1), pp.1-16.

Song, H., Price, P.W. and Cerny, J., (1997). Age-related changes in antibody repertoire: contribution from T cells. *Immunological reviews*, *160*(1), pp.55-62.

Soriano, J.B., Abajobir, A.A., Abate, K.H., Abera, S.F., Agrawal, A., Ahmed, M.B., Aichour, A.N., Aichour, I., Aichour, M.T.E., Alam, K. and Alam, N., (2017). Global, regional, and national deaths, prevalence, disability-adjusted life years, and years lived with disability for chronic obstructive pulmonary disease and asthma, 1990–2015: a systematic analysis for the Global Burden of Disease Study 2015. *The Lancet Respiratory Medicine*, *5*(9), pp.691-706.

Specks, U., Nerlich, A., Colby, T.V., Wiest, I. and Timpl, R., (1995). Increased expression of type VI collagen in lung fibrosis. *American journal of respiratory and critical care medicine*, *151*(6), pp.1956-1964.

Spencer, J.P., (2007). The interactions of flavonoids within neuronal signalling pathways. *Genes & Nutrition*, *2*(3), pp.257-273.

Squires, P.E., Harris, T.E., Persaud, S.J., Curtis, S.B., Buchan, A.M. and Jones, P.M., (2000). The extracellular calcium-sensing receptor on human beta-cells negatively modulates insulin secretion. *Diabetes*, *49*(3), pp.409-417.

Stamos, J.L. and Weis, W.I., (2013). The β-catenin destruction complex. *Cold Spring Harbor perspectives in biology*, *5*(1), p.a007898.

Starling, C.M., Prado, C.M., Leick-Maldonado, E.A., Lanças, T., Reis, F.G., Aristóteles, L.R., Dolhnikoff, M., Martins, M.A. and Tibério, I.F., (2009). Inducible nitric oxide synthase inhibition attenuates lung tissue responsiveness and remodeling in a model of chronic pulmonary inflammation in guinea pigs. *Respiratory physiology & neurobiology*, *165*(2-3), pp.185-194.

Stirling DR, Swain-Bowden MJ, Lucas AM, Carpenter AE, Cimini BA, Goodman A (2021). CellProfiler 4: improvements in speed, utility and usability. *BMC Bioinformatics*, 22(1), 433.

Stolk, J., Rudolphus, A., Davies, P., Osinga, D., Dijkman, J.H., Agarwal, L., Keenan, K.P., Fletcher, D. and Kramps, J.A., (1992). Induction of emphysema and bronchial mucus cell hyperplasia by intratracheal instillation of lipopolysaccharide in the hamster. *The Journal of pathology*, *167*(3), pp.349-356.

Stolz, D., Leeming, D.J., Kristensen, J.H.E., Karsdal, M.A., Boersma, W., Louis, R., Milenkovic, B., Kostikas, K., Blasi, F., Aerts, J. and Sand, J.M., (2017). Systemic biomarkers of collagen and elastin turnover are associated with clinically relevant outcomes in COPD. *Chest*, *151*(1), pp.47-59.

Stow, J.L. and Murray, R.Z., (2013). Intracellular trafficking and secretion of inflammatory cytokines. *Cytokine & growth factor reviews*, *24*(3), pp.227-239.

Stripp, B.R. and Reynolds, S.D., (2008). Maintenance and repair of the bronchiolar epithelium. *Proceedings of the American Thoracic Society*, *5*(3), pp.328-333.

Strutz, F., Zeisberg, M., Renziehausen, A., Raschke, B., Becker, V., Van Kooten, C. and Müller, G.A., (2001). TGF-β1 induces proliferation in human renal fibroblasts via induction of basic fibroblast growth factor (FGF-2). *Kidney international*, *59*(2), pp.579-592.

Südhof, T.C., (2004). The synaptic vesicle cycle. *Annu. Rev. Neurosci.*, *27*, pp.509-547.

Sueblinvong, V., Neujahr, D.C., Mills, S.T., Roser-Page, S., Guidot, D., Rojas, M., Ritzenthaler, J.D. and Roman, J., (2012). Predisposition for disrepair in the aged lung. *The American journal of the medical sciences*, *344*(1), pp.41-51.

Sueblinvong, V., Neujahr, D.C., Mills, S.T., Roser-Page, S., Guidot, D., Rojas, M., Ritzenthaler, J.D. and Roman, J., (2012). Predisposition for disrepair in the aged lung. *The American journal of the medical sciences*, *344*(1), pp.41-51.

Sun, Q., He, Q., Xu, J., Liu, Q., Lu, Y., Zhang, Z., Xu, X. and Sun, B., (2019). Guanine nucleotide–binding protein G (i) α2 aggravates hepatic ischemia-reperfusion injury in mice by regulating MLK3 signaling. *The FASEB Journal*, *33*(6), pp.7049-7060.

Sundarakrishnan, A., Chen, Y., Black, L.D., Aldridge, B.B. and Kaplan, D.L., (2018). Engineered cell and tissue models of pulmonary fibrosis. *Advanced drug delivery reviews*, *129*, pp.78-94.

Surolia, R., Li, F.J., Wang, Z., Li, H., Liu, G., Zhou, Y., Luckhardt, T., Bae, S., Liu, R.M., Rangarajan, S. and de Andrade, J., (2017). 3D pulmospheres serve as a personalized and predictive multicellular model for assessment of antifibrotic drugs. *JCI insight*, *2*(2).

Suzuki, R., Kato, T., Miyazaki, Y., Iwata, M., Noda, Y., Takagi, K., Nakashima, N. and Torii, K., (2001). Matrix Metalloproteinases and Tissue lnhibitors of Matrix Metalloproteinases in Sputum from Patients with Bronchial Asthma. *Journal of Asthma*, *38*(6), pp.477-484.

Swaby, C., Wilmsen, K., Wally, A., Lagowala, A., Cortez, C., Niederkofler, A., Ghosh, B. and Sidhaye, V.K., (2023). Role of LIM Kinase 1 in Driving Epithelial Plasticity in COPD. In C108. IMMUNITY AND INFLAMMATION IN COPD: NOVEL FINDINGS (pp. A6142-A6142). American Thoracic Society.

Sysa, P., Potter, J.J., Liu, X. and Mezey, E., (2009). Transforming growth factor-β1 up-regulation of human α1 (I) collagen is mediated by Sp1 and Smad2 transacting factors. *DNA and cell biology*, *28*(9), pp.425-434.

Takahashi, M., Kubo, S., Kiryu, S., Gee, J. and Hatabu, H., (2007). MR microscopy of the lung in small rodents. *European journal of radiology*, *64*(3), pp.367-374.

Tang, L., Cheng, C.Y., Sun, X., Pedicone, A.J., Mohamadzadeh, M. and Cheng, S.X., (2016). The extracellular calcium-sensing receptor in the intestine: evidence for regulation of colonic absorption, secretion, motility, and immunity. *Frontiers in physiology*, *7*, p.245.

Tang, W., Smith, S.G., Beaudin, S., Dua, B., Howie, K., Gauvreau, G. and O'byrne, P.M., (2014). IL-25 and IL-25 receptor expression on eosinophils from subjects with allergic asthma. *International archives of allergy and immunology*, *163*(1), pp.5-10.

Tanna, A.P. and Johnson, M., (2018). Rho kinase inhibitors as a novel treatment for glaucoma and ocular hypertension. *Ophthalmology*, *125*(11), pp.1741-1756.

Tanner, L. and Single, A.B., (2020). Animal models reflecting chronic obstructive pulmonary disease and related respiratory disorders: translating pre-clinical data into clinical relevance. *Journal of innate immunity*, *12*(3), pp.203-225.

Tashiro, J., Rubio, G.A., Limper, A.H., Williams, K., Elliot, S.J., Ninou, I., Aidinis, V., Tzouvelekis, A. and Glassberg, M.K., (2017). Exploring animal models that resemble idiopathic pulmonary fibrosis. *Frontiers in medicine*, *4*, p.118.

Tatler, A.L., Philp, C.J., Hill, M.R., Cox, S., Bullock, A.M., Habgood, A., John, A., Middlewick, R., Stephenson, K.E., Goodwin, A.T. and Billington, C.K., (2023). Differential remodeling in small and large murine airways revealed by novel whole lung airway analysis. American Journal of Physiology-Lung Cellular and Molecular Physiology, 324(3), pp.L271-L284.

Terbuch, A., Tiu, C., Candilejo, I.M., Scaranti, M., Curcean, A., Bar, D., Estevez Timon, M., Ameratunga, M., Ang, J.E., Ratoff, J. and Minchom, A.R., (2020). Radiological Patterns of Drug-induced Interstitial Lung Disease (DILD) in Early-phase Oncology Clinical TrialsDrug-induced Interstitial Lung Disease in Phase I Trials. *Clinical Cancer Research*, *26*(18), pp.4805-4813.

Tfelt-Hansen, J., MacLeod, R.J., Chattopadhyay, N., Yano, S., Quinn, S., Ren, X., Terwilliger, E.F., Schwarz, P. and Brown, E.M., (2003). Calcium-sensing receptor stimulates PTHrP release by pathways dependent on PKC, p38 MAPK, JNK, and ERK1/2 in H-500 cells. *American Journal of Physiology-Endocrinology and Metabolism*, *285*(2), pp.E329-E337.

Thannickal, V.J. and Horowitz, J.C., (2006). Evolving concepts of apoptosis in idiopathic pulmonary fibrosis. *Proceedings of the American Thoracic Society*, *3*(4), pp.350-356.

Thannickal, V.J., (2013). Mechanistic links between aging and lung fibrosis. *Biogerontology*, *14*(6), pp.609-615.

Tharmalingam, S. and Hampson, D.R., (2016). The Calcium-Sensing Receptor and Integrins in Cellular Differentiation and Migration. *Frontiers in physiology*, 7, p. 190.Frontiers Media SA,

Thiel, G., Lesch, A. and Keim, A., (2012). Transcriptional response to calcium-sensing receptor stimulation. *Endocrinology*, *153*(10), pp.4716-4728.

Thomas, B., Rutman, A., Hirst, R.A., Haldar, P., Wardlaw, A.J., Bankart, J., Brightling, C.E. and O'Callaghan, C., (2010). Ciliary dysfunction and ultrastructural abnormalities are features of severe asthma. *Journal of Allergy and Clinical Immunology*, *126*(4), pp.722-729.

Thompson, B.J., (2010). Developmental control of cell growth and division in Drosophila. *Current opinion in cell biology*, *22*(6), pp.788-794.

Thomsen, A.R.B., Hvidtfeldt, M. and Bräuner-Osborne, H., (2012). Biased agonism of the calcium-sensing receptor. *Cell calcium*, *51*(2), pp.107-116.

Tian, X., Liu, Z., Niu, B., Zhang, J., Tan, T.K., Lee, S.R., Zhao, Y., Harris, D.C. and Zheng, G., (2011). E-cadherin/β-catenin complex and the epithelial barrier. *Journal of Biomedicine and Biotechnology*, *2011*.

Tillie-Leblond, I., Pugin, J., Marquette, C.H., Lamblin, C., Saulnier, F., Brichet, A., Wallaert, B., Tonnel, A.B. and Gosset, P., (1999). Balance between proinflammatory cytokines and their inhibitors in bronchial lavage from patients with status asthmaticus. *American journal of respiratory and critical care medicine*, *159*(2), pp.487-494.

Tjin, G., White, E.S., Faiz, A., Sicard, D., Tschumperlin, D.J., Mahar, A., Kable, E.P. and Burgess, J.K., (2017). Lysyl oxidases regulate fibrillar collagen remodelling in idiopathic pulmonary fibrosis. *Disease models & mechanisms*, *10*(11), pp.1301-1312.

Tjin, G., White, E.S., Kable, E. and Burgess, J., (2016). TGF-Β Induced Collagen Remodelling by IPF Fibroblasts is Alleviated by Inhibition of Lysyl Oxidase Enzyme Activity. *QJM: An International Journal of Medicine*, *109*(suppl_1), pp.S14-S14.

Tjin, G., Xu, P., Kable, S.H., Kable, E.P. and Burgess, J.K., (2014). Quantification of collagen I in airway tissues using second harmonic generation. *Journal of biomedical optics*, *19*(3), p.036005.

Tkach, V., Bock, E. and Berezin, V., (2005). The role of RhoA in the regulation of cell morphology and motility. *Cell motility and the cytoskeleton*, *61*(1), pp.21-33.

Togo, S., Liu, X., Wang, X., Sugiura, H., Kamio, K., Kawasaki, S., Kobayashi, T., Ertl, R.F., Ahn, Y., Holz, O. and Magnussen, H., (2009). PDE4 inhibitors roflumilast and rolipram augment PGE2 inhibition of TGF-Β1-stimulated fibroblasts. *American Journal of Physiology-Lung Cellular and Molecular Physiology*, *296*(6), pp.L959-L969.

Tomasek, J.J., Vaughan, M.B., Kropp, B.P., Gabbiani, G., Martin, M.D., Haaksma, C.J. and Hinz, B., (2006). Contraction of myofibroblasts in granulation tissue is dependent on Rho/Rho kinase/myosin light chain phosphatase activity. *Wound repair and regeneration*, *14*(3), pp.313-320.

Tominaga, K. and Suzuki, H.I., (2019). TGF-Β signaling in cellular senescence and aging-related pathology. *International journal of molecular sciences*, *20*(20), p.5002.

Tourkina, E., Richard, M., Gooz, P., Bonner, M., Pannu, J., Harley, R., Bernatchez, P.N., Sessa, W.C., Silver, R.M. and Hoffman, S., (2008). Antifibrotic properties of caveolin-1 scaffolding domain in vitro and in vivo. *American Journal of Physiology-Lung Cellular and Molecular Physiology*, *294*(5), pp.L843-L861.

Toward, T.J. and Broadley, K.J., (2001). Chronic lipopolysaccharide exposure on airway function, cell infiltration, and nitric oxide generation in conscious guinea pigs: effect of rolipram and dexamethasone. *Journal of Pharmacology and Experimental Therapeutics*, *298*(1), pp.298-306.

Toward, T.J. and Broadley, K.J., (2002). Goblet cell hyperplasia, airway function, and leukocyte infiltration after chronic lipopolysaccharide exposure in conscious Guinea pigs: effects of rolipram and dexamethasone. *Journal of Pharmacology and Experimental Therapeutics*, *302*(2), pp.814-821.

Trian, T., Benard, G., Begueret, H., Rossignol, R., Girodet, P.O., Ghosh, D., Ousova, O., Vernejoux, J.M., Marthan, R., Tunon-de-Lara, J.M. and Berger, P., (2007). Bronchial smooth muscle remodeling involves calcium-dependent enhanced mitochondrial biogenesis in asthma. *Journal of Experimental Medicine*, *204*(13), pp.3173-3181.

Tsuji, T., Aoshiba, K. and Nagai, A., (2006). Alveolar cell senescence in patients with pulmonary emphysema. *American journal of respiratory and critical care medicine*, *174*(8), pp.886-893.

Tsukada, S., Westwick, J.K., Ikejima, K., Sato, N. and Rippe, R.A., (2005). SMAD and p38 MAPK signaling pathways independently regulate α1 (I) collagen gene expression in unstimulated and transforming growth factor-β-stimulated hepatic stellate cells. *Journal of Biological Chemistry*, *280*(11), pp.10055-10064.

Tsukui, T., Sun, K.H., Wetter, J.B., Wilson-Kanamori, J.R., Hazelwood, L.A., Henderson, N.C., Adams, T.S., Schupp, J.C., Poli, S.D., Rosas, I.O. and Kaminski, N., (2020). Collagen-producing lung cell atlas identifies multiple subsets with distinct localization and relevance to fibrosis. *Nature communications*, *11*(1), pp.1-16.

Tu, C.L., Celli, A., Mauro, T. and Chang, W., (2019). Calcium-sensing receptor regulates epidermal intracellular Ca2+ signaling and re-epithelialization after wounding. *Journal of Investigative Dermatology*, *139*(4), pp.919-929.

Tu, C.L., Chang, W. and Bikle, D.D., (2011). The calcium-sensing receptor-dependent regulation of cell–cell adhesion and keratinocyte differentiation requires Rho and filamin A. *Journal of investigative dermatology*, *131*(5), pp.1119-1128.

Tyner, J.W., Kim, E.Y., Ide, K., Pelletier, M.R., Roswit, W.T., Morton, J.D., Battaile, J.T., Patel, A.C., Patterson, G.A., Castro, M. and Spoor, M.S., (2006). Blocking airway mucous cell metaplasia by inhibiting EGFR antiapoptosis and IL-13 transdifferentiation signals. *The Journal of clinical investigation*, *116*(2), pp.309-321.

Tzavlaki, K. and Moustakas, A., (2020). TGF-β Signaling. *Biomolecules*, *10*(3), p.487.

Tzilas, V., Bouros, E., Barbayianni, I., Karampitsakos, T., Kourtidou, S., Ntassiou, M., Ninou, I., Aidinis, V., Bouros, D. and Tzouvelekis, A., (2019). Vitamin D prevents experimental lung fibrosis and predicts survival in patients with idiopathic pulmonary fibrosis. *Pulmonary Pharmacology & Therapeutics*, *55*, pp.17-24.

Uchida, D.A., Ackerman, S.J., Coyle, A.J., Larsen, G.L., Weller, P.F., Freed, J. and Irvin, C.G., (1993). The Effect of Human Eosinophil Granule Major Basic Protein on Airway Responsiveness in the Rat *In Vivo* : A Comparison with Polycations. *American Review of Respiratory Disease*, *147*(4), pp. 982–988.

Uchiyama-Tanaka, Y., Matsubara, H., Mori, Y., Kosaki, A., Kishimoto, N., Amano, K., Higashiyama, S. and Iwasaka, T., (2002). Involvement of HB-EGF and EGF receptor transactivation in TGF-β–mediated fibronectin expression in mesangial cells. *Kidney international*, *62*(3), pp.799-808.

Uhal, B.D., (2002). Apoptosis in lung fibrosis and repair. *Chest*, *122*(6), pp.293S-298S.

Uhlén, M., Fagerberg, L., Hallström, B.M., Lindskog, C., Oksvold, P., Mardinoglu, A., Sivertsson, Å., Kampf, C., Sjöstedt, E., Asplund, A. and Olsson, I., (2015). Tissue-based map of the human proteome. *Science*, *347*(6220).

Ulich, T.R., Watson, L.R., Yin, S.M., Guo, K.Z., Wang, P.E.N.G., Thang, H.D.J.C. and Del Castillo, J., (1991). The intratracheal administration of endotoxin and cytokines. I. Characterization of LPS-induced IL-1 and TNF mRNA expression and the LPS-, IL-1-, and TNF-induced inflammatory infiltrate. *The American journal of pathology*, *138*(6), p.1485.

Underwood, D.C., Osborn, R.R., Bochnowicz, S., Webb, E.F., Rieman, D.J., Lee, J.C., Romanic, A.M., Adams, J.L., Hay, D.W. and Griswold, D.E., (2000). SB 239063, a p38 MAPK inhibitor, reduces neutrophilia, inflammatory cytokines, MMP-9, and fibrosis in lung. *American Journal of Physiology-Lung Cellular and Molecular Physiology*, *279*(5), pp.L895-L902.

Undevia, N.S., Dorscheid, D.R., Marroquin, B.A., Gugliotta, W.L., Tse, R. and White, S.R., (2004). Smad and p38-MAPK signaling mediates apoptotic effects of transforming growth factor-β1 in human airway epithelial cells. *American Journal of Physiology-Lung Cellular and Molecular Physiology*, *287*(3), pp.L515-L524.

Van der Velden, J., Harkness, L.M., Barker, D.M., Barcham, G.J., Ugalde, C.L., Koumoundouros, E., Bao, H., Organ, L.A., Tokanovic, A., Burgess, J.K. and Snibson, K.J., (2016). The effects of tumstatin on vascularity, airway inflammation and lung function in an experimental sheep model of chronic asthma. *Scientific reports*, *6*(1), pp.1-10.

Van der Velden, J.L., Ye, Y., Nolin, J.D., Hoffman, S.M., Chapman, D.G., Lahue, K.G., Abdalla, S., Chen, P., Liu, Y., Bennett, B. and Khalil, N., (2016). JNK inhibition reduces lung remodeling and pulmonary fibrotic systemic markers. *Clinical and translational medicine*, *5*(1), pp.1-18.

van Dijk, E.M., Menzen, M.H., Spanjer, A.I., Middag, L.D., Brandsma, C.A.A. and Gosens, R., (2016). Noncanonical WNT-5B signaling induces inflammatory responses in human lung fibroblasts. *American Journal of Physiology-Lung Cellular and Molecular Physiology*, *310*(11), pp.L1166-L1176.

van Heusden, C., Grubb, B.R., Button, B. and Lazarowski, E.R., (2021). Airway epithelial nucleotide release contributes to mucociliary clearance. *Life*, *11*(5), p.430.

Van Lommel, A. and Lauweryns, J.M., (1997). Postnatal development of the pulmonary neuroepithelial bodies in various animal species. *Journal of the autonomic nervous system*, *65*(1), pp.17-24.

van Manen, M.J., Geelhoed, J.M., Tak, N.C. and Wijsenbeek, M.S., (2017). Optimizing quality of life in patients with idiopathic pulmonary fibrosis. *Therapeutic Advances in Respiratory Disease*, *11*(3), pp.157-169.

Vanacker, N.J., Palmans, E., Pauwels, R.A. and Kips, J.C., (2002a). Dose-related effect of inhaled fluticasone on allergen-induced airway changes in rats. *European Respiratory Journal*, *20*(4), pp.873-879.

Vanacker, N.J., Palmans, E., Pauwels, R.A. and Kips, J.C., (2002b). Effect of combining salmeterol and fluticasone on the progression of airway remodeling. *American journal of respiratory and critical care medicine*, *166*(8), pp.1128-1134.

Vanacker, N.J., Palmans, E.L.S., Kips, J.C. and Pauwels, R.A., (2001). Fluticasone inhibits but does not reverse allergen-induced structural airway changes. *American Journal of Respiratory and Critical Care Medicine*, *163*(3), pp.674-679.

Vander Ark, A., Cao, J. and Li, X., (2018). TGF-β receptors: In and beyond TGF-β signaling. *Cellular Signalling*, 52, pp. 112–120.Pergamon,

Varela-Rey, M., Montiel-Duarte, C., Oses-Prieto, J.A., Lopez-Zabalza, M.J., Jaffrezou, J.P., Rojkind, M. and Iraburu, M.J., (2002). p38 MAPK mediates the regulation of α1 (I) procollagen mRNA levels by TNF-α and TGF-β in a cell line of rat hepatic stellate cells. *FEBS letters*, *528*(1-3), pp.133-138.

Varet, H., Brillet-Guéguen, L., Coppée, J.Y. and Dillies, M.A., (2016). SARTools: a DESeq2-and EdgeR-based R pipeline for comprehensive differential analysis of RNA-Seq data. *PloS one*, *11*(6), p.e0157022.

Verbeken, E.K., Cauberghs, M., Mertens, I., Clement, J., Lauweryns, J.M. and Van de Woestijne, K.P., (1992). The senile lung: comparison with normal and emphysematous lungs 2. Functional aspects. *Chest*, *101*(3), pp.800-809.

Vernooy, J.H., Dentener, M.A., Van Suylen, R.J., Buurman, W.A. and Wouters, E.F., (2002). Long-term intratracheal lipopolysaccharide exposure in mice results in chronic lung inflammation and persistent pathology. *American journal of respiratory cell and molecular biology*, *26*(1), pp.152-159.

Vernooy, J.H., Dentener, M.A., Van Suylen, R.J., Buurman, W.A. and Wouters, E.F., (2001). Intratracheal instillation of lipopolysaccharide in mice induces apoptosis in bronchial epithelial cells: no role for tumor necrosis factor-α and infiltrating neutrophils. *American journal of respiratory cell and molecular biology*, *24*(5), pp.569-576.

Verrecchia, F., Chu, M.L. and Mauviel, A., (2001). Identification of novel TGF-β/Smad gene targets in dermal fibroblasts using a combined cDNA microarray/promoter transactivation approach. *Journal of biological chemistry*, *276*(20), pp.17058-17062.

Vicent, G.P., Zaurin, R., Ballaré, C., Nacht, A.S. and Beato, M., (2009). Erk signaling and chromatin remodeling in MMTV promoter activation by progestins. *Nuclear receptor signaling*, *7*(1), pp.nrs-07008.

Vignola, A.M., Chanez, P., Chiappara, G., Merendino, A., Pace, E., Rizzo, A., la ROCCA, A.M., Bellia, V., Bonsignore, G. and Bousquet, J., (1997). Transforming growth factor-β expression in mucosal biopsies in asthma and chronic bronchitis. *American journal of respiratory and critical care medicine*, *156*(2), pp.591-599.

Vignola, A.M., Chanez, P., Chiappara, G., Merendino, A., Pace, E., Rizzo, A., la ROCCA, A.M., Bellia, V., Bonsignore, G. and Bousquet, J., (1997). Transforming growth factor-β expression in mucosal biopsies in asthma and chronic bronchitis. *American journal of respiratory and critical care medicine*, *156*(2), pp.591-599.

Vignola, A.M., Riccobono, L., Mirabella, A., Profita, M., Chanez, P., Bellia, V., Mautino, G., D'accardi, P., Bousquet, J. and Bonsignore, G., (1998). Sputum metalloproteinase-9/tissue inhibitor of metalloproteinase-1 ratio correlates with airflow obstruction in asthma and chronic bronchitis. *American journal of respiratory and critical care medicine*, *158*(6), pp.1945-1950.

Virchow Jr, J.C., Kroegel, C., Walker, C. and Matthys, H., (1996). Inflammatory determinants of asthma severity: mediator and cellular changes in bronchoalveolar lavage fluid of patients with severe asthma. *Journal of Allergy and Clinical Immunology*, *98*(5), pp.S27-S40.

Vitenberga, Z. and Pilmane, M., (2018). Age-related lung tissue remodeling due to the local distribution of MMP-2, TIMP-2, TGF-β and Hsp70. *Biotechnic & Histochemistry*, *93*(4), pp.239-248.

Vitenberga, Z. and Pilmane, M., (2018). Age-related lung tissue remodeling due to the local distribution of MMP-2, TIMP-2, TGF-β and Hsp70. *Biotechnic & Histochemistry*, *93*(4), pp.239-248.

Vlahos, R. and Bozinovski, S., (2014). Recent advances in pre-clinical mouse models of COPD. *Clinical science*, *126*(4), pp.253-265.

Vlahovic, G., Russell, M.L., Mercer, R.R. and Crapo, J.D., (1999). Cellular and connective tissue changes in alveolar septal walls in emphysema. *American journal of respiratory and critical care medicine*, *160*(6), pp.2086-2092.

Vogelzang, P.F., van der Gulden, J.W., Folgering, H., Kolk, J.J., Heederik, D., Preller, L., Tielen, M.J. and van Schayck, C.P., (1998). Endotoxin exposure as a major determinant of lung function decline in pig farmers. *American journal of respiratory and critical care medicine*, *157*(1), pp.15-18.

Vos, T., Lim, S.S., Abbafati, C., Abbas, K.M., Abbasi, M., Abbasifard, M., Abbasi-Kangevari, M., Abbastabar, H., Abd-Allah, F., Abdelalim, A. and Abdollahi, M., (2020). Global burden of 369 diseases and injuries in 204 countries and territories, 1990–2019: a systematic analysis for the Global Burden of Disease Study 2019. *The Lancet*, *396*(10258), pp.1204-1222.

Vyleta, N.P. and Smith, S.M., (2011). Spontaneous glutamate release is independent of calcium influx and tonically activated by the calcium-sensing receptor. *Journal of Neuroscience*, *31*(12), pp.4593-4606.

Wadsworth, S.J., Sin, D.D. and Dorscheid, D.R., (2011). Clinical update on the use of biomarkers of airway inflammation in the management of asthma. *Journal of asthma and allergy*, *4*, p.77.

Waghray, M., Cui, Z., Horowitz, J.C., Subramanian, I.M., Martinez, F.J., Toews, G.B. and Thannickal, V.J., (2005). Hydrogen peroxide is a diffusible paracrine signal for the induction of epithelial cell death by activated myofibroblasts. *The FASEB journal*, *19*(7), pp.1-16.

Wakahara, K., Tanaka, H., Takahashi, G., Tamari, M., Nasu, R., Toyohara, T., Takano, H., Saito, S., Inagaki, N., Shimokata, K. and Nagai, H., (2008). Repeated instillations of Dermatophagoides farinae into the airways can induce Th2-dependent airway hyperresponsiveness, eosinophilia and remodeling in mice: effect of intratracheal treatment of fluticasone propionate. *European journal of pharmacology*, *578*(1), pp.87-96.

Walker, E.J., Heydet, D., Veldre, T. and Ghildyal, R., (2019). Transcriptomic changes during TGF-β-mediated differentiation of airway fibroblasts to myofibroblasts. *Scientific reports*, *9*(1), pp.1-14.

Walters, E.H., Soltani, A., Reid, D.W. and Ward, C., (2008). Vascular remodelling in asthma. *Current opinion in allergy and clinical immunology*, *8*(1), pp.39-43.

Wang, J., Faiz, A., Ge, Q., Vermeulen, C.J., Van der Velden, J., Snibson, K.J., van de Velde, R., Sawant, S., Xenaki, D., Oliver, B. and Timens, W., Hacken, N.T., van den Berge, M., James, A., Elliot, J.G., Dong, L., Burgess, J.K., Ashton, A.W., (2018).

Unique mechanisms of connective tissue growth factor regulation in airway smooth muscle in asthma: Relationship with airway remodelling. *Journal of cellular and molecular medicine*, *22*(5), pp.2826-2837.

Wang, J., Hu, K., Cai, X., Yang, B., He, Q., Wang, J. and Weng, Q., (2022). Targeting PI3K/AKT signaling for treatment of idiopathic pulmonary fibrosis. *Acta Pharmaceutica Sinica B*, *12*(1), pp.18-32.

Wang, L., Ma, R., Flavell, R.A. and Choi, M.E., (2002). Requirement of mitogen-activated protein kinase kinase 3 (MKK3) for activation of p38α and p38δ MAPK isoforms by TGF-ß1 in murine mesangial cells. *Journal of Biological Chemistry*, *277*(49), pp.47257-47262.

Wang, X.R., Zhang, H.X., Sun, B.X., Dai, H.L., Hang, J.Q., Eisen, E.A., Wegman, D.H., Olenchock, S.A. and Christiani, D.C., (2005). A 20-year follow-up study on chronic respiratory effects of exposure to cotton dust. *European Respiratory Journal*, *26*(5), pp.881-886.

Wansleeben, C., Bowie, E., Hotten, D.F., Yu, Y.R.A. and Hogan, B.L., (2014). Age-related changes in the cellular composition and epithelial organization of the mouse trachea. *PloS one*, *9*(3), p.e93496.

Warburton, D., Shi, W. and Xu, B., (2013). TGF-ß-Smad3 signaling in emphysema and pulmonary fibrosis: an epigenetic aberration of normal development?. *American Journal of Physiology-Lung Cellular and Molecular Physiology*, *304*(2), pp.L83-L85.

Ward, D.T. and Riccardi, D., (2012). New concepts in calcium-sensing receptor pharmacology and signalling. *British journal of pharmacology*, *165*(1), pp.35-48.

Ward, D.T., McLarnon, S.J. and Riccardi, D., (2002). Aminoglycosides increase intracellular calcium levels and ERK activity in proximal tubular OK cells expressing the extracellular calcium-sensing receptor. *Journal of the American Society of Nephrology*, *13*(6), pp.1481-1489.

Warshamana, G.S., Pociask, D.A., Fisher, K.J., Liu, J.Y., Sime, P.J. and Brody, A.R., (2002). Titration of non-replicating adenovirus as a vector for transducing active TGF-ß1 gene expression causing inflammation and fibrogenesis in the lungs of C57BL/6 mice. *International journal of experimental pathology*, *83*(4), pp.183-202.

Wasserstein, R.L., and Lazar, N.A., (2016) The ASA Statement on *p*-Values: Context, Process, and Purpose. *The American Statistician*, *70*(2), pp.129-133.

Waters, D.W., Schuliga, M., Fogarty, E., Burgess, J.K., Grainge, C., Westall, G., Laurent, G., Prele, C.M., Mutsaers, S.E. and Knight, D., (2017). Dysregulated Stat3 Signaling Induces And Reinforces Fibroblast Senescence In Lung Fibroblasts Of Ipf Patients. In *A74. REGULATORY MECHANISMS OF THE MOLECULAR PATHWAYS IN FIBROSIS* (pp. A2457-A2457). American Thoracic Society.

Weichselbaum, M., Sparrow, M.P., Hamilton, E.J., Thompson, P.J. and Knight, D.A., (2005). A confocal microscopic study of solitary pulmonary neuroendocrine cells in human airway epithelium. *Respiratory Research*, *6*(1), pp.1-11.

Weng, A., Maciel Herrerias, M., Watanabe, S., Welch, L.C., Flozak, A.S., Grant, R.A., Aillon, R.P., Dada, L.A., Han, S.H., Hinchcliff, M. and Misharin, A.V., (2022). Lung injury induces alveolar type 2 cell hypertrophy and polyploidy with implications for

repair and regeneration. *American journal of respiratory cell and molecular biology*, *66*(5), pp.564-576.

West, J.B., (2011). Respiratory physiology: the essentials. 9th edn. Lippincott Williams & Wilkins, Philadelphia/London

White, E.S., (2015). Lung extracellular matrix and fibroblast function. *Annals of the American Thoracic Society*, *12*(Supplement 1), pp.S30-S33.

White, E.S., Lazar, M.H. and Thannickal, V.J., (2003). Pathogenetic mechanisms in usual interstitial pneumonia/idiopathic pulmonary fibrosis. *The Journal of Pathology: A Journal of the Pathological Society of Great Britain and Ireland*, *201*(3), pp.343-354.

Wilkinson, J.E., Burmeister, L., Brooks, S.V., Chan, C.C., Friedline, S., Harrison, D.E., Hejtmancik, J.F., Nadon, N., Strong, R., Wood, L.K. and Woodward, M.A., (2012). Rapamycin slows aging in mice. *Aging cell*, *11*(4), pp.675-682.

Wilkinson, T.M., Hurst, J.R., Perera, W.R., Wilks, M., Donaldson, G.C. and Wedzicha, J.A., (2006). Effect of interactions between lower airway bacterial and rhinoviral infection in exacerbations of COPD. *Chest*, *129*(2), pp.317-324.

Willemse, B.W., Ten Hacken, N.H., Rutgers, B., Postma, D.S. and Timens, W., (2005a). Association of current smoking with airway inflammation in chronic obstructive pulmonary disease and asymptomatic smokers. *Respiratory research*, *6*(1), pp.1-10.

Williams, C.M., Rahman, S., Hubeau, C. and Ma, H.L., (2012). Cytokine pathways in allergic disease. *Toxicologic pathology*, *40*(2), pp.205-215.

Williams, K. and Roman, J., (2016). Studying human respiratory disease in animals–role of induced and naturally occurring models. *The Journal of pathology*, *238*(2), pp.220-232.

Williams, O.W., Sharafkhaneh, A., Kim, V., Dickey, B.F. and Evans, C.M., (2006). Airway mucus: from production to secretion. *American journal of respiratory cell and molecular biology*, *34*(5), pp.527-536.

Wills-Karp, M., (2004). Interleukin-13 in asthma pathogenesis. *Immunological reviews*, *202*(1), pp.175-190.

Wilson, R., Templeton, A., Leemereise, C., Eames, R., Banham-Hall, E., Hessel, E.M. and Cahn, A., (2019). Safety, tolerability, and pharmacokinetics of a new formulation of nemiralisib administered via a dry powder inhaler to healthy individuals. *Clinical therapeutics*, *41*(6), pp.1214-1220.

Wilson, S.J., Ward, J.A., Pickett, H.M., Baldi, S., Sousa, A.R., Sterk, P.J., Chung, K.F., Djukanovic, R., Dahlen, B., Billing, B. and Shaw, D., (2021). Airway Elastin is increased in severe asthma and relates to proximal wall area: histological and computed tomography findings from the U-BIOPRED severe asthma study. *Clinical & Experimental Allergy*, *51*(2), pp.296-304.

Wipff, P.J., Rifkin, D.B., Meister, J.J. and Hinz, B., (2007). Myofibroblast contraction activates latent TGF-β1 from the extracellular matrix. *Journal of Cell Biology*, 179(6), pp. 1311–1323.

Wnuk, D., Paw, M., Ryczek, K., Bochenek, G., Sładek, K., Madeja, Z. and Michalik, M., (2020). Enhanced asthma-related fibroblast to myofibroblast transition is the result of profibrotic TGF-ß/Smad2/3 pathway intensification and antifibrotic TGF-ß/Smad1/5/(8) 9 pathway impairment. *Scientific reports*, *10*(1), pp.1-16.

Wójcik-Pszczoła, K., Chłoń-Rzepa, G., Jankowska, A., Ślusarczyk, M., Ferdek, P.E., Kusiak, A.A., Świerczek, A., Pociecha, K., Koczurkiewicz-Adamczyk, P., Wyska, E. and Pękala, E., (2020). A novel, Pan-PDE inhibitor exerts anti-fibrotic effects in human lung fibroblasts via inhibition of TGF-ß signaling and activation of cAMP/PKA signaling. *International journal of molecular sciences*, *21*(11), p.4008.

Wolffs, K.L., (2022). *Determining the role of the calcium-sensing receptor (CASR) in pulmonary fibrosis (PF) and the ability of a CASR inhibitor to reverse profibrotic changes in an in vitro model of PF* (Doctoral dissertation, Cardiff University).

Wolter, P., Collard, H.R. and Jones, K., (2014). Pathogenesis of Idiopathic Pulmonary Fibrosis. *Annual review of pathology*, (9), pp. 157–179.

Wong, C., Rougier-Chapman, E.M., Frederick, J.P., Datto, M.B., Liberati, N.T., Li, J.M. and Wang, X.F., (1999). Smad3-Smad4 and AP-1 complexes synergize in transcriptional activation of the c-Jun promoter by transforming growth factor ß. *Molecular and cellular biology*, *19*(3), pp.1821-1830.

Wong, S.L. and Sukkar, M.B., (2017). The SPARC protein: an overview of its role in lung cancer and pulmonary fibrosis and its potential role in chronic airways disease. *British journal of pharmacology*, *174*(1), pp.3-14.

Woodruff, P.G., Dolganov, G.M., Ferrando, R.E., Donnelly, S., Hays, S.R., Solberg, O.D., Carter, R., Wong, H.H., Cadbury, P.S. and Fahy, J.V., (2004). Hyperplasia of smooth muscle in mild to moderate asthma without changes in cell size or gene expression. *American journal of respiratory and critical care medicine*, *169*(9), pp.1001-1006.

Woodworth, B.A., Zhang, S., Tamashiro, E., Bhargave, G., Palmer, J.N. and Cohen, N.A., (2010). Zinc increases ciliary beat frequency in a calcium-dependent manner. *American journal of rhinology & allergy*, *24*(1), pp.6-10.

World Health Organisation, (2020). Global Health Estimates 2020: Deaths by Cause, Age, Sex, by Country and by Region, 2000-2019. Geneva, World Health Organization; 2020.

Wright, J.L. and Churg, A., (1990). Cigarette Smoke Causes Physiologic and Morphologic Changes of Emphysema in the Guinea Pig1–3. *Am Rev Respir Dis*, *142*, pp.1422-8.

Wright, J.L., Cosio, M. and Churg, A., (2008). Animal models of chronic obstructive pulmonary disease. *American journal of physiology-lung cellular and molecular physiology*, *295*(1), pp.L1-L15.

Wright, J.L., Tazelaar, H.D. and Churg, A., (2011). Fibrosis with emphysema. *Histopathology*, *58*(4), pp.517-524.

Wu, M., Wang, S.S., Cao, J.Y., Tang, T.T., Gao, M., Ma, K.L. and Liu, B.C., (2019). Calcium-sensing receptor mediates interleukin-1ß-induced collagen expression in mouse collecting duct cells. *Journal of Cellular Biochemistry*, 120(5), pp. 7353–7362.

Wylam, M.E., Sathish, V., VanOosten, S.K., Freeman, M., Burkholder, D., Thompson, M.A., Pabelick, C.M. and Prakash, Y.S., (2015). Mechanisms of cigarette smoke effects on human airway smooth muscle. *PloS one*, *10*(6), p.e0128778.

Wynn, T.A. and Vannella, K.M., (2016). Macrophages in tissue repair, regeneration, and fibrosis. *Immunity*, *44*(3), pp.450-462.

Wynn, T.A., (2007). Common and unique mechanisms regulate fibrosis in various fibroproliferative diseases. *The Journal of clinical investigation*, *117*(3), pp.524-529.

Xiao, L., Du, Y., Shen, Y., He, Y., Zhao, H. and Li, Z., (2012). TGF-beta 1 induced fibroblast proliferation is mediated by the FGF-2/ERK pathway. *Frontiers in Bioscience-Landmark*, *17*(7), pp.2667-2674.

Xie, T., Luo, G.Y., Zhang, Y., Wang, X., Wang, X.Y., Wu, M. and Li, G.P., (2015). Rho-kinase inhibitor fasudil reduces allergic airway inflammation and mucus hypersecretion by regulating STAT 6 and NF κB. *Clinical & Experimental Allergy*, *45*(12), pp.1812-1822.

Xu, K., Ma, J., Lu, R., Shao, X., Zhao, Y., Cui, L., Qiu, Z., Tian, Y. and Li, J., (2023). Effective-compound combination of Bufei Yishen formula III combined with ER suppress airway mucus hypersecretion in COPD rats: via EGFR/MAPK signaling. *Bioscience Reports*, p.BSR20222669.

Yamauchi, K., (2006). Airway remodeling in asthma and its influence on clinical pathophysiology. *The Tohoku journal of experimental medicine*, *209*(2), pp.75-87.

Yan, F., Gao, H., Zhao, H., Bhatia, M. and Zeng, Y., (2018). Roles of airway smooth muscle dysfunction in chronic obstructive pulmonary disease. *Journal of translational medicine*, *16*(1), pp.1-9.

Yang, H., Juliy, M.P., Victor, P.K. and Zhou, X., (2014a). Role of calcium-sensing receptor in hypoxia-induced airway mucous hypersecretion. *Zhonghua yi xue za zhi*, *94*(12), pp.944-947.

Yang, H.J., Perelman, J.M., Kolosov, V.P. and Zhou, X.D., (2014b). Calcium-sensing receptor mediation of hypoxia-induced mucous hypersecretion of human airway epithelial cells by ERK signaling pathway. *Basic & Clinical Medicine*, *34*(7), pp.877-881.

Yarova, P.L., Davies, C., Price, S.A., Huang, Q., Graca, J.A., Maleki-Toyserkani, S., Lowe, A.P.P., Kidd, E.J., Ford, W.R., Broadley, K.J. and Ward, J.P.T., Corrigan, J. C., Prakash, Y. S., Kemp, P. J. and Riccardi, D. (2016). Inhaled calcilytics: effects on airway inflammation and remodeling. In *Respiratory Drug Delivery* (Vol. 1, pp. 1-12).

Yarova, P.L., Huang, P., Schepelmann, M.W., Bruce, R., Ecker, R., Nica, R., Telezhkin, V., Traini, D., Dos Reis, L.G., Kidd, E.J. and Ford, W.R., Broadley, K.J., Kariuki, B.M., Corrigan, C.J., Ward, J.P.T., Kemp, P.J., and Riccardi, D., (2021). Characterization of negative allosteric modulators of the calcium-sensing receptor for repurposing as a treatment of asthma. *Journal of Pharmacology and Experimental Therapeutics*, *376*(1), pp.51-63.

Yarova, P.L., Stewart, A.L., Sathish, V., Britt, R.D., Thompson, M.A., Lowe, A.P., Freeman, M., Aravamudan, B., Kita, H., Brennan, S.C., Schepelmann, M., Davies,

T., Yung, S., Cholisoh, Z., Kidd, E.J., Ford, W.R., Broadley K.J., Rietdorf, K., Chang, W., Bin Khayat, M.E., Ward, D.T., Corrigan, C.J., Ward, J.P.T., Kemp, P.J., Pabelick, C.M., Prakash, Y.S., and Riccardi, D., (2015). Calcium-sensing receptor antagonists abrogate airway hyperresponsiveness and inflammation in allergic asthma. *Science translational medicine*, *7*(284), pp.284ra60-284ra60.

Ying, S., Robinson, D.S., Varney, V., Meng, Q., Tsicopoulos, A., Moqbel, R., Durham, S.R., Kay, A.B. and Hamid, Q., (1991). TNFα mRNA expression in allergic inflammation. *Clinical & Experimental Allergy*, *21*(6), pp.745-750.

Yokoyama, A., Kohno, N., Fujino, S., Hamada, H., Inoue, Y., Fujioka, S., Ishida, S. and Hiwada, K., (1995). Circulating interleukin-6 levels in patients with bronchial asthma. *American journal of respiratory and critical care medicine*, *151*(5), pp.1354-1358.

Young, A.R. and Narita, M., (2010). Connecting autophagy to senescence in pathophysiology. *Current opinion in cell biology*, *22*(2), pp.234-240.

Yu, Q.Y. and Tang, X.X., (2022). Irreversibility of pulmonary fibrosis. *Aging and disease*, *13*(1), p.73.

Yuan, H., Fan, Y., Wang, Y., Gao, T., Shao, Y., Zhao, B., Li, H., Xu, C. and Wei, C., (2019). Calcium-sensing receptor promotes high glucose-induced myocardial fibrosis via upregulation of the TGF-β1/Smads pathway in cardiac fibroblasts. *Molecular medicine reports*, *20*(2), pp.1093-1102.

Yue, X., Shan, B. and A Lasky, J., (2010). TGF-β: titan of lung fibrogenesis. *Current enzyme inhibition*, *6*(2), pp.67-77.

Zahm, J.M., Chevillard, M. and Puchelle, E., (1991). Wound repair of human surface respiratory epithelium. *Am. J. Respir. CeUMol. Biol. Vol. S. pp*, *242*, p.248.

Zahm, J.M., Kaplan, H., Hérard, A.L., Doriot, F., Pierrot, D., Somelette, P. and Puchelle, E., (1997). Cell migration and proliferation during the in vitro wound repair of the respiratory epithelium. *Cell motility and the cytoskeleton*, *37*(1), pp.33-43.

Zahm, J.M., Pierrot, D., Chevillard, M. and Puchelle, E., (1992). Dynamics of cell movement during the wound repair of human surface respiratory epithelium. *Biorheology*, *29*(5-6), pp.459-465.

Zeki, A.A., Bratt, J.M., Rabowsky, M., Last, J.A. and Kenyon, N.J., (2010). Simvastatin inhibits goblet cell hyperplasia and lung arginase in a mouse model of allergic asthma: a novel treatment for airway remodeling?. *Translational Research*, *156*(6), pp.335-349.

Zhang, P., Li, J., Liu, H., Han, N., Ju, J., Kou, Y., Chen, L., Jiang, M., Pan, F., Zheng, Y. and Gao, Z., (2020). Long-term bone and lung consequences associated with hospital-acquired severe acute respiratory syndrome: a 15-year follow-up from a prospective cohort study. *Bone research*, *8*(1), p.8.

Zhang, W., Ou, J., Inagaki, Y., Greenwel, P. and Ramirez, F., (2000). Synergistic cooperation between Sp1 and Smad3/Smad4 mediates transforming growth factor β1 stimulation of α2 (I)-collagen (COL1A2) transcription. *Journal of Biological Chemistry*, *275*(50), pp.39237-39245.

Zhang, X., Zhang, T., Wu, J., Yu, X., Zheng, D., Yang, F., Li, T., Wang, L., Zhao, Y., Dong, S. and Zhong, X., (2014). Calcium sensing receptor promotes cardiac fibroblast

proliferation and extracellular matrix secretion. *Cellular Physiology and Biochemistry*, *33*(3), pp.557-568.

Zhang, Y., Alexander, P.B. and Wang, X.F., (2017). TGF-ß family signaling in the control of cell proliferation and survival. *Cold Spring Harbor perspectives in biology*, *9*(4), p.a022145.

Zhang, Y., Feng, X.H. and Derynck, R., (1998). Smad3 and Smad4 cooperate with c-Jun/c-Fos to mediate TGF-ß-induced transcription. *Nature*, *394*(6696), pp.909-913.

Zhang, Y., Li, S., Huang, S., Cao, L., Liu, T., Zhao, J., Wu, J., Wang, J., Cao, L., Xu, J. and Dong, L., (2019). IL33/ST2 contributes to airway remodeling via p-JNK MAPK/STAT3 signaling pathway in OVA-induced allergic airway inflammation in mice. *Experimental lung research*, *45*(3-4), pp.65-75.

Zhang, Y.E., (2009). Non-Smad pathways in TGF-ß signaling. *Cell research*, *19*(1), pp.128-139.

Zhao, J., Shi, W., Chen, H. and Warburton, D., (2000). Smad7 and Smad6 differentially modulate transforming growth factor ß-induced inhibition of embryonic lung morphogenesis. *Journal of Biological Chemistry*, *275*(31), pp.23992-23997.

Zhao, J., Shi, W., Wang, Y.L., Chen, H., Bringas Jr, P., Datto, M.B., Frederick, J.P., Wang, X.F. and Warburton, D., (2002). Smad3 deficiency attenuates bleomycin-induced pulmonary fibrosis in mice. *American Journal of Physiology-Lung Cellular and Molecular Physiology*, *282*(3), pp.L585-L593.

Zhao, Y., Ma, J., Fan, Y., Wang, Z., Tian, R., Ji, W., Zhang, F. and Niu, R., (2018). TGF-ß transactivates EGFR and facilitates breast cancer migration and invasion through canonical Smad3 and ERK/Sp1 signaling pathways. *Molecular oncology*, *12*(3), pp.305-321.

Zhou, L.F., Jiang, L., Li, Z.H. and Kang, J., (2010). Change of matrix metalloproteinase-1 and matrix metalloproteinase-7 in serum and bronchoalveolar lavage fluid of patients with idiopathic pulmonary fibrosis and sarcoidosis. *Zhonghua jie he he hu xi za zhi= Zhonghua jiehe he huxi zazhi= Chinese journal of tuberculosis and respiratory diseases*, *33*(6), pp.441-444.

Zhou-Suckow, Z., Duerr, J., Hagner, M., Agrawal, R. and Mall, M.A., (2017). Airway mucus, inflammation and remodeling: emerging links in the pathogenesis of chronic lung diseases. *Cell and tissue research*, *367*(3), pp.537-550.

Zhu, J. and Thompson, C.B., (2019). Metabolic regulation of cell growth and proliferation. *Nature reviews Molecular cell biology*, *20*(7), pp.436-450.

Zhu, X., Wang, L., Zhang, B., Li, J., Dou, X. and Zhao, R.C., (2011). TGF-ß1-induced PI3K/Akt/NF-κB/MMP9 signalling pathway is activated in Philadelphia chromosome-positive chronic myeloid leukaemia hemangioblasts. *The Journal of Biochemistry*, *149*(4), pp.405-414.

Zimmermann, N., King, N.E., Laporte, J., Yang, M., Mishra, A., Pope, S.M., Muntel, E.E., Witte, D.P., Pegg, A.A., Foster, P.S. and Hamid, Q., (2003). Dissection of experimental asthma with DNA microarray analysis identifies arginase in asthma pathogenesis. *The Journal of clinical investigation*, *111*(12), pp.1863-1874.

Zou, J., Lei, T., Guo, P., Yu, J., Xu, Q., Luo, Y., Ke, R. and Huang, D., (2019). Mechanisms shaping the role of ERK1/2 in cellular senescence. *Molecular medicine reports*, *19*(2), pp.759-770.

Zurek, M. and Crémillieux, Y., (2011). MRI of the lung: non-invasive protocols and applications to small animal models of lung disease. In *In vivo NMR Imaging*. Humana Press. pp. 459-474

CHAPTER 9: APPENDICES

9.1.1 Aniline blue is a lesser known, but similarly effective, mucosubstance stain

One aim of the novel quantitative histomorphometry of airway cross-section components (qHACC) analysis was to standardise a single stain for the determination of many airway remodelling markers. Here Masson's trichrome staining with aniline blue was used to identify epithelial tissues and smooth muscle by distinct shades and textures of red as well as collagens and mucosubstances by distinct shades and loci of blue staining, as described in Chapter 2. However, aniline blue is not well established as a mucosubstance stain and although it is known to bind preferentially to a proteinaceous core, its binding specificity is not well understood (Aumann, 1994). **Figure S9.1** shows a serial section comparison of goblet cell staining in multiple airways where positive staining shows a high degree of specificity to goblet cells. Furthermore, Alcian blue-periodic acid Schiff (PAS) staining identifies positively stained cells in a deep purple in harsh contrast to negatively stained airways that are poorly visible against the counter stain. This may represent a source of bias towards the selection of positively stained airways using Alcian blue-PAS staining. Masson's trichrome with aniline blue is not limited by this staining bias and allows the quantification of numerous other markers, simultaneously. For these reasons, aniline blue was selected to determine mucosubstances and is recommended for future studies.

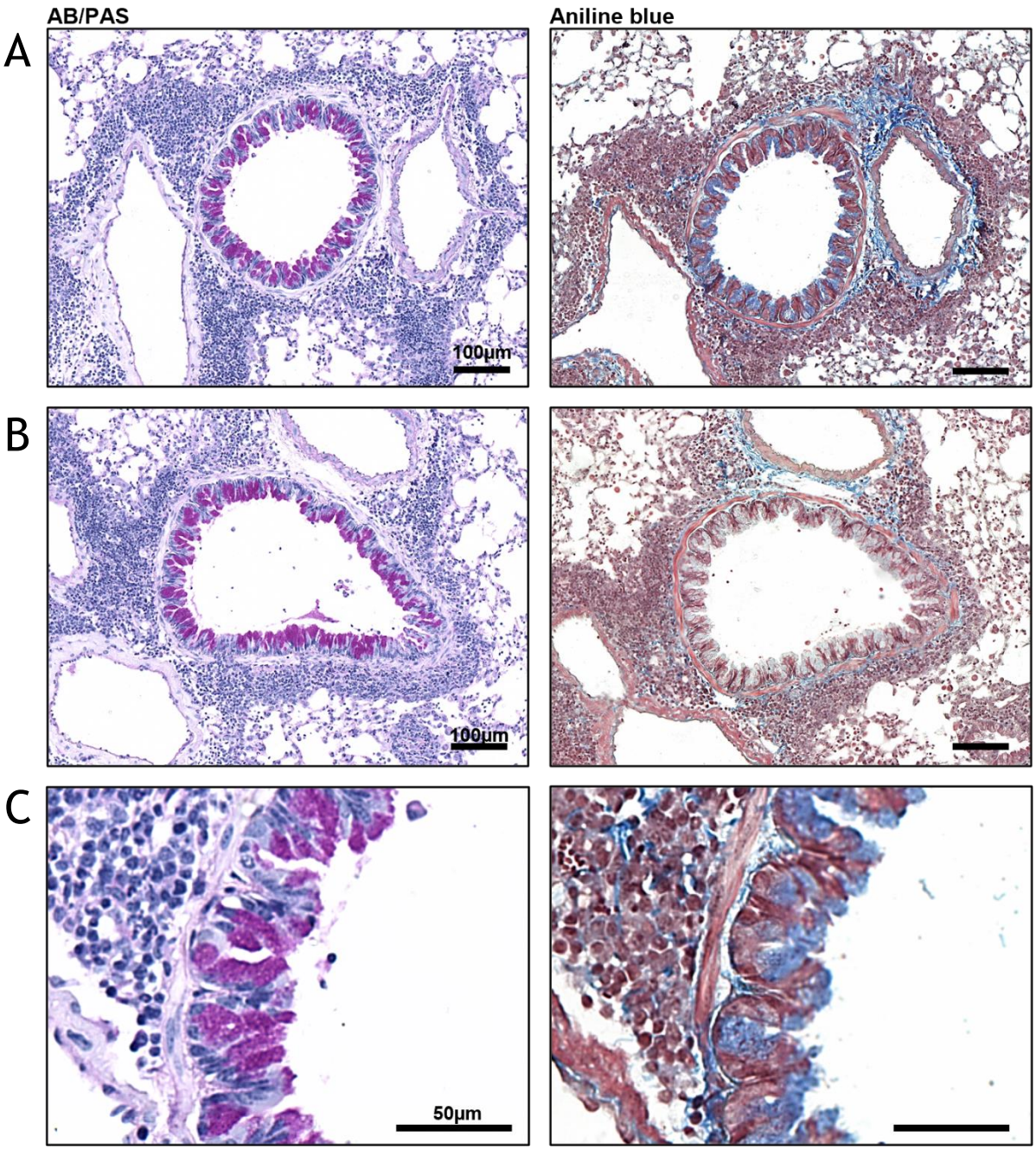

Figure S9.1. Comparison of goblet cell mucosubstance staining using Alcian blue (AB) & periodic acid Schiff (PAS) vs Masson's trichrome with aniline blue. Alcian blue & PAS staining is the industry standard for identifying acidic and neutral mucosubstances in the lung but this stain lacks versatility as it stains only mucosubstances in the lung. Here we show Masson's trichrome using aniline blue stains mucosubstances in a comparable manner, while also providing differential tissue and collagen stains, eliminating the need to repeat the sectioning, staining, imaging and analysis procedure and maintains the airway

sample population for multiple measurements and reduced variability. Images are the same airway in serial sections from the animal coded OVA 6 from the model of shorter-term IgE/Th2 asthma delivered by intranasal instillation. Graticule: (A and B) 100 µm or © 50 µm. AB: Alcian blue; PAS: Periodic acid-Schiff; IgE: Immunoglobulin E.

9.1.2 Isotype control confirms CaSR antibody specificity

As shown in **Figure S9.2**, an immunoglobulin (Ig)G2a isotype control was used to match the isotype of the calcium-sensing receptor (CaSR) antibody (ab19347) used in these studies and determine whether the CaSR antibody was binding to other molecules based on its isotype specificity and not its antibody specificity. The isotype control resulted in no staining other than the nuclear DAPI stain used. This was confirmed by the negative control group.

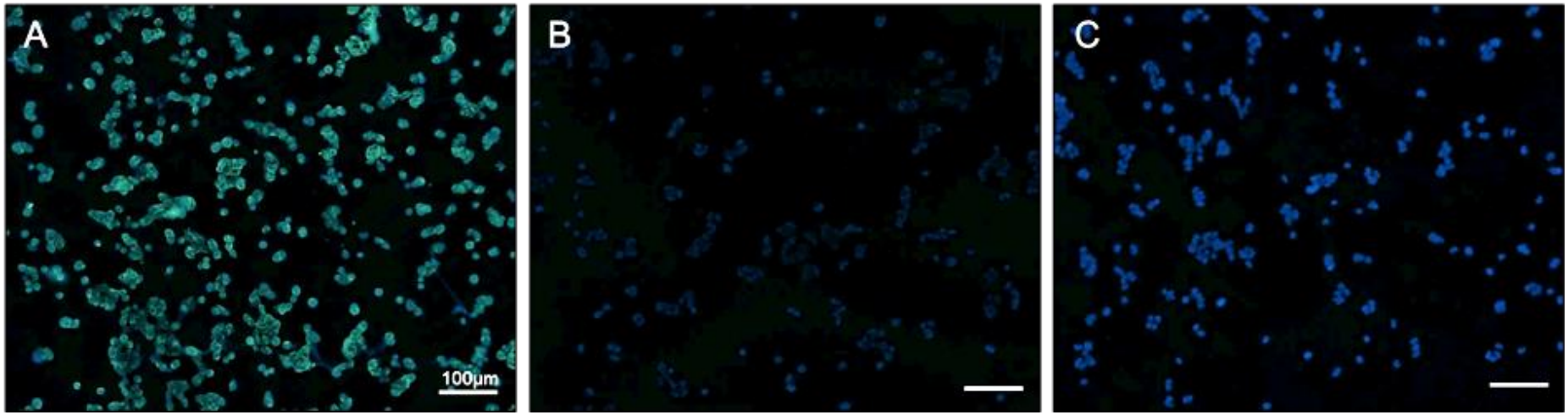

Figure S9.2. Specificity of CaSR immunoreactivity using the anti-CaSR antibody (ab19347). CaSR-HEK 293 cells were fixed with 2% paraformaldehyde and blocked with 1% BSA, 3% SeaBlock and 0.1% Triton X100. Following this cells were exposed to (**A**) anti-CaSR antibody (ab19347; 1:200) (**B**) anti-IgG2a isotype control (Thermofisher, Cat# 02-6200) antibody and (**C**) no primary antibody (negative control) to determine non-specific immunoreactivity of the ab19347 anti-CaSR antibody. Blue represents nuclear immunoreactivity (DAPI) and green represents primary antibody (or isotype control) immunoreactivity with AlexaFluor 488 (ab150077) secondary antibody. Regions of interest selected at random using the DAPI field; 10x objective; brightness + 40%. Background subtracted using ImageJ ("separate colour"; 50.0 pixels). Graticule: 100 µm. IgG2A: Immungoblulin G isotype 2a; CaSR: calcium-sensing receptor; CaSR-HEK 293: Human embryonic kidney cells transfected with the calcium-sensing receptor.

9.1.3 NAM treatment downregulates markers of fibroblast migration induced by TGF-β

Fibroblast migration is a process associated with the spread of fibrosis around the lung. Cell shape can be an indicator of a migratory phenotype as well as markers such as collagen triple helix repeat containing 1 (CTHRC1), fascin actin-bundling protein 1 (FSCN1), and heat shock protein family B1 (HSPB1). Fibroblasts exposed to TGF-β exhibited increased cell surface area (**p_{adj} = 0.020**). Here, NAM treatment significantly reduced cell surface area (**p_{adj} < 0.0001**), as shown in **Figure S9.3B**. TGF-β upregulated markers of fibroblast migration, as shown in **Figure S9.3C**, including *CTHRC1*, *FSCN1* and *HSPB1* (**$\log_2$ fold change; *CTHRC1* = 1.06, *FSCN1* = 0.41, *HSPB1* = 0.97; p_{adj} < 0.05; TGF-β vs vehicle**). NAM treatment significantly reduced the expression of *CTHRC1*, *FSCN1* and *HSPB1* (**$\log_2$ fold change; *CTHRC1* = -0.78, *FSCN1* = -0.40, *HSPB1* = -1.04; p_{adj} < 0.05; TGF-β + NAM vs TGF-β**). Furthermore, inhibition of cAMP-producing adenyl cyclase has been shown to play a role in fibroblast motility (Kohyama et al., 2009; Togo et al., 2009). Fibroblast differentiation is accompanied by migratory phenotype that increases the number of fibrogenic cells in fibrotic foci (Wynn, 2007; Fujisawa et al., 2020). Fibroblasts expressing CTHRC1 are more migratory than other subsets of collagen-producing cells (Tsukhui et al., 2020) and FSCN1 and HSPB1 are genes code for components of motility in fibroblasts (Chilosi et al., 2006). In this study, increased cell surface area was used as a surrogate measurement for the rounding phenotype associated with the migratory phenotype (Tkach et al., 2005) and was significantly increased and accompanied by increased mRNA expression of CTHRC1, FSCN1 and HSPB1, contributing to the proposed spread of fibrosis around the lung.

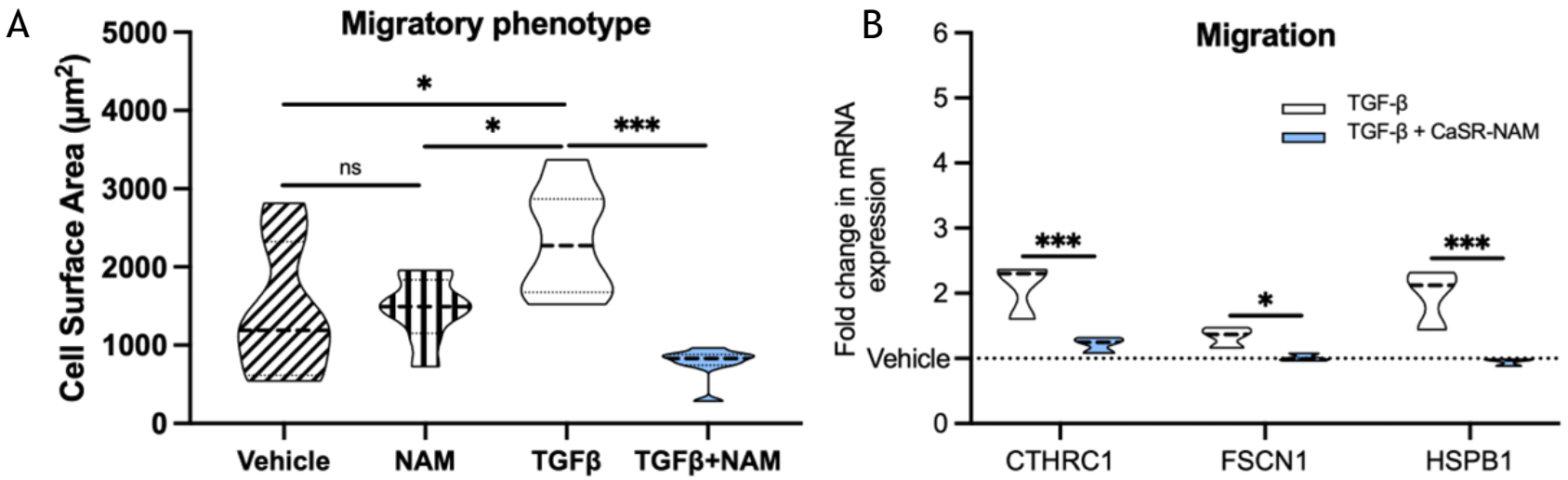

Figure S9.3. NAM treatment ameliorates TGF-ß-induced migration in human lung fibroblasts. (**A**) Primary normal human lung fibroblasts (Lonza, UK) were treated with and without remodelling mediator TGF-ß and/or a NAM (NPS2143). (**B**) Cell surface area was quantified using StrataQuest and found that NAM treatment significantly abrogated the TGF-ß-induced cell shape change that is indicative of a migratory phenotype. (**C**) Markers of fibroblast migration, including CTHRC1, FSCN1, and HSPB1, were also significantly reduced by NAM treatment suggesting CaSR activation plays a central role in fibroblast migration and the spread of fibrosis in the lung. Quantification was achieved using RNA-sequencing and p value adjustment using the Benjamini-Hochberg correction. A truncated violin plot was used to demonstrate frequency distribution of the data where dashed lines represent the median and dotted lines represent the upper and lower quartiles, respectively. N = 3, (B) n = 8 and

(C) n = 6. ns (p_{adj} > 0.05), * (p_{adj} < 0.05), ** (p_{adj} < 0.01), *** (p_{adj} < 0.001). Graticule: 50 µm. IPF: Idiopathic pulmonary fibrosis; CaSR: Calcium-sensing receptor; NAM: Negative allosteric modulator of the calcium-sensing receptor; TGF-ß: Transforming growth factor beta; CTHRC1: Collagen triple helix repeat containing 1; FSCN1: Fascin actin-bundling protein 1; HSPB1: Heat shock protein family B1.

9.1.4 Physiological relevance of TGF-β exposure in normal human lung fibroblasts

The evidence supporting the physiological relevance of 5 ng/ml TGF-β is largely anecdotal. However, Kotecha et al. (1996) demonstrated infants with bronchopulmonary dysplasia exhibited TGF-β concentrations as high as 39.5 ± 26.0 ng/ml in the bronchoalveolar lavage fluid (BALF), compared to maximum concentrations of 2.8 ± 2.3 ng/ml in control infants. This suggests 5 ng/ml TGF-β may be more closely related to physiological conditions than pathophysiology.

9.1.5 NAMs evoke no fibroblast response in the absence of TGF-β

As expected, untreated fibroblasts exposed to NAM treatment alone exhibited no alteration to CaSR (p_{adj} **= 0.50**), αSMA (p_{adj} **= 0.37**) or rho associated coiled-coil containing protein kinase 1 (ROCK1) (p_{adj} **= 0.25**) protein expression and no change in cell surface area was detected (p_{adj} **= 0.95**). Furthermore, 0 differentially expressed genes (p_{adj} **< 0.05**) were identified in untreated fibroblasts exposed to NAM treatment alone. This evidence supports the proposed mechanism of action whereby NAMs only elicit their dampening effect on CaSR activation in the presence of an orthosteric ligand and indicates that TGF-β evokes an extracellular environment consistent with CaSR activation.

9.1.6 Treatment with NAM in human lung fibroblasts does not induce cytotoxicity

Lactate dehydrogenase (LDH) release, a marker of cell viability that is increased in all cell types following damage to the plasma membrane, was assessed in all treatment groups of the normal human lung fibroblast experiment to investigate whether the proposed experimental protocol would induce cytotoxicity. Here, compared to the vehicle treatment group, the assay positive control group (10% cell lysis solution) induced a significant increase in LDH release (p_{adj} **< 0.0001 vs vehicle**). On the other hand, LDH release following treatment with NAM alone, TGF-β or TGF-β + NAM, in the absence of cell lysis solution, was indistinguishable from baseline levels (p_{adj} **> 0.05 vs vehicle**). This suggests cytotoxicity was not induced using this experimental protocol using human lung fibroblasts from a single donor. This experiment was performed by Dr Kasope Wolffs.

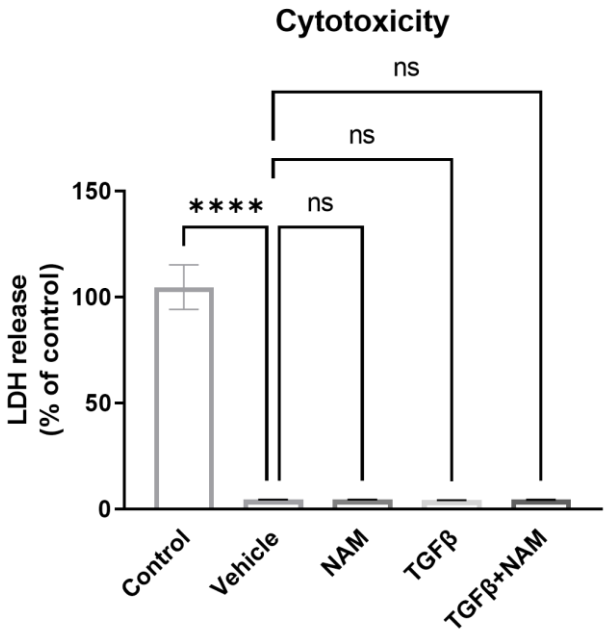

Figure S9.4 NAM treatment does not induce cytotoxicity. LDH release, a marker of cytotoxicity, was assessed in normal human lung fibroblasts to assess the effect of NAM treatment on cell viability. Here, the positive control group, treated with 10% cell lysis solution induced a significant effect on LDH release, compared to the negative vehicle control, but treatment with NAM alone, TGF-ß or TGF-ß + NAM did not. Statistical significance identified using a one-way ANOVA with Bonferroni post hoc test. This figure was created by Dr Kasope Wolffs (unpublished). N = 1, n = 3. ns (p_{adj} > 0.05), **** (p_{adj} < 0.0001). LDH; lactate dehydrogenase; TGF-ß: transforming growth factor ß; NAM: negative allosteric modulator of the CaSR.